

# UNIVERSITÀ DELLA CALABRIA



Dipartimento di Dipartimento di Chimica e Tecnologie Chimiche  
Dipartimento di Farmacia e Scienze della Salute e della Nutrizione

---

*Scuola di Dottorato Scienza e Tecnica "Bernardino Telesio"*

*Organic Molecules of Pharmacological Interest (OMPI)*

(XXVI ciclo)

Settore scientifico disciplinare Chim/06

## ***Different medicinal chemistry approaches towards the identification of novel targets in breast cancer***

*Direttore:* **Ch.mo Prof. Roberto Bartolino**

*Coordinatore:* **Ch.mo Prof. Bartolo Gabriele**

*Supervisori*

**Ch.mo Prof. Giovanni Sindona**

**Ch.mo Prof. Marcello Maggiolini**

*Dottoranda*

**Dott.ssa Assunta Pisano**

---

*Anno Accademico 2012/2013*

---

---

# Contents

<b>Abstract</b>	1
<b>Section 1: GPER characterization</b>	3
<b>Chapter 1</b>	
<b>Introduction</b>	<b>3</b>
1.1 G protein-coupled receptors (GPCRs)	3
1.2 The G protein-coupled estrogen receptor (GPER)	5
1.3 Bisphenol A	10
1.4 Searching for GPER ligands	12
1.5 Mass spectrometry as a novel tool for GPER characterization	14
1.6 Aim of the study	16
<b>Chapter 2</b>	
<b>Materials and Methods</b>	<b>18</b>
2.1 Reagents	18
2.2 Cell Cultures	18
2.2.1 Isolation and characterization of CAFs	19
2.3 Western Blotting	20
2.4 RT-PCR and real-time PCR	21
2.5 Transient transfections	21
2.5.1 Plasmids	22
2.5.2 Gene silencing experiments	23
2.5.3 Luciferase assays	23
2.6 Wound-healing assays	24
2.7 Proliferation assays	25
2.8 Molecular modeling	25
2.9 Synthesis of GPER ligands	26
2.9.1 General	26
2.9.2 Preparation of 1,4-dimethyl-9H-carbazol-3-yl-methylene)-hydrazines (2a-c) and N,N'-bis-(6-bromo-1,4-dimethyl-9H-carbazol-3-yl-methylene)-hydrazine	26
2.9.3 Spectral data	27
2.10 Protein depletion	28
2.11 Chemical Fractionation	28
2.12 Solid-Phase Extraction	29
2.13 Isolation of GPER	29
2.14 Solid-Phase Extraction	29
2.15 Protein Digestion	30

2.16 Protein Identification by MALDI MS	30
<b>Chapter 3</b>	
<b>Results</b>	<b>31</b>
3.1 BPA acts as a GPER agonist	31
3.1.1 BPA induces ERK1/2 activation through GPER	31
3.1.2 BPA stimulates the expression of GPER target genes	33
3.1.3 BPA induces cell proliferation and migration through GPER	36
3.2 Carbhydraz (2a) as a new selective GPER ligand	39
3.2.1 Synthesis of Carbhydraz (2a)	39
3.2.2 Docking simulations	40
3.2.3 Carbhydraz induces ERK 1/2 phosphorylation through GPER in breast cancer cells	42
3.2.4 Carbhydraz (2a) does not activate ER $\alpha$	43
3.3 Isolation & Identification of GPER by Mass spectrometry	44
3.3.1 Isolation of GPER	44
3.3.2 GPER Identification by MALDI-TOF/TOF mass spectrometry	45
<b>Chapter 4</b>	
<b>Discussion</b>	<b>47</b>
<b>Section 2: Synthesis and biological activity of new half-titanocene derivatives</b>	<b>51</b>
Chapter 1	
<b>Introduction</b>	<b>51</b>
1.1 Titanocenes: novel metal based compounds as anticancer drugs	51
1.2 Aim of the study	54
<b>Chapter 2</b>	
<b>Materials and Methods</b>	<b>55</b>
2.1 Synthesis of new half-titanocene	55
2.1.1 General	55
2.1.2 Synthesis of half-titanocene complexes 5a,b	56
2.1.3 Spectral data	56
2.2 Cell Cultures	58
2.8 MTT assays	58
<b>Chapter 3</b>	
<b>Results</b>	<b>59</b>
3.1 Synthesis of titanocene derivatives	59
3.2 New half-titanocene derivatives inhibit breast cancer cell growth	62
<b>Chapter 4</b>	
<b>Discussion</b>	<b>63</b>



Contents

---

<b>References</b>	<b>65</b>
<b>Pubblications</b>	<b>80</b>



# ABSTRACT

G protein-coupled receptors (GPCRs) belong to the largest family of cell-surface molecules representing the targets of approximately 40% of current medicinal drugs (Overington, J.P et al 2006). GPCRs are ubiquitous in mammalian (Bockaert, J. et al. 1999), regulate several physiological processes and play an important role in multiple diseases ranging from cardiovascular dysfunction, depression, pain, obesity to cancer (Rosenbaum D.M. et al. 2011). One member of this superfamily, named GPR30/GPER, mediates estrogen signaling in different cell contexts, leading to gene expression changes and relevant biological responses (Filardo E.J et al. 2000, Bologna C.G. et al. 2006, Maggiolini M. and Picard D. 2010). GPER acts by transactivating the Epidermal Growth Factor Receptor (EGFR), which thereafter induces the increase of intracellular cyclic AMP (cAMP), calcium mobilization and the activation of the phosphatidylinositol 3-kinase (PI3K) and the mitogen-activated protein kinases (MAPKs) (Maggiolini M. and Picard D. 2010). Moreover, the GPER-mediated transduction pathways activated by estrogens trigger the expression of a typical gene signature, including the expression of c-fos and the gene encoding the connective tissue growth factor (CTGF), which are involved in the proliferation and migration of diverse cell types (Lappano R. et al 2012a, Madeo A. and Maggiolini M. 2010).

On the basis of these findings, the first objective of the present study was the characterization of GPER from different points of view: GPER-mediated signaling pathways and biological functions, selective ligands and molecular characterization of the receptors. In particular, the research project focused on:

1. the transduction pathways by which the environmental contaminant Bisphenol A (BPA) influences cell proliferation and migration of human breast cancer cells and cancer-associated fibroblasts (CAFs);
2. the characterization of novel carbazole derivatives as GPER agonists in ER-negative breast cancer cells;
3. the isolation and characterization of GPER in estrogen-sensitive cancer cells by Mass Spectrometry.

Additionally, the second section of this doctoral thesis was focused on the evaluation of the cytotoxic activity of novel synthesized compounds, given the interest and the need to discover new molecules against cancer. In particular, novel titanocene-complexes were studied evaluating their ability to elicit repressive effects on the growth of estrogen-sensitive breast cancer cells.

# SECTION 1

## GPER characterization

### Chapter 1

#### Introduction

##### 1.1 G protein-coupled receptors (GPCRs)

The seven-transmembrane G protein-coupled receptors (GPCRs), which belong to the largest superfamily of signal transduction proteins, regulate multiple biological functions coupling to a heterotrimeric G-protein associated with the inner surface of the plasma membrane (Pierce KL et al. 2002; Lappano R and Maggiolini M., 2011). The heterotrimer that is composed of the  $G\alpha$ ,  $G\beta$ , and  $G\gamma$  subunits, binds to the guanine nucleotide GDP in its basal state. Upon activation by ligand binding, GDP is released and replaced by GTP, which leads to subunit dissociation into a  $\beta\gamma$  dimer and the GTP bound  $\alpha$  monomer (Neves S.R. et al 2002) (Figure 1.1).

GPCRs include more than 900 members, representing the most prominent family of validated pharmacological targets in biomedicine (Pierce K.L. et al. 2002).

As only a small number of these GPCRs are targeted by current drugs, huge efforts are currently being made to exploit the remaining receptors, including approximately 120 members for which no existing ligands have been identified (Chung S. et al. 2008). Several studies have demonstrated

that GPCRs are involved in multiple physiological functions as well as in human disease including cancer (Lappano R. and Maggiolini M., 2011). For example, various GPCRs such as chemokines, thrombin, lysophosphatidic acid (LPA), gastrin-releasing peptide, endothelin and prostaglandin receptors play a key role in angiogenesis and metastasis (Lui V. W. et al. 2003, Greenhough A. et al. 2009) as well as in inflammation-associated cancer (Dorsam R. T. et al. 2007). In addition, constitutively active GPCRs can be expressed from the genomes of human oncogenic viruses (Dorsam R. T. et al. 2007). As more data linking GPCRs to cancer are currently emerging, the pharmacological manipulation of these receptors is attractive for the development of novel strategies to target tumour progression and metastasis.

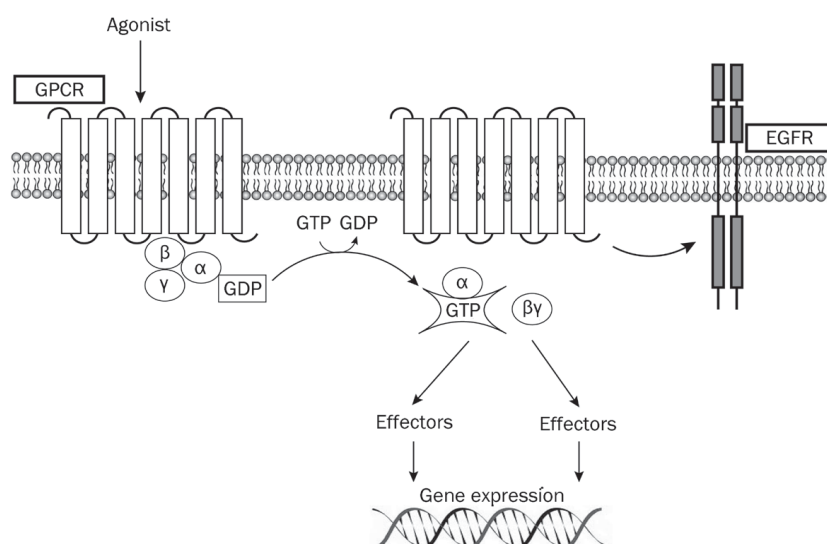


**Figure 1.1.** Agonist binding to GPCRs promotes the dissociation of GDP bound to the  $G\alpha$  subunit and its replacement with GTP leading to the activation of the heterotrimeric G proteins and the subunit dissociation into a  $\beta\gamma$  dimer and the GTP-bound  $\alpha$  monomer. Both subunits activate multiple downstream effectors which induce gene transcription and relevant biological responses.

## 1.2 The G protein-coupled estrogen receptor (GPER)

Among the GPCR family members, GPR30/GPER, was recently shown to mediate the multifaceted actions of estrogens in different tissues including cancer cells (Maggiolini M. and Picard D. 2010). GPER was first identified as an orphan member of the 7-transmembrane receptor family by multiple groups in the late 1990s (Carmeci C. et al, 1997, O'Dowd B.F. et al. 1998, Owman C. et al. 1996, Takada Y. et al. 1997). It belongs to the rhodopsin-like receptor superfamily and its gene is mapped to chromosome 7p22.3 (Carmeci C. et al, 1997). There are four alternate transcriptional splicing variants encoding the same protein which is comprised of 375 amino acids, and contains seven transmembrane spanning segments (Wang C. et al. 2007). Although GPER is a seven-transmembrane receptor, its subcellular localization remains to be fully elucidated. Indeed, several studies have reported the presence of GPER at the plasma membrane, in the endoplasmic reticulum, in the Golgi apparatus as well as in the nucleus of CAFs extracted from mammary biopsies (Filardo E.J. et al. 2007, Madeo A. and Maggiolini M. 2010, Thomas P. et al. 2005, Revankar C.M. et al. 2007).

Several studies demonstrated that the ligand-dependent activation of GPER trigger the activation of the heterotrimeric G proteins and subsequently Src and adenylyl cyclase (AC) resulting in intracellular cAMP production. Src is involved in matrix metalloproteinases (MMP) activation, which cleave pro-heparan-bound epidermal growth factor (pro-HB-EGF) releasing free HB-EGF. The latter activates EGF receptor (EGFR), leading to multiple downstream events, for example the activation of phospholipase C (PLC), PI3K and MAPK (Maggiolini

M. and Picard D. 2010). Activated PLC produces inositol triphosphate (IP3), which further binds to IP3 receptor and leads to intracellular calcium mobilization (Filardo E.J. and Thomas P. 2012). The downstream signal of PI3K is AKT pathway, closely related to cancer cell growth as involved in cell survival and proliferation (Vivanco I. et al. 2002). The activation of MAPK and PI3K results in the activation of numerous cytosolic pathways and nuclear proteins, which in turn regulate transcription factors such as SRF, CREB and members of the E26 transformation specific (ETS) family by direct phosphorylation (Pandey D.P. et al. 2009, Posern G. and Treisman R. 2006). These promotes the expression of a second wave of transcription factors such as FOS, JUN, EGR1, ATF3, C/EBP $\delta$ , and NR4A2. Cells are literally reprogrammed under the effect of this network of transcription factors and a series of GPER target genes such as CTGF are up-regulated (Pandey D.P. et al. 2009) (Figure 1.2).



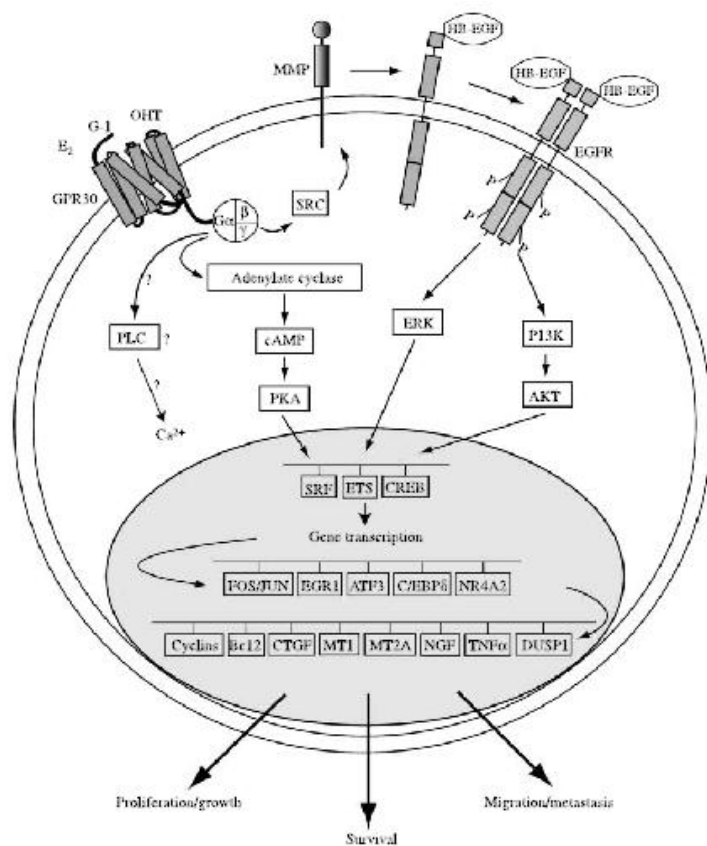


**Figure 1.2.** Schematic representation of the GPER signaling network.

In addition, there may be a variety of signaling crosstalk pathways and both negative and positive feedback loops. For example, it has been demonstrated that EGF up-regulates GPER expression through the EGFR/MAPK pathway in ER-negative breast cancer cells, most likely by promoting the recruitment of the c-FOS-containing transcription factor AP-1 to the GPER promoter (Albanito L. et al. 2008b). Considering that GPER signaling uses the EGFR/MAPK pathway, a positive feedback loop is conceivable. This mechanism is also operational for EGF and the related growth factor TGF $\alpha$  in ER $\alpha$ -positive breast cancer cells (Vivacqua A. et al. 2009). GPER gene expression has been detected in at least four kinds

of human tumor specimens or cell lines, including breast cancer (Albanito L. et al. 2008b, Carmeci C. et al. 1997, Filardo E.J. 2002, Filardo E.J. et al. 2008, Filardo E.J. et al. 2000, Filardo E.J. et al. 2006, Kuo W.H. et al. 2007, Pandey D.P. et al. 2009, Thomas P. et al. 2005), endometrial cancer (He Y.Y. et al. 2009, Leblanc K. et al. 2007, Smith H.O. et al. 2007, Vivacqua A. et al. 2006b), ovarian cancer (Albanito L. et al. 2008a, Albanito L. et al. 2007, Henic E. et al. 2009), thyroid cancer (Vivacqua A. et al. 2006a), and a rat pheochromocytoma cell line PC-12. (Alyea R.A et al. 2008).

In addition, there is a growing body of evidence supporting that GPER is strongly associated with cancer proliferation (Albanito L. et al. 2008b, Albanito L. et al. 2007, Filardo E.J. et al. 2000, He Y.Y. et al. 2009, Kang K. et al. 2009, Liu Z. et al. 2008, Maggiolini M. et al. 2004, Vivacqua A. et al. 2006a, 2006b), migration (Henic E. et al. 2009, Pandey D.P. et al. 2009), invasion (He Y.Y. et al. 2009), metastasis (Filardo E.J. et al. 2006, Filardo E.J. et al. 2008), differentiation (He Y.Y. et al. 2009), and drug resistance (Kleuser B. et al. 2008, Lapensee E.W. et al. 2009). Indeed, as estrogens stimulate the progression of breast cancer in approximately two-thirds of patients who express ER (Ali S. and Coombes R.C. 2000, Hanstein B. et al. 2004), some selective estrogen receptor modulators (SERMs), such as tamoxifen, have been clinically used to antagonize the binding of estrogen to its classic ERs, which is an effective therapeutic strategy in attenuating the growth of ER-positive breast cancers.

However, there are around 25% of ER-positive breast cancer patients who do not respond to anti-estrogen therapy (Early Breast Cancer Trialists' Collaborative Group 2005). It implies that the blockade of classic ERs alone may be not enough to completely abolish estrogen-induced breast

cancer cell growth, since estrogen may promote it through other receptors besides classic ERs. Such hypothesis is further supported by the discovery of GPER as the third specific ER with different structure and function respect to ER $\alpha$  and ER $\beta$ . GPER has a high binding affinity to not only for estrogen, but also for some ER antagonists, such as tamoxifen and ICI 182,780. Notably, estrogen and the aforementioned antiestrogens stimulate GPER signaling (Thomas P. et al. 2005). These important findings provide a further possible mechanism for the progression of estrogen-related cancers, and raise a novel potential target for antiestrogen therapy. As it concerns clinical findings, GPER overexpression was associated with lower survival rates in endometrial and ovarian cancer patients (Smith H.O. et al. 2007, Smith H.O. et al. 2009) as well as with a higher risk of developing metastatic disease in breast cancer patients (Filardo E.J et al. 2006). Moreover, in a previous extensive survey, GPER was found to be highly expressed and significantly associated with tumor size (>2 cm), with the presence of distant metastases and increased human EGFR-2 (HER-2)/neu expression (Filardo E.J. et al. 2006). Likewise, a recent study demonstrated that the majority of the aggressive inflammatory breast tumors examined resulted GPER positive (Arias-Pulido H. et al. 2010), suggesting that the expression of the receptor may be considered a predictor of an aggressive disease. In addition to the aforementioned studies on the potential functions of GPER in cancer and possibly other pathological conditions, this receptors was implicated in a broad range of physiological functions regarding reproduction, metabolism, bone, cardiovascular, nervous and immune systems (Olde B. and Leeb-Lundberg L.M. 2009). Estrogen binds to GPER with a high affinity of a reported Kd 2.7 nM (Thomas P. et al. 2005) or 6 nM (Prossnitz E.R. et al. 2008).

Moreover, in the last few years a great attention was focused on the identification of synthetic ligands of GPER acting as agonists or antagonists. In particular different compounds named G-1 (Bologa C.G. et al. 2006) G-15 (Dennis M.K. et al. 2011), GPER-L1 and GPER-L2 (Lappano R. et al. 2012a) and MIBE (Lappano R. et al. 2012b), were identified using virtual and bio-molecular screening and are used to evaluate the GPER-mediated signaling and functions. In addition, different studies shows that ICI 182,780 (Filardo E.J. et al. 2002, Thomas P. et al. 2005) and 4-hydroxytamoxifen (OHT) (Filardo E.J. et al. 2002, Pandey D.P. et al. 2009, Vivacqua A. et al. 2006a, 2006b) are also able to bind GPER and mimic estrogen effects. It has been reported that a variety of xenoestrogens, including bisphenol A, can bind and activate GPER leading to important biological responses (Thomas P. and Dong J. 2006).

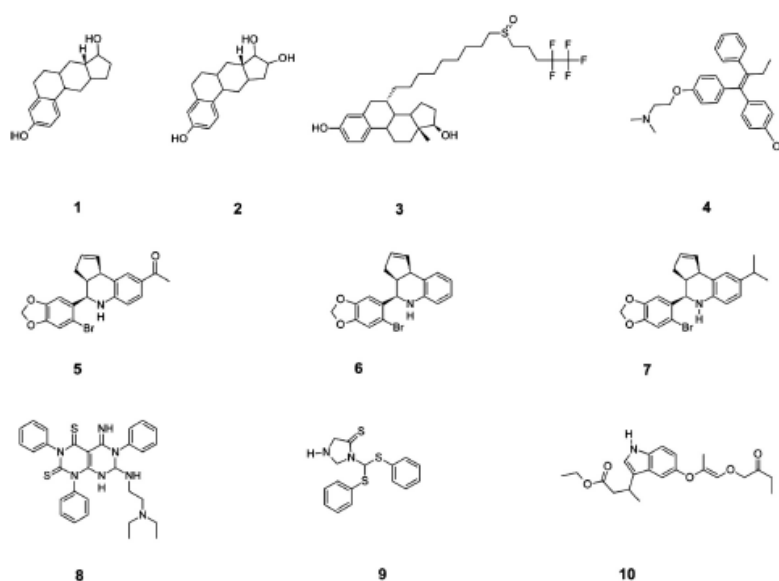


**Figure 1.3.** Structures of some GPER ligands: (1) 17-β estradiol, (2) estriol, (3) ICI 182 780, (4) 4-hydroxytamoxifen, (5) G-1, (6) G-15, (7) G-36, (8) GPER-L1,(9) GPER-L2, (10) MIBE.

### 1.3 Bisphenol A

Bisphenol-A (BPA) (Figure 1.3) was first synthesized by Dianin in 1891 and reported to be a synthetic estrogen in the 1930s (Dodds E.C. and Lawson W.1936). In the 1950s, BPA was rediscovered as a compound that could be polymerized to make polycarbonate plastic, and from that moment on until now, it has been commonly used in the plastic industry.

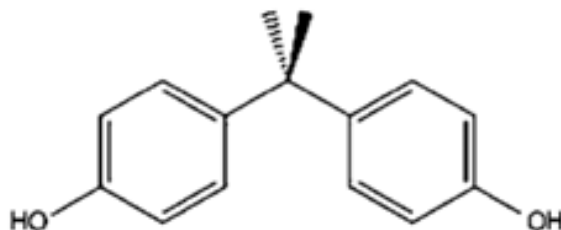


*Figure 1.4* Chemical structure of Bisphenol A

BPA is one of the highest volume chemicals produced worldwide, with over 6 billion pounds produced each year and over 100 tons released into the atmosphere by the yearly production (Vandenberg L.N. et al. 2009). It is used as the base compound in the manufacture of polycarbonate plastic and the resin lining of food and beverage cans, and as an additive in other widely used plastics such as polyvinyl chloride and polyethylene terephthalate (Welshons W.V. et al. 2006). It is present not only in food and beverage containers, but also in some dental material (Olea N. et al. 1996). Numerous studies have found that BPA can leach from polycarbonate containers; heat and either acidic or basic conditions accelerate the hydrolysis of the ester bond linking BPA monomers, leading to a release of BPA with the concomitant potential human exposure (Kang J.H. et al. 2006, Richter C.A. et al. 2007). Indeed, the

potential for BPA exposure has already been demonstrated since BPA was detected in 95% of the urine samples in the USA (Calafat A.M. et al. 2005). Moreover, it has been detected in amniotic fluid, neonatal blood, placenta, cord blood and human breast milk (Richter C.A. et al. 2007). Concerning the potential risk of this compound, in the 1980s the lowest-observable-adverse effect-level (LOAEL) for BPA was determined at 50 mg/kgbw/day, and the Environmental Protection Agency (EPA) calculated a “reference dose” or safe dose of 50 lg/kgbw/day in a series of studies in which the changes of body weight in animals fed diets containing BPA were analysed ([http:// www.epa.gov/iris/subst/0356.htm](http://www.epa.gov/iris/subst/0356.htm), U.E.P.A.). However, since that time, numerous scientific evidence supports that BPA can interfere with the endocrine signaling pathways at doses below the calculated safe dose, particularly after fetal, neonatal or perinatal exposure, but also after adult exposure. In this regard, fetal and perinatal exposures to BPA in rodents were shown to affect the brain, mammary gland and reproductive tract as well as to stimulate the development of hormone-dependent tumors (Durando M. et al. 2007, Ho S.M. et al. 2006; Maffini M.V. et al. 2006, Munoz-de-Toro M. et al. 2005). Although since its discovery has been highlighted as BPA could have estrogen like activity, this was rediscovered in 1993 and confirmed by performing different assays such as: competitive binding to ER, proliferation of MCF-7 breast cancer cells, induction of progesterone receptors, and reversal estrogen action by tamoxifen (Krishnan A.V. et al. 1993). Indeed, BPA, with its two benzene rings and two (4, 4')-OH substituents, fits in the ER binding pocket (Gould J.C. et al. 1998) (Figure 1.4).

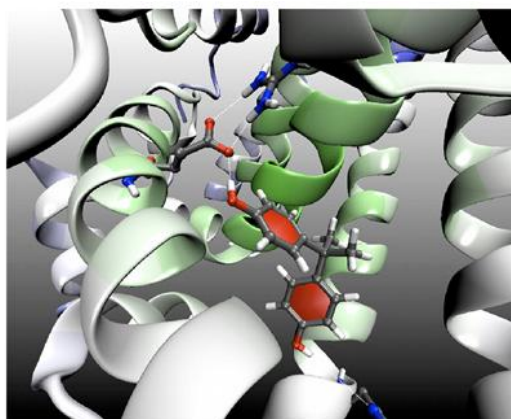


*Figure 1.5.* Binding of Bisphenol A to the estrogen receptor  $\alpha$

Biochemical assays have examined the kinetics of BPA binding to ER and have determined that BPA binds both ER $\alpha$  and ER $\beta$ , with approximately 10-fold higher affinity to ER $\beta$  (Kuiper et al. 1998, Routledge et al. 2000). However, the affinity of BPA for the ERs is approximately 10,000-fold weaker than that of estradiol (Andersen H.R. et al. 1999, Kuiper G.G. et al. 1998, Fang H. et al. 2000). Therefore, the low dose effects exerted by BPA in different cell types, can be explained at least partially because this endocrine disruptors may bind differently than E2 within the ligand domain of estrogen receptors (ERs) (Gould J.C. et al. 1998). There are also differences in the BPA co-activator recruitment, as is indicated by the fact that the BPA/ER $\beta$  complex showed over a 500-fold greater potency than BPA/ER $\alpha$  in recruiting the coactivator TIF2. This is a reflection of the more efficient capacity that ER $\beta$  has to potentiate receptor gene activity in some cell types (Routledge E.J. et al. 2000, Safe S.H. et al. 2002). In addition, it has been largely demonstrated that BPA elicits rapid responses via non-classical estrogen triggered pathways (Nadal A. et al. 2000, Quesada I. et al. 2002; Watson C.S. et al. 2005). BPA has been

shown to bind to both the membrane-bound form of ER (mER) and GPER in different cellular contexts (Wetherill Y.B. et al. 2007). In particular, it has been evidenced that BPA, upon binding to GPER, activates intracellular pathways that may be involved in the biological responses of normal and neoplastic cells (Bouskine A. et al. 2009, Dong S. et al. 2011, Sheng Z.G. and Zhu B.Z. 2011).

#### **1.4 Searching for GPER ligands**

Although different compounds have demonstrated the ability to bind both GPER and the classical ERs, a major challenge in dissecting estrogen signaling is the identification of novel compounds able to differentiate the pharmacology of the novel GPER over that of the classical ERs by targeting each receptor subtype in a selective manner (Lappano et al 2012a).

In this respect the identification of G-1, GPER-L1 and GPER-L2, which act as selective GPER agonists (Bologa C. G. et al. 2006; Lappano et al., 2012a), and G-15 and G-36 (Dennis M. et al. 2009; Dennis M. et al. 2011), which act as GPER antagonists, provided new opportunities towards the characterization of GPER signaling as well as the evaluation of both common and distinct estrogen receptors-mediated functions.



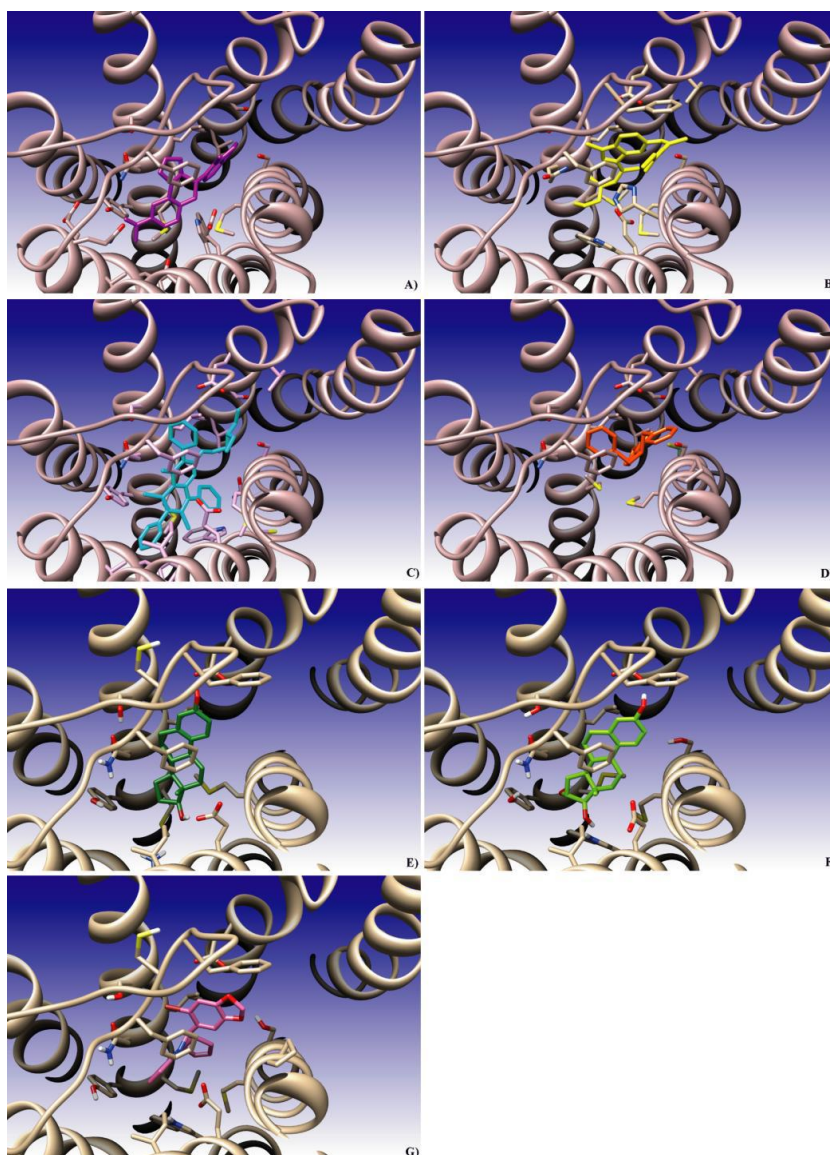


**Figure 1.6.** GPER binding site. Protein TM helices are represented as solid ribbons while ligands are reported as sticks. Panel A, G-1 in purple sticks; panel B, MIBE in yellow; panel C, GPER-L1 in cyan; panel D, GPER-L2 in orange; panel E, 17-Estradiol in dark green; panel F, estriol in light green; panel G, G-15 in pink.

In this context, *in silico* models allowed us to identify novel compounds which could be used as selective GPER ligands. In particular, the

molecular structure of carbazoles derivatives displays a favourable interaction with GPER.

Carbazole alkaloids exhibit a wide variety of activities including antibacterial, anti-inflammatory, psychotropic and anti-histamine properties (Caruso A. et al. 2008). Moreover, carbazoles show significant antitumor activity in multiple cells derived from leukemia, melanoma, colon adenocarcinoma, kidney, brain and breast tumors (Panno A. et al. 2013, Moody D.L. et al. 2007). For instance, a series of simple benzo[a]carbazoles has been shown to bind to estrogen receptor (ER) and inhibit the growth of mammary tumors of rats as well breast cancer cell proliferation (Von Angerer E. et al. 1986).

### **1.5 Mass spectrometry as a novel tool for GPER characterization**

The identification of different GPER-selective ligands as well as the characterization of the GPER-mediated biological functions has provided novel information regarding the possibility to use this receptor as new drugs target.

However, the complete structural and functional behaviour of this receptor has not yet been fully characterized. Today, one of the most important tool used to study the structure and function of proteins is mass spectrometry. Mass spectrometry is a gel-free proteomic technique used to elucidate the chemical structures of molecules, such as peptides and other chemical compounds (Aebersold R. and Mann M. 2003) and has become the technique of choice for protein identification as these methods are very sensitive, require small amounts of sample (femtomole to attomole concentrations) and have the capacity for high sample throughput. Peptide

mass fingerprinting (PMF) is the primary tool for protein identification. PMF is based on a set of peptide masses obtained by mass spectroscopic analysis which is then used to search against protein databases created by *in silico* cleavage of all known, predicted, or partial protein sequences (Fenyo D. et al. 2000).

Mass spectrometric measurements are carried out in the gas phase on ionized analytes (Aebersold R. and Mann M. 2003). In order to measure the characteristics of individual molecules, a mass spectrometer converts them to ions, so that, they can be moved about and manipulated by external electric or magnetic fields. The mass spectrometer is based on the principle of measurement of the mass-to-charge ( $m/z$ ) of gas-phase ions. This technique has both qualitative and quantitative purposes. The three fundamental components of a mass spectrometer are the ionization source, the mass analyzer, and the detector (Aebersold R. and Goodlet D. R. 2001). Protein identification made from peptide mass fingerprints can be confirmed by using post source decay (PSD) matrix-assisted laser desorption/ionization (MALDI-MS) or tandem mass spectrometry (LC-MS/MS) fragmentation of individual peptides.

In the present study, MALDI-TOF/TOF mass spectrometry is used for protein identification and characterization.

Matrix-assisted laser desorption/ionization was first introduced in the late 1980s by the group of Hillenkamp (Aebersold R. and Goodlet D. R. 2001). MALDI allows the analysis of biomolecules (biopolymers such as proteins, peptides, and sugars) and large organic molecules such as polymers, dendrimers, and other macromolecules that tend to be fragile and fragment when ionized by conventional ionization methods (Aebersold R. and Goodlet D. R. 2001). MALDI sublimates and ionizes

the analytes out of a dry, crystalline matrix via laser pulses (Aebersold R. and Mann M. 2003).

Generally, the matrix consists of crystallized molecules and may be prepared with any one of the following chemical agent: 3,5-dimethoxy-4-hydroxycinnamic acid (sinapinic acid),  $\alpha$ -cyano-4-hydroxycinnamic acid (alpha-cyano or alpha-matrix), or 2,5-dihydroxybenzoic acid (DHB) (Aebersold R. and Mann M. 2003). In order to prepare the matrix solution, any one of the above mentioned chemical reagent is added to a mixture of highly purified water and an organic solvent, normally acetonitrile (ACN) or ethanol. Trifluoroacetic acid (TFA) may also be added to the matrix solution (Aebersold R. and Mann M. 2003). Matrix should be of low molecular weight to allow facile vaporization. It is often acidic and acts as a proton source to encourage ionization. Matrix should have strong optical absorption either in ultra violet (UV)

or in infrared (IR) range and can be functionalized with polar groups allowing their use in aqueous solutions (Aebersold R. and Mann M. 2003).

The ionization is triggered by a laser beam. UV laser such as nitrogen lasers (337 nm) and frequency tripled and quadrupled Neodymium-doped yttrium aluminium garnet (Nd:YAG) lasers (355 nm and 266 nm respectively) are used. IR lasers are also used at some point due to their softer mode of ionization (Aebersold R. and Mann M. 2003). MALDI is usually coupled to TOF analyzer that measure the mass of intact peptides, however, several other analyzers can also couple with MALDI depends on the type of analysis. MALDI-TOF MS comes with two modes, functionally linear mode and reflectron mode. The MALDI-TOF MS used in the present study is of linear mode.

The advantages of MALDI-TOF include good sensitivity and good tolerance to biochemical buffers and salts. In addition, since there is usually only a singly charged ion formed it is a good choice for the analysis of heterogeneous samples. The advantages of MALDI-TOF MS for peptide analysis and protein identification are speed, ease of analysis, and accuracy of the molecular weights obtained by the TOF detector. The major mass spectrometric applications in the biomedical field, includes analysis of proteins, peptides, oligonucleotides in biochemistry; drug discovery, drug metabolism, combinatorial chemistry, pharmacokinetics in pharmaceuticals; neonatal screening, haemoglobin analysis, drug testing in clinical and microbiological field; and proteomics/functional genomics.

### **1.6 Aim of the study**

On the basis of these findings, the first objective of this doctoral thesis was the study of GPER-mediated signaling pathways and biological functions, selective ligands and molecular characterization of GPER. In particular, the research focused on:

1. the transduction pathways by which the environmental contaminant Bisphenol A (BPA) influences cell proliferation and migration of human breast cancer cells and cancer-associated fibroblasts (CAFs);
2. the characterization of novel carbazole derivatives as GPER agonists in ER-negative breast cancer cells;
3. the isolation and characterization of GPER in estrogen-sensitive cancer cells by Mass Spectrometry.



## Chapter 2

### Materials and Methods

#### 2.1 Reagents

Bisphenol A (BPA), N-[2-(p-bromocinnamylamino)ethyl]-5-soquinolinesulfonamide dihydrochloride (H89), PD98059 (PD) and arsenic trioxide (As<sub>2</sub>O<sub>3</sub>) were purchased from Sigma-Aldrich (Milan, Italy); AG1478 (AG) was bought from Biomol Research Laboratories (DBA, Milan, Italy), and 1-(4-(6-bromobenzo[1,3]dioxol-5-yl)-3a,4,5,9b-tetrahydro-3H-cyclopenta[c]quinolin-8-yl)-ethanone (G-1) from Calbiochem (Merck KGaA, Frankfurt, Germany). As<sub>2</sub>O<sub>3</sub> was dissolved in phosphate-buffered saline; BPA and PD were dissolved in ethanol; AG1478, H89, G-1 and carbazole derivatives were solubilized in dimethyl sulfoxide (DMSO).

#### 2.2 Cell cultures

SkBr3 human breast cancer cells were maintained in RPMI 1640 without phenol red supplemented with 10% FBS. MCF7 human breast cancer cells were maintained in DMEM with phenol red supplemented with 10% FBS. Cells were grown in a 37° C incubator with 5% CO<sub>2</sub>. The day before experiments for immunoblots cells were switched to medium without serum, thereafter cells were treated as indicated.

### ***2.2.1 Isolation and characterization of CAFs***

CAFs were extracted as previously described (Madeo A. and Maggiolini M. 2010). Briefly, breast cancer specimens were collected from primary tumors of patients who had undergone surgery. Tissues from tumors were cut into smaller pieces (1–2 mm diameter), placed in digestion solution (400 IU collagenase, 100 IU hyaluronidase, and 10% serum, containing antibiotic and antimycotic solution), and incubated overnight at 37°C. The cells were then separated by differential centrifugation at  $90 \times g$  for 2 min. Supernatant containing fibroblasts was centrifuged at  $485 \times g$  for 8 min; the pellet obtained was suspended in fibroblasts growth medium (Medium 199 and Ham's F12 mixed 1:1 and supplemented with 10% FBS) and cultured at 37°C in 5% CO<sub>2</sub>. Primary cells cultures of breast fibroblasts were characterized by immunofluorescence. Briefly cells were incubated with human anti-vimentin (V9) and human anti-cytokeratin 14 (LL001), both from Santa Cruz Biotechnology DBA (Milan, Italy). To assess fibroblasts activation, we used anti-fibroblast activated protein  $\alpha$  (FAP $\alpha$ ) antibody (H-56; Santa Cruz Biotechnology DBA) (Figure 2.3).



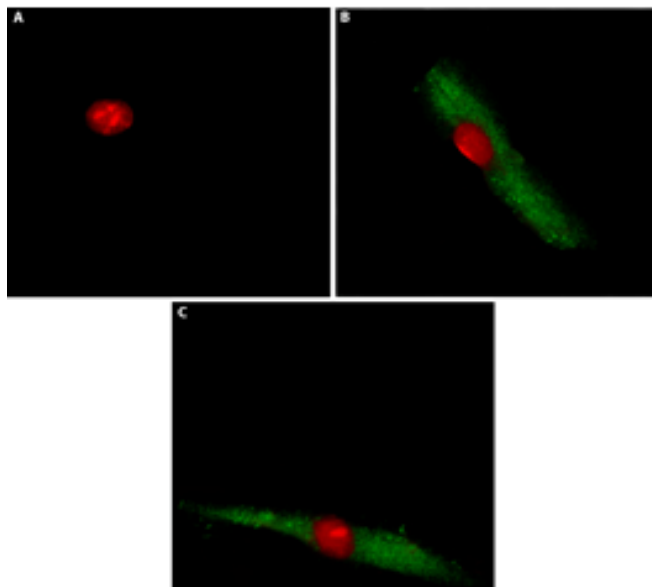


**Figure 2.3.** Characterization of CAFs. CAFs were immunostained by anti-cytokeratin 14 (A), anti-vimentin (B) and anti FAP $\alpha$  (C)antibody.

### 2.3 Western blotting

SkBr3 cells and CAFs were grown in 10-cm dishes, exposed to treatments or ethanol (or DMSO), which was used as the vehicle, and then lysed in 500  $\mu$ L of 50 mmol/L NaCl, 1.5 mmol/L MgCl<sub>2</sub>, 1 mmol/L EGTA, 10% glycerol, 1% Triton X-100, 1% sodium dodecylsulfate (SDS), and a mixture of protease inhibitors containing 1 mmol/L aprotinin, 20 mmol/L phenylmethylsulfonyl fluoride, and 200 mmol/L sodium orthovanadate. Then, we diluted samples 10 times and determined protein concentration using Bradford reagent (Sigma-Aldrich, Milan, Italy). The method of Bradford is based on the observation that the absorbance maximum of a solution of Coomassie Brilliant Blue G250 shifts from 465 to 595 nm upon binding with proteins. The amount of bound colorant depends on the content of basic amino acids in proteins in solution. Equal amounts of

whole protein extract were resolved on a 10% SDS polyacrylamide. After electrophoresis, the proteins were transferred from the gel onto a nitrocellulose membrane by electroblotting in buffer with low salt content (25 mM TRIS, 192 mM Glycine pH 8.3, 0.1% SDS, 20% Methanol). Then, the membrane was placed in a solution of no-fat milk at 5% in 1X TBST (Tris HCl 100 mM pH 7.5, 1M NaCl, 1% Tween 20) for one hour at room temperature in order to block all sites of non-specific hydrophobic interactions. Afterward, nitrocellulose filter were probed overnight at 4°C with the antibody against c-Fos (H-125),  $\beta$ -Actin (C-2), phosphorylated extracellular signal-regulated kinase 1/2 (p-ERK1/2; E-4), EGR-1 (588), CTGF (L-20), ERK2 (C-14), ER $\alpha$  (F-10), or GPR30 (N-15), all from Santa Cruz Biotechnology, DBA (Milan, Italy), or ER $\beta$  from Serotec (Space Import Export, Milan, Italy). Membranes were then incubated with horseradish peroxidase (HRP)-conjugated secondary antibodies (Santa Cruz Biotechnology, DBA Milan, Italy) and immunoreactive bands were visualized with the ECL western blotting detection system (GE Healthcare, Milan, Italy). Results of densitometric analyses of Western blots were obtained using ImageJ software (Abramoff M.D. et al. 2004).

#### **2.4 RT-PCR and real-time PCR**

Total RNA was extracted from cells maintained for 24 hours in medium without serum and treated with ligand for indicated times using Trizol commercial kit (Invitrogen, Milan, Italy) according to the manufacturer's protocol. RNA was quantified spectrophotometrically, and cDNA was synthesized from the RNA by reverse transcription using murine leukemia virus reverse transcriptase (Invitrogen). We quantified the expression of selected genes by real-time PCR. This method is based on the use of

intercalating agents which bind to double stranded DNA. These molecules, when excited by laser beams, emit fluorescence and allow to follow in real-time the progress of the reaction and the increase of the amount of nucleic acid. In this study we used SYBR Green as the detection method and the Step One sequence detection system (Applied Biosystems Inc., Milan, Italy). Specific primers for the genes c-FOS, CTGF, EGR-1 and the control gene 18S were designed using Primer Express software (version 2.0; Applied Biosystems Inc.). Assays were performed in triplicate. We used mean values to calculate expression levels by the relative standard curve method. The sequences of primer used are:

5'-CGAGCCCTTTGATGACTTCCT-3' (c-FOS Fw);

5'-GGAGCGGGCTGTCTCAGA-3' (c-FOS Rv);

5'-ACCTGTGGGATGGGCATCT-3' (CTGF Fw);

5'-CAGGCGGCTCTGCTTCTCTA-3' (CTGF Rv);

5'-GCCTGCGACATCTGTGGAA-3' (EGR-1 Fw);

5'-CGCAAGTGGATCTTGGGTATGC-3' (EGR-1 Rv);

5'- GCGTCCCCCACTTCTTA-3' (18S Fw);

5'-GGGCATCACAGACCTGTTATT-3' (18S Rv).

## 2.5 Transient transfections

The transfections allow to insert exogenous biological material, such as nucleic acids, into the eukaryotic cell. The transfection is defined “transient” when the inserted genetic material remains in the cell as an extrachromosomal fragment and does not integrate into the cellular genome; in this case the features induced by transfection persist for a short

time, usually disappear prior to 72 hours. The main problem in the transfer of nucleic acids is provided by the presence of negative charges, due to phosphate groups, in the skeleton of the molecules. Because of these charges, the exogenous material is not able to overcome the cell membrane, as electrostatic forces of repulsion occur. One of the methods of transfection more employed to mask the anionic groups of the DNA is represented by the use of cationic lipids. This method is included in the field of chemical techniques of transfection and requires the use of amphipathic lipid molecules which associate to form liposomes. These, being constituted by amphipathic lipids, in contact with the aqueous environment form a phospholipid bilayer very similar to cell membranes. Moreover, the liposomes may contain within them charged molecules, such as DNA, as their polar heads are turned towards the inner of the vesicle. This complex lipid/DNA can fuse with the plasma membrane and carry the exogenous material within the cell. The cationic lipids most commonly used have characteristics such as high efficiency, low cytotoxicity, quick and simple protocol for usage and some can be used also in the presence of serum.

### ***2.5.1 Plasmids***

The CTGF luciferase reporter plasmid p(-1999/+36)-luc (Chaour B. et al. 2006), which is based on the backbone of vector pGL3-basic (Promega), was a gift from B. Chaour (Department of Anatomy and Cell Biology, State University of New York Downstate Medical Center, Brooklyn, NY, USA). The luciferase reporter plasmid for c-FOS

(Kaneyama J.K. et al. 2002) encoding a -2.2-kb 5' upstream fragment of human c-FOS was a gift from

K. Nose (Department of Microbiology, Showa University School of Pharmaceutical Sciences, Hatanodai, Shinagawa-ku, Tokyo, Japan). The EGR-1 luciferase reporter plasmid pEgr-1A (Chen C.C. et al. 2004), which contains the -600 to +12 5'-flanking sequence from the human EGR-1 gene was a gift from S. Safe (Department of Veterinary Physiology and Pharmacology, Texas A&M University, Houston, TX, USA). The short hairpin (sh) RNA constructs to knock down the expression of GPER and CTGF and the unrelated shRNA control construct were obtained and used as previously described (Pandey D.P. et al. 2009).

### ***2.5.2 Gene silencing experiments***

To silence GPER and CTGF expression, we used the technique of shRNA (short hairpin RNA). These are small molecules of double-stranded RNA hairpin-shaped (hairpin) which are processed by a specific enzyme called DICER. This enzyme cuts the double-stranded RNA and form fragments of double-stranded RNA of about 19-25 nucleotides. Where after, the enzyme complex RISC separates the two strands and transfers one near the mRNA containing the sequence of gene which should be to be silenced. This filament will bind with the complementary sequence at the mRNA level and causes the block of translation or degradation of the mRNA itself. For gene silencing experiments, cells were plated onto 10-cm dishes, maintained in serum-free medium for 24 hr, and then

transfected for an additional 24 hours before treatments with shRNA, shGPER or ShCTGF using Fugene6.

### **2.5.3 Luciferase assays**

To perform the luciferase assay two "reporter" enzymes are simultaneously expressed in a single system and their activities are measured. The activity of the experimental reporter is correlated to the specific conditions of treatment, while the basal cell activity is compared to that of the co-transfected control reporter (pRL-CMV). Comparing the activity of the experimental and control reporters, it is possible to normalize experimental variability which generally is caused by the differences between the number of cells and effectiveness of the transfection. In this assay in one sample are measured sequentially the activities of two luciferase: the firefly or firely luciferase (*Photius pyralis*) and the Renilla luciferase (*Renilla reniformis*). These enzymes have different structures and requires different substrates, so that it is possible to discriminate selectively the respective bioluminescent reactions. The activity of firefly luciferase is measured initially adding the LAR II (Luciferase Assay Reagent II) to the cell lysate. This generates a light signal that is appropriately quantified using a luminometer (Lumat model LB 9507, Berthold Technology). Then, adding in the same tube the Stop & Glo reagent, the first enzymatic reaction is stopped and simultaneously start the second reaction catalyzed by Renilla which also generates a light signal. Finally, the values of the Luciferase activity are compared with the corresponding values of Renilla and expressed as "relative Luciferase units". In this study for the luciferase assays, cells were transferred into 24-well plates containing 500  $\mu$ L of regular growth

medium per well the day before transfection. On the day of transfection, SkBr3 cell medium was replaced with RPMI without phenol red and serum, and transfection was performed using Fugene6 Reagent (Roche Molecular Biochemicals, Milan, Italy) and a mixture containing 0.5  $\mu\text{g}$  of each reporter plasmid. Renilla luciferase (pRL-CMV; 1 ng) was used as a transfection control. After 5–6 hours, ligands were added and cells were incubated for 16–18 hr. We measured luciferase activity using the Dual Luciferase Kit (Promega, Milan, Italy) according to the manufacturer's recommendations. Firefly luciferase values generated by the reporter plasmid were normalized to Renilla luciferase values. Normalized values obtained from cells treated with ethanol vehicle were set as 1-fold induction, and the activity induced by treatments was calculated based on this value.

## 2.6 Wound-healing assays

CAFs were seeded into 12-well plates in regular growth medium. When at 70% to 80% confluency, the cells were transfected with shGPER using Fugene6 reagent for 24 hr. Transfected cells were washed once, medium was replaced with 2.5% charcoal-stripped FBS, and cells were treated. We then used a p200 pipette tip to scratch the cell monolayer. In experiments performed using conditioned medium, CAFs were plated into 12-well plates and transfected with 500 ng shRNA control plasmid or shGPER or shCTGF plasmids using Fugene6, as recommended by the manufacturer. After 24 hr, CAFs were treated with 1  $\mu\text{M}$  BPA, and the conditioned medium was collected and filtered through a sterile nonpyrogenic 0.2  $\mu\text{m}$  filter. The conditioned medium obtained was added to subconfluent SkBr3 cells, and a series of scratches were made using a p200 pipette tip. We

evaluated cell migration in three independent experiments after 48 hr. of treatment; data are expressed as a percentage of cells in the wound area upon treatment compared with cells receiving vehicle.

## 2.7 Proliferation assays

SkBr3 cells and CAFs were seeded in 24-well plates in regular growth medium. After cells attached, they were washed, incubated in medium containing 2.5% charcoal-stripped FBS, and transfected with 500 ng shGPER or control shRNA plasmids using Fugene6 reagent. After 24 hr, cells were treated with 1  $\mu$ M BPA, and the transfection and treatment were renewed every 2 days. We counted the cells using the COUNTESS automated cell counter (Invitrogen) following the manufacturer's recommendations.

## 2.8 Molecular modeling

We used the program GOLD v.5.0.1 (the Cambridge Crystallographic Data Center, UK) to perform docking simulations. GOLD is a program using a genetic algorithm that allows to investigate the full range of ligand conformational flexibility and a partial protein side chain flexibility. We used, as the protein target for our docking simulation the three dimensional atomic coordinates of the GPER molecular model built by homology as described elsewhere (Lappano R. et al. 2010). We identified Phe 208 O atom, as the protein active site centre on the basis of our previous docking simulations (Lappano R. et al. 2010) and we considered as the active site atoms, those located within 20 Å from this point. The default GOLD settings were used running the simulations. Residues Tyr123, Gln138, Phe206, Phe208, Glu275, Phe278 and His282 of GPER



were defined with flexible side chains, allowing their free rotation. Ligand molecular structure was built and energy minimized with the programs InsightII and Discover3 (Biosym/MSI, San Diego, CA, USA). Figures were drawn with the program Chimera (Pettersen E.F. et al. 2004) and interaction diagram was built using the program Ligplot (Wallace A.C. et al. 1996).

## 2.9 Synthesis of GPER ligands

### 2.9.1 General

Commercial reagents were purchased from Aldrich, Acros Organics and Alfa Aesar and were used without additional purification. Melting points were determined on a Gallenkamp melting point apparatus. The IR spectra were recorded on a Fourier Transform Infrared Spectrometer FT/IR-4200 for KBr pellets. <sup>1</sup>H-NMR (300 MHz) and <sup>13</sup>C-NMR (100 MHz) spectra were recorded on a Bruker 300 spectrometer. Chemical shifts are expressed in parts per million downfield from tetramethylsilane as an internal standard. Thin layer chromatography (TLC) was performed on silica gel 60F-264 (Merck). The 6-bromo-1,4-dimethyl-9H-carbazole-3-carbaldehyde 1 was prepared as described in the literature (Vehar B. et al. 2011).

### 2.9.2 Preparation of 1,4-dimethyl-9H-carbazol-3-yl-methylene-hydrazines (2a-c) and N,N'-bis-(6-bromo-1,4-dimethyl-9H-carbazol-3-yl-methylene)-hydrazine (3)

Hydrazine hydrate, 98% (d= 1.029 g/mL; 5.97x10<sup>-3</sup> mol; 0.29 mL) and 1,4-dimethyl-9H-carbazole-3-carbaldehyde 1a-b (1.48x10<sup>-3</sup> mol) were dissolved in absolute ethanol (37.4 mL).

The resulting solution was heated under reflux for 3h. After cooling to room temperature, the reaction solution was evaporated under reduced pressure. The remaining residue was washed twice with Et<sub>2</sub>O (20 mL). The filtrate was dried under reduced pressure and the solid residue obtained was recrystallized from Et<sub>2</sub>O to give 2a-b as powder. The compound 3 has been isolated as cream powder for filtration of the reaction of 1a.

### ***2.9.3 Spectral data of newly synthesized compounds***

6-Bromo-1,4-dimethyl-9H-carbazol-3-yl-methylene)-hydrazine (2a).

Orange powder; yield 60%; mp > 270 °C. IR spectrum,  $\nu$ , cm<sup>-1</sup>: 3398-3354 (NH<sub>2</sub>); 3169 (NH); 1613 (CH=N); 1589; 1442; 857. <sup>1</sup>H NMR spectrum (DMSO-d<sub>6</sub>),  $\delta$ , ppm: 2.49 (s, 3H, CH<sub>3</sub>); 2.78 (s, 3H, CH<sub>3</sub>); 6.51 (s, 2H, NH<sub>2</sub>); 7.45-7.49 (m, 2H, Ar); 7.61 (s, 1H, Ar); 8.22 (s, 1H, CH=N-NH<sub>2</sub>); 8.26 (s, 1H, Ar); 11.47 (s, 1H, NH). <sup>13</sup>C NMR spectrum (DMSO-d<sub>6</sub>),  $\delta$ , ppm: 15.12; 16.77; 110.73; 112.95; 117.92; 119.87; 124.32; 124.39; 125.30; 125.38; 127.04; 127.45; 138.48; 138.68; 139.11. Found, %: C 56.98; H 4.46; N 13.29. C<sub>15</sub>H<sub>14</sub>BrN<sub>3</sub>. Calculated, %: C 56.95; H 4.50; N 13.31.

(6-Methoxy-1,4-dimethyl-9H-carbazol-3-yl-methylene)-hydrazine (2b).

Green powder; yield 48%; mp > 270 °C. IR spectrum,  $\nu$ , cm<sup>-1</sup>: 3430-3379 (NH<sub>2</sub>); 2924 (NH); 1612 (CH=N); 1464; 1210; 1130; 863. <sup>1</sup>H NMR spectrum (DMSO-d<sub>6</sub>),  $\delta$ , ppm:  $\delta$  2.79 (s, 3H, CH<sub>3</sub>); 3.53 (s, 3H, CH<sub>3</sub>); 3.87 (s, 3H, OCH<sub>3</sub>); 6.51 (s, 2H, NH<sub>2</sub>); 6.92-7.27 (m, 1H, Ar); 7.50-7.91 (m, 3H, 2 Ar, CH=N-NH<sub>2</sub>); 8.30 (s, 1H, Ar); 11.29 (s, 1H, NH). <sup>13</sup>C NMR spectrum (DMSO-d<sub>6</sub>),  $\delta$ , ppm: 15.32; 19.77; 55.87; 102.13; 105.95; 109.62; 112.19; 117.62; 121.39; 124.20; 125.05; 127.24;

134.67; 139.65; 143.06; 154.10. Found, %: C 71.89; H 6.41; N 15.72. C<sub>16</sub>H<sub>17</sub>N<sub>3</sub>O. Calculated, %: C 71.92; H 6.39; N 15.69.

N,N'-bis-(6-bromo-1,4-dimethyl-9H-carbazol-3-yl-methylene)-hydrazine (3).

Yield 15%; mp > 270 °C. IR spectrum,  $\nu$ , cm<sup>-1</sup>: 3419 (NH); 1614 (CH=N); 1589; 1438; 1247; 798. <sup>1</sup>H NMR spectrum (DMSO-d<sub>6</sub>),  $\delta$ , ppm: 2.58 (s, 6H, CH<sub>3</sub>); 3.00 (s, 6H, CH<sub>3</sub>); 7.55 (s, 4H, Ar); 8.01 (s, 2H, Ar); 8.34 (s, 2H, Ar); 9.18 (s, 2H, CH=N-); 11.52 (s, 2H, NH). <sup>13</sup>C NMR spectrum (DMSO-d<sub>6</sub>),  $\delta$ , ppm: 15.09; 16.72; 110.68; 112.94; 117.88; 119.86; 124.34; 124.38; 125.28; 125.37; 127.00; 127.41; 138.49; 138.68; 139.10. Found, %: C 60.02; H 4.03; N 9.33. C<sub>30</sub>H<sub>24</sub>Br<sub>2</sub>N<sub>4</sub>. Calculated, %: C 60.05; H 4.00; N 9.29.

## 2.10 Protein Depletion

High abundant proteins such as albumin & IgG were depleted using ProteoPrep Blue Albumin and IgG depletion medium (Sigma Aldrich). The buffers supplied by the manufacturer contain surfactants & salts that can cause signal suppression, therefore an alternative protocol was used. The cartridge was conditioned with 200  $\mu$ l of 50 mM NH<sub>4</sub>HCO<sub>3</sub> pH 8, three times giving 10 min incubation followed by centrifugation. 200  $\mu$ l of total protein extract was loaded onto the column and incubated for 10 min at room temperature. After centrifugation at 3000 rpm for 1 min, the flow-through was loaded again and collected. The column was washed two times with 200  $\mu$ l of 50 mM NH<sub>4</sub>HCO<sub>3</sub> and the relative flow-throughs were collected and pooled. The bound proteins were eluted with 200  $\mu$ l of (NH<sub>4</sub>)<sub>2</sub>CO<sub>3</sub> pH 10, two times giving 10 min incubation followed by centrifugation. The eluate fractions were collected and pooled.

### 2.11 Chemical Fractionation

Chemical Fractionation: 100  $\mu$ l of depleted protein solution was precipitated with 800  $\mu$ l CHCl<sub>3</sub>/CH<sub>3</sub>OH 1:3 (v/v). The pellet was partitioned with 200  $\mu$ l of CH<sub>3</sub>CN/NH<sub>4</sub>HCO<sub>3</sub> (60:40,v/v), 200  $\mu$ l of H<sub>2</sub>O and 200  $\mu$ l of TFA 0.1%/CH<sub>3</sub>CN (90:10,v/v) respectively at room temperature under magnetic stirring. Each step was followed by centrifugation at 12000 rpm for 5 min.

### 2.12 Solid-Phase Extraction

Solid-Phase Extraction: The total protein lysate was fractionated using a reversed-phase C18 cartridges (6 ml, 1 g). Conditionation: 2 ml of CH<sub>3</sub>CN/TFA 0.1% (50:50,v/v) followed by 2 ml of TFA 0.1% were drawn slowly through the column, avoiding column from drying. Sample Adsorption: 4 ml of sample (200  $\mu$ l of total protein extract + 3.8 ml of TFA 0.1 %) was slowly drawn through the column. Washing: 3 ml of TFA 0.1% was drawn completely through the column. Elution: The analytes were eluted by loading different solutions of CH<sub>3</sub>CN/TFA 0.1% (500  $\mu$ l each time) increasing the concentration of organic phase (from 10 to 100%).

### 2.13 Isolation of GPER

Spin column with hydroxyapatite (HTP) – 200  $\mu$ l of total protein lysate was diluted with 25  $\mu$ l of equilibration buffer (10 mM TRIS, 1 mM EDTA, pH 7) and loaded onto HTP (100 g) spin column. After 30 min incubation at room temperature, the column was centrifuged at 8000 rpm for 2 min. The filtrate was collected and reloaded for second time to achieve

maximum removal. The bound proteins were eluted with 200  $\mu$ l of elution buffer (100 mM KCl, 40 mM TRIS, 2 mM EDTA, pH 8), three times giving 30 min incubation followed by centrifugation at 8000 rpm for 2 min. Eluate concentrated to 100  $\mu$ l in speedvac. Spin column with C18 – 200  $\mu$ l of total protein lysate was diluted with 25  $\mu$ l of equilibration solution (H<sub>2</sub>O:C<sub>2</sub>H<sub>6</sub>O, 90:10) and loaded onto C18 (100 g) spin column. After 1 hr incubation at room temperature, the column was centrifuged at 8000 rpm for 2 min. The filtrate was collected and reloaded for second time to achieve maximum removal. The bound proteins were eluted with 200  $\mu$ l of elution solution containing 1  $\mu$ M 17 $\beta$  Estradiol in H<sub>2</sub>O:C<sub>2</sub>H<sub>6</sub>O, 50:50 giving 5 hr incubation and centrifugation, then followed by two more times with 200  $\mu$ l of H<sub>2</sub>O:C<sub>2</sub>H<sub>6</sub>O, 50:50 giving 30 min incubation and centrifugation. Concentrated to 100  $\mu$ l.

#### ***2.14 SDS-PAGE Electrophoresis***

SDS-PAGE Electrophoresis: 12.5% poly acrylamide gel was used. After electrophoresis, the gel was stained with Coomassie blue stain solution and destained with 40% CH<sub>3</sub>OH, 10% acetic acid to 1 L H<sub>2</sub>O.

#### **2.15 Protein Digestion**

In the present study, digestion was performed extensively on gel, in solution and also on membrane. Proteolytic enzymes such as trypsin,  $\alpha$ -chymotrypsin and pepsin were used for digestion.

**2.16 Protein Identification by MALDI MS**

MS and MS/MS experiments were carried out on AB SCIEX TOF/TOF™ 5800 System equipped with a 1 kHz variable rate laser. MS data were acquired at a laser repetition rate of 400 Hz with 4000 laser shots/spectrum (100 laser shots/sub-spectrum) with a mass accuracy of 50 ppm. MS spectra were evaluated using Mascot program ([www.matrixscience.com](http://www.matrixscience.com)). Database searches were performed against Swiss-Prot & NCBI, with taxonomy restricted to Homo sapiens and pepsin enzyme cleavage specificity with an initial mass tolerance of 50 ppm.

# Chapter 3

## Results

### 3.1 BPA acts as a GPER agonist

#### 3.1.1 BPA induces ERK1/2 activation through GPER

To evaluate the ability of BPA to induce ERK1/2 activation through GPER we used the SKBR3 cells and CAFs which both express GPER and lack ERs (Figure 3.1)

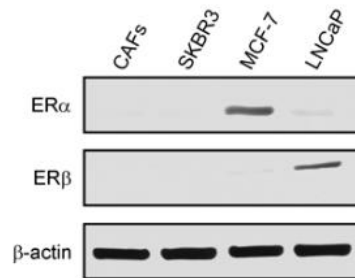


**Figure 3.1.** CAFs and SKBR3 cells are ER $\alpha$  and ER $\beta$  negative. Western blot analyses of ER $\alpha$  and ER $\beta$  protein expression in CAFs, SKBR3 and MCF-7 breast cancer cells and LNCaP prostate cancer cells.  $\beta$ -actin antibody was used as a loading control.

Considering that in our (Maggiolini M. and Picard D. 2010) and other (Dong S. et al. 2011) previous investigations ERK1/2 phosphorylation was found as a downstream signaling induced by the ligand activation of

GPER, we began the present study evaluating the ERK1/2 activation by increasing concentrations of BPA and the selective GPER agonist G-1 in SKBR3 cells and CAFs. BPA (Figure 3.2 A,C) and G-1 (Figure 3.2 B,D) induced ERK1/2 phosphorylation in both cell types in a dose-dependent manner.

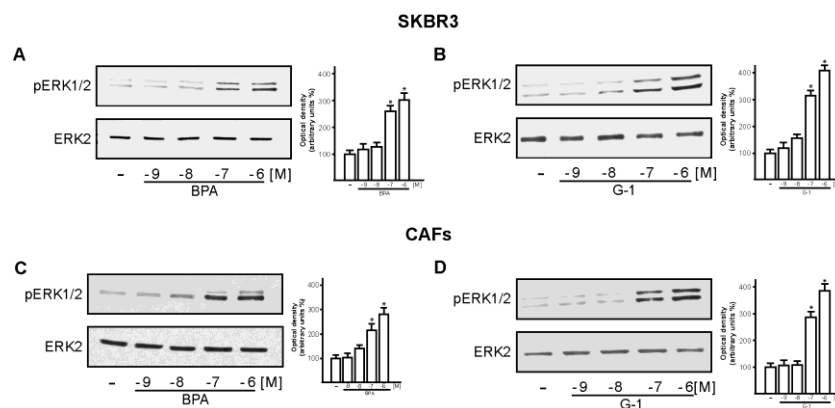


**Figure 3.2.** Induction of ERK1/2 phosphorylation (pERK1/2) by BPA and G-1 through GPER in SKBR3 cells and CAFs. (A,B) SKBR3 cells were treated for 30 min with vehicle (–) or increasing concentrations of BPA (A) or G-1 (B). (C,D) CAFs were treated for 30 min with vehicle (–) or increasing concentrations of BPA (c) or G-1 (d). Graphs show densitometric analyses of the blots normalized to ERK2; values shown represent the mean  $\pm$  SD of three independent experiments. \* $p < 0.05$  compared with vehicle.

Moreover, to elucidate the intracellular pathway through which BPA induces ERK1/2 activation in SKBR3 cells, we used the inhibitors specific for EGFR (AG), ERK (PD) and PKA (H-89). As shown in Figure 3.3 (panel A), when AG or PD was added, ERK1/2 activation was not evident, but it was present when H89 was added. Interestingly, ERK1/2 phosphorylation by BPA was abolished by silencing GPER expression in both SKBR3 and CAFs (Figure 3.3 B,D), suggesting that GPER is required for ERK1/2 activation after exposure to BPA. We ascertained the



efficacy of GPER silencing using immunoblots in SKBR3 cells and CAFs as shown in Figures 3.3 panels C and E, respectively.

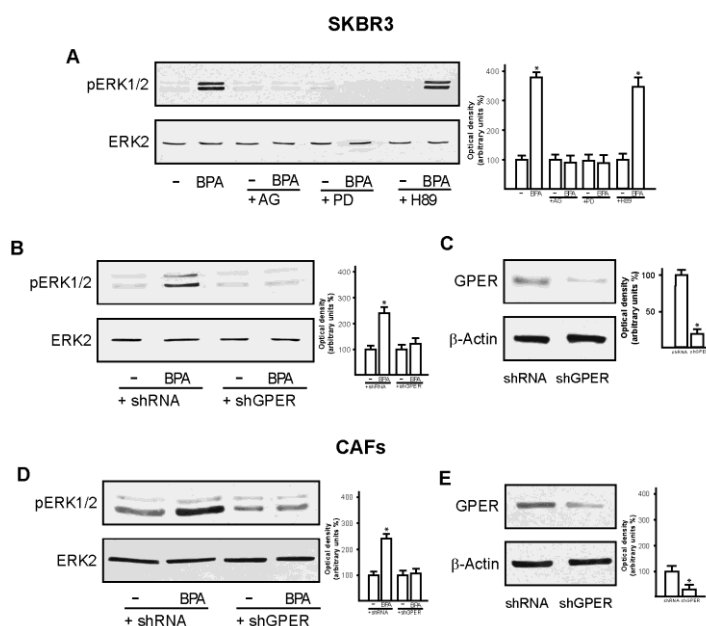


**Figure 3.3.** BPA induces ERK1/2 phosphorylation (pERK1/2) in SKBR3 cells and CAFs through the GPER/EGFR/ERK signaling pathway. (A) ERK1/2 phosphorylation in SKBR3 cells treated for 30 min with vehicle or 1  $\mu$ M BPA alone or in combination with 10  $\mu$ M AG1478, PD, or H89 (inhibitors of EGFR, MEK, and PKA, respectively). (B) ERK1/2 phosphorylation in SKBR3 cells transfected with shRNA or shGPER and treated with vehicle or 1  $\mu$ M BPA for 30 min. (C) Efficacy of GPER silencing. (D) ERK1/2 phosphorylation in CAFs transfected with shRNA or shGPER and treated with vehicle or 1  $\mu$ M BPA for 30 min. (E) Efficacy of GPER silencing in CAFs. Graphs show densitometric analyses of the blots normalized to ERK 2 (A,B,D) or  $\beta$ -Actin (C,E); values shown represent the mean  $\pm$  SD of three independent experiments. \* $p < 0.05$  compared with vehicle.

Moreover, to demonstrate the specificity of BPA action, we used the environmental contaminant arsenic (Nordstrom D.K. 2002), which elicits the ability of breast cancer cells to activate ERK1/2 (Ye J. et al. 2005). We observed that ERK1/2 phosphorylation induced by 10  $\mu$ M As<sub>2</sub>O<sub>3</sub> was still present in SKBR3 cells transfected with shGPER (data not shown).

### 3.1.2 BPA stimulates the expression of GPER target genes

GPER-mediated signaling regulates the transcription of diverse target genes (Pandey D.P et al. 2009). In the present study, BPA transactivated the promoter sequence of c-FOS, EGR-1, and CTGF (Figure 3.4 A) in SKBR3 cells, and accordingly stimulated mRNA expression of these genes in both SKBR3 cells and CAFs (Figures 3.4 B,C).

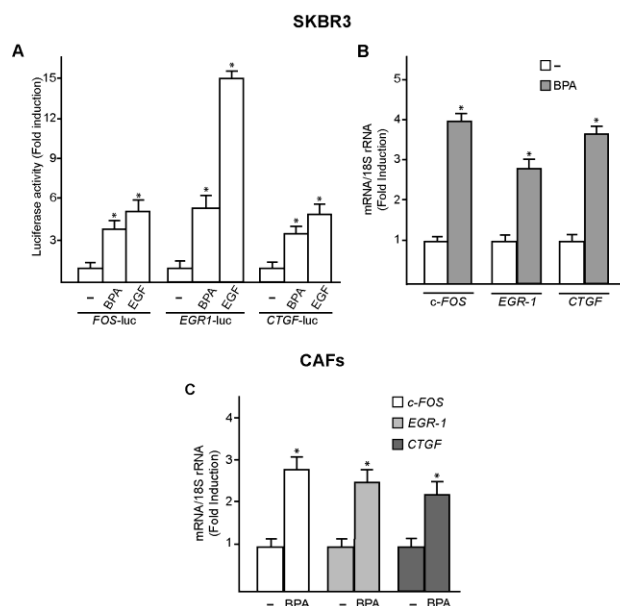


**Figure 3.4.** Expression of GPER target genes (c-FOS, EGR-1, and CTGF) in SKBR3 cells and CAFs in response to BPA treatment. (a) Evaluation of c-FOS, EGR-1, and CTGF luciferase reporter genes in transfected SKBR3 cells treated with vehicle (–), 1  $\mu$ M BPA, or EGF (50 ng/mL; positive control). Luciferase activity was normalized to the internal transfection control; values are presented as fold change (mean  $\pm$  SD) of vehicle control and represent three independent experiments, each performed in triplicate. (B,C) Evaluation of c-FOS, EGR-1, and CTGF mRNA expression by real-time PCR in SKBR3 cells (B) and CAFs (C) treated with 1  $\mu$ M BPA for 4 hr. Gene expression was normalized to 18S expression, and values are presented as fold change (mean  $\pm$  SD) of vehicle control. \* $p < 0.05$  compared with vehicle.

In accordance with these findings, BPA induced the protein levels of c-FOS, EGR-1, and CTGF (Figure 3.5 A). As observed with ERK1/2 activation, the EGFR inhibitor AG1478 and the ERK inhibitor PD, but not the PKA inhibitor H89, repressed the up-regulation of these proteins by BPA in SKBR3 cells (Figure 3.5 A). Notably, the c-FOS, EGR-1, and CTGF protein increases after exposure to BPA were abrogated by silencing GPER in both SKBR3 cells and CAFs (Figures 3.5 B,D). The efficacy of GPER silencing was ascertained by immunoblotting experiments in SKBR3 cells and CAFs as shown in Figure 3.5 panels C and E, respectively.

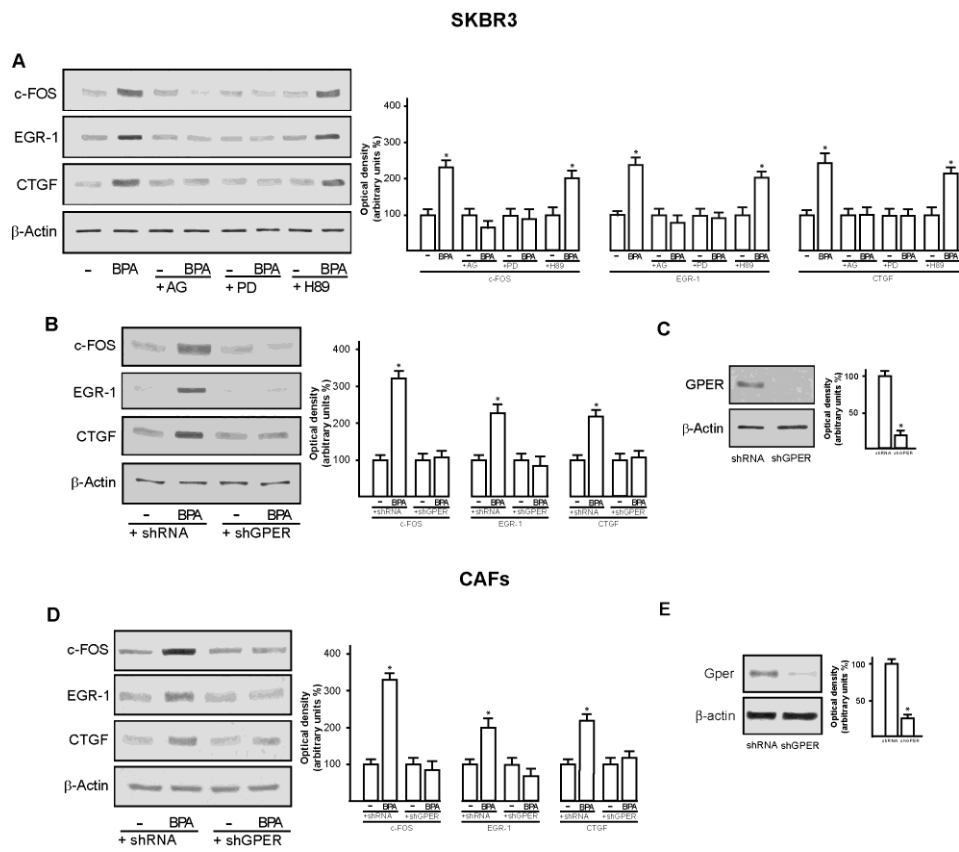


**Figure 3.5.** BPA induces protein levels of GPER target genes through the GPER/EGFR/ERK transduction pathway. (A) Immunoblots showing c-FOS, EGR-1, and CTGF protein expression in SKBR3 cells treated with vehicle or 1  $\mu$ M BPA alone or in combination with 10  $\mu$ M AG1478, PD, or H89 (inhibitors of EGFR, MEK, and PKA respectively). (B) Protein levels of c-FOS, EGR-1, and CTGF in SKBR3 cells transfected with shRNA or shGPER and treated with vehicle or 1  $\mu$ M BPA for 6 hr. (C) Efficacy of GPER silencing in SKBR3 cells. (D) Expression of c-FOS, EGR-1, and CTGF protein in CAFs transfected with shRNA or shGPER and treated with vehicle or 1  $\mu$ M BPA for 6 hr. (E) Efficacy of GPER silencing in CAFs. Graphs show densitometric analyses of the blots normalized to  $\beta$ -actin; values represent the mean  $\pm$  SD of three independent experiments. \* $p < 0.05$  compared with vehicle.

### 3.1.3 BPA induces cell proliferation and migration through GPER

The aforementioned results were recapitulated in the complex physiologic responses such as cell proliferation and migration. The proliferative effects observed in both SKBR3 cells and CAFs after 5-day treatment with BPA were cancelled when GPER expression was silenced by shGPER (Figure 3.6 A,B).

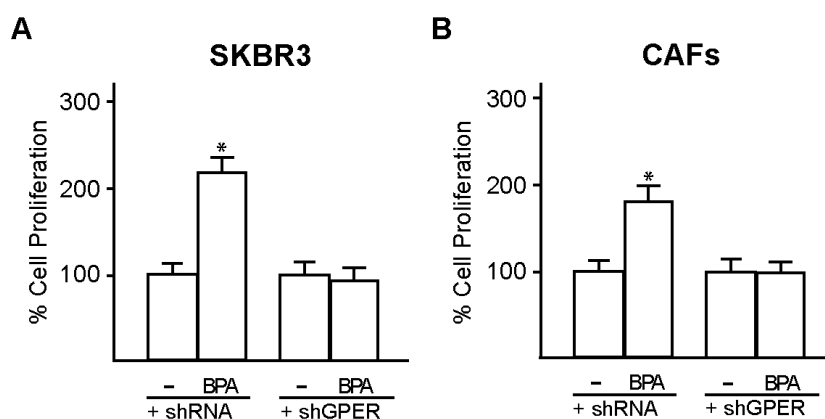


**Figure 3.6.** Induction of proliferation in SKBR3 cells and CAFs. Proliferation in SKBR3 cells (A) and CAFs (B) treated with vehicle (–) or 1  $\mu$ M BPA for 5 days after silencing GPER expression. Values shown represent the mean  $\pm$  SD percent of vehicle control of three independent experiments, each performed in triplicate.  $p < 0.05$  compared with vehicle.

Moreover, in wound-healing assays in CAFs, migration induced by BPA was abolished by knocking down GPER expression (Figure 3.7).

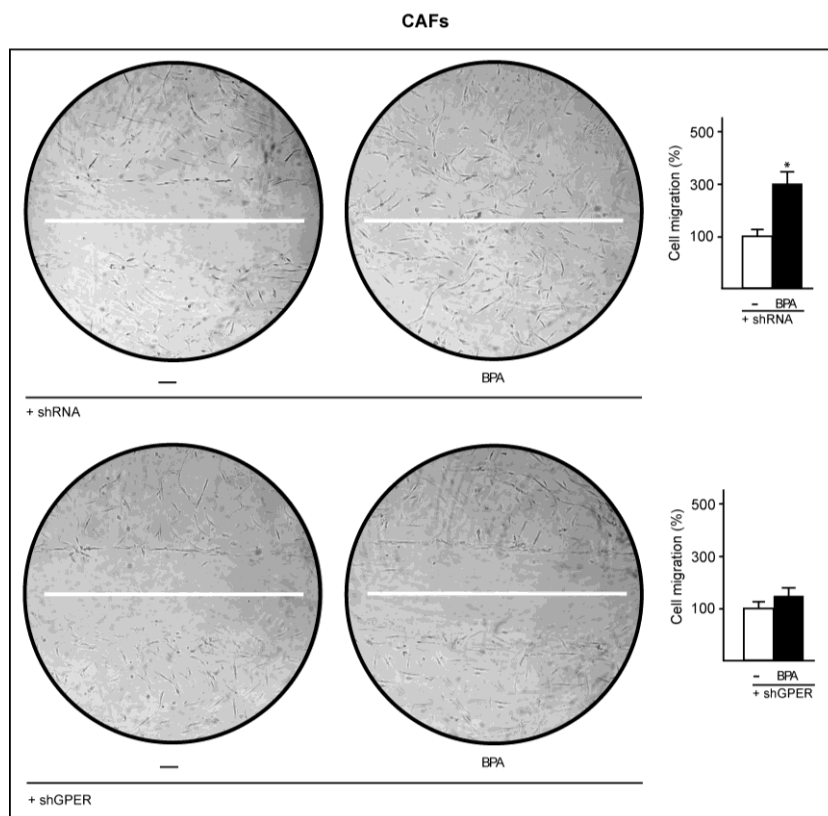


**Figure 3.7.** BPA induces migration of CAFs. Migration in CAFs treated with vehicle or 1  $\mu$ M BPA for 48 hr after silencing GPER expression. Values shown represent the mean  $\pm$  SD percent of vehicle control of three independent experiments, each performed in triplicate. \* $p < 0.05$  compared with vehicle.

In addition, to evaluate whether the treatment of CAFs with BPA could induce the migration of tumor cells through secreted factor(s), we performed wound-healing assays in SkBr3 cells cultured with conditioned medium from CAFs. Interestingly, the migration of SkBr3 cells was not evident after silencing GPER or CTGF expression in CAFs (Figure 3.8). Overall, these findings demonstrate that BPA induces stimulatory effects as GPER agonist in both ER-negative SKBR3 breast cancer cells and CAFs.

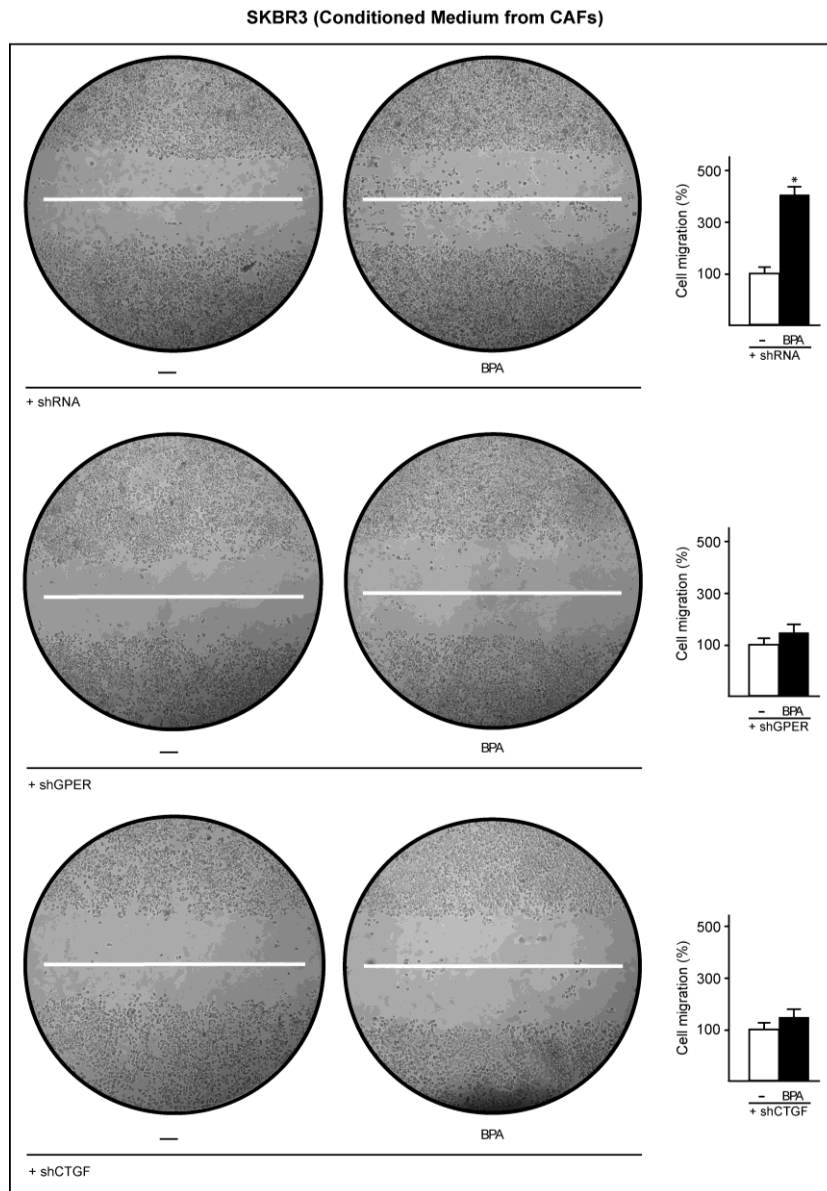
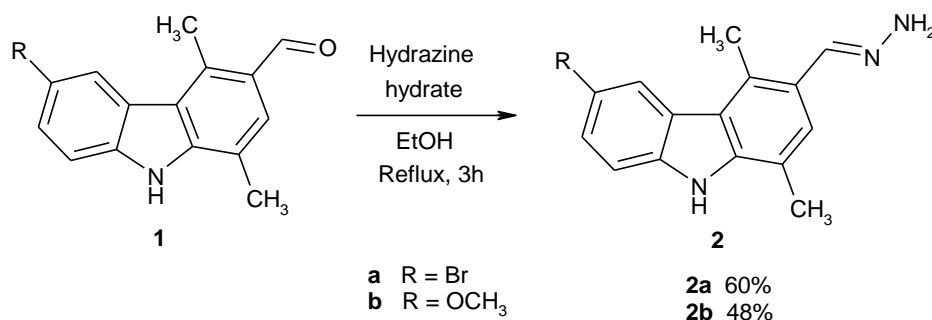


**Figure 3.8** Induction of migration of SKBR3 cells through the stimulation of CAFs with BPA. Migration in SKBR3 cells cultured in conditioned medium from CAFs with silenced expression of GPER and CTGF. Values shown represent the mean  $\pm$  SD percent of vehicle control of three independent experiments, each performed in triplicate. \* $p < 0.05$  compared with vehicle

## 3.2 Carbohydraz (2a) as a new selective GPER ligand

### 3.2.1 Synthesis of Carbohydraz (2a)

The starting 6-bromo-1,4-dimethyl-9H-carbazole-3-carbaldehyde (1) was prepared by a known procedure (Vehar B. et al. 2011). The synthesis of (6-bromo-1,4-dimethyl-9H-carbazol-3-yl-methylene)-hydrazine, referred to as Carbohydraz (2a), and its analogue 2b was depicted in Scheme 1.



*Scheme 1.* Synthesis of Carbohydraz (2a) and of 2b.

This is a convenient modification of the Wolff-Kishner (Wolff L. 1912) reduction and requires the heating of the aldehydic compound 1 with hydrazine hydrate in absolute ethanol by one-pot reaction. The desired hydrazines 2 were obtained in good yield (48-60%). From reaction of 1a was also isolated, as a product, bis-carbazole 3 (yield of 15%).

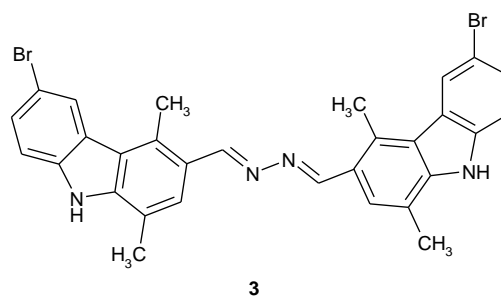


*Figure 3.9* N,N'-bis-(6-bromo-1,4-dimethyl-9H-carbazol-3-yl-methylene)-hydrazine (3).



### 3.2.2 Docking simulation

Several studies (Lappano R. et al 2012a, Dennis M.K. et al 2011) described the GPER binding pocket as a deep cleft in the protein core, surrounded by both hydrophobics and polar residues belonging to transmembrane helices TM III, TM V, TM VI and TM VII. Using a previously tested GPER molecular model as target (Lappano R. et al. 2010), docking simulations confirmed a good affinity of the selective agonist G-1 for the protein, as previously demonstrated both in silico and in vitro (Bologa C.G. et al. 2006). Subsequently, we performed a docking simulation of the novel compounds, Carbohydraz (2a) and 2b, for GPER using the same settings and parameters as used for G-1. Both molecules were positioned within the GPER binding site (Figure 3.10 A-B), similarly to G-1 (Figure 3.10 C-D). Particularly, the bromine atom of Carbohydraz (2a) is positioned about 2.9Å from the nitrogen atom of H307, which is a residue belonging to helix TM VII. The primary amine of Carbohydraz (2a) forms a hydrogen bond with N118 (TM II), while the carbazole moiety forms hydrophobic interactions with V116, L119, M133, F206 and F208, which contribute to stabilize the complex.

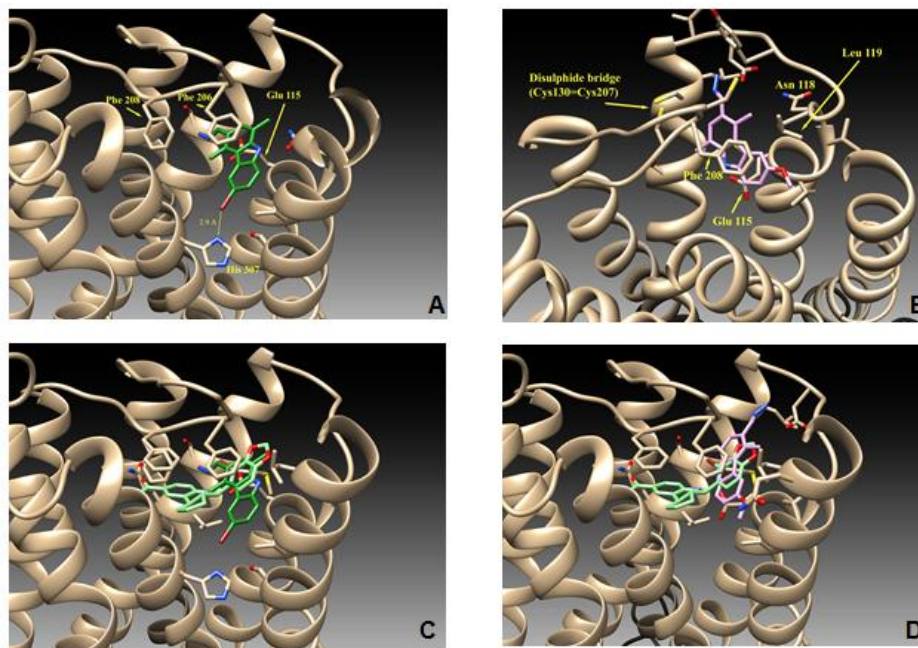


**Figure 3.10** Ribbon representation of GPER (drawn in tan) bound to different compounds. Panel A reports the binding mode of Carbhdyraz (2a), drawn as dark green sticks. A yellow line connects the bromine to the histidine indolic nitrogen atom. In Panel B the compound 2b is drawn in purple. The G-1 moiety is drawn in light green and superposed to Carbhdyraz (2a) in Panel C and to moiety (2b) in Panel D.

The hydrazinic group of Carbhdyraz (2a) is in a favourable position to form hydrogen bonds with the carboxyl group of E115 and the hydroxyl group of C207. It should be noted that the functionalization of the carbazole nucleus in position 6 with a bromine present in Carbhdyraz (2a) could be strategic for the affinity with GPER. In fact, the substitution of Br with OCH<sub>3</sub> in the same position (2b) could determine a 180° rotation of the carbazole ring and a subsequent reduction of interaction between this compound and GPER helices TM I and TM VII.

### ***3.2.3 Carbhydraz induces ERK 1/2 phosphorylation through GPER in breast cancer cells***

In order to verify the results obtained by docking simulation regarding the potential of the two novel synthesized compounds to potentially interact with GPER, we evaluated in ER-negative SkBr3 breast cancer cells the ERK1/2 phosphorylation, which is known to be a hallmark of ligand GPER activation (Maggiolini M. et al. 2004, Lappano et al. 2012a). As in dose-response studies only the compound referred to as Carbhydraz (2a) induced ERK1/2 phosphorylation (Figure 3.11 A-B), we aimed to determine whether this effect occurs through GPER. To this end, we knocked-down GPER expression in SkBr3 cells by a shGPER, which abrogated the ability of Carbhydraz (2a) to induce ERK1/2 activation (Figure 3.11 C-D). Taken together, these data suggest that Carbhydraz triggers ERK1/2 phosphorylation through GPER, confirming the findings obtained by docking simulation.

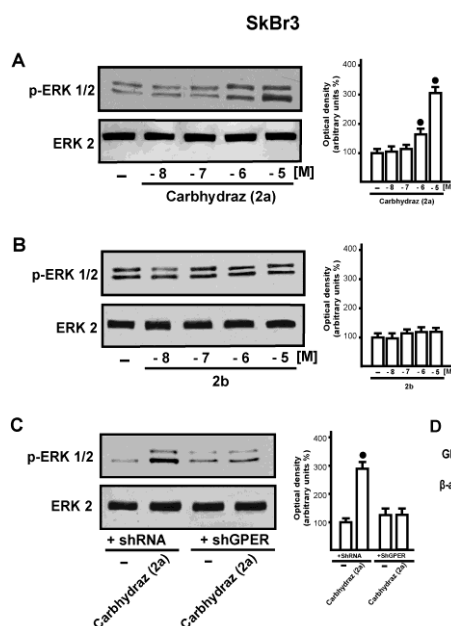


**Figure 3.11.** Carbohydraz (2a) activates ERK1/2 in a GPER-dependent manner. (A-B) ERK1/2 activation in SkBr3 cells treated for 15 min with increasing concentrations of Carbohydraz (2a) or 2b. (C) ERK1/2 activation in SkBr3 cells transfected with shRNA or shGPER and then treated for 15 min with vehicle (–) or 10  $\mu$ M Carbohydraz (2a). Side panels show densitometric analysis of the blots normalized to ERK2. (D) Efficacy of GPER silencing. Each data point represents the mean  $\pm$ SD of three independent experiments. (●) indicate  $p < 0.05$  for cells receiving vehicle (–) versus treatment.

### 3.2.4 Carbohydraz (2a) does not activate ER $\alpha$

To further evaluate whether the synthesized compounds might be able to activate the classical ER $\alpha$ , we transiently transfected an ER reported gene in MCF7 breast cancer cells, which express ER $\alpha$  and not ER $\beta$  as judged by RT-PCR (data not shown). Only E2 transactivated the endogenous ER $\alpha$  in MCF7 cells demonstrating that Carbohydraz (2a) is selective for GPER, since did not exhibit activating properties for ER $\alpha$  (Figure 3.12).

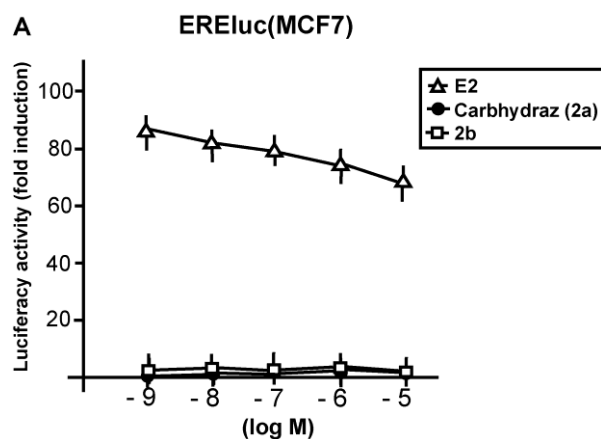


**Figure 3.12** Carbhydraz (2a) and 2b do not activate ER $\alpha$ . MCF7 cells were transfected with an ER luciferase reporter gene along with the internal transfection control Renilla Luciferase and treated with increasing concentrations (logarithmic scale) of E2, Carbhydraz (2a) and 2b. The normalized luciferase activity values of cells treated with vehicle were set as 1-fold induction, upon which the activity induced by treatments was calculated. Each data point represents the mean  $\pm$  SD of three experiments performed in triplicate.

### 3.3 Isolation & Identification of GPER by Mass spectrometry

#### 3.3.1 Isolation of GPER

In the last few years, several studies have been directed towards GPER in order to better understand its role in different cell contexts (Maggiolini M. and Picard D., 2010), however, some information about this receptor, such as the complete structure and its behaviour in breast cancer cells are now poorly understood. In this regard, we tried mass spectrometry-based proteomic approach toward GPER characterization. Initially, we started with developing a new protocol to isolate and enrich GPER from complex mixture of proteins. Therefore, we extracted protein samples from breast cancer cells and then we subjected these samples to a spin column containing hydroxyapatite resin. We hypothesized that hydroxyapatite may be a good choice for isolation and enrichment of GPER on the basis of previously published reports (Fonslow BR 2012, Prossnitz ER 2007).

Thereafter, the bound proteins were eluted from the hydroxyapatite resin bed and concentrated in speed vac. The concentrated protein sample was further subjected to Western Blotting to confirm the presence of GPER. The protein extracts were resolved on a 10% sodium dodecyl sulfate-polyacrylamide gel and transferred to a nitrocellulose membrane. The blot was incubated with a generic protein (such as milk protein) to bind to any remaining sticky places on the nitrocellulose. A specific antibody against GPER (N-15, SantaCruz Biotechnology, Milan, Italy) was then added to the solution (overnight at 4°C). After rinsing the membrane to remove unbound primary antibody, the membrane was exposed to another antibody (secondary antibody), directed at a species-specific portion of the primary antibody and linked to a reporter enzyme. A sensitive sheet of photographic film was placed against the membrane and the exposure to the light created an image of the antibodies bound to the blot (ECL™ Western Blotting Analysis System, GE Healthcare, Milan, Italy). The immunoblot revealed the presence of GPER, by showing a single band approximately of 42 kDa (Fig. 3.13).

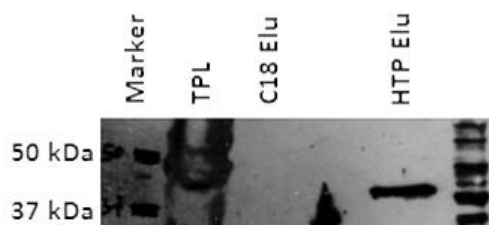
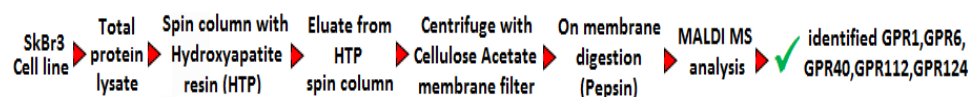


**Figure 3.13.** Figure 3.13 Western Blot analysis confirmed effective GPER isolation

### ***3.3.2 GPER Identification by MALDI-TOF/TOF mass spectrometry***

In order to identify GPER, the sample was processed and prepared for MALDI-TOF/TOF mass spectrometry analysis. The eluate from hydroxyapatite resin was concentrated in speed vac and subjected to

enzymatic digestion. Different proteolytic enzymes such as trypsin, pepsin,  $\alpha$ -chymotrypsin were used for protein digestion. The digested samples were desalted and concentrated with C18 ziptips before MS analysis. Then, the sample was mixed with matrix ( $\alpha$ -cyano-4-hydroxycinnamic acid) and analyzed in AB Sciex TOF/TOF 5800 MS. The spectra were acquired from both MS and MS/MS mode. The acquired spectra were stored on the system. Later, rigorous database search was performed to identify and characterize GPER. After intensive data analysis, the peptide mass fingerprint (PMF) showed the presence of several GPCRs (figure 3.14, 3.15).



## *{MATRIX}* SCIENCE Mascot Search Results

Database : SwissProt (74019 sequences; 26840295 residues)  
 Taxonomy : Homo sapiens (human) (4980 sequences)  
 Timestamp : 31 Jul 2012 at 11:17:27 GMT  
 Top Score : 58 for **P46091**, PROBABLE G PROTEIN-COUPLED RECEPTOR GPR1.

### Probability Based Mowse Score

Score is  $-10 \cdot \log(P)$ , where P is the probability that the observed match is a random event.

Protein scores greater than 49 are significant ( $p < 0.05$ ).

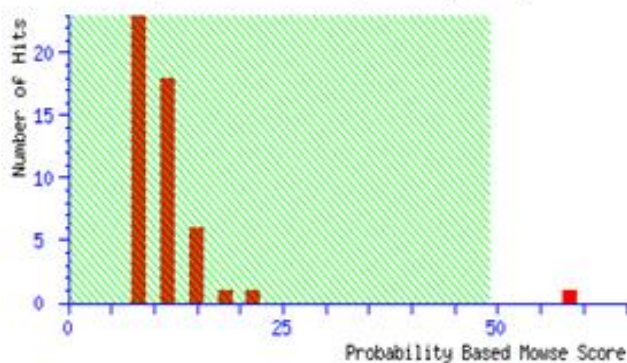


*Figure 3.14.* GPCRs identifications

int of GPR1 (a member of GPCR family)

### Protein View

Match to: P46091; Score: 58  
 PROBABLE G PROTEIN-COUPLED RECEPTOR GPR1.  
 Nominal mass ( $M_r$ ): 41370; Calculated pI value: 6.98  
 NCBI BLAST search of [P46091](#) against nr  
 Unformatted [sequence string](#) for pasting into other applications  
 Taxonomy: [Homo sapiens](#)  
 Variable modifications: Acetyl (K),Acetyl (N-term),Oxidation (M)  
 Cleavage by PepsinA: cuts C-term side of FLWYEQA  
 Number of mass values searched: 56  
 Number of mass values matched: 56  
 Sequence Coverage: 72%

Matched peptides shown in **Bold Red**

```

1 MEDLEETLFE EFENYSYDLD YYSLESDLEE KVQLGVVHWV SLVLYCLAFV
51 LGIPGNAIVI WFTGLKWKKT VTTLWFLNLA IADPIFLLFL PLYISYVAMN
101 FHWPPGIWLC KANSFTAQLN MPASVFPLTV ISLDHYIHLI HPVLSHRHRT
151 LKNSLIVIIIF IWLLASLIGG PALYFRDTVE FNNHTLCYNN FQRHDPDLTL
201 IRHHVLTWVK PIIGYLFPLL TMSICYLCLI PKVKKRTVLI SSRHFWTILV
251 VVVAFVVCWT PYHLFSIWEL TIHNSYSHH VMQAGIPLST GLAFLNSCLN
301 PILYVLISKK FQARFRSSVA EILKYTLWEV SCSGTVSEQL RNSETRNLCCL
351 LETAQ

```

Figure 3.15 Peptide Mass Fingerpr



# Chapter 4

## Discussion

G-protein-coupled receptors (GPCRs) represent the largest class of membrane proteins in the human genome. They are important in the control of fundamental processes such as vision, olfaction, hormone signaling, stress responses as well as nervous system functions. Controlled GPCR expression, localization and signaling are essential for normal physiology as malfunction leads to disease, leading GPCRs as targets for drug discovery. Despite extensive research in structural proteomics, only limited information is available for the three-dimensional structure of GPCRs, as these seven trans-membrane domain (7-TM) receptors are difficult to recover in sufficient quantities from native contexts (Lappano and Maggiolini 2011).

One member of this family, named GPR30/GPER, has largely proven to be a key mediator in the development and progression of several types of tumors, however it can also mediate relevant physiological responses in the reproductive, nervous, endocrine, immune and cardiovascular systems. As it concerns the potential role of GPER in cancer, its expression has been associated with aggressive features of breast, endometrial and ovarian tumors (Filardo E.J. et al. 2006, Smith H.O. et al. 2009). In line with these findings, numerous investigations proved GPER expression and activation in different tumor cells, including breast, endometrial, ovarian,

thyroid, prostate and testicular germ cells (Filardo E.J. et al. 2000, Vivacqua A. et al. 2006, Chevalier N. et al. 2011). Although several GPCR family members, as GPER, control key biological functions in both physiological and pathological conditions, existing drugs that target this receptor superfamily are directed towards only a few members. Consequently, huge efforts are currently underway to develop new GPCR-based drugs, particularly for cancer treatment. Although their overexpression and solubility and consequently the crystallization process result particularly problematic, computer based methods have been increasing successful in identifying the atomic structure of a biological target like a GPCR on the basis of its primary structure (Rosano C. et al. 2012). In this context, the availability of a GPER 3D model allowed us to pursue a “protein-based” approach in order to characterize the potential interaction of different molecules with this receptor (Rosano C. et al. 2012). Moreover, following different approaches (“ligand-based” as well as mixed biomolecular and virtual screening), several GPER natural and synthetic ligands have been identified by several groups (Bologa C.G. et al. 2006, Dennis M.K. et al. 2009; Lappano et al., 2010; Dennis M.K. et al. 2011; Lappano et al., 2012a,b). Ligand binding studies validated the results obtained by molecular modeling and docking simulations. Moreover, functional assays allowed the characterization of the biological effects elicited by numerous compounds through GPER in multiple contexts. In particular, the two well-known ER $\alpha$  ligands and activators 17 $\beta$ -estradiol and estriol, as GPER ligands, showed the ability to activate or inhibit, respectively, GPER signalling (Lappano R. et al. 2010). The ER antagonists tamoxifen and ICI 182,780 displayed a high binding affinity for GPER and surprisingly acted as agonists of this receptor (Maggiolini

M. et al. 2004). In addition a series of natural, synthetic compounds and environmental contaminants, such as Bisphenol A (Thomas and Dong 2006), have been identified and characterized as GPER ligands with either agonist or antagonist properties (Lappano R. et al. 2012b).

In the present study, GPER is involved in the biological action elicited by BPA in breast cancer cells and CAFs, both of which express GPER and lack ERs. Interestingly, we found that in both cell types BPA triggers rapid ERK activation through the GPER/EGFR transduction pathway and induces the expression of genes that characterize estrogenic GPER-mediated signaling (Pandey D.P. et al. 2009). In addition, we determined that BPA stimulates the proliferation and migration of SKBR3 cells and CAFs through GPER. Of note, conditioned medium from BPA-treated CAFs induced the migration of SKBR3 cells, suggesting that BPA may also promote a functional crosstalk between cancer cells and CAFs. These data regarding CAFs are particularly intriguing given that these cells actively contribute to cancer growth and progression even at metastatic sites (Bhowmick N.A. and Moses H.L. 2005).

Moreover, we have designed and synthesized novel carbazole derivatives and performed docking simulations as well as functional assays in order to assess their potential affinity and activity for GPER. In particular, a compound, which we termed Carbohydraz (2a), displayed a high affinity for the receptor in docking simulations. Accordingly, Carbohydraz (2a) showed the capability to trigger in breast cancer cells intracellular molecular signaling, such as ERK phosphorylation, which is known to characterize the ligand-induced activation of GPER. Moreover, Carbohydraz (2a) did not exhibit any activating properties for ER $\alpha$ , suggesting its specificity for GPER. Indeed, the ability of diverse

molecules to bind to and activate both the classical estrogen receptors and GPER made difficult to differentiate the pharmacology of GPER over that of the classical ERs. In this context, Carbohydraz (2a) together with the other previously identified GPER selective ligands, either agonists or antagonists, could contribute to better dissect the distinct functions selectively mediated by each estrogen receptor.

Knowledge of a GPCR structure enables us to gain a mechanistic insight into its function and dynamics, and further aid rational drug design. Despite intensive research carried out over the last three decades, resolving the structural basis of GPCR function is still a major activity. The crystal structures obtained in the last 5 years provide the first opportunity to understand how protein structure dictates the unique functional properties of these complex signalling molecules. However, owing to the intrinsic hydrophobicity, flexibility and instability of membrane proteins, it is still a challenge to crystallize GPCRs, and, when this is possible, it is no longer in its native membrane environment and no longer without modification. Furthermore, the conformational change of the transmembrane  $\alpha$ -helices associated with the structure activation increases the difficulty of capturing the activation state of a GPCR to a higher resolution by X-ray crystallography. On the other hand, solid-state NMR may offer a unique opportunity to study membrane protein structure, ligand binding and activation at atomic resolution in the native membrane environment, as well as described functionally significant dynamics. In this context, the present study focused also on the isolation of GPER from estrogen-sensitive cancer cells by using a combination of Western Blot and MALDI MS.

This could provide the basis for further investigations, based on biochemical, biophysical and molecular techniques, aimed to determine the high-resolution structure of GPER and other GPCRs which revealed to play a key role in cancer development and progression, thus shedding light on structural bases of GPCR allosteric modulation.



## **SECTION 2**

# **Synthesis and biological activity of new half-titanocene derivatives**

## **Chapter 1**

### **Introduction**

#### **1.1 Titanocenes: novel metal based compounds as anticancer drugs**

Although female breast cancer incidence rate began decreasing in the America, breast cancer is still the most common cancer among women worldwide and the second leading cause of cancer death in women, exceeded only by lung cancer (Landis S. H. et al. 1999). According to the American Cancer Society (ACS), there are 232,340 cases diagnosed and 39,620 cases of patients die from breast cancer every year ([www.cancer.org](http://www.cancer.org)). Death rates from breast cancer have been declining since about 1989, mainly resulting from the earlier detection through screening and increased awareness. However, there are still more patients were diagnosed as invasive or advanced breast cancer which request intensive treatments and is associated with poor outcomes. Treatments of breast cancers include surgery, radiotherapy and chemotherapy. Among

the chemotherapeutic agents, Cis-platin (cis-diamminedichloroplatinum II), a metal-based anti-cancer drug (figure 1.1), (Jamieson ER and Lippard SJ 1999, Rosenberg B et al. 1969), is commonly used to inhibit the growth of different types of tumors including breast cancer (Basu and Krishnamurthy 2010, Florea and Busselberg, 2011, Pines et al., 2011).

Cis-platin exerts antitumour activity like classical alkylating agents. In particular, Cis-platin is known to cause DNA damage by forming Pt-DNA adducts at the 1,2-intrastrand crosslink, leading to the activation of various signal transduction pathways (Zeidan et al. 2008, Basu and Krishnamurthy 2010, Florea and Busselberg 2011). However, its exact mechanism of action and specificity are still not well established.

Moreover, like most commonly used chemotherapy drugs, Cis-platin treatment lacks specificity toward tumor cells and its clinical efficacy was limited by side-effects, toxicity and drug resistance (Decatris et al. 2004).

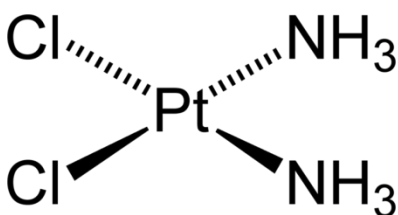


*Figure 1.1.* Cis-platin (cis-diamminedichloroplatinum II)

Therefore, over the last few years several researches have been addressed towards the development of novel metal-based anticancer drugs, with the aim of improving clinical effectiveness, reducing general toxicity and broadening the spectrum of activity (Zanella,A. et al. 2011).



The search for novel metal-based antitumor drugs, other than Pt agents, includes the investigation of the cytotoxic activity of copper (I/II) (Zanella, A. et al 2011) and titanocene (Napoli, M. et al 2011) compounds. In this context, particular attention has been recently devoted to new copper(I) complexes. Some of these were tested for their cytotoxic properties against several human tumor cell lines, such as HL60 (promyelocytic leukemia), MCF7 (breast cancer), HCT-15 (colon cancer), HeLa (cervix cancer), A549 (lung cancer), 2008 (ovarian cancer sensitive to cis platin) and C13 (ovarian cancer resistant to cis-platin) (Napoli M. et al 2011).

A great deal of research has been focused on a variety of transition metal complexes bearing labile cis chlorides or similar ligands. Among the candidate drugs, the pseudotetrahedral metallocene complexes of the type  $(C_5H_5)_2MCl_2$  represent a seemingly logical extension of cis-platin derivatives and have received much attention (Clarke M.J. et al. 1999). These complexes are made up of a metal core consisting of transition metals as Ti, Nb, Mo, etc. The coordination sites of the metal are occupied by two cyclopentadienyl rings ( $C_5H_5$  or Cp) and two labile ligands (i.e., Cl). Köpf-Maier and Köpf (Köpf-Maier, P. et al. 1979) have investigated the antitumor activities of a whole series of metallocene dichloride complexes (varying the transition metal) *in vivo*.

From this research, titanocene dichloride (TDC) exhibited the most promising chemotherapeutic activity among all other metallocenes tested (Dombrowski, K.E. et al. 1986). Consequently, numerous analogues of TDC (figure 1.2) were developed and well-studied, such as titanocene Y.

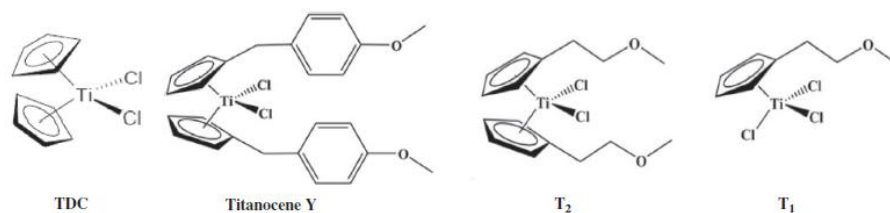


**Figure 1.2** Titanocene dichloride (TDC);bis-[(p-methoxybenzyl) cyclopentadienyl] titaniumdichloride (titanoceneY); bis-cyclopentadienyl – ethenylmethoxyl – titanium dichloride T2 and cyclopentadienyl-ethenylmethoxyltitanium trichloride T1.

In particular, the anti-proliferative activity of titanocene Y and other titanocenes has been studied in 36 human tumor cell lines (Kelter G. et al. 2005). In vitro and in vivo experiments showed that renal cancer is a major target for this novel class of titanocenes, although they showed a significant activity also against ovarian, prostate, cervix, lung, colon and breast tumors (Claffey J. et al..2008).

## 1.2 Aim of the study

On the basis of the aforementioned findings, the aim of this study was the synthesis and the evaluation of the biological activity of novel titanocene derivatives in breast cancer cells.

# Chapter 2

## Materials and methods

### 2.1 Synthesis of new half-titanocene

#### 2.1.1 General

The elemental analyses for C, H, N, were recorded on a ThermoFinnigan Flash EA1112 series and performed according to standard microanalytical procedures.

<sup>1</sup>H NMR, homodecoupled <sup>1</sup>H NMR, <sup>1</sup>H COSY and <sup>13</sup>C NMR spectra were recorded at 298 K on a Bruker Avance 300 Spectrometer operating at 300 MHz (<sup>1</sup>H) and 75 MHz (<sup>13</sup>C) and referred to internal tetramethylsilane. Molecular weights were determined by ESI mass spectrometry. ESI-MS analysis in positive and negative ion mode, were made using a Finnigan LCQ ion trap instrument, manufactured by Thermo Finnigan (San Jose, CA, USA), equipped with the Excalibur software for processing the data acquired. The sample was dissolved in acetonitrile and injected directly into the electrospray source, using a syringe pump, which maintains constant flow at 5 l/min. The temperature of the capillary was set at 220 °C. All manipulations were carried out under oxygen- and moisture-free atmosphere in an MBraun MB200 glove-box. All the solvents were thoroughly deoxygenated and dehydrated under argon by refluxing over suitable drying agents, while NMR deuterated solvents (Euriso-Top products) were kept in the dark over molecular sieves. TiCl<sub>4</sub>, Titanium(IV) chloride tetrahydrofuran complex, Super Hydride (LiBEt<sub>3</sub>H,

1.0 M solution in THF), and all chemicals were obtained from Aldrich chemical Co. and used without further purification.

### 2.1.2 Synthesis of half-titanocene complexes 5a,b

Lithium cyclopentadienide intermediate (1.83mmol) was dissolved in dry THF (20ml) to give a colourless solution.  $TiCl_4$  (18.30mmol) was added at 0°C to give a dark red solution. This was refluxed overnight and then cooled. The solvent was removed under reduced pressure. The remaining residue was extracted with dichloromethane (30ml) and filtered through celite to remove the LiCl. The filtrate was washed twice with hexane (20ml) and then dried under reduced pressure to give a solid.

### 2.1.3 Spectral data

[(4-Methoxybenzyl) cyclopentadienyl]-titanium-trichloride [ $C_5H_4-CH_2-C_6H_4-OCH_3$ ] $TiCl_3$  (5a). Black solid.  $^1H$ NMR (ppm,  $CD_2Cl_2$ , 300 MHz): 3.78 [s, 3H,  $C_5H_4-CH_2-C_6H_4-OCH_3$ ], 4.01 [s, 2H,  $C_5H_4-CH_2-C_6H_4-OCH_3$ ], 6.80 [m, 4H,  $C_5H_4-CH_2-C_6H_4-OCH_3$ ], 6.83–7.01 [d, 4H,  $C_5H_4-CH_2-C_6H_4-OCH_3$ ].  $^{13}C$ NMR (ppm,  $CD_2Cl_2$ , 75 MHz): 55.90 [ $C_5H_4-CH_2-C_6H_4-OCH_3$ ], 45.0 [ $C_5H_4-CH_2-C_6H_4-OCH_3$ ], 114.0–128.70–130.0–132.0–135.90–147.80–158.60 [ $C_5H_4-CH_2-C_6H_4-OCH_3$ ]. Mass (E.I., 70 eV, m/z): 273 [ $L-TiCl-Li$ ]<sup>+</sup>, 186 [ $L$ ]<sup>+</sup>. Calcd for  $C_{13}H_{13}Cl_3OTi$  (%): C, 46.00; H, 3.86. Found (%): C, 46.21; H, 3.84.

[(3,4-Di-methoxybenzyl)-cyclopentadienyl]-titanium-trichloride [ $C_5H_4-CH_2-C_6H_3-(OCH_3)_2$ ] $TiCl_3$  (5b). Brown solid.  $^1H$ NMR (ppm, THF- $d_8$ , 300 MHz): 3.73 [s, 6H,  $C_5H_4-CH_2-C_6H_3-(OCH_3)_2$ ], 3.98 [s, 2H,  $C_5H_4-CH_2-C_6H_3-(OCH_3)_2$ ], 6.29–6.42 [m, 4H,  $C_5H_4-CH_2-C_6H_3-$

(OCH<sub>3</sub>)<sub>2</sub>], 6.71–6.76 [d, 2H, C<sub>6</sub>H<sub>3</sub>–(OCH<sub>3</sub>)<sub>2</sub>], 6.84 [s, 1H, C<sub>6</sub>H<sub>3</sub>–(OCH<sub>3</sub>)<sub>2</sub>]. <sup>13</sup>CNMR (δppm, CD<sub>2</sub>Cl<sub>2</sub>, 75 MHz): 55.50 [C<sub>5</sub>H<sub>4</sub>–CH<sub>2</sub>–C<sub>6</sub>H<sub>3</sub>–(OCH<sub>3</sub>)<sub>2</sub>], 36.80 [C<sub>5</sub>H<sub>4</sub>–CH<sub>2</sub>–C<sub>6</sub>H<sub>3</sub>–(OCH<sub>3</sub>)<sub>2</sub>], 112.20–113.30–115.40–120.80–122.50–132.80–137.10–149.20–150.30 [C<sub>5</sub>H<sub>4</sub>–CH<sub>2</sub>–C<sub>6</sub>H<sub>3</sub>–(OCH<sub>3</sub>)<sub>2</sub>]. Mass (E.I., 70 eV, m/z): 286 [L-Ti-Na]<sup>+</sup>. Calcd for C<sub>14</sub>H<sub>15</sub>Cl<sub>3</sub>O<sub>2</sub>Ti (%): C, 45.51; H, 4.09. Found (%): C, 45.91; H, 4.04.

(4-(N,N-Dimethylbenzylidene)-cyclopentadienyl)-titanium-trichloride [C<sub>5</sub>H<sub>4</sub>–CH<sub>2</sub>–C<sub>6</sub>H<sub>4</sub>–N(CH<sub>3</sub>)<sub>2</sub>]<sub>2</sub>TiCl<sub>3</sub>(5c). Red solid. <sup>1</sup>HNMR (δppm, THF, 300 MHz): 2.98 [s, 6H, C<sub>5</sub>H<sub>4</sub>–CH<sub>2</sub>–C<sub>6</sub>H<sub>4</sub>–N(CH<sub>3</sub>)<sub>2</sub>], 3.89 [s, 2H, C<sub>5</sub>H<sub>4</sub>–CH<sub>2</sub>–C<sub>6</sub>H<sub>4</sub>–N(CH<sub>3</sub>)<sub>2</sub>], 6.45–6.67 [m, 4H, C<sub>5</sub>H<sub>4</sub>–CH<sub>2</sub>–C<sub>6</sub>H<sub>4</sub>–N(CH<sub>3</sub>)<sub>2</sub>], 7.10–7.31 [d, 4H, C<sub>5</sub>H<sub>4</sub>–CH<sub>2</sub>–C<sub>6</sub>H<sub>4</sub>–N(CH<sub>3</sub>)<sub>2</sub>]. <sup>13</sup>CNMR (δppm, THF- d<sub>8</sub>, 75 MHz): 41.70 [C<sub>5</sub>H<sub>4</sub>–CH<sub>2</sub>–C<sub>6</sub>H<sub>4</sub>–N(CH<sub>3</sub>)<sub>2</sub>], 33.10 [C<sub>5</sub>H<sub>4</sub>–CH<sub>2</sub>–C<sub>6</sub>H<sub>4</sub>–N(CH<sub>3</sub>)<sub>2</sub>], 115.90–117.60–119.20–128.70–130.70–136.0–137.10 [C<sub>5</sub>H<sub>4</sub>–CH<sub>2</sub>–C<sub>6</sub>H<sub>4</sub>–N(CH<sub>3</sub>)<sub>2</sub>]. Mass (E.I., 70 eV, m/z): 371 [L-TiCl<sub>3</sub>-Na]<sup>+</sup>. Calcd for C<sub>14</sub>H<sub>16</sub>Cl<sub>3</sub>NTi (%): C, 47.70; H, 4.57. Found (%): C, 47.92; H, 4.17; N, 3.79.

(Benzyl)-cyclopentadienyl-titanium-trichloride [C<sub>5</sub>H<sub>4</sub>–CH<sub>2</sub>–C<sub>6</sub>H<sub>5</sub>]<sub>2</sub>TiCl<sub>3</sub>(5d). Red solid. <sup>1</sup>HNMR (δppm, THF- d<sub>8</sub>, 300 MHz): 4.06 [s, 2H, C<sub>5</sub>H<sub>4</sub>–CH<sub>2</sub>–C<sub>6</sub>H<sub>5</sub>], 6.33–6.45 [m, 4H, C<sub>5</sub>H<sub>4</sub>–CH<sub>2</sub>–C<sub>6</sub>H<sub>5</sub>], 7.22–7.24 [m, 5H, C<sub>5</sub>H<sub>4</sub>–CH<sub>2</sub>–C<sub>6</sub>H<sub>5</sub>]. <sup>13</sup>CNMR (δppm, THF- d<sub>8</sub>, 75 MHz): 36.70 [C<sub>5</sub>H<sub>4</sub>–CH<sub>2</sub>–C<sub>6</sub>H<sub>5</sub>], 110.90–115.10–122.60–128.0–128.60–140.60 [C<sub>5</sub>H<sub>4</sub>–CH<sub>2</sub>–C<sub>6</sub>H<sub>5</sub>]. Mass (E.I., 70 eV, m/z): 242 [L-Ti-K]<sup>+</sup>, 163 [L-Li]<sup>+</sup>. Calcd for C<sub>12</sub>H<sub>11</sub>Cl<sub>3</sub>Ti (%): C, 46.58; H, 3.58. Found (%): C, 46.17; H, 3.32.

(2,4-Dimethoxybenzyl)-cyclopentadienyl-titanium-trichloride [C<sub>5</sub>H<sub>4</sub>–CH<sub>2</sub>–C<sub>6</sub>H<sub>3</sub>–(OCH<sub>3</sub>)<sub>2</sub>]<sub>2</sub>TiCl<sub>3</sub>(5e). Brown solid. <sup>1</sup>HNMR (δppm, THF- d<sub>8</sub>, 300 MHz): 3.72–3.76 [s, 6H, C<sub>5</sub>H<sub>4</sub>–CH<sub>2</sub>–C<sub>6</sub>H<sub>3</sub>–(OCH<sub>3</sub>)<sub>2</sub>], 3.90

[s,2H,C5H4-CH2-C6H3-(OCH3)2],6.28-6.29[m,4H,C5H4-CH2-C6H3-(OCH3)2],6.40-6.46[d,2H,C 5H4-CH2-C6H3-(OCH3)2]7.01[s,1H,C5H4-CH2-C6H3-(OCH3)2].<sup>13</sup>CNMR (dppm,CD<sub>2</sub>Cl<sub>2</sub>,75MHz):55.40-55.50[C5H4-CH2-C6H3-(OCH3)2],31.80 [C5H4-CH2-C6H3-(OCH3)2],99.10-104.80-116.60-121.90-123.30-131.40-137.60-159.20 161.0[C5H4-CH2-C6H3-(OCH3)2].Mass (E.I.,70eV,m/z):286 [L-Ti- Na]<sup>+</sup>.Calcd for C<sub>14</sub>H<sub>15</sub>Cl<sub>3</sub>O<sub>2</sub>Ti(%):C,45.51;H,4.09.Found (%):C,45.91;H,4.04.

(2,4,6-Tri-methoxybenzyl)-cyclopentadienyl-titanium-trichloride [C5H4-CH2-C6H2-(OCH3)3]TiCl<sub>3</sub>(5f).Black solid. <sup>1</sup>HNMR (dppm,THF,300 MHz):3.72-3.77 [s,9H,C5H4-CH2-C6H2-(OCH3)3],3.90 [s,2H,C5H4-CH2-C6H2-(OCH3)3],6.30-6.34[m,4H,C5H4-CH2-C6H2-(OCH3)3],6.47[s,2H,C5H4-CH2-CH2-(OCH3)3]. <sup>13</sup>CNMR (dppm,THF- d<sub>8</sub>,75MHz):54.70 [C5H4-CH2-C6H2-(OCH3)3],31.05 [C5H4-CH2-C6H2-(OCH3)3],98.40-104.0-115.80-122.50-130.60-137.70-158.30-160.30[C5H4-CH2-C6H2-(OCH3)3].Mass (E.I.,70eV,m/z):317 [L-Ti-Na]<sup>+</sup>.Calcd for C<sub>15</sub>H<sub>17</sub>Cl<sub>3</sub>O<sub>3</sub>Ti(%):C,45.09;H,4.29.Found (%):C,45.39;H,4.24.

## 2.2 Cell cultures

MCF7 breast cancer cells were maintained in DMEM/F-12 supplemented with 10% fetal bovine serum (FBS), 100 mg/ml penicillin/streptomycin and 2mM L-glutamine (Invitrogen,Gibco,Milan,Italy). SkBr3 breast cancer cells were cultured in RPMI-1640 medium supplemented with 10% FBS,100 mg/ml penicillin/streptomycin and 2mM L-glutamine (Invitrogen,Gibco,Milan,Italy). Cells were switched to medium without

serum the day before experiments and thereafter treated in medium supplemented with 1% FBS.

### **2.3 MTT assay**

Cells were switched to medium without serum the day before experiments and thereafter treated in medium supplemented with 1% FBS. The effects of each compound on cell viability were determined with the MTT [3-(4,5-dimethylthiazol-2-yl)-2,5-diphenyltetrazolium bromide] assay, which is based on the conversion of MTT to MTT-formazan by mitochondrial enzyme. Cells were seeded in quadruplicate in 96-well plates in regular growth medium and grown until 70–80% confluence. Cells were washed once they had attached and then treated with 10  $\mu$ M each compound for indicated time (for 1 day up to 5 days). Relative cell viability was determined by MTT assay according to the manufacturer's protocol (Sigma–Aldrich, Milan, Italy). Mean absorbance for each drug dose was expressed as a percentage of the control untreated well absorbance and plotted versus drug concentration. IC<sub>50</sub> values represent the drug concentrations that reduced the mean absorbance at 570 nm to 50% of those in the untreated control wells.





# Chapter 3

## Results

### 3.1 Synthesis of titanocene derivatives

In order to investigate the potential cytotoxic activity of titanocene derivatives, we have synthesized and characterized some half-titanocenes compounds (Figure 3.1) by nuclear magnetic resonance (NMR), mass spectroscopy and elemental analysis.

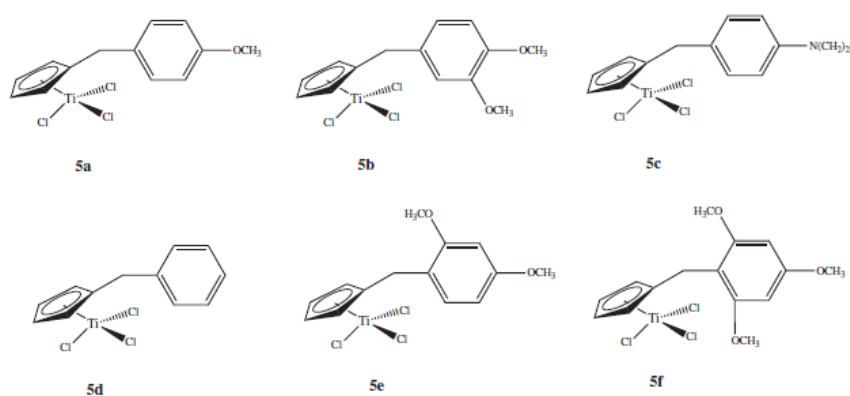
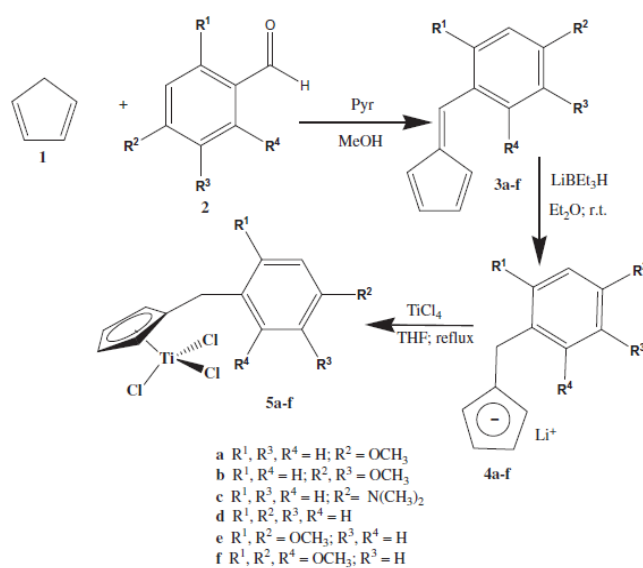


*Figure 3.1.* Structures of synthesized complexes.

All these complexes contain different substituents on the Cp ligands, able to stabilize the titanium cation by intramolecular coordination. Preliminary cytotoxic studies of these titanium based compounds have been carried out:

- compound 5a was synthesized in order to verify whether the activity was higher for half-titanocene Y than titanocene Y, as it was for the bis-cyclopentadienyl-ethenylmethoxyl-titanium dichloride T2 and cyclopentadienyl-ethenylmethoxyl-titanium trichloride T1;
- compounds 5b, 5e and 5f bear in different positions methoxyl groups, which may make ligands much more coordinating, except for the methoxyl in position 4;
- compound 5d has no substituents on the aryl, but the phenyl is able to coordinate to titanium. Finally, the dimethylamino group in position 4 of the aryl moiety of 5c has a strong capability to bond metal-cation.

The synthesis of complexes was carried out according to Scheme 1.



**Scheme 1.** Synthetic route for the preparation of ligands and half-titanocene complexes 5 a–f.

The syntheses of proligands fulvene were carried out as performed by Tacke, M. et al. 1987, whereas (2,4-dimethoxyphenyl) fulvene was synthesized in good yield according to literature method (Claffey J. et al. 2008) starting from 2,4-dimethoxy benzaldehyde.

Hydrolysis stability of the six half-titanocene complexes (5a–f in figure 3.1) has been determined in aqueous solution, 90% DMSO by  $^1\text{H NMR}$  spectroscopy, in order to correlate the chemical stability and coordination chemistry of these complexes with their observed cytotoxic activity. Since we can expect that rapid hydrolysis of leaving group ( $-\text{Cl}$ ) and cyclopentadienyl ligands could give way to biologically inactive species, active species could be generated if the Cp rings remain metal bound.

Hydrolysis of aromatic rings of 5a–f was evaluated by integration of two signals of protons of cyclopentadienyl bonded to metal, as to newly formed multiplet of substituted cyclopentadiene. Table 1 reports the results of our hydrolysis tests.

**Table 1**  
Hydrolysis results of 5a–f complexes in DMSO/D<sub>2</sub>O solution at rt followed by  $^1\text{H NMR}$

Complex	% Cp ring hydrolysis			
	5 min	4 h	8 h	24 h
5a	<1	<1	<1	<5
5b	<1	<1	<1	<5
5c	<1	<1	<5	17
5d	9	24	40	41
5e	<1	<1	<1	<5
5f	<1	<1	<1	<5

**Table 1** Hydrolysis results of 5a–f complexes in DMSO/D<sub>2</sub>O solution at rt followed by  $^1\text{H NMR}$ .

The complexes that show the highest hydrolytic stability are 5a, 5b, 5e and 5f. In particular, the cyclopentadienyl rings of complexes are hydrolyzed only for less than 5% after 24h, whereas complexes 5c and 5d are hydrolyzed for 17 % and 41%, respectively.

These data provide sufficient evidence that the presence of coordinating groups on the aryl substituent of the cyclopentadienyl is effective for the stabilization of the complexes. Therefore, these coordinating groups might be fundamental to increase, if active, their biological effectiveness.

### **3.2 New half-titanocene derivatives inhibit breast cancer cell growth**

In order to investigate the effects on cancer cell proliferation of the novel synthesized compounds, we treated for 5 days MCF7 and SkBr3 breast cancer cells with each compound. Cells were also exposed to cis-platin in order to compare the anticancer effects of the complexes to this well-known chemotherapeutic. It should be noted that by using the compounds mentioned above, SkBr3 cells resulted to be more responsive to the treatment compared to MCF7 cells. Among all tested compounds, 5d, 5e and 5f elicited repressive effects on the proliferation of both cell lines (figure 3.4).

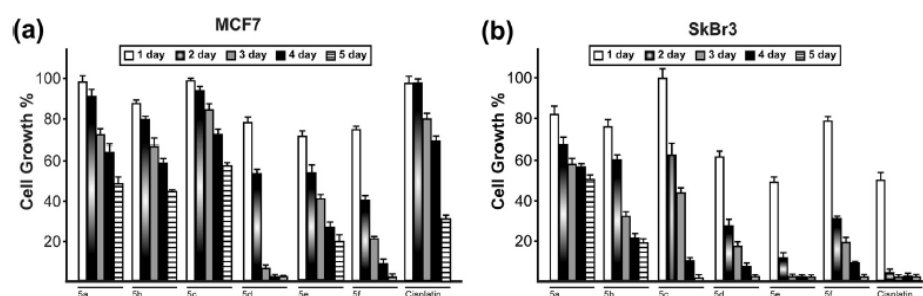


**Figure 3.2** Evaluation of growth responses to 10  $\mu$ M of 5 a–f in MCF7 (a) and SkBr3 (b) breast cancer cells, as determined by using the MTT assay. Cell viability was expressed as the percentage of cells treated with the different compounds respect to cells treated with vehicle. Cells ( $5-8 \times 10^4$  ml) were treated for 1 day up to 5 days, as indicated.

In particular, 5d strongly decreased the viability of MCF7 cells after 3 days of treatment, whereas 5e showed the highest antitumor activity on SkBr3 cells after a 2 days exposure, being the most active compound on this cell line. In particular, 5d, 5e and 5f showed a strongest cytotoxic effect on MCF7 than Cis-platin. Moreover 5e showed a similar cytotoxic activity on SkBr3 compared to cis-platin.



# Chapter 4

## Discussion

Cis-platin is a metal-based anti-cancer drug (Rosenberg et al.1969) which is considered one of the most efficient drugs for the treatment of certain types of cancer, including breast, testicular, ovarian, cervical, head and neck, and small cell lung cancers (Basu A. and Krishnamurthy 2010, Florea and Busselberg 2011, Pines et al. 2011). However, drug toxicity and resistance limit its utilization for a broad range of diseases. Therefore, in recent years, a growing interest was focused on the development of nonplatinum-based anticancer therapeutics. The main goal was to increase the variety of potential drugs, which may lead to higher activity enabling the administration of lower doses, target different types of tumour cells, better selectivity and lower toxicity (Koleros E. et al. 2010). Non-platinum complexes may introduce numerous options for coordination numbers and geometries, oxidation states, affinity for certain types of biological ligands, and may operate by different mechanisms. Among the candidate drugs, the pseudotetrahedral metallocene complexes of the type  $(C_5H_5)_2MCl_2$  (M= Ti, V, Nb, Mo, Re) represent a seemingly logical extension of Cis-platin derivatives and have received much attention (Clarke M.J. et al. 1999). These compounds belong to a relatively new class of small hydrophobic organometallic anticancer agents that exhibit antitumour activities against diverse cancer cell lines, such as leukemia,

melanoma colon, lung and renal tumor cells (Zanella A. et al. 2011, Napoli M. et al. 2011, Clarke M.J. et al. 1979). Titanocene dichloride (TDC), is the most widely studied metallocene compound as cytotoxic anticancer agent. In particular, it can selectively kill cancer cells and was used in phase I and II clinical trials (Christodoulou C. V. et al. 1998, Desoize B. 2004, Caruso F. and Rossi M. 2004, Kröger N. et al. 2000). However, the efficacy of TDC in phase II clinical trials in patients with metastatic renal cell carcinoma (Lümmen G. et al. 1998) or metastatic breast cancer (Kröger N. et al. 2000) was too low to be pursued. As titanium is present, in the form of a whitening pigment, in many biomaterials, such as in food, it is not unreasonable to conceive that it may be incorporated into drugs and into living systems, without showing high toxicity (Peri D. and Tshuva E. Y. 2009). In this context, we synthesized a series of novel titanocene-complexes and evaluated their growth regulatory effects in MCF7 and SkBr3 breast cancer cells. Among these compounds, that showed moderate to high antitumor activity, the strongest anti-proliferative activity against MCF7 cells was displayed especially by 5d, whereas 5e elicited relevant repressive effects on SkBr3 cells. Hence, the capability of these compounds to elicit inhibitory effects on cancer cell growth could be taken into account towards novel pharmacological approaches in cancer therapy. Therefore, further experiments would be helpful to investigate the molecular mechanism involved.



# References

- Abramoff M.D., Magalhaes P.J., Ram S.J.** *Image processing with ImageJ*. *Biophotonics Int*, 11(7): 36–42, 2004.
- Aebersold R., Mann M.** *Mass spectrometry-based proteomics*. *Nature*, 422, 2003.
- Aebersold, R., and Goodlet, D. R..** *Mass Spectrometry in Proteomics*. *Chemical Reviews*, Vol. 101, No. 2, p. 269-295 2001.
- Albanito L., Lappano R., Madeo A., Chimento A., Prossnitz E.R., Cappello A.R., Dolce V., Abonante S., Pezzi V., Maggiolini M.** *G-protein-coupled receptor 30 and estrogen receptor- $\alpha$  are involved in the proliferative effects induced by atrazine in ovarian cancer cells*. *Environ Health Perspect* 116:1648–1655, 2008a.
- Albanito L., Madeo A., Lappano R., Vivacqua A., Rago V., Carpino A., Oprea T.I., Prossnitz E.R., Musti A.M., Andò S., Maggiolini M.** *G protein-coupled receptor 30 (GPR30) mediates gene expression changes and growth response to 17 $\beta$ -estradiol and selective GPR30 ligand G-1 in ovarian cancer cells*. *Cancer Res*, 67: 1859–1866 2007.
- Albanito L., Sisci D., Aquila S., Brunelli E., Vivacqua A., Madeo A., Lappano R., Pandey D. P., Picard D., Mauro L., Ando` S., Maggiolini M.** *EGF induces GPR30 expression in estrogen receptor negative breast cancer cells*. *Endocrinology*, 149: 3799–3808, 2008b.
- Ali S., Coombes R.C.** *Estrogen receptor alpha in human breast cancer: occurrence and significance*. *J Mammary Gland Biol Neoplasia*, (3): 271-81, 2000.

- Alyea RA; Laurence SE; Kim SH; Katzenellenbogen BS; Katzenellenbogen JA; and Watson CS.** *The roles of membrane estrogen receptor subtypes in modulating dopamine transporters in PC-12 cells.* J Neurochem., 106(4): 1525–1533 2008.
- Andersen H.R., Andersson A.M., Arnold S.F., Autrup H., Barfoed M., Beresford N.A., Bjerregaard P., Christiansen L.B., Gissel B., Hummel R., Jorgensen E.B., Korsgaard, B., Le Guevel R., Leffers H., McLachlan J., Moller A., Nielsen J.B., Olea, N., Oles-Karasko A., Pakdel F., Pedersen K.L., Perez P., Skakkeboek N.E., Sonnenschein C., Soto A.M., et al.** *Comparison of short-term estrogenicity tests for identification of hormone-disrupting chemicals.* Environ Health Perspect, 107 (Suppl. 1): 89–108, 1999.
- Arias-Pulido H., Royce M., Gong Y., Joste N., Lomo L., Lee S.J., Chaher N., Verschraegen C., Lara J., Prossnitz E.R., Cristofanilli M.** *GPR30 and estrogen receptor expression: new insights into hormone dependence of inflammatory breast cancer.* Breast Cancer Res Treat, 123:51-58, 2010.
- Basu A., Krishnamurthy S.** *Cellular Responses to Cisplatin-Induced DNA Damage .* J Nucleic Acids, 2010: 201367, 2010.
- Bhowmick NA, Moses HL.** *Tumor-stroma interactions.* Curr Opin Genet Dev, 15:97–101, 2005.
- Bockaert, J., Pin J.P.** *Molecular tinkering of G protein-coupled receptors: an evolutionary success.* EMBO J., 18:1723–1729 1999.
- Bologa, C.G., Revankar, C.M., Young, S.M., Edwards, B.S., Arterburn, J.B., Kiselyov, A.S., Parker, M.A., Tkachenko, S.E., Savchuck, N.P., Sklar, L.A., Oprea, T.I., Prossnitz, E.R.** *Virtual and biomolecular screening converge on a selective agonist for GPR30.* Nat Chem Biol, 4:207–12 2006.

- Bouskine A., Nebout M., Brücker-Davis F., Benahmed M., Feniche P.** *Low doses of Bisphenol A promote human seminoma cell proliferation by activating PKA and PKG via a membrane G-protein-coupled estrogen receptor.* Environ Health Perspect, 117: 1053-1058, 2009.
- Calafat A.M., Kuklennyik Z., Reidy J.A., Caudill S.P., Ekong J., Needham L.L.** *Urinary concentrations of bisphenol A and 4-nonylphenol in a human reference population.* Environ Health Perspect, 113: 391–395, 2005.
- Carmeci C., Thompson D.A., Ring H.Z., Francke U., Weigel R.J.** *Identification of a gene (GPR30) with homology to the G-protein-coupled receptor superfamily associated with estrogen receptor expression in breast cancer.* Genomics, 45: 607–617, 1997.
- Caruso F., Rossi M.** “*Antitumor titanium compounds.*” Mini-Reviews in Medicinal Chemistry, 4: 49–60, 2004.
- Caruso, A., Voisin-Chiret, A.S., Lancelot, J.C., Sinicropi, M.S., Garofalo, A., Rault, S.** *Efficient and Simple Synthesis of 6-Aryl-1,4-dimethyl-9H-carbazoles.* Molecules, 13:1312-1320, 2008.
- Chaour B., Yang R., Sha Q.** *Mechanical stretch modulates the promoter activity of the profibrotic factor CCN2 through increased actin polymerization and NF-kappaB activation.* J Biol Chem, 281: 20608–20622, 2006.
- Chevalier, N., Bouskine, A., Fenichel, P.** *Role of GPER/GPR30 in tumoral testicular germ cells proliferation.* Cancer Biol. Ther., 12: 2-3, 2011.
- Christodoulou CV, Ferry DR, Fyfe DW, Young A, Doran J, Sheehan TM, Eliopoulos A, Hale K, Baumgart J, Sass G, Kerr DJ.** *Phase I trial of weekly scheduling and pharmacokinetics of titanocene dichloride in patients with advanced cancer.* Journal of Clinical Oncology, 16(8):2761-9, 1998.

- Chung S., Funakoshi T., Civelli O.** *Orphan GPCR research.* Br. J. Pharmacol. 153: 339–346, 2008.
- Claffey J, Hogan M, Müller-Bunz H, Pampillón C, Tacke M.** *Oxali-titanocene Y: a potent anticancer drug.* Chem. Med. Chem., 3(5): 729-31, 2008.
- Claffey J, Hogan M, Müller-Bunz H, Pampillón C, Tacke M.** *Oxali-titanocene Y: a potent anticancer drug.* ChemMedChem. 3(5):729-31, 2008.
- Clarke M.J., Zhu F. Frasca, D.R** *Non-platinum chemotherapeutic metallopharmaceuticals.* Chem.Rev., 99(9):2511-34, 1999.
- Decatris MP, Sundar S, O'Byrne KJ.** *Platinum-based chemotherapy in metastatic breast cancer: current status.* Cancer Treat Rev. 30(1):53-81, 2004.
- Dennis M.K., Field A.S., Burai R., Ramesh C., Petrie W.K., Bologna C.G., Oprea T.I., Yamaguchi Y., Hayashi S.I., Sklar L.A., Hathaway H.J., Arterburn J.B., Prossnitz E.R.** *Identification of a GPER/GPR30 antagonist with improved estrogen receptor counterselectivity.* J Steroid Biochem Mol Biol, 127: 358-366, 2011.
- Desoize B.** “*Metals and metal compounds in cancer treatment.*” Anticancer Research vol. 24, no. 3 A :1529–1544, 2004.
- Dodds E.C., Lawson W.** *Synthetic estrogenic agents without the phenanthrene nucleus.* Nature 137: 996, 1936.
- Dombrowski KE, Sheats JE, Prockop DJ.** *Iron-containing metallocenes as active site directed inhibitors of the proteinase that cleaves the NH2-terminal propeptides from type I procollagen.* Biochemistry, 29;25(15):4302-9, 1986.
- Dong S., Terasaka S., Kiyama R.** *Bisphenol A induces a rapid activation of Erk1/2 through GPR30 in human breast cancer cells.* Environ Pollut, 159: 212–218, 2011.

- Dorsam, R. T., Gutkind J. S.** *G-protein-coupled receptors and cancer.* Nature Rev. Cancer 7: 79–94, 2007.
- Durando M., Kass L., Piva J., Sonnenschein C., Soto A.M., Luque E.H., Muñoz-de-Toro M.** *Prenatal bisphenol A exposure induces preneoplastic lesions in the mammary gland in Wistar rats.* Environ Health Perspect, 115: 80-86, 2007.
- Early Breast Cancer Trialists' Collaborative Group (EBCTCG).** *Effects of chemotherapy and hormonal therapy for early breast cancer on recurrence and 15-year survival: an overview of the randomised trials.* Lancet, 365(9472): 1687-717, 2005.
- Fang H., Tong W., Perkins R., Soto A.M., Prechtel N.V., Sheehan D.M.** *Quantitative comparisons of in vitro assays for estrogenic activities.* Environ Health Perspect, 108: 723–729, 2000.
- Fenyo D.** *Identifying the proteome: software tools.* Current opinion in Biotechnology, 11:391-395, 2000.
- Filardo E.J., Quinn J.A., Frackelton Jr A.R., Bland K.I.** *Estrogen action via the G protein-coupled receptor, GPR30: stimulation of adenylyl cyclase and cAMP-mediated attenuation of the epidermal growth factor receptor to MAPK signaling axis.* Mol Endocrinol, 16 (1): 70–84, 2002.
- Filardo E.J., Graeber C.T., Quinn J.A., Resnick M.B., Giri D., DeLellis R.A., Steinhoff M. M., Sabo E.** *Distribution of GPR30, a seven membrane spanning estrogen receptor, in primary breast cancer and its association with clinicopathologic determinants of tumor progression.* Clin Cancer Res, 12(21): 6359-66, 2006.
- Filardo E.J., Quinn J., Pang Y., Graeber C., Shaw S., Dong J., Thomas P.** *Activation of the novel estrogen receptor G Protein-Coupled Receptor 30 (GPR30) at the plasma membrane.* Endocrinology, 148: 3236–3245, 2007.

- Filardo E.J., Quinn J.A., Bland K.I., Frackelton Jr A.R.** *Estrogen induced activation of Erk-1 and Erk-2 requires the G protein coupled receptor homolog, GPR30, and occurs via trans-activation of the epidermal growth factor receptor through release of HB-EGF.* Mol Endocrinol, 14: 1649–1660, 2000.
- Filardo E.J., Quinn J.A., Sabo E.** *Association of the membrane estrogen receptor, GPR30, with breast tumor metastasis and transactivation of the epidermal growth factor receptor.* Steroids, 73: 870–873, 2008.
- Filardo E.J., Thomas P.** *Minireview: G protein-coupled estrogen receptor-1, GPER-1: its mechanism of action and role in female reproductive cancer, renal and vascular physiology.* Endocrinology., 153(7): 2953-62, 2012.
- Florea AM, Büsselberg D.** *Cisplatin as an anti-tumor drug: cellular mechanisms of activity, drug resistance and induced side effects.* Cancers (Basel), 15;3(1):1351-71, 2011.
- Fonslow BR, Niessen SM, Singh M, Wong CC, Xu T, Carvalho PC, Choi J, Park SK, Yates JR 3rd.** *Single-step inline hydroxyapatite enrichment facilitates identification and quantitation of phosphopeptides from mass-limited proteomes with MudPIT.* J Proteome Res, 4;11(5):2697-709, 2012.
- Gould J.C., Leonard L.S., Maness S.C., Wagner B.L., Conner K., Zacharewski T., Safec S., McDonnell D.P., Gaido K.W.** *Bisphenol A interacts with the estrogen receptor  $\alpha$  in a distinct manner from estradiol.* Mol Cell Endocrinol, 142: 203–214, 1998.
- Greenhough, A., Smartt HJ, Moore AE, Roberts HR, Williams AC, Paraskeva C, Kaidi A.** *The COX-2/PGE2 pathway: key roles in the hallmarks of cancer and adaptation to the tumour microenvironment.* Carcinogenesis 30, 377–386 2009. Carcinogenesis, 30(3):377-86, 2009.

- Hanstein B, Djahansouzi S, Dall P, Beckmann MW, Bender HG.** *Insights into the molecular biology of the estrogen receptor define novel therapeutic targets for breast cancer.* Eur J Endocrinol, 150(3):243-55, 2004.
- He Y.Y., Cai B., Yang Y.X., Liu X.L., Wan X.P.** *Estrogenic G protein-coupled receptor 30 signaling is involved in regulation of endometrial carcinoma by promoting proliferation, invasion potential, and interleukin-6 secretion via the MEK/ERK mitogen-activated protein kinase pathway.* Cancer Science 100(6): 1051–1061, 2009.
- Henic E., Noskova V., Høyer-Hansen G., Hansson S., Casslén B.** *Estradiol attenuates EGF-induced rapid uPAR mobilization and cell migration via the G-protein-coupled receptor 30 in ovarian cancer cells.* Int J Gynecol Cancer, 19(2): 214-22, 2009.
- Ho S.M., Tang W.Y., Belmonte de Frausto J., Prins G.S.** *Developmental exposure to estradiol and bisphenol A increases susceptibility to prostate carcinogenesis and epigenetically regulates phosphodiesterase type 4 variant 4.* Cancer Res, 66(11): 5624–5632, 2006.
- Jamieson ER, Lippard SJ.** *Structure, recognition, and processing of cisplatin-DNA adducts.* Chem Rev 99:2467–2498, 1999.
- Kaneyama J.K., Shibamura M., Nose K.** *Transcriptional activation of the c-fos gene by a LIM protein, Hic-5.* Biochem Biophys Res Commun, 299(3): 360-365, 2002.
- Kang J.H., Kondo F., Katayama, Y.** *Human exposure to bisphenol A.* Toxicology, 226: 79–89, 2006.
- Kang K., Lee S.B., Jung S.H., Cha K.H., Park W.D., Sohn Y.C., Nho C.W.** *Tectoridin, a poor ligand of estrogen receptor alpha, exerts its estrogenic effects via an ERK-dependent pathway.* Mol Cell, 27(3): 351-7, 2009.

- Kelter G, Sweeney NJ, Strohfeltd K, Fiebig HH, Tacke M.** *In-vitro anti-tumor activity studies of bridged and unbridged benzyl-substituted titanocenes.* *Anticancer Drugs.* 16(10):1091-8, 2005.
- Kleuser B, Malek D, Gust R, Pertz HH, Potteck H.** *17-Beta-estradiol inhibits transforming growth factor-beta signaling and function in breast cancer cells via activation of extracellular signal-regulated kinase through the G protein-coupled receptor 30.* *Mol Pharmacol.* 74(6):1533-43, 2008.
- Koleros E, Stamatatos TC, Psycharis V, Raptopoulou CP, Perlepes SP, Klouras N.** *Perlepes, and Nikolaos Klouras In Search for Titanocene Complexes with Improved Cytotoxic Activity: Synthesis, X-Ray Structure, and Spectroscopic Study of Bis ( $\eta^5$ -cyclopentadienyl) difluorotitanium (IV).* *Bioinorganic Chemistry and Applications.* Bioinorg Chem Appl. 914580, 2010.
- Köpf-Maier,P.; Köpf,H .** *Titanocene dichloride--the first metallocene with cancerostatic activity.* *Angew. Chem., Int. Ed.,*18,477, 1979.
- Kröger N., Kleeberg U. R., Mross K, Edler L., Saß G., Hossfeld D.K.** *Phase II clinical trial of titanocene dichloride in patients with metastatic breast cancer.* *Onkologie,* 23:60–62, 2000.
- Krishnan A.V., Stathis P., Permuth S.F., Tokes L., Feldman D.** *Bisphenol-A: an estrogenic substance is released from polycarbonate flasks during autoclaving.* *Endocrinology,* 132: 2279–2286, 1993.
- Kuiper G.G., Lemmen J.G., Carlsson B., Corton J.C., Safe S.H., Van Der Saag P.T., van der Burg B., Gustafsson J.Å.** *Interaction of estrogenic chemicals and phytoestrogens with estrogen receptor  $\beta$ .* *Endocrinology,* 139: 4252–4263, 1998.



- Kuo W.H., Chang L.Y., Liu D.L., Hwa H.L., Lin J.J., Lee P.H., Chen C.N., Lien H.C., Yuan R.H., Shun C.T., Chang K.J., Hsieh F.J.** *The interactions between GPR30 and the major biomarkers in infiltrating ductal carcinoma of the breast in an Asian population.* Taiwan J Obstet Gynecol, 46(2): 135-45, 2007.
- L'ummen G., Sperling H., Luboldt H, Otto T., R'ubben H.** *Phase II trial of titanocene dichloride in advanced renal-cell carcinoma.* Cancer Chemotherapy and Pharmacology, 5:415–417, 1998.
- Landis, S. H., Murray, T., Bolden, S., Wingo, P. A.** *Cancer statistics, CA Cancer J. Clin., 49: 8–31, 1999.*
- Lapensee E.W., Tuttle T.R., Fox S.R., Ben-Jonathan N.** *Bisphenol A at low nanomolar doses confers chemoresistance in estrogen receptor- $\alpha$ -positive and -negative breast cancer cells.* Environ Health Perspect, 117:175–180, 2009.
- Lappano R., Rosano C., De Marco P., De Francesco E.M., Pezzi V., Maggiolini, M.** *Estriol acts as a GPR30 antagonist in estrogen receptor-negative breast cancer cells.* Mol. Cell. Endocrinol., 320: 162-170, 2010.
- Lappano R., Rosano C., Santolla M.F., Pupo M., De Francesco E.M., De Marco P., Ponassi M., Spallarossa A., Ranise A., Maggiolini M.** *Two novel GPER agonists induce gene expression changes and growth effects in cancer cells.* Curr Cancer Drug Targets., 12: 531-42, 2012a.
- Lappano, R., Maggiolini M.** *G protein-coupled receptors: novel targets for drug discovery in cancer.* Nat Rev Drug Discov., 10:47-60, 2011.
- Lappano, R., Santolla M.F., Pupo M., Sinicropi M.S., Caruso A., Rosano C., Maggiolini M.** *MIBE acts as antagonist ligand of both estrogen receptor alpha and GPER in breast cancer cells.* Breast Cancer Res., 14(1), R12, 2012b.

- Leblanc K., Sexton E., Parent S., Bélanger G., Déry M.C., Boucher V., Asselin E.** *Effects of 4-hydroxytamoxifen, raloxifene and ICI 182 780 on survival of uterine cancer cell lines in the presence and absence of exogenous estrogens.* Int J Oncol, 30(2): 477-87, 2007.
- Liu Z., Yu X., Shaikh Z.A.** *Rapid activation of ERK1/2 and AKT in human breast cancer cells by cadmium.* Toxicol Appl Pharmacol, 228(3): 286-94, 2008.
- Lui V. W., Thomas SM, Zhang Q, Wentzel AL, Siegfried JM, Li JY, Grandis JR.** *Mitogenic effects of gastrin-releasing peptide in head and neck squamous cancer cells are mediated by activation of the epidermal growth factor receptor.* Oncogene, 22:6183–6193, 2003.
- Madeo, A., Maggiolini, M.** *Nuclear alternate estrogen receptor GPR30 mediates 17 $\beta$ -estradiol-induced gene expression and migration in breast cancer-associated fibroblasts.* Cancer Res., 70: 6036–6046, 2010.
- Maffini M.V., Rubin B.S., Sonnenschein C., Soto A.M.** *Endocrine disruptors and reproductive health: the case of bisphenol-A.* Mol Cell Endocrinol, 255: 179–186, 2006.
- Maggiolini M., Vivacqua A., Fasanella G., Recchia A.G., Sisci D., Pezzi V., Montanaro D., Musti A.M., Picard D., Andò, S.** *The G protein-coupled receptor GPR30 mediates c-fos up-regulation by 17 $\beta$ -estradiol and phytoestrogens in breast cancer cells.* J. Biol. Chem., 279: 27008-27016 2004.
- Maggiolini, M., Picard D.** *The unfolding stories of GPR30, a new membrane bound estrogen receptor.* J Endocrinol., 204:105–14, 2010.
- Moody D.L., Dyba M., Kosakowska-Cholody T., Tarasova N.I., Michejda C.J.** *Synthesis and biological activity of 5-aza-ellipticine derivatives.* Bioorg. Med. Chem. Lett., 17(8): 2380-2384, 2007.

- Muñoz-de-Toro M, Markey CM, Wadia PR, Luque EH, Rubin BS, Sonnenschein C, Soto AM.** *Perinatal exposure to bisphenol-A alters peripubertal mammary gland development in mice.* *Endocrinology.*146(9):4138-47, 2005.
- Nadal A., Ropero A.B., Laribi O., Maillet M., Fuentes E., Soria B.** *Nongenomic actions of estrogens and xenoestrogens by binding at a plasma membrane receptor unrelated to estrogen receptor alpha and estrogen receptor beta.* *Proc Natl Acad Sci USA,* 97: 11603–11608, 2000.
- Napoli M, Saturnino C, Sirignano E, Popolo A, Pinto A, Longo P.** *Synthesis, characterization and cytotoxicity studies of methoxy alkyl substituted metallocenes.* *Eur J Med Chem.* , 46(1):122-8, 2011.
- Neves S.R., Ram P.T, Iyengar R.** *G protein pathways.* *Science.* 296: 1636–9, 2002.
- Nordstrom D.K.** *Public health. Worldwide occurrences of arsenic in ground water.* *Science,* 296: 2143–2145, 2002.
- O’Dowd B.F., Nguyen T., Marchese A., Cheng R., Lynch K.R., Heng H.H., Kolakowski Jr. L.F., George S.R.** *Discovery of three novel G-protein-coupled receptor genes.* *Genomics,* 47: 310–313, 1998.
- Olde B, Leeb-Lundberg LM.** *GPR30/GPER1: searching for a role in estrogen physiology.* *Trends Endocrinol Metab.* , 20(8):409-16, 2009.
- Olea N, Olea-Serrano MF.** *Oestrogens and the environment.* *Eur J Cancer, Prev.* 5(6):491-6, 1996 .
- Overington J.P., Al-Lazikani B., Hopkins A.L.** **How many drug targets are there?** *Nature Rev Drug Discov.,* 5: 993-996, 2006.

- Owman C., Blay P., Nilsson C., Lolait S.J.** *Cloning of human cDNA encoding a novel heptahelix receptor expressed in Burkitt's lymphoma and widely distributed in brain and peripheral tissues.* *Biochem Biophys Res Commun*, 228: 285–292, 1996.
- Pandey D.P., Lappano R., Albanito L., Madeo A., Maggiolini M., Picard D.** *Estrogenic GPR30 signalling induces proliferation and migration of breast cancer cells through CTGF.* *EMBO J*, 28: 523–532, 2009.
- Panno A., Sinicropi M.S., Caruso A., El-Kashef H., Lancelot J.C., Aubert G., Lesnard A., Cresteil T., Rault S.** *New trimethoxybenzamides and trimethoxyphenylureas derived from dimethylcarbazole as cytotoxic agents. Part I.* *J. Heterocyclic Chem.*, DOI 10.1002/jhet.1951, 2013.
- Peri D, Meker S, Shavit M, Tshuva EY.** *Synthesis, characterization, cytotoxicity, and hydrolytic behavior of C2- and C1-symmetrical Ti(IV) complexes of tetradentate diamine bis(phenolato) ligands: a new class of antitumor agents.* *Chemistry*: 15(10):2403-15, 2009.
- Pettersen E.F., Goddard T.D., Huang C.C., Couch G.S., Greenblatt DM, Meng EC, Ferrin TE.** *UCSF Chimera--a visualization system for exploratory research and analysis.* *J. Computational Chem.*, 25:1605-1612, 2004.
- Pierce KL, Premont RT, Lefkowitz RJ.** *Seven-transmembrane receptors.* *Nature Rev Mol Cell Biol*, 3: 639–50, 2002.
- Pines A, Kelstrup CD, Vrouwe MG, Puigvert JC, Typas D, Misovic B, de Groot A, von Stechow L, van de Water B, Danen EH, Vrieling H, Mullenders LH, Olsen JV.** *Global phosphoproteome profiling reveals unanticipated networks responsive to cisplatin treatment of embryonic stem cells.* *Mol Cell Biol*, 31(24): 4964-77, 2011.

- Posern G., Treisman R.** *Actin' together: serum response factor, its cofactors and the link to signal transduction.* Trends Cell Biol, 16(11): 588-96, 2006.
- Prossnitz E.R., Arterburn J.B., Smith H.O., Oprea T.I., Sklar L.A., Hathaway H.J.** *Estrogen signaling through the transmembrane G protein-coupled receptor GPR30.* Annual Review of Physiology, 70: 165–190, 2008.
- Prossnitz E.R., Maggiolini M.** *Mechanisms of estrogen signaling and gene expression via GPR30.* Mol Cell Endocrinol, 308: 32–38, 2009.
- Prossnitz ER, Arterburn JB, Sklar LA.** *GPR30: A G protein-coupled receptor for estrogen.* Mol Cell Endocrinol., 265-266:138-42, 2007.
- Quesada I., Fuentes E., Viso-Leon M.C., Soria B., Ripoll C., Nadal A.** *Low doses of the endocrine disruptor bisphenol-A and the native hormone 17betaestradiol rapidly activate transcription factor CREB.* Faseb J, 16: 1671– 1673, 2002.
- Revankar C.M., Mitchell H.D., Field A.S., Burai R., Corona C., Ramesh C., Sklar L.A., Arterburn J.B., Prossnitz E.R.** *Synthetic estrogen derivatives demonstrate the functionality of intracellular GPR30.* ACS Chem Biol, 2(8): 536-44, 2007.
- Richter C.A., Birnbaum L.S., Farabollini F., Newbold R.R., Rubin B.S., Talsness C.E., Vandenberg J.G., Walser-Kuntz D.R., vom Saal F.S.** *In vivo effects of bisphenol A in laboratory rodent studies.* Reprod Toxicol, 24: 199–224, 2007.
- Rosano C., Lappano R., Santolla M.F., Ponassi M., Donadini A., Maggiolini M.** *Recent advances in the rationale design of GPER ligands.* Curr. Med. Chem., 19(36): 6199-6206, 2012.
- Rosenbaum D.M., Rasmussen S.G., Kobilka B.K.** *The structure and function of G-protein-coupled receptors.* Nature., 459: 356-63, 2009.

- Rosenberg B, VanCamp L, Trosko JE, Mansour VH.** *Platinum compounds: A new class of potent antitumour agents.* Nature, 222:385–386.10, 1969.
- Routledge E.J., White R., Parker M.G., Sumpter J.P.** *Differential effects of xenoestrogens on coactivator recruitment by estrogen receptor (ER) alpha and ERbeta.* J Biol Chem, 275: 35986–35993, 2000.
- Safe S.H., Pallaroni L., Yoon K., Gaido K., Ross S., McDonnell D.** Problems for risk assessment of endocrine-active estrogenic compounds. Environ Health Perspect, 110 (Suppl 6): 925–929, 2002.
- Sheng Z.G., Zhu B.Z.** *Low concentrations of Bisphenol A induce mouse spermatogonial cell proliferation by G-Protein-Coupled Receptor 30 and estrogen Receptor- $\alpha$ .* Environ Health Perspect, 119(12): 1775-80, 2011.
- Smith H.O., Arias-Pulido H., Kuo D.Y., Howard T., Qualls C.R., Lee S.J., Verschraegen C.F., Hathaway H.J., Joste N.E., Prossnitz E.R.** *GPR30 predicts poor survival for ovarian cancer.* Gynecologic Oncology, 114: 465–471, 2009.
- Smith H.O., Leslie K.K., Singh M., Qualls C.R., Revankar C.M., Joste N.E., Prossnitz E.R.** *GPR30: a novel indicator of poor survival for endometrial carcinoma.* American Journal of Obstetrics and Gynecology, 196: 386.e1–386.e9, 2007.
- Tacke M, Cuffe LP, Gallagher WM, Lou Y, Mendoza O, Müller-Bunz H, Rehmann FJ, Sweeney N.** *Methoxy-phenyl substituted ansa-titanocenes as potential anti-cancer drugs derived from fulvenes and titanium dichloride.* J Inorg Biochem\_ 98(12):1987-94, 2004.
- Takada Y., Kato C., Kondo S., Korenaga R., Ando J.** *Cloning of cDNAs encoding G protein-coupled receptor expressed in human endothelial cells exposed to fluid shear stress.* Biochem Biophys Res Commun 240: 737–741, 1997.

- Thomas P., Dong J.** *Binding and activation of the seven-transmembrane estrogen receptor GPR30 by environmental estrogens: a potential novel mechanism of endocrine disruption.* J Steroid Biochem Mol Biol, 102: 175–179, 2006.
- Thomas P., Pang Y., Filardo E.J., Dong J.** *Identity of an estrogen membrane receptor coupled to a G protein in human breast cancer cells.* Endocrinology, 146: 624–632, 2005.
- Vandenberg L.N., Maffini M.V., Sonnenschein C., Rubin B.S., Soto A.M.** *Bisphenol-A and the great divide: a review of controversies in the field of endocrine disruption.* Endocr Rev, 30(1): 75–95, 2009.
- Vehar B., Hrast M., Kovac A., Konc J., Mariner K., Chopra I., O'Neill A., Janezic D., Gobec S.** *Ellipticines and 9-acridinylamines as inhibitors of D-alanine:D-alanine ligase.* Bioorg. Med. Chem., 5137-5146, 2011.
- Vivacqua A., Bonofiglio D., Albanito L., Madeo A., Rago V., Carpino A., Musti A.M., Picard D., Andò S., Maggiolini M.** *17 $\beta$ -Estradiol, genistein and 4-hydroxytamoxifen induce the proliferation of thyroid cancer cells through the G protein-coupled receptor GPR30.* Mol Pharmacol, 70: 1414–1423, 2006a.
- Vivacqua A., Bonofiglio D., Recchia A.G., Musti A.M., Picard D., Andò S., Maggiolini M.** *The G protein-coupled receptor GPR30 mediates the proliferative effects induced by 17 $\beta$ -estradiol and hydroxytamoxifen in endometrial cancer cells.* Mol Endocrinol, 20: 631–646, 2006b.
- Vivacqua A., Lappano R., De Marco P., Sisci D., Aquila S., De Amicis F., Fuqua S.A., Ando` S., Maggiolini M.** *G protein-coupled receptor 30 expression is up-regulated by EGF and TGF $\alpha$  in estrogen receptor positive cancer cells.* Molecular Endocrinology 23: 1815–1826, 2009.

- Vivanco I., Sawyers C.L.** *The phosphatidylinositol 3-Kinase AKT pathway in human cancer.* Nat Rev Cancer, 2(7): 489-501, 2002.
- Von Angerer E., Prekajac J.** *Benzo[a]carbazole derivatives. Synthesis, estrogen receptor binding affinities and mammary tumor inhibiting activity.* J. Med. Chem., 26: 113-116, 1986,
- Wallace A.C., Laskowski R.A., Thornton J.N.** *Ligplot. A program to generate schematic diagrams of protein-ligand interactions.* Protein Eng., 8: 127-134, 1996.
- Wang C., Prossnitz E.R., Roy S.K.,** *Expression of GPR30 in the hamster ovary: differential regulation by gonadotropins and steroid hormones.* Endocrinology, 148: 4853–4864, 2007.
- Watson C.S., Bulayeva N.N., Wozniak A.L., Finnerty C.C.** *Signaling from the membrane via membrane estrogen receptor- $\alpha$ : estrogens, xenoestrogens, and phytoestrogens.* Steroids, 70: 364–371, 2005.
- Welshons W.V., Nagel S.C., vom Saal F.S.** *Large effects from small exposures. III. Endocrine mechanisms mediating effects of bisphenol A at levels of human exposure.* Endocrinology, 147: S56–S69, 2006.
- Wetherill Y.B., Akingbemi B.T., Kanno J., McLachlan J.A., Nadal A., Sonnenschein C., Watson C.S., Zoeller R.T., Belcher S.M.** *In vitro molecular mechanisms of bisphenol A action.* Reprod Toxicol, 24: 178–198, 2007.
- Wolff L.** *Chemischen Institut der Universität Jena: Methode zum Ersatz des Sauerstoffatoms der Ketone und Aldehyde durch Wasserstoff.* Justus Liebigs Annalen der Chemie, 394(1):86-108, 1912.
- Ye J., Li A., Liu Q., Wang X., Zhou J.** *Inhibition of mitogen-activated protein kinase enhances apoptosis induced by arsenic trioxide in human breast cancer MCF-7 cells.* Clin Exp Pharmacol Physiol, 32(12): 1042–1048, 2005.



**Zanella A., Gandin V., Porchia M., Refosco F., Tisato F., Sorrentino F., Scutari G., Rigobello M.P.** *Cytotoxicity in human cancer cells and mitochondrial dysfunction induced by a series of new copper(I) complexes containing tris(2-cyanoethyl)phosphines.* Invest.New Drugs, 29(6):,1213-23, 2011.

**Zeidan YH, Jenkins RW, Hannun YA.** *Remodeling of cellular cytoskeleton by the acid sphingomyelinase/ceramide pathway.* J Cell Biol, 21;181(2):335-50, 2008.

## Publications

Pupo M., **Pisano A.**, Abonante S., Maggiolini M., Musti A.M., *GPER activates Notch signaling in breast cancer cells and cancer-associated fibroblasts (CAFs)*. The International Journal of Biochemistry & Cell Biology. 2013, <http://dx.doi.org/10.1016/j.biocel.2013.11.011>

Sinicropi M.S., Lappano R., Caruso A., Santolla M.F., **Pisano A.**, Rosano C., Capasso A., Panno A., Lancelot J.C., Rault S., Saturnino C., Maggiolini M., *(6-Bromo-1,4-dimethyl-9H-carbazol-3-yl-methylene)-hydrazine ("Carbhydraz") as a novel GPER agonist*. Current Topics in Medicinal Chemistry, 2013, SUBMITTED.

Sirignano E., Saturnino C., Botta A., Sinicropi M.S., Caruso A., **Pisano A.**, Lappano R., Maggiolini M., Longo P., *Synthesis, characterization and cytotoxic activity on breast cancer cells of new half-titanocene derivatives*. Bioorg Med Chem Lett. 2013 Jun 1;23(11):3458-62.

Pupo M., Vivacqua A., Perrotta I., **Pisano A.**, Aquila S., Abonante S., Gasperi-Campani A., Pezzi V., Maggiolini M., *The nuclear localization signal is required for nuclear GPER translocation and function in breast Cancer-Associated Fibroblasts (CAFs)*. Mol Cell Endocrinol. 2013 Aug 25;376(1-2):23-32.

Pupo M., **Pisano A.**, Lappano R., Santolla M.F., De Francesco E.M., Abonante S., Rosano C., Maggiolini M., *Bisphenol A induces gene expression changes and proliferative effects through GPER in breast cancer cells and cancer-associated fibroblasts*. Environmental Health Perspectives, 2012, Aug;120(8):1177-82.

## Accepted Manuscript

Title: GPER activates Notch signaling in breast cancer cells and cancer-associated fibroblasts (CAFs)

Authors: Marco Pupo Assunta Pisano Sergio Abonante  
Marcello Maggiolini Anna Maria Musti



PII: S1357-2725(13)00349-X  
DOI: <http://dx.doi.org/doi:10.1016/j.biocel.2013.11.011>  
Reference: BC 4178

To appear in: *The International Journal of Biochemistry & Cell Biology*

Received date: 14-6-2013  
Revised date: 3-10-2013  
Accepted date: 5-11-2013

Please cite this article as: Pupo, M., Pisano, A., Abonante, S., Maggiolini, M., & Musti, A. M., GPER activates Notch signaling in breast cancer cells and cancer-associated fibroblasts (CAFs), *International Journal of Biochemistry and Cell Biology* (2013), <http://dx.doi.org/10.1016/j.biocel.2013.11.011>

This is a PDF file of an unedited manuscript that has been accepted for publication. As a service to our customers we are providing this early version of the manuscript. The manuscript will undergo copyediting, typesetting, and review of the resulting proof before it is published in its final form. Please note that during the production process errors may be discovered which could affect the content, and all legal disclaimers that apply to the journal pertain.

**GPER activates Notch signaling in breast cancer cells  
and cancer-associated fibroblasts (CAFs)**

Marco Pupo<sup>a</sup>, Assunta Pisano<sup>a</sup>, Sergio Abonante<sup>b</sup>, Marcello Maggiolini<sup>a</sup>, Anna Maria Musti<sup>a,c</sup>

<sup>a</sup> Department of Pharmacy, Health and Nutritional Sciences, University of Calabria, Rende, Italy

<sup>b</sup> Regional Hospital, Cosenza, Italy

<sup>c</sup> Institut for Clinical Institut for Clinical Neurobiology, University of Würzburg, Würzburg,  
Germany

**Corresponding Authors:**

Prof. Marcello Maggiolini, Department of Pharmacy, Health and Nutritional Sciences, University of Calabria, 87036 Rende, Italy; Tel: +39 0984 493076; Fax: +39 0984 493458; E-mail: marcellomaggiolini@yahoo.it

Prof. Anna Maria Musti, Institut for Clinical Institut for Clinical Neurobiology, University of Würzburg, D-97078 Würzburg, Germany; Tel: +49 (0)931-201 44030; Fax: +49 (0)931-201 44009; E-mail: E\_Musti\_A@klinik.uni-wuerzburg.de

Manuscript word count: 4361

**Abstract**

The G protein-coupled receptor GPR30/GPER has been shown to mediate rapid effects of 17 $\beta$ -estradiol (E2) in diverse types of cancer cells. Here, we provide evidence for a novel crosstalk between GPER and the Notch signaling pathway in breast cancer cells and cancer-associated fibroblasts (CAFs). We show that E2 and the GPER selective ligand G-1 induce both the  $\gamma$ -secretase-dependent activation of Notch-1 and the expression of the Notch target gene Hes-1. These inductions are prevented by knocking down GPER or by using a dominant-negative mutant of the Notch transcriptional co-activator Master-mind like-1 (DN-MAML-1), hence suggesting the involvement of GPER in the Notch-dependent transcription. By performing chromatin-immunoprecipitation experiments and luciferase assays, we also demonstrate that E2 and G-1 induce the recruitment of the intracellular domain of Notch-1 (NICD) to the Hes-1 promoter and the transactivation of a Hes-1-reporter gene, respectively. Functionally, the E2 and G-1-induced migration of breast cancer cells and CAFs is abolished in presence of the  $\gamma$ -secretase inhibitor GSI or DN-MAML-1, which both inhibit the Notch signaling pathway. In addition, we demonstrate that E2 and G-1 prevent the expression of VE-Cadherin, while both compounds induce the expression of Snail, a Notch target gene acting as a repressor of cadherins expression. Notably, both GSI and DN-MAML-1 abolish the up-regulation of Snail-1 by E2 and G-1, whereas the use of GSI rescues VE-Cadherin expression. Taken together, our results prove the involvement of the Notch signaling pathway in mediating the effects of estrogenic GPER signaling in breast cancer cells and CAFs.

**Keywords:** GPER, Estrogens signaling, Notch signaling, Breast cancer, Cancer-associated fibroblasts.

## 1 Introduction

Estrogens regulate critical signaling pathways involved in the control of cell proliferation and differentiation in reproductive and non-reproductive tissues (Liang and Shang, 2013). These steroids influence also the pathological processes of hormone-dependent tumors, like breast cancer, activating the estrogen receptor (ER) $\alpha$  and ER $\beta$  which act as transcription factors binding to cognate the responsive elements located in the promoter regions of target genes (Ascenzi et al., 2006; Panno et al., 1996).

Although estrogens act mostly by this classic genomic mechanism, they are also able to rapidly activate transduction pathways in an ER-independent manner. In the last few years the membrane-associated G protein-coupled receptor GPR30/GPER has been widely shown to mediate signals triggered by estrogens, antiestrogens and phyto-xenoestrogens, including the quick MAPK activation, the induction of early gene expression, the proliferation and migration in different types of cancer cells (Albanito et al., 2008a, 2008b, 2007; Chimento et al., 2012; De Marco et al., 2013; Filice et al., 2009; Lappano et al., 2010; Maggiolini et al., 2004; Pupo et al., 2012; Recchia et al., 2011; Santolla et al., 2012; Thomas et al., 2005; Vivacqua et al., 2012, 2006a, 2006b). Moreover, the identification of synthetic molecules acting either as agonistic or antagonist ligands of GPER has extended our knowledge regarding the estrogenic GPER signaling (Bologa et al., 2006; Dennis et al., 2011; Lappano et al., 2012a, 2012b; Rosano et al., 2012). Among these molecules, the GPER-agonist ligand G-1 has been shown to induce both gene expression changes and proliferation in diverse tumor cells. In this regard, several studies have shown that these effects mediated by ligand-activated GPER require a functional interaction with the EGFR transduction pathway, the activation of the MAPK cascade, PI3K kinase and phospholipase C signaling (Maggiolini and Picard, 2010). Moreover, in ER-negative cancer cells like SkBr3 cells or cancer-associated fibroblasts (CAFs), GPER contributed to the stimulation of migration as its silencing drastically reduced the pro-migratory effects of 17 $\beta$ -Estradiol (E2) and G-1, which involved EGFR-dependent activation of one

important GPER target gene named connective tissue growth factor (*CTGF*) (Madeo and Maggiolini 2010; Pandey et al., 2009).

The Notch signaling and its crosstalk with several transduction pathways plays an important role in different aspects of breast cancer biology, including cell growth, EMT transition and cell migration (Guo et al., 2011). Notch consists of a family of single-pass transmembrane receptors (Notch1-4), which can be activated by the interaction with membrane-tethered ligands, including Dll (Delta-like 1-4) and Jagged (Jagged 1-2) (Miele, 2006). Up-regulated expression of Notch receptors and/or their ligands have been found in several human malignancies, including breast cancer (Al-Hussaini et al., 2011; Kopan and Ilagan, 2009). In addition, the expression of the Notch ligand Jagged-1 has been correlated with more aggressive malignant features (Reedijk et al., 2005) . Upon ligand activation, Notch is cleaved by an ADAM metalloproteinase and  $\gamma$ -secretase and thereafter the membrane-released Notch intracellular domain (NICD) translocates to the nucleus (Guo et al., 2011). In the nucleus, NICD releases the expression of Notch target genes by recruiting transcriptional regulators, hence converting the RBP-J/CSL transcriptional repressor complex in a transcriptional activator (Yin et al., 2010). The most characterized transcriptional targets of Notch signaling are bHLH transcriptional repressors of the *Hes* (*Hes-1 to 7*) and *Hey* (*Hey-1 and 2, L*) subfamilies (Iso et al., 2003). Notch-induced activation of *Hes* and *Hey* genes play an important role in cell fate determination during organ development (Guo et al., 2011) Furthermore, Notch-dependent expression of *Hes* and *Hey* genes has been described in different types of cancer cells and correlates with Notch tumorigenic activities (Miele, 2006). An additional Notch-target gene is the zinc-finger transcriptional repressor *Snail*, which has been shown to trigger EMT by directly repressing E-cadherin expression (Wang et al., 2010). Notch-dependent up-regulation of *Snail* and the consequent E-cadherin repression represent the main pathway mediating the Notch-dependent migration in diverse tumor cells (Chen et al., 2010; Guo et al., 2011; Matsuno et al., 2012).

In the present study, we provide novel evidence showing that ligand-activated GPER triggers Notch activation and expression of Notch target genes. Moreover, we have assessed that Notch signaling contributes to GPER-mediated migration in ER-negative breast cancer cells and cancer-associated fibroblasts.

Accepted Manuscript



## 2 Materials and methods

### 2.1 Reagents

17 $\beta$ -Estradiol (E2) was purchased from Sigma-Aldrich (Milan, Italy);  $\gamma$ -Secretase inhibitor cbz-Leu-Leu-Nle-CHO (GSI) and 1-[4-(-6-bromobenzol[1,3]diodo-5-yl)-3a,4,5,9b-tetrahydro3H-cyclopenta[c]quinolin-8yl]-ethanone (G-1) were purchased from Calbiochem (Merck KGaA, Frankfurt, Germany); Notch ligand Jagged-1 (DSL Peptide 188-204) (JAG-1) was obtained from AnaSpec (DBA Milan, Italy). E2 was dissolved in ethanol while G-1, GSI and JAG-1 were solubilized in DMSO.

### 2.2 Cell cultures

The SkBr3 breast cancer cells were maintained in RPMI-1640 (Invitrogen, Gibco, Milan, Italy) without phenol red, supplemented with 10% fetal bovine serum (FBS). MCF7 breast cancer cells were maintained in DMEM with phenol red supplemented with 10% FBS. Cells were switched to medium without serum the day before experiments for immunoblots, reverse transcription polymerase chain reaction (RT-PCR) and chromatin immunoprecipitation (ChIP). Both cell lines were grown in a 37° C incubator with 5% CO<sub>2</sub>. CAFs were extracted as previously described (Madeo and Maggiolini 2010; Pupo et al., 2013, 2012) maintained in a mixture of MEDIUM 199 and HAM'S F-12 (1:1) supplemented with 10% FBS. Primary cells cultures of breast fibroblasts were characterized by immunofluorescence. Briefly cells were incubated with human anti-vimentin (V9) and human anti-cytokeratin 14 (LL001), all antibodies were from Santa Cruz Biotechnology, DBA (Milan, Italy). In order to assess fibroblasts activation, we used anti-fibroblast activated protein  $\alpha$  (FAP $\alpha$ ) antibody (H-56) purchased from Santa Cruz Biotechnology, DBA (Milan, Italy) (data not shown). We used CAFs passaged for up to five population doublings for the experiments performed using these cells. CAFs were also switched to medium without serum the day before experiments for immunoblots and reverse transcription polymerase chain reaction (RT-PCR)

### 2.3 Western blotting

Western blotting experiments were performed as previously described (Madeo et al., 2010). Briefly, cells were exposed to ligands, and then lysed in a buffer containing 1% SDS and a mixture of protease inhibitors. Equal amounts of whole protein extract were resolved on SDS-polyacrylamide gel, transferred to a nitrocellulose membrane (Amersham Biosciences, Milan, Italy), probed overnight at 4°C with antibodies against *Hes-1* (H-140), *Notch-1* (C-20), Snai 1 (G-7), *VE-Cadherin* (N-14), *ERα* (F-10), *GPER* (N-15) and *β-actin* (C-2) purchased from Santa Cruz Biotechnology (DBA, Milan, Italy), and then revealed using the ECL® Western Blotting Analysis System (GE Healthcare, Milan, Italy). Results of densitometric analyses of Western blots, obtained using ImageJ software, are presented as optical density (OD; expressed in arbitrary units) relative to the control ( $\beta$ -actin).

### 2.4 Reverse transcription and quantitative RT-PCR

Total RNA was extracted using Trizol commercial kit (Invitrogen, Milan, Italy) according to the manufacturer's protocol. RNA was quantified spectrophotometrically and its quality was checked by electrophoresis through agarose gel stained with ethidium bromide. Only samples that were not degraded and showed clear 18S and 28S bands under ultraviolet light were used for real-time PCR. Total cDNA was synthesized from RNA by reverse transcription using the murine leukemia virus reverse transcriptase (Invitrogen, Milan, Italy) following the protocol provided by the manufacturer. The expression of selected genes was quantified by quantitative RT-PCR carried out as previously described (Maggiolini et al., 1999). *Hes-1*, *Notch-1*, *Snail*, *VE-cadherin* and the internal control *RPLP0* (also known as *36B4*) cDNAs yielded bands of 346, 289, 406, 319 and 408 bp with 21, 25, 22, 23 and 10 PCR cycles, respectively. The primers pairs used to amplify the fragments were: 5'-CCCAGCCAGTGTCAACACGAC-3' (forward) and 5'-ATTAACGCCCTCGCACGTGG-3' (reverse) for *Hes-1*; 5'-GCATAGTCCAAAAGCTCCTG-3' (forward) and 5'-GTGCACTCTTGGCATAACAC-3' (reverse) for *Notch-1*; 5'-CTCACCGGCTCCTTCGTCCT-3'

(forward) and 5'-ACACGCCTGGCACTGGTACT-3' (reverse) for *Snail*; 5'-TCTCCGCAATAGACAAGGAC-3' (forward) and 5'-AGTAAGATGGCTACCACTGC-3' (reverse) for *VE-Cadherin*; 5'-CTCAACATCTCCCCCTTCTC-3' (forward) and 5'-CAAATCCCATATCCTCGTCC-3' (reverse) for *RPLP0*. Results of densitometric analyses of blots, obtained using ImageJ software, are presented as optical density (OD; expressed in arbitrary units) relative to the control (*RPLP0*).

## 2.5 Real-Time PCR

Gene expression was evaluated also by real-time PCR as we previously described (Lappano et al, 2011). For *Hes-1*, *Snail*, *VE-Cadherin*, and the ribosomal protein *18S*, which was used as a control gene to obtain normalized values, the primers were: 5'-TCAACACGACACCGGATAAA-3' (*Hes-1* forward) and 5'-CCGCGAGCTATCTTTCTTCA-3' (*Hes-1* reverse); 5'-CTTCCAGCAGCCCTACGAC-3' (*Snail* forward) and 5'-CGGTGGGGTTGAGGATCT-3' (*Snail* reverse); 5'-TTTCCAGCAGCCTTTCTACCA-3' (*VE-Cadherin* forward) and 5'-GGAAGAACTGGCCCTTGTC-3' (*VE-Cadherin* reverse) and 5'-GGCGTCCCCCAACTTCTTA-3' (*18S* forward) and 5'-GGGCATCACAGACCTGTTATT-3' (*18S* reverse), respectively.

## 2.6 Chromatin Immunoprecipitation (ChIP) Assay

Cells were grown in 10-cm plates and then exposed to ligands for 8 hours. Thereafter, cells were cross-linked with 1% formaldehyde and sonicated. Supernatants were immunocleared with sonicated salmon DNA/protein A agarose (Upstate Biotechnology, Inc., Lake Placid, NY) and immunoprecipitated with the anti-*Notch-1* (C-20) antibody or non specific IgG (Santa Cruz Biotechnology, DBA, Milan, Italy). Pellets were washed, eluted with a buffer consisting of 1% SDS and 0.1 mol/L NaHCO<sub>3</sub>, and digested with proteinase K. DNA was obtained by phenol/chloroform extraction and precipitated with ethanol. A 4μl volume of each sample was used as template to amplify by real-time PCR a RBP-J binding site corresponding to -167 to +6 located in the 5'-

flanking region of *Hes-1* gene. The primers used were Fwd: 5'-CAGACCTTGTGCCTGGCG-3' and Rev: 5'-TGTGATCCCTAGGCCCTG-3'. data were normalized with respect to unprocessed lysates (input DNA). Inputs DNA quantification was performed by using 4µl of the template DNA. The relative antibody-bound fractions were normalized to a calibrator that was chosen to be the basal, untreated sample. Final results were expressed as percent differences with respect to the relative inputs.

## 2.7 Plasmids

The luciferase reporter plasmid Hes1-Luc (-467 to +46 of the Hes1 promoter with the luciferase gene) was a kind gift from Dr. Hee-Sae Park (Hormone Research Center, School of Biological Sciences and Technology, Chonnam National University, Yongbong-dong, Buk-ku, Gwangju, Republic of Korea). The plasmid encoding dominant-negative MAML-1 (DN-MAML-1) was a gift from Dr. M. Bocchetta (Cardinal Bernardin Cancer Center, Loyola University Chicago, Illinois, USA). The Sure Silencing (sh) ER $\alpha$  and the respective control plasmid (shRNA), generated in pGeneClip Puromycin Vector, were purchased from SA Bioscience Corp (Frederick, MD, USA) and used according to the manufacturer's recommendations. Short hairpin RNA construct against human GPER (shGPR30/shGPER) and the unrelated shRNA control construct were previously described (Pandey et al., 2009).

## 2.8 Transfection, Luciferase assays and gene silencing experiments

For luciferase assays, cells were plated into 24-well plates with 500 µl of regular growth medium/well the day before transfection. Cell medium was replaced with medium supplemented with 1% charcoal-stripped (CS) FBS lacking phenol red and serum on the day of transfection, which was performed using the X-treme Gene 9 reagent as recommended by the manufacturer (Roche Diagnostics, Milan, Italy) with a mixture containing 0.5 µg of reporter plasmid and 2 ng of pRL-TK. After 5-6 hr, ligands were added and cells were incubated for 24 hours. Luciferase activity was then measured using the Dual Luciferase Kit (Promega, Milan, Italy) according to the

manufacturer's recommendations. Firefly luciferase activity was normalized to the internal transfection control provided by the Renilla luciferase activity. The normalized relative light unit values obtained from cells treated with vehicle were set as one-fold induction upon which the activity induced by treatments was calculated. For the gene silencing experiments, cells were plated into 10-cm dishes, transfected in serum-free medium for 24 hours before treatments using X-treme Gene 9 (Roche Diagnostics, Milan, Italy), according to the manufacturer's recommendations with shRNA, shGPER, shER $\alpha$ , DN MAML-1 and the unrelated empty vector.

### **2.9 Wound-healing assay**

SkBr3 cells and CAFs were seeded into 12-well plates in regular growth medium. When at 70% to 80% confluence, the cells were washed once and medium was replaced with 2.5% charcoal-stripped FBS. Cells were then pre-treated with GSI and treated with E2, G-1 and JAG-1. Then, a p200 pipette tip was used to scratch the cell monolayer. We evaluated cell migration in three independent experiments after 24 hours of treatment; data are expressed as a percentage of cells in the wound area upon treatment compared with cells receiving vehicle.

### **2.10 Transwell cell migration assay**

Migration assays were performed with SkBr3 cells and CAFs in triplicate using boyden chambers (Costar Transwell, 8 mm polycarbonate membrane). For knockdown experiments, cells were transfected with the plasmid DN-MAML1 or with an empty vector construct using X-treme Gene 9 reagent in medium without serum. After 24 hours, cells were seeded in the upper chambers. Treatments were added to the medium without serum in the bottom wells. After 24 hours, cells on the bottom side of the membrane were fixed, stained with GIEMSA (Sigma-Aldrich Milan, Italy), photographed and counted.

### **2.11 Statistical analysis**

Statistical analysis was performed using analysis of variance followed by Newman-Keuls testing to determine differences in means. p-Values < 0.05 are considered statistically significant.

### 3 Results

#### 3.1 E2 and G-1 induce Notch-dependent expression of Hes-1

In order to investigate a possible functional interaction between GPER and Notch signaling, we first investigated whether ligand-activated GPER triggers Notch-dependent transcription. Hence, we evaluated the *Hes-1* mRNA expression in SkBr3 cells treated with E2, G-1 or the soluble Notch ligand JAG-1. As shown in Figure 1A-B and in Supplementary Figure 1A, all three ligands induced the levels of *Hes-1* particularly upon 24 hours treatments. To assess the direct involvement of GPER in the up-regulation of *Hes-1*, we transfected SkBr3 cells with a shGPER which abrogated the expression of *Hes-1* induced by E2 and G-1 (Figure 1C-F and Supplementary Figure 1B). In contrast, in SkBr3 cells transfected with the shGPER and exposed to JAG-1, the induction of *Hes-1* was still evident (Figure 1E-F and Supplementary Figure 1B). To confirm the Notch-dependent up-regulation of *Hes-1* by E2 and G-1, we used the  $\gamma$ -secretase inhibitor named GSI which impaired the *Hes-1* response to these treatments along that promoted by JAG-1 as expected (Figure 1G-H and Supplementary Figure 1C). In order to corroborate these results, we transfected SkBr3 cells with a dominant-negative mutant of the Master-mind like 1 (DN-MAML-1), which is a transcriptional co-activator of Notch-1 (Guo et al., 2011). As shown in Figure 1I-J and in Supplementary Figure 1D, the induction of *Hes1* mRNA by E2, G-1 and JAG-1 was no longer observed in presence of DN-MAML-1. To confirm these findings, we also evaluated *Hes-1* protein levels by western blot analysis. As shown in Figure 2A-F, we found in all treatments described above, variations of *Hes-1* protein which reflected those of mRNAs.

Next, to corroborate the role elicited by GPER in mediating the Notch dependent transcription of *Hes-1*, upon E2 and G-1 treatments, we evaluated the expression of *Hes-1* mRNA also using the ER-positive MCF-7 breast cancer cells (Supplementary Figure 2A-H). As previous reports have shown that in ER-positive breast cancer cells low doses of E2 may inhibit Notch activity (Rizzo et al., 2008), we evaluated the expression of *Hes-1* mRNA by increasing concentrations of E2 in both

MCF-7 (ER-positive) and SkBr3 (ER-negative) breast cancer cells. As shown in Supplementary Figure 3A-C, in SkBr3 cells, E2 induces the expression of *Hes-1* mRNA already at concentration of 1 nM. In contrast, in MCF-7 cells the expression of *Hes-1* mRNA was up-regulated only at higher concentrations of E2 (Supplementary Figure 3D-F). Moreover, ER $\alpha$  silencing by shER $\alpha$  had no effect on the up-regulation of *Hes-1* mRNA by E2 (Supplementary Figure 3G-K).

### **3.2 E2 and G-1 induce Notch activation and the recruitment of N1ICD to the *Hes-1* promoter sequence**

Having established that E2 and G-1 trigger *Hes-1* expression in a GSI dependent fashion, we then verified whether these ligands induce the  $\gamma$ -secretase-mediated release of Notch intracellular domain (N1ICD), which is a hallmark of Notch activation. As shown in Figure 3A-B, both E2 and G-1 along with JAG-1 stimulated the membrane-release of N1ICD in a GSI-sensitive manner. In addition, the abrogation of GPER expression by shGPER abolished only the membrane-release of N1ICD induced by E2 and G-1 (Figure 3C-D), suggesting that GPER ligands trigger Notch activation.

As SkBr3 cells express constitutive levels of JAG-1 (data not shown), we asked whether the effects of E2 and G-1 on Notch activation could rely on the up-regulation of *Notch-1* expression. As shown in Figure 3E-H, we found that E2 and G-1 induced both mRNA and protein levels of *Notch-1*, further supporting the aforementioned data.

Performing ChIP experiments in SkBr3 cells, we next determined that E2 and G-1 together with JAG-1 induce in a GSI dependent fashion the recruitment of N1ICD to the RBP-J/CSL binding site located within the *Hes-1* promoter sequence (Figure 4A). In accordance with these results, the transactivation of a *Hes-1* promoter reporter gene induced by E2, G-1 and JAG-1 was no longer evident in presence of GSI (Figure 4B). Taken together, these results suggest that ligand-activated GPER triggers the expression of the Notch target gene *Hes-1* by inducing *Notch-1* expression, the membrane-release of N1ICD which is consequently recruited to the *Hes-1* promoter sequence.

### 3.3 Notch signaling is involved in the migration of SkBr3 cells induced by E2 and G-1

In order to address the biological response to Notch activation upon E2 and G-1 treatment, we evaluated the effects of Notch signaling in the migration of SkBr3 cells. As determined by wound-healing assays, the migration of SkBr3 cells induced by E2 and G-1 as well as JAG-1 was abolished using GSI (Figure 5A and Supplementary Figure 4). Performing boyden chamber assays, we confirmed the aforementioned results (Figure 5B and Supplementary Figure 5A) and we demonstrated that the migration induced by E2, G-1 or JAG-1 is also prevented in SkBr3 cells transfected with DN-MAML-1 (Figure 5C and Supplementary Figure 5B). Moreover, shGPER transfection abolished SkBr3 migration induced by E2 and G-1, whereas JAG-1-induced migration was not affected (Figure 5D and Supplementary Figure 6). Taken together, these data suggest that GPER and Notch signaling pathways are involved in the migration of SkBr3 cells stimulated by E2 and G-1.

### 3.4 E2 and G-1 up-regulate *Snail* and inhibit *VE-Cadherin* expression through the Notch signaling

In different types of cancer cells, the Notch-target gene *Snail* has been shown to repress the expression of cell-cell adhesion molecules, including E-cadherins and vascular endothelial (VE)-cadherin. In this regard, it has been shown that these genes are involved in the epithelial to mesenchymal transition (EMT) which is a biological process regulated by a network of transduction pathways including Notch signaling (Grego-Bessa et al., 2004). Hence, we investigated whether E2 and G-1 induced the expression of *Snail* at both mRNA and protein levels in a Notch-dependent manner. As shown in Figure 6A-D and in Supplementary Figure 7A, we found that E2 and G-1, as well as JAG-1, induced the expression of *Snail* which was abrogated by co-expression of DN-MAML-1. Next, we investigated whether the up-regulation of *Snail* by E2 and G-1 is coupled to an altered expression of cell-cell adhesion molecules. As SkBr3 cells lack *E-Cadherin* expression (Hiraguri et al., 1998), we evaluated the response of *VE-Cadherin*, which is expressed in SkBr3



cells (Endo et al., 2008). As shown in Figure 6E-H and in Supplementary Figure 7B, E2 and G-1 reduced the expression of *VE-Cadherin* at both mRNA and protein levels, in a GSI-sensitive fashion.

### 3.5 The GPER and Notch pathways cooperate in cancer-associated fibroblasts (CAFs)

Given the relevant contribution of the microenvironment to cancer cell growth and invasiveness (Kalluri and Zeisberg, 2006), we examined whether the cross-talk between Notch and GPER signaling pathways occurs in CAFs which play a pivotal role in the functional interaction between stroma and cancer cells towards tumor progression. Hence, we determined that GPER mediates the mRNA and protein expression of *Hes-1* induced by E2 and G-1 in CAFs obtained from breast cancer patients, whereas the *Hes-1* response to JAG-1 was not altered transfecting cells with a shGPER (Figure 7A-F). Using GSI, the up-regulation of *Hes-1*, at both mRNA and protein levels, triggered by all agents was no longer observed (Figure 7G-J). As biological counterpart, the migration of CAFs stimulated by E2, G-1 and JAG-1 was abolished using GSI, as assessed performing both wound-healing and boyden chamber assays (Figure 8A-B, Supplementary Figure 8 and Supplementary Figure 9). Collectively, these data confirmed the results obtained in breast cancer cells and extended the potential of E2 and G-1 to engage the Notch signaling through GPER in main components of the tumor microenvironment like CAFs

#### 4 Discussion

A wide number of studies have shown that the functional interactions among steroid receptors and growth factor receptors play a crucial role towards breast cancer progression (Bartella et al., 2012; Lappano et al., 2013; Vivacqua et al., 2009). In this regard, the estrogen action mediated by GPER via EGFR activation has made clear that GPER may facilitate the response to estrogens independently of the classical ERs. Accordingly, the functional cross-talk between GPER and EGFR has been documented in different types of malignancies and involved in relevant biological outcomes like the proliferation and migration of cancer cells (Maggiolini and Picard, 2010).

On the other side, deregulation of the Notch pathway by oncogenic signaling represents a further crossroad in tumor growth and invasion (Guo et al., 2011; Rizzo et al., 2008). In particular, the Notch interaction with ER-mediated signaling as well as growth factor receptors has been shown in breast cancer cells (Al-Hussaini et al., 2011; Guo et al., 2011; Osipo et al., 2008; Rizzo et al., 2008). Therefore, the response of breast cancer cells to estrogens may be dependent on the repertoire of receptors expressed in different cell contexts and the downstream transduction pathways that functionally cooperate towards tumor progression.

In the present study, we have used the ER-negative SkBr3 breast cancer cells in order to evaluate in a peculiar model system the potential cross talk between the Notch pathway and the GPER signaling. Worthy, we provide novel evidence showing that ligand-activated GPER triggers Notch-mediated gene expression changes and biological responses as cell migration. These findings were confirmed in CAFs derived from breast cancer patients, suggesting that the GPER/Notch signaling may be engaged by estrogens also in the tumor microenvironment that mainly contribute to tumor development (Kalluri and Zeisberg, 2006).

As the activation of the Notch transduction pathway induces the nuclear translocation of N1ICD and the transactivation of Notch-target genes (Miele, 2006), we initially assessed whether the ligand-activated GPER could stimulate the expression of one main Notch-regulated gene like *Hes-*

1. Three independent lines of evidence support that indeed this is the case: (i) E2 and the selective GPER ligand G-1 increased the mRNA levels of *Hes-1*, (ii) E2 and G-1 triggered both the release of the Notch-1 intracellular domain (N1ICD) and its recruitments to the *Hes-1* promoter sequence, (iii) E2 and G-1 transactivated the *Hes-1* promoter, hence recapitulating the aforementioned findings. Notably, *Hes-1* up regulation by E2 or G-1 was confirmed also in ER-positive MCF-7 cells. Interestingly, our results (see Supplementary Figure 3) show that high doses of E2 (100nM) were necessary to induce *Hes-1* expression in MCF-7 cells, whereas *Hes-1* induction was already achieved at low dosage of E2 (1nM) in SkBr3 cells. Moreover, we found that knockdown of ER $\alpha$  expression had no effect on *Hes-1* up-regulation in MCF-7 cells, whereas GPER silencing completely abrogated *Hes-1* up-regulation by E2 or G-1. These results indicate that ER-positive and ER-negative breast cancer cells have a different dose-response to E2, presumably relying on the different binding affinity of E2 for ER $\alpha$  and GPER, as demonstrated in previous studies (Revankar et al., 2005; Thomas et al., 2005). Importantly, the dose response curve of E2 on *Hes-1* expression in MCF-7 cells overcomes the apparent discrepancy between our data and the previous study by Rizzo and colleagues, showing that low doses of E2 reduce Delta-dependent activation of Notch signalling (Rizzo et al., 2008).

The ability of E2 and G-1 to trigger Notch-dependent transcription was clearly demonstrated by the evidence that the up-regulation of *Hes-1* was abolished by using both GSI or DN-MAML-1, a dominant-negative mutant of Master-mind like 1, which is a Notch-1 transcriptional co-activator (Wu and Griffin, 2004). Likewise, the knockdown of GPER abrogated both the induction of *Hes-1* and the release of N1ICD upon E2 and G-1 treatments, hence demonstrating the involvement of GPER in the activation of Notch signaling by these ligands.

The mechanism through which GPER leads to *Notch-1* activation seems to be transcriptional, as an increase of *Notch-1* mRNA levels was found in response to E2 and G-1. Remarkably, this increase preceded the induction of the *Hes-1* mRNA levels (see Figure 1A-B and Figure 3E-F), suggesting

that the deregulation of Notch-1 expression mediates the effects elicited by GPER on both Notch activation and Notch-dependent transcription. Conversely, in SkBr3 cells the constitutive JAGGED-1 expression was not altered by E2 and G-1 (data not shown), indicating that the boost of Notch induced by E2 and G-1 is sufficient to activate the Notch signaling. Accordingly, it has been reported that high *Notch-1* levels are associated with a poor prognosis in breast cancer (Al-Hussaini et al., 2011). Although the molecular mechanisms involved in the induction of Notch-1 by GPER remain to be fully elucidated, the cross talk between GPER and EGFR may be ruled out, as the inhibition of EGFR does not interfere with the up-regulation of *Hes-1* induced by E2 or G-1 (our published data). In this regard, further studies are required to investigate whether GPER may trigger the expression of Notch-1 through other transduction mechanisms.

The aforementioned findings were recapitulated and further highlighted by evaluating the role of Notch in a relevant biological response like cell migration. Of note, the ability of E2 and G-1 to stimulate the migration of SkBr3 cells was abolished using GSI or DM-MALM-1, hence indicating that both Notch activation and Notch-dependent transcription contribute to the migratory effects elicited by E2 and G-1.

The invasive and migratory ability of cancer cells have been previously associated with EMT (Matsuno et al., 2012; Thiery, 2002), that particularly in breast tumor involved the deregulation of E-cadherin expression through Notch and its target gene *Snail* (Wang et al., 2010) In this regard, the up-regulation of *Snail* coupled to an altered expression of *VE-cadherin* induced by E2 and G-1 in a GSI-dependent fashion, further corroborates the contribution of the Notch-dependent transcription in cell migration and EMT triggered by these ligands.

Our results demonstrate for the first time that estrogen-activated GPER engages Notch signaling towards gene expression changes and biological responses in breast tumor cells and CAFs, hence providing a further mechanism through which estrogens may stimulate the progression of breast cancer.

**Acknowledgements**

This work was supported by Associazione Italiana per la Ricerca sul Cancro (AIRC, project n.12849/2012), AIRC project Calabria 2011 and Fondazione Cassa di Risparmio di Calabria e Lucania.

Accepted Manuscript

## References

- Albanito L, Lappano R, Madeo A, Chimento A, Prossnitz ER, Cappello AR, Dolce V, Abonante S, Pezzi V, Maggiolini M. G-protein-coupled receptor 30 and estrogen receptor-alpha are involved in the proliferative effects induced by atrazine in ovarian cancer cells. *Environ Health Perspect* 2008a; 116: 1648-1655.
- Albanito L, Madeo A, Lappano R, Vivacqua A, Rago V, Carpino A, Oprea TI, Prossnitz ER, Musti AM, Andò S, Maggiolini M. G protein-coupled receptor 30 (GPR30) mediates gene expression changes and growth response to 17 $\beta$ -estradiol and selective GPR30 ligand G-1 in ovarian cancer cells. *Cancer Res* 2007; 67: 1859-1866.
- Albanito L, Sisci D, Aquila S, Brunelli E, Vivacqua A, Madeo A, Lappano R, Pandey DP, Picard D, Mauro L, Andò S, Maggiolini M. Epidermal growth factor induces G protein-coupled receptor 30 expression in estrogen receptor-negative breast cancer cells. *Endocrinology* 2008b; 149: 3799-3808.
- Al-Hussaini H, Subramanyam D, Reedijk M, Sridhar SS. Notch signaling pathway as a therapeutic target in breast cancer. *Mol Cancer Ther* 2011; 10: 9-15.
- Ascenzi P, Bocedi A, Marino M. Structure–function relationship of estrogen receptor alpha and beta: impact on human health. *Mol Aspects Med* 2006; 27: 299-402.
- Bartella V, De Marco P, Malaguarnera R, Belfiore A, Maggiolini M. New advances on the functional cross-talk between insulin-like growth factor-I and estrogen signaling in cancer. *Cell Signal* 2012; 24: 1515-1521.
- Bologa CG, Revankar CM, Young SM, Edwards BS, Arterburn JB, Kiselyov AS, Parker MA, Tkachenko SE, Savchuck NP, Sklar LA, Oprea TI, Prossnitz ER. Virtual and biomolecular screening converge on a selective agonist for GPR30. *Nat Chem Biol* 2006; 2: 207-212.

- Chen J, Imanaka N, Chen J, Griffin JD. Hypoxia potentiates Notch signaling in breast cancer leading to decreased E-cadherin expression and increased cell migration and invasion. *British Journal of Cancer* 2010; 102: 351-360.
- Chimento A, Sirianni R, Casaburi I, Ruggiero C, Maggiolini M, Andò S, Pezzi V. 17 $\beta$ -Estradiol activates GPER- and ESR1-dependent pathways inducing apoptosis in GC-2 cells, a mouse spermatocyte-derived cell line. *Mol Cell Endocrinol* 2012; 355: 49-59.
- De Marco P, Bartella V, Vivacqua A, Lappano R, Santolla MF, Morcavallo A, Pezzi V, Belfiore A, Maggiolini M. Insulin-like growth factor-I regulates GPER expression and function in cancer cells. *Oncogene* 2013; 32: 678-688.
- Dennis MK, Field AS, Burai R, Ramesh C, Petrie WK, Bologna CG, Oprea TI, Yamaguchi Y, Hayashi S, Sklar LA, Hathaway HJ, Arterburn JB, Prossnitz ER. Identification of a GPER/GPR30 antagonist with improved estrogen receptor counterselectivity. *J Steroid Biochem Mol Biol* 2011; 127: 358-366.
- Endo Y, Deonauth K, Prahalad P, Hoxter B, Zhu Y, Byers SW. Role of Sox-9, ER81 and VE-cadherin in retinoic acid-mediated trans-differentiation of breast cancer cells. *PLoS One* 2008; 3: e2714.
- Filice E, Recchia AG, Pellegrino D, Angelone T, Maggiolini M, Cerra MC. A new membrane G protein-coupled receptor (GPR30) is involved in the cardiac effects of 17beta-estradiol in the male rat. *J Physiol Pharmacol* 2009; 60: 3-10.
- Grego-Bessa J, Díez J, Timmerman L, de la Pompa JL. Notch and epithelial-mesenchyme transition in development and tumor progression: another turn of the screw. *Cell Cycle* 2004; 3: 718-721.

- Guo S, Liu M, Gonzalez-Perez RR. Role of Notch and its oncogenic signaling crosstalk in breast cancer. *Biochim Biophys Acta* 2011; 15: 197-213.
- Hiraguri S, Godfrey T, Nakamura H, Graff J, Collins C, Shayesteh L, Doggett N, Johnson K, Wheelock M, Herman J, Baylin S, Pinkel D, Gray J. Mechanisms of inactivation of E-cadherin in breast cancer cell lines. *Cancer Res* 1998; 58: 1972-1977.
- Iso T, Kedes L, Hamamori Y. HES and HERP families: multiple effectors of the Notch signaling pathway. *J Cell Physiol* 2003; 194: 237-255.
- Kalluri R, Zeisberg M. Fibroblasts in cancer. *Nat Rev Cancer* 2006; 6: 392-401.
- Kopan R, Ilagan MX. The canonical Notch signaling pathway: unfolding the activation mechanism. *Cell* 2009; 137: 216-233.
- Lappano R, De Marco P, De Francesco EM, Chimento A, Pezzi V, Maggiolini M. Cross-talk between GPER and growth factor signaling. *J Steroid Biochem Mol Biol* 2013; doi: 10.1016/j.jsbmb.2013.03.005.
- Lappano R, Recchia AG, De Francesco EM, Angelone T, Cerra MC, Picard D, Maggiolini M: The cholesterol metabolite 25-hydroxycholesterol activates estrogen receptor  $\alpha$ -mediated signaling in cancer cells and in cardiomyocytes. *PLoS One* 2011; 6: e16631.
- Lappano R, Rosano C, De Marco P, De Francesco EM, Pezzi V, Maggiolini M. Estriol acts as a GPR30 antagonist in estrogen receptor-negative breast cancer cells. *Mol Cell Endocrinol* 2010; 320: 162-170.
- Lappano R, Rosano C, Santolla MF, Pupo M, De Francesco EM, De Marco P, Ponassi M, Spallarossa A, Ranise A, Maggiolini M. Two novel GPER agonists induce gene expression changes and growth effects in cancer cells. *Curr Cancer Drug Targets* 2012a; 12: 531-542.



- Lappano R, Santolla MF, Pupo M, Sinicropi MS, Caruso A, Rosano C, Maggiolini M. MIBE acts as antagonist ligand of both estrogen receptor  $\alpha$  and GPER in breast cancer cells. *Breast Cancer Res* 2012b; 14: R12.
- Liang J, Shang Y. Estrogen and cancer. *Annual Review of Physiology* 2013; 75: 225-240.
- Madeo A, Maggiolini M. Nuclear alternate estrogen receptor GPR30 mediates 17 $\beta$ estradiol-induced gene expression and migration in breast cancer-associated fibroblasts. *Cancer Res* 2010; 70: 6036-6046.
- Madeo A, Vinciguerra M, Lappano R, Galgani M, Gasperi-Campani A, Maggiolini M, Musti AM. c-Jun activation is required for 4-hydroxytamoxifen-induced cell death in breast cancer cells. *Oncogene* 2010; 29: 978-991.
- Maggiolini M, Donzé O, Picard D. A non-radioactive method for inexpensive quantitative RT-PCR. *Biol Chem* 1999; 380: 695-697.
- Maggiolini M, Picard D. The unfolding stories of GPR30, a new membrane-bound estrogen receptor. *J Endocrinol* 2010; 204: 105-114.
- Maggiolini M, Vivacqua A, Fasanella G, Recchia AG, Sisci D, Pezzi V, Montanaro D, Musti AM, Picard D, Andò S. The G protein-coupled receptor GPR30 mediates c-fos up-regulation by 17 $\beta$ -estradiol and phytoestrogens in breast cancer cells. *J Biol Chem* 2004; 279: 27008-27016.
- Matsuno Y, Coelho AL, Jarai G, Westwick J, Hogaboam CM. Notch signaling mediates TGF- $\beta$ 1-induced epithelial-mesenchymal transition through the induction of Snai1. *Int J Biochem Cell Biol* 2012; 44: 776-789.
- Miele L. Notch signaling. *Clin Cancer Res* 2006; 12: 1074-1079.

- Osipo C, Patel P, Rizzo P, Clementz AG, Hao L, Golde TE, Miele L. ErbB-2 inhibition activates Notch-1 and sensitizes breast cancer cells to a gamma-secretase inhibitor. *Oncogene* 2008; 27: 5019-5032.
- Pandey DP, Lappano R, Albanito L, Madeo A, Maggiolini M, Picard D. Estrogenic GPR30 signalling induces proliferation and migration of breast cancer cells through CTGF. *EMBO J* 2009; 28: 523-532.
- Panno ML, Salerno M, Pezzi V, Sisci D, Maggiolini M, Mauro L, Morrone EG, Andò S. Effect of oestradiol and insulin on the proliferative pattern and on oestrogen and progesterone receptor contents in MCF-7 cells. *J Cancer Res Clin Oncol* 1996; 122: 745-749.
- Pupo M, Pisano A, Lappano R, Santolla MF, De Francesco EM, Abonante S, Rosano C, Maggiolini M. Bisphenol A induces gene expression changes and proliferative effects through GPER in breast cancer cells and cancer-associated fibroblasts. *Environ Health Perspect* 2012; 120: 1177-1182.
- Pupo M, Vivacqua A, Perrotta I, Pisano A, Aquila S, Abonante S, Gasperi-Campani A, Pezzi V, Maggiolini M. The nuclear localization signal is required for nuclear GPER translocation and function in breast Cancer-Associated Fibroblasts (CAFs). *Mol Cell Endocrinol* 2013; 376: 23-32.
- Recchia AG, De Francesco EM, Vivacqua A, Sisci D, Panno ML, Andò S, Maggiolini M. The G protein-coupled receptor 30 is up-regulated by hypoxia inducible factor-1 $\alpha$ (HIF-1 $\alpha$ ) in breast cancer cells and cardiomyocytes. *J Biol Chem* 2011; 286: 10773-10782.
- Reedijk M, Odorcic S, Chang L, Zhang H, Miller N, McCready DR, Lockwood G, Egan SE. High-level coexpression of JAG1 and NOTCH1 is observed in human breast cancer and is associated with poor overall survival. *Cancer Res*; 2005 65: 8530-8537.

Revankar CM, Cimino DF, Sklar LA, Arterburn JB, Prossnitz ER. A transmembrane intracellular estrogen receptor mediates rapid cell signalling. *Science*; 2005 307: 1625-1630.

Rizzo P, Miao H, D'Souza G, Osipo C, Song LL, Yun J, Zhao H, Mascarenhas J, Wyatt D, Antico G, Hao L, Yao K, Rajan P, Hicks C, Siziopikou K, Selvaggi S, Bashir A, Bhandari D, Marchese A, Lendahl U, Qin JZ, Tonetti DA, Albain K, Nickoloff BJ, Miele L. Cross-talk between notch and the estrogen receptor in breast cancer suggests novel therapeutic approaches. *Cancer Res* 2008; 68: 5226-5235.

Rizzo P, Osipo C, Foreman K, Golde T, Osborne B, Miele L. Rational targeting of Notch signaling in cancer. *Oncogene* 2008; 27: 5124-5131.

Rosano C, Lappano R, Santolla MF, Ponassi M, Donadini A, Maggiolini M. Recent advances in the rationale design of GPER ligands. *Curr Med Chem* 2012; 19: 6199-6206.

Santolla MF, Lappano R, De Marco P, Pupo M, Vivacqua A, Sisci D, Abonante S, Iacopetta D, Cappello AR, Dolce V, Maggiolini M. GPER mediates the up-regulation of fatty acid synthase (FASN) induced by 17 $\beta$ -estradiol in cancer cells and cancer-associated fibroblasts (CAFs). *J Biol Chem* 2012; 287: 43234-43245.

Thiery JP. Epithelial-mesenchymal transitions in tumour progression. *Nat Rev Cancer* 2002; 2: 442-454.

Thomas P, Pang Y, Filardo EJ, Dong J. Identity of an estrogen membrane receptor coupled to a G protein in human breast cancer cells. *Endocrinology* 2005; 146: 624-632.

Vivacqua A, Bonofiglio D, Albanito L, Madeo A, Rago V, Carpino A, Musti AM, Picard D, Andò S, Maggiolini M. 17 $\beta$ -Estradiol, genistein, and 4-hydroxytamoxifen induce the proliferation of

thyroid cancer cells through the G protein coupled-receptor GPR30. *Mol Pharmacol* 2006a; 70: 1414-1423.

Vivacqua A, Bonofiglio D, Recchia AG, Musti AM, Picard D, Andò S, Maggiolini M. The G protein-coupled receptor GPR30 mediates the proliferative effects induced by 17 $\beta$ -estradiol and hydroxytamoxifen in endometrial cancer cells. *Mol Endocrinol* 2006b; 20: 631-646.

Vivacqua A, Lappano R, De Marco P, Sisci D, Aquila S, De Amicis F, Fuqua SA, Andò S, Maggiolini M. G protein-coupled receptor 30 expression is up-regulated by EGF and TGF  $\alpha$  in estrogen receptor alpha-positive cancer cells. *Mol Endocrinol* 2009; 23: 1815-1826.

Vivacqua A, Romeo E, De Marco P, De Francesco EM, Abonante S, Maggiolini M. GPER mediates the Egr-1 expression induced by 17 $\beta$ -estradiol and 4-hydroxytamoxifen in breast and endometrial cancer cells. *Breast Cancer Res Treat* 2012; 133: 1025-1035.

Wang Z, Li Y, Kong D, Sarkar FH. The role of Notch signaling pathway in epithelial-mesenchymal transition (EMT) during development and tumor aggressiveness. *Curr Drug Targets* 2010; 11: 745-751.

Wu L, Griffin JD. Modulation of Notch signaling by mastermind-like (MAML) transcriptional co-activators and their involvement in tumorigenesis. *Semin Cancer Biol* 2004; 14: 348-356.

Yin L, Velazquez OC, Liu ZJ. Notch signaling: emerging molecular targets for cancer therapy. *Biochem Pharmacol* 2010; 80: 690-701.

## Figure legends

### Figure 1: Ligand-activated GPER induces the Notch-dependent expression of *Hes-1* mRNA in SkBr3 breast cancer cells

(A) mRNA expression of *Hes-1* in SkBr3 cells treated with 100 nM E2, 1  $\mu$ M G-1 and 1  $\mu$ M JAG-1, as indicated. (B) Densitometric analysis of *Hes-1* mRNA expressions normalized to *RPLP0*. (C) Immunoblots of GPER expression in SkBr3 cells transfected for 48 hours with shRNA or shGPER. (D) Densitometric analysis of GPER expressions normalized to beta-actin. (E) Expression of *Hes-1* mRNA in SkBr3 cells transfected with shRNA or shGPER for 24 hours and then treated with 100 nM E2, 1  $\mu$ M G-1 and 1  $\mu$ M JAG-1 for additional 24 hours. (F) Densitometric analysis of *Hes-1* mRNA expressions normalized to *RPLP0*. (G) mRNA expression of *Hes-1* in SkBr3 cells treated for 24 hours with 100 nM E2, 1  $\mu$ M G-1 and 1  $\mu$ M JAG-1 alone or in combination with 100 nM of  $\gamma$ -secretase inhibitor (GSI). (H) Densitometric analysis of *Hes-1* mRNA expressions normalized to *RPLP0*. (I) mRNA expression of *Hes-1* in SkBr3 cells transfected for 24 hours with an empty vector or a dominant-negative mutant of the Master-mind like 1 (DN-MAML-1) and then treated for additional 24 hours with 100 nM E2, 1  $\mu$ M G-1 and 1  $\mu$ M JAG-1. (J) Densitometric analysis of *Hes-1* mRNA expressions normalized to *RPLP0*. Columns represent the mean  $\pm$  SD of three independent experiments. ( $\circ$ ), ( $\bullet$ ), ( $\square$ ) Indicate  $P < 0.05$  for cells receiving vehicle (-) versus treatments. In panel D, ( $\circ$ ) indicates  $P < 0.05$  for cells transfected with shRNA respect to cells transfected with shGPER

### Figure 2: Ligand-activated GPER induced the Notch-dependent expression of *Hes-1* at protein level in SkBr3 breast cancer cells

(A) Immunoblots of *Hes-1* protein expression in SkBr3 cells transfected for 24 hours with a shRNA or shGPER and then treated for additional 24 hours with 100 nM E2, 1  $\mu$ M G-1 and 1  $\mu$ M JAG-1. (B) Densitometric analysis of *Hes-1* protein expressions normalized to beta-actin. (C) *Hes-1* protein expression in SkBr3 cells treated for 24 hours with 100 nM E2, 1  $\mu$ M G-1 and 1  $\mu$ M JAG-1 alone or

in combination with 100 nM of  $\gamma$ -secretase inhibitor (GSI). (D) Densitometric analysis of *Hes-1* protein expressions normalized to beta-actin. (E) *Hes-1* protein expression in SkBr3 cells transfected for 24 hours with an empty vector or a dominant-negative mutant of the Master-mind like 1 (DN-MAML-1) and then treated for additional 24 hours with 100 nM E2, 1  $\mu$ M G-1 and 1  $\mu$ M JAG-1. (F) Densitometric analysis of *Hes-1* protein expressions normalized to beta-actin. Columns represent the mean  $\pm$  SD of three independent experiments. ( $\circ$ ), ( $\bullet$ ) Indicate  $P < 0.05$  for cells receiving vehicle (-) versus treatments.

**Figure 3: Ligand-activated GPER up-regulates the expression of both N1ICD and *Notch-1* in SkBr3 breast cancer cells**

(A) N1ICD protein expression in SkBr3 cells treated for 24 hours with 100 nM E2, 1  $\mu$ M G-1 and 1  $\mu$ M JAG-1 alone or in combination with 100 nM of  $\gamma$ -secretase inhibitor (GSI). (B) Densitometric analysis of N1ICD protein expressions normalized to beta-actin. (C) N1ICD protein expression in SkBr3 cells transfected for 24 hours with a shRNA or shGPER and then treated for additional 24 hours with 100 nM E2, 1  $\mu$ M G-1 and 1  $\mu$ M JAG-1. (D) Densitometric analysis of N1ICD protein expressions normalized to beta-actin. (E) mRNA expression of *Notch-1* in SkBr3 cells treated with 100 nM E2 and 1  $\mu$ M G-1, as indicated. (F) Densitometric analysis of *Notch-1* mRNA expressions normalized to *RPLP0*. (G) *Notch-1* full length (*Notch-1 FL*) protein expression in SkBr3 cells treated for 8 hours with 100 nM E2 and 1  $\mu$ M G-1. (H) Densitometric analysis of *Notch-1 FL* protein expressions normalized to beta-actin. Columns represent the mean  $\pm$  SD of three independent experiments. ( $\circ$ ), ( $\bullet$ ) Indicate  $P < 0.05$  for cells receiving vehicle (-) versus treatments.

**Figure 4: Ligand-activated GPER induces both the recruitment of N1ICD to *Hes-1* promoter and the transactivation of a *Hes-1* promoter reporter gene in SkBr3 cells**

(A) The recruitment of N1ICD to the RBP-J site located within the *Hes-1* promoter induced in SkBr3 cells treated for 8 hours with 100 nM E2, 1  $\mu$ M G-1 and 1  $\mu$ M JAG-1 was abolished treating cells also with 100 nM of  $\gamma$ -secretase inhibitor (GSI). The amplified sequences were evaluated by

real-time PCR. Bar graphs show the mean  $\pm$ SD of three independent experiments. (B) SkBr3 cells were transfected with a *Hes-1* promoter reporter gene plasmid and then treated for 24 hours with 100 nM E2, 1  $\mu$ M G-1 and 1  $\mu$ M JAG-1 alone or in combination with 100 nM GSI. The luciferase activities were normalized to the internal transfection control, and values of cells receiving vehicle (-) were set as 1-fold induction upon which the activity induced by treatments was calculated. Bar graphs represent the mean  $\pm$ SD of three independent experiments each performed in triplicate. (○) Indicates  $P < 0.05$  for cells receiving vehicle (-) versus treatments.

**Figure 5: Inhibition of Notch signaling abrogates the migration of SkBr3 cells induced by E2, G-1 and JAG-1**

The migration of SkBr3 cells evaluated by wound-healing (A) and boyden chamber assays (B) upon exposure to 100 nM E2, 1  $\mu$ M G-1 and 1  $\mu$ M JAG-1 for 24 hours was abolished in presence of 100 nM of  $\gamma$ -secretase inhibitor (GSI). The migration of SkBr3 cells evaluated by boyden chamber assays (C) upon exposure to 100 nM E2, 1  $\mu$ M G-1 and 1  $\mu$ M JAG-1 for 24 hours was abolished transfecting cells with a dominant-negative mutant of the Master-mind like 1 (DN-MAML-1). The migratory effects stimulated by E2 and G-1 were abrogated transfecting cells with shGPER (D). Columns show mean of three independent experiments done in triplicate and standardized to cells receiving vehicle (-), bars represent SD. (○) Indicates  $P < 0.05$  for cells receiving vehicle (-) versus treatments.

**Figure 6: Notch signaling is required for up-regulation of *Snail* and inhibition of *VE-Cadherin* expression in SkBr3 cells**

(A) The up-regulation of the *Snail* mRNA expression induced in SkBr3 cells by a 24 hours exposure to 100 nM E2, 1  $\mu$ M G-1 and 1  $\mu$ M JAG-1 was abolished transfecting cells for 24 hours with a dominant-negative mutant of the Master-mind like 1 (DN-MAML-1) before treatments. (B) Densitometric analysis of *Snail* mRNA expressions normalized to *RPLP0*. (C) The induction of the *Snail* protein expression stimulated in SkBr3 cells by a 24 hours treatment with 100 nM E2, 1  $\mu$ M

G-1 and 1  $\mu$ M JAG-1 was abrogated transfecting cells for 24 hours with a dominant-negative mutant of the Master-mind like 1 (DN-MAML-1) before treatments. (D) Densitometric analysis of *Snail* protein expressions normalized to beta-actin. (E) The down-regulation of *VE-Cadherin* mRNA expression in SkBr3 cells treated for 24 hours with 100 nM E2, 1  $\mu$ M G-1 and 1  $\mu$ M JAG-1 was rescued treating cells with 100 nM of the  $\gamma$ -secretase inhibitor (GSI). (F) Densitometric analysis of *VE-Cadherin* mRNA expressions normalized to *RPLP0*. (G) The reduction of *VE-Cadherin* protein expression in SkBr3 cells treated for 24 hours with 100 nM E2, 1  $\mu$ M G-1 and 1  $\mu$ M JAG-1 was prevented treating cells with 100 nM of the  $\gamma$ -secretase inhibitor (GSI). (H) Densitometric analysis of *VE-Cadherin* protein expressions normalized to beta-actin. Columns represent the mean  $\pm$  SD of three independent experiments. ( $\circ$ ) Indicates  $P < 0.05$  for cells receiving vehicle (-) versus treatments.

**Figure 7: Ligand-activated GPER induces *Hes-1* expression in CAFs.**

(A) Evaluation of *Hes-1* mRNA expression in CAFs transfected for 24 hours with a shRNA or a shGPER and treated for 8 hours with 100 nM E2, 1  $\mu$ M G-1 and 1  $\mu$ M JAG-1. (B) Densitometric analysis of *Hes-1* mRNA expressions normalized to *RPLP0*. (C) Immunoblots of *Hes-1* protein expression in CAFs transfected for 24 hours with a shRNA or shGPER and then treated for additional 18 hours with 100 nM E2, 1  $\mu$ M G-1 and 1  $\mu$ M JAG-1. (D) Densitometric analysis of *Hes-1* protein expressions normalized to beta-actin. (E) Immunoblots of GPER expression in CAFs transfected for 48 hours with shRNA or shGPER. (F) Densitometric analysis of GPER expressions normalized to beta-actin, (G) Evaluation of *Hes-1* mRNA expression in CAFs treated for 8 hours with 100 nM E2, 1  $\mu$ M G-1 and 1  $\mu$ M JAG-1 alone or in combination with 100 nM of the  $\gamma$ -secretase inhibitor (GSI). (H) Densitometric analysis of *Hes-1* mRNA expressions normalized to *RPLP0*. (I) *Hes-1* protein expression in CAFs treated for 8 hours with 100 nM E2, 1  $\mu$ M G-1 and 1  $\mu$ M JAG-1 alone or in combination with 100 nM of  $\gamma$ -secretase inhibitor (GSI). (J) Densitometric analysis of *Hes-1* protein expressions normalized to beta-actin. Columns represent the mean  $\pm$  SD



of three independent experiments. (○), (●) Indicate  $P < 0.05$  for cells receiving vehicle (-) versus treatments. In panel F, (○) indicates  $P < 0.05$  for cells transfected with shRNA respect to cells transfected with shGPER.

**Figure 8: Inhibition of Notch signaling abolishes the migratory effects stimulated by E2, G-1 and JAG-1 in CAFs.**

(A) Wound-healing and (B) boyden chamber assays performed in CAFs to evaluate the migration in presence of 100 nM E2, 1  $\mu$ M G-1 and 1  $\mu$ M JAG-1 alone or in combination with 100 nM of the  $\gamma$ -secretase inhibitor (GSI). Bar graphs show representative experiments with means of triplicate samples. Results were standardized to data of cells receiving vehicle which were set to 100%. (○), Indicates  $P < 0.05$  for cells receiving vehicle (-) versus treatments.

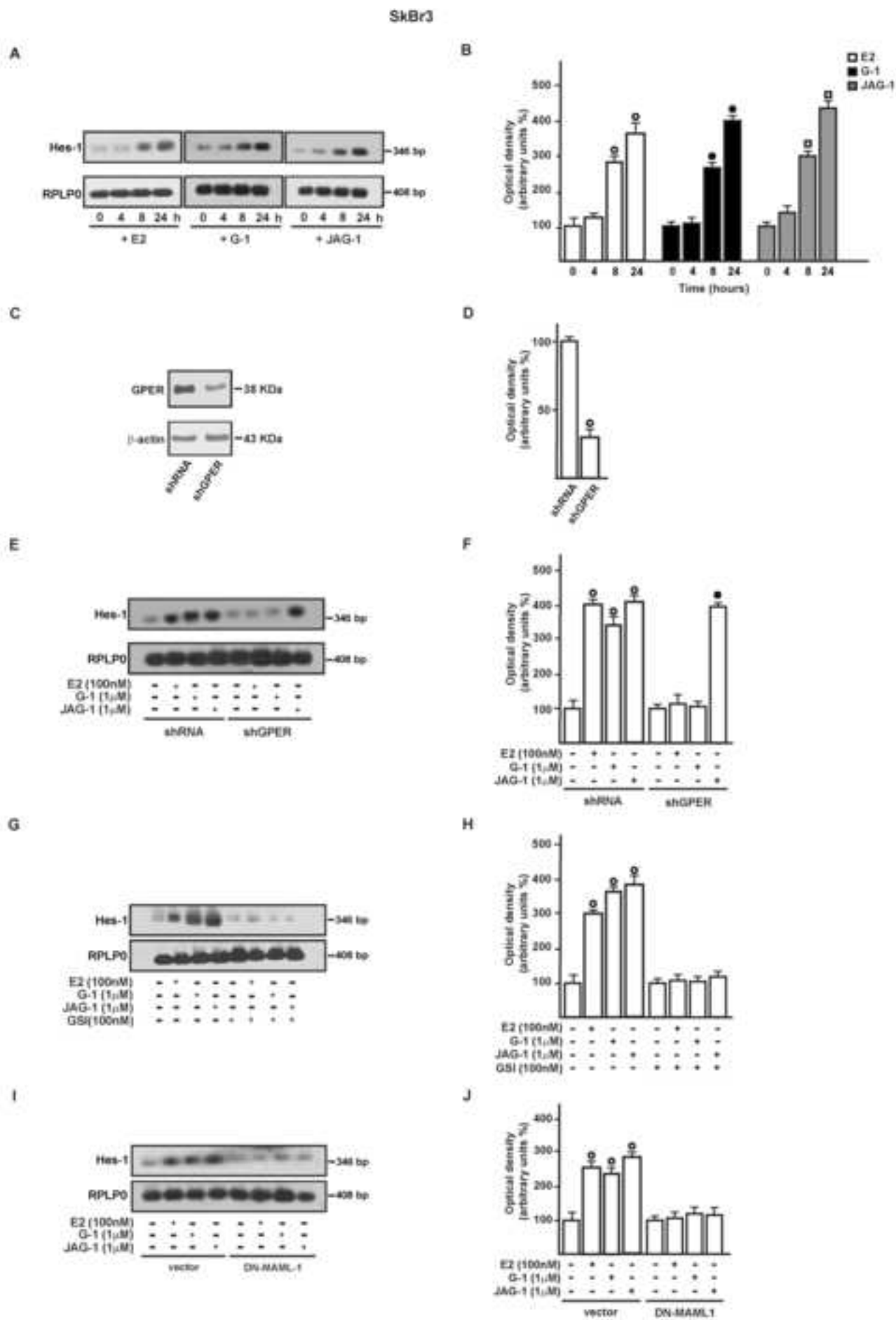
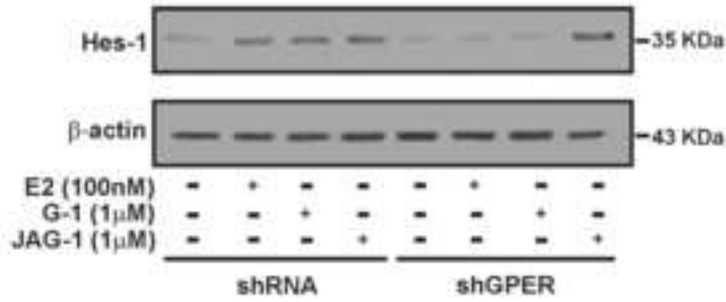


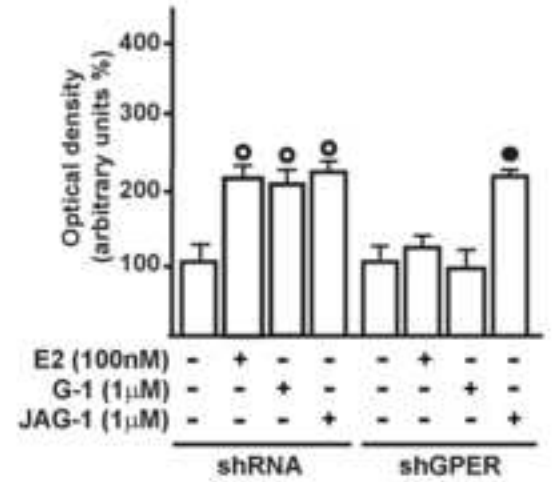
Fig. 1

## SkBr3

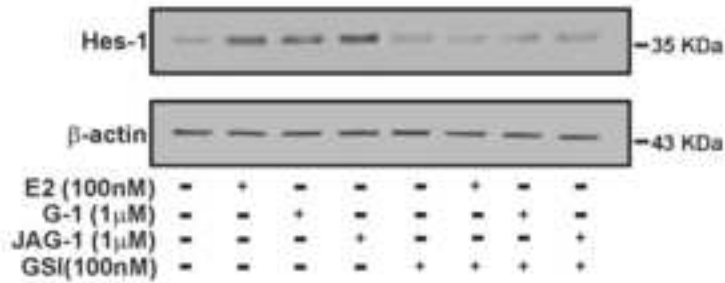
A



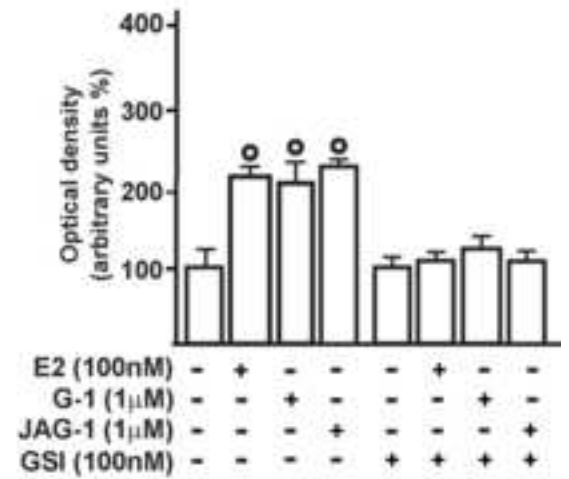
B



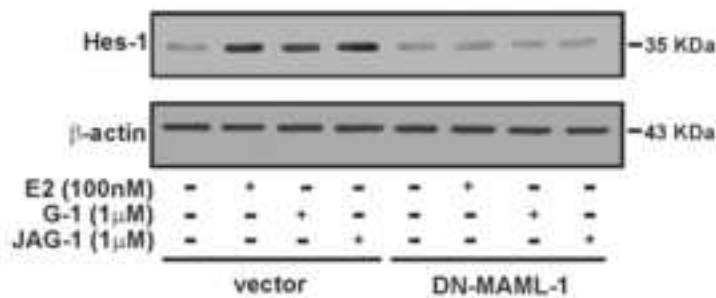
C



D



E



F

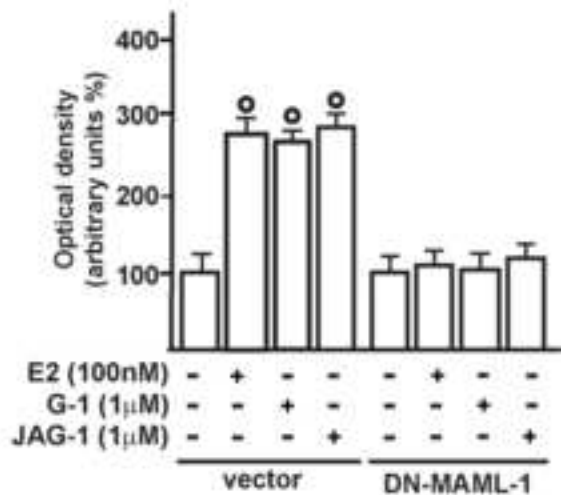


Fig. 2

## SkBr3

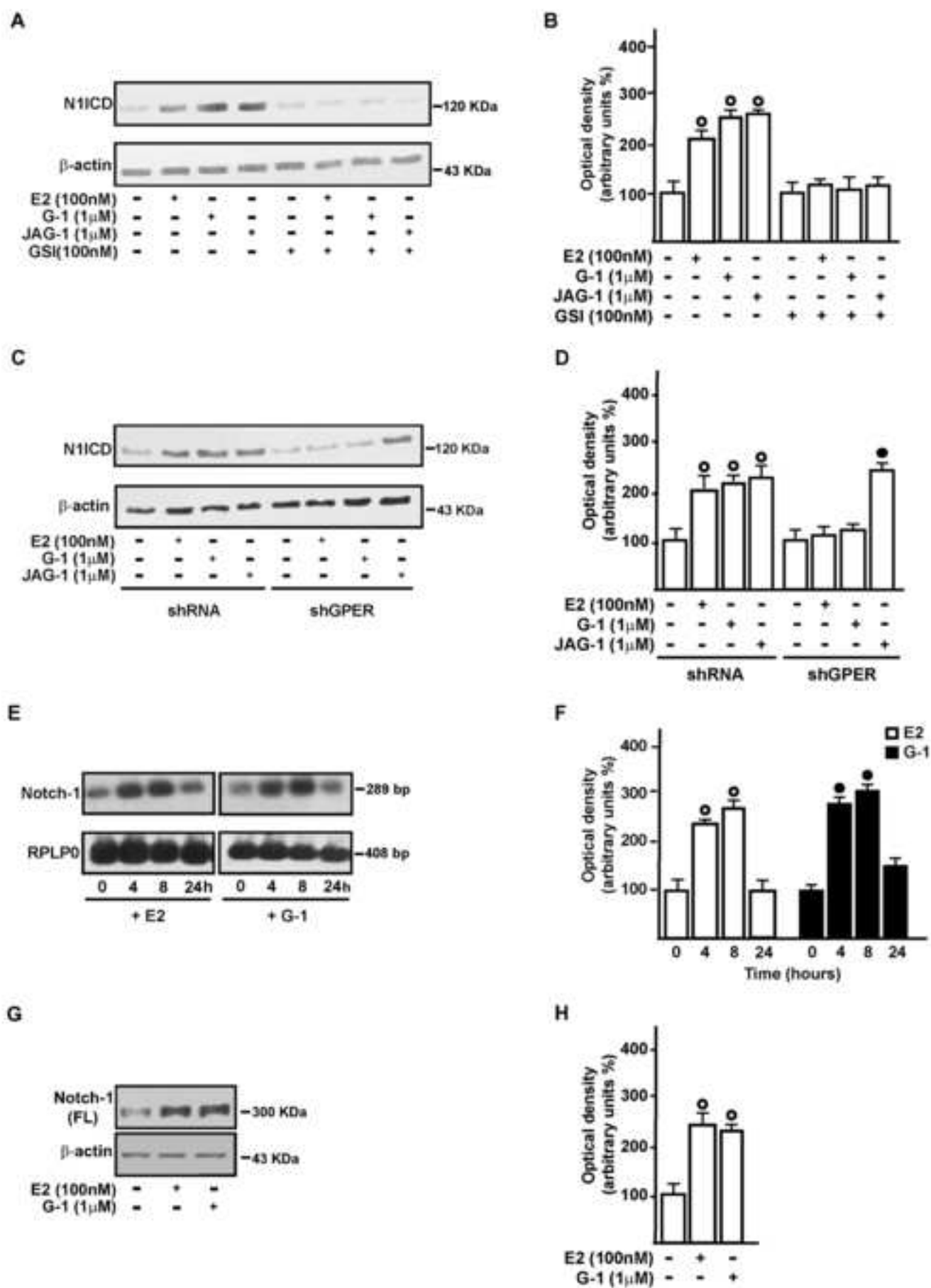
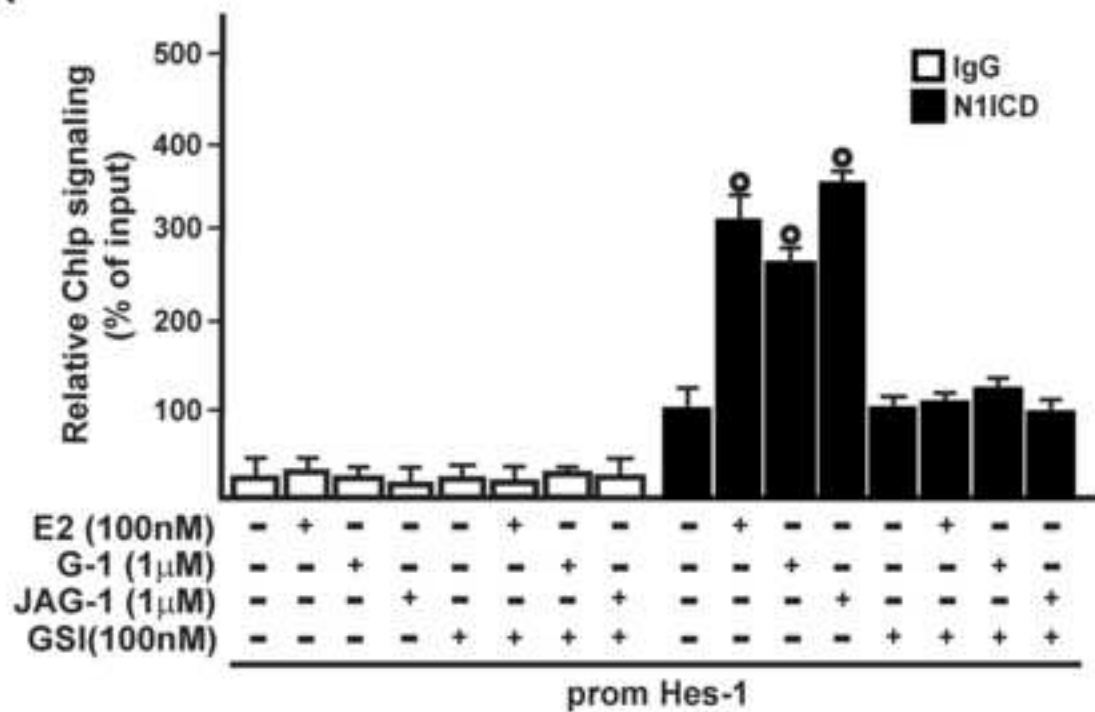


Fig. 3

SkBr3

A



B

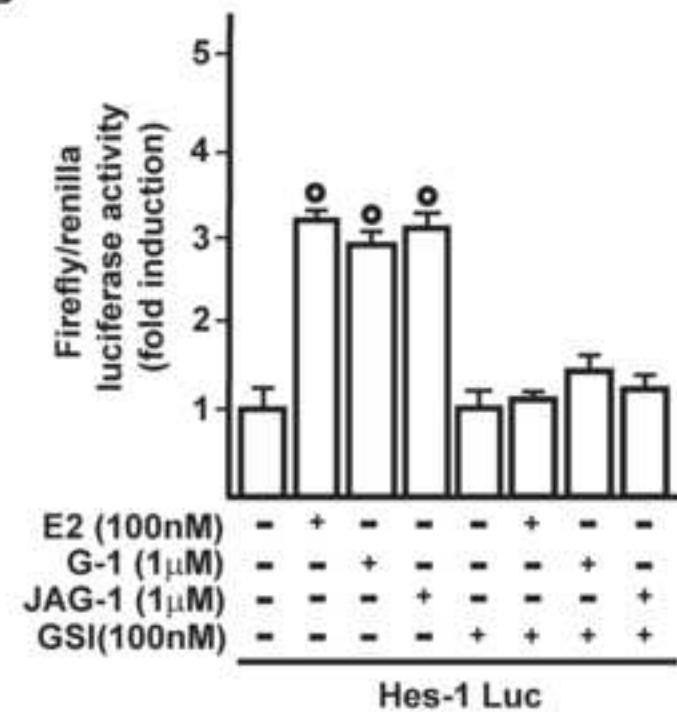
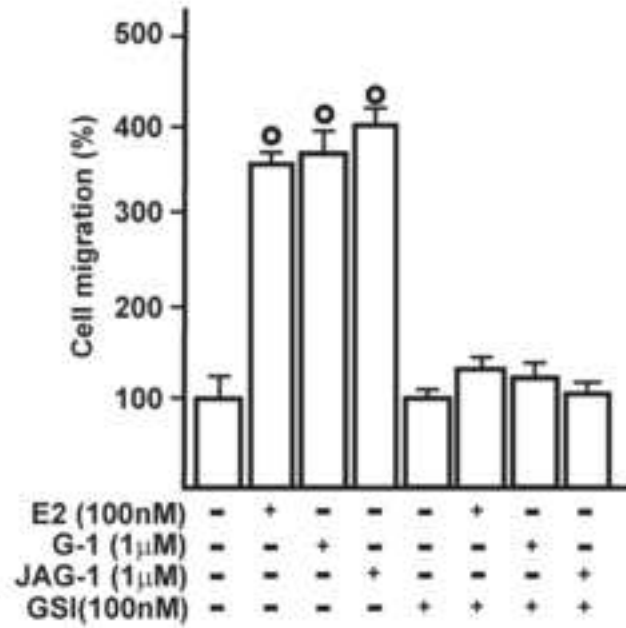


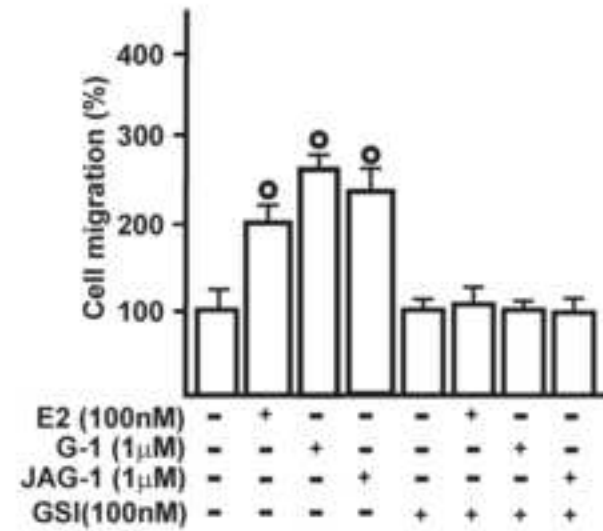
Fig. 4

SkBr3

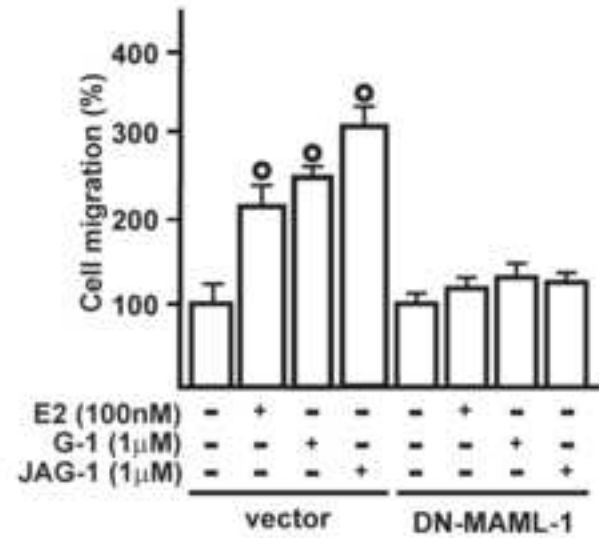
A



B



C



D

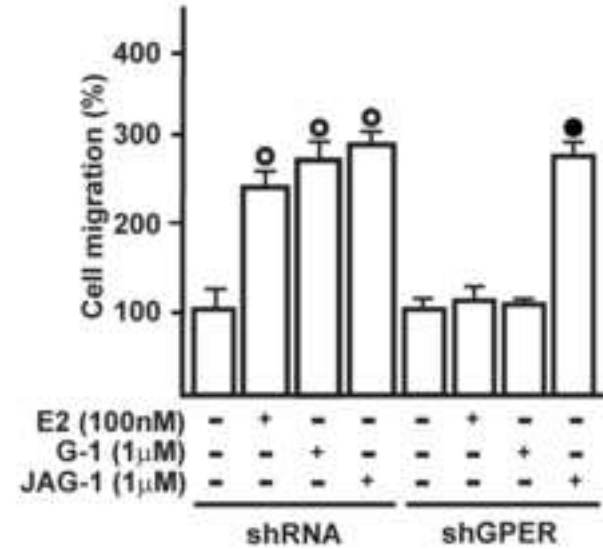


Fig. 5

## SkBr3

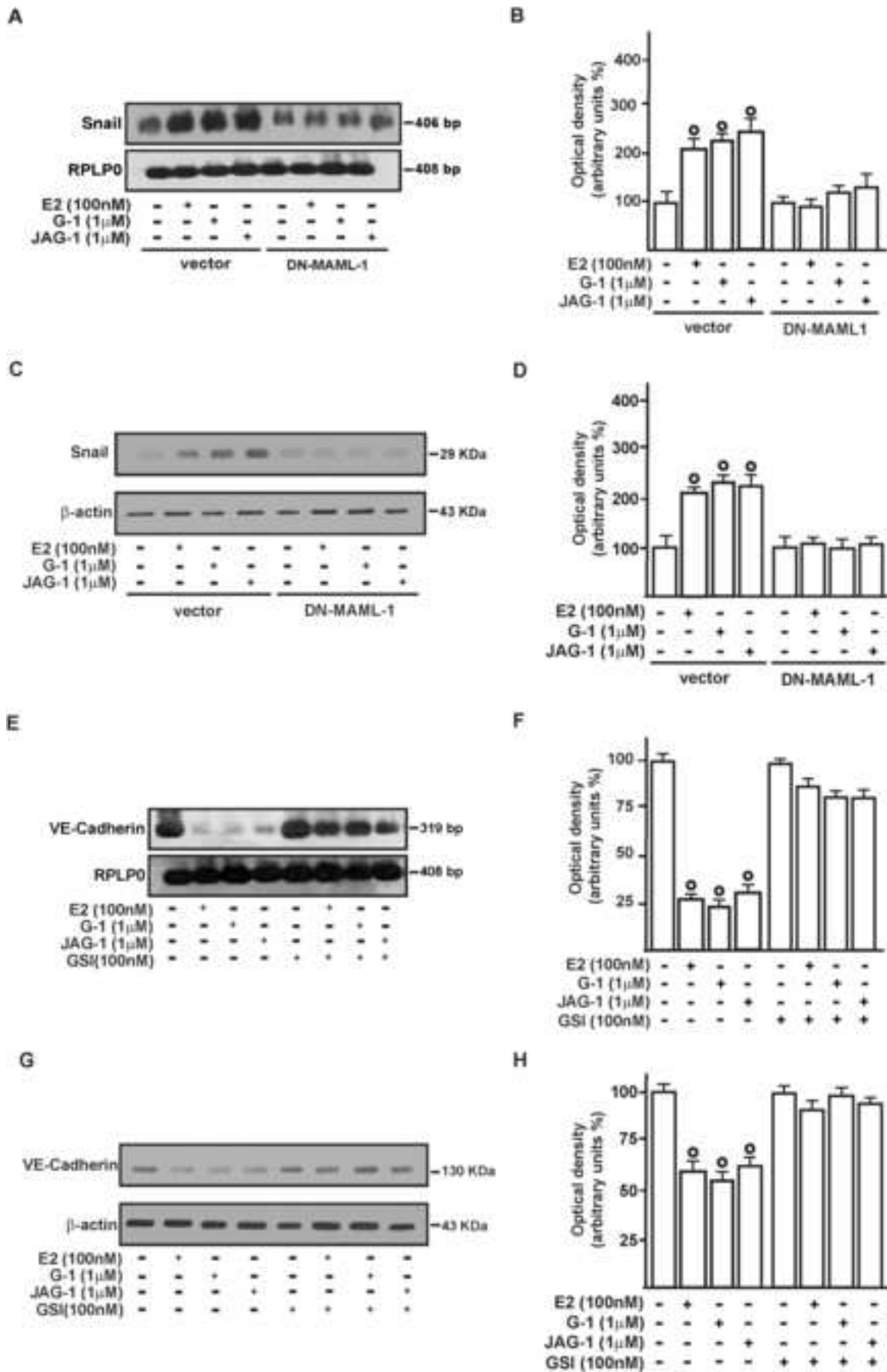


Fig. 6

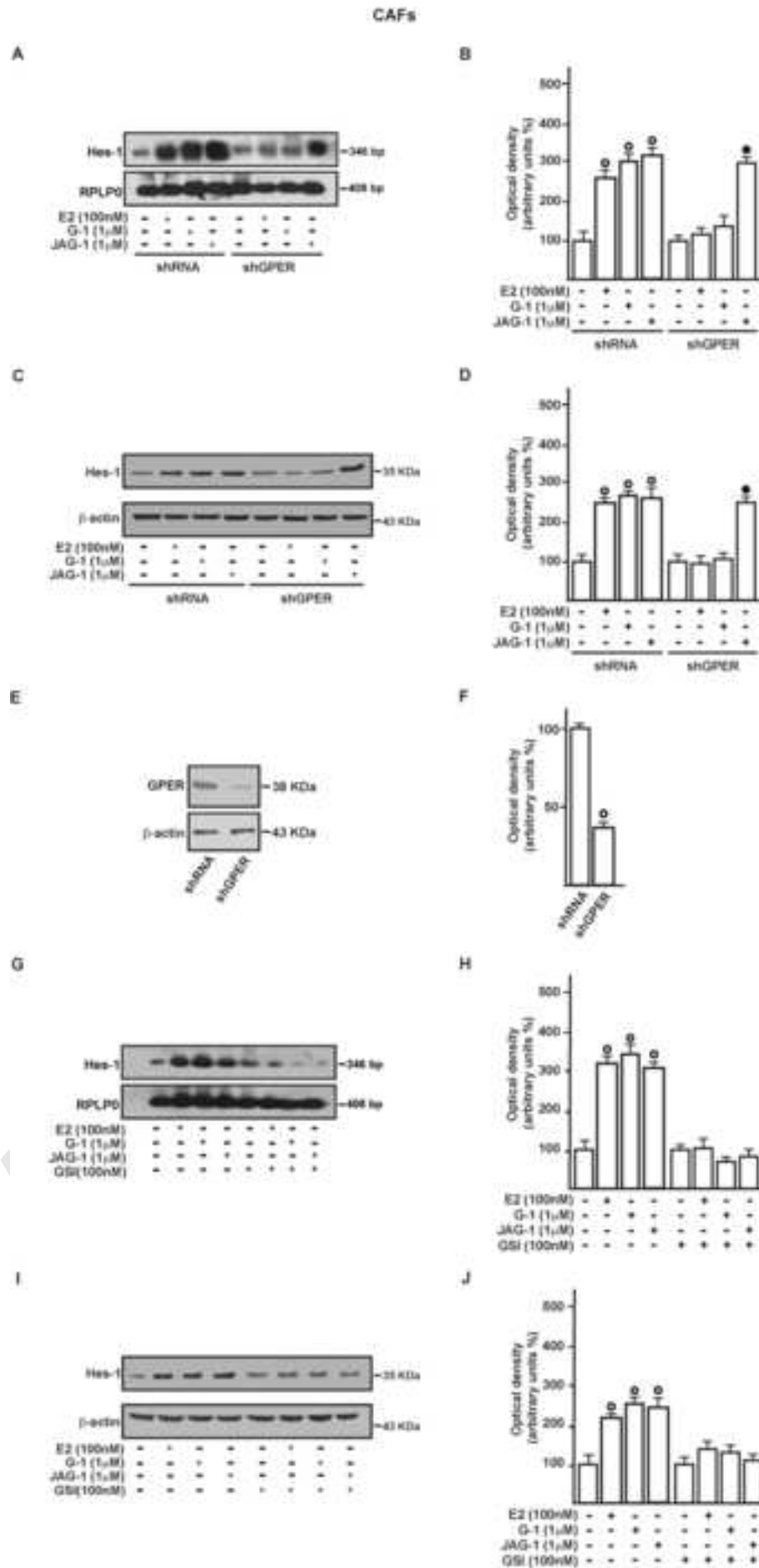
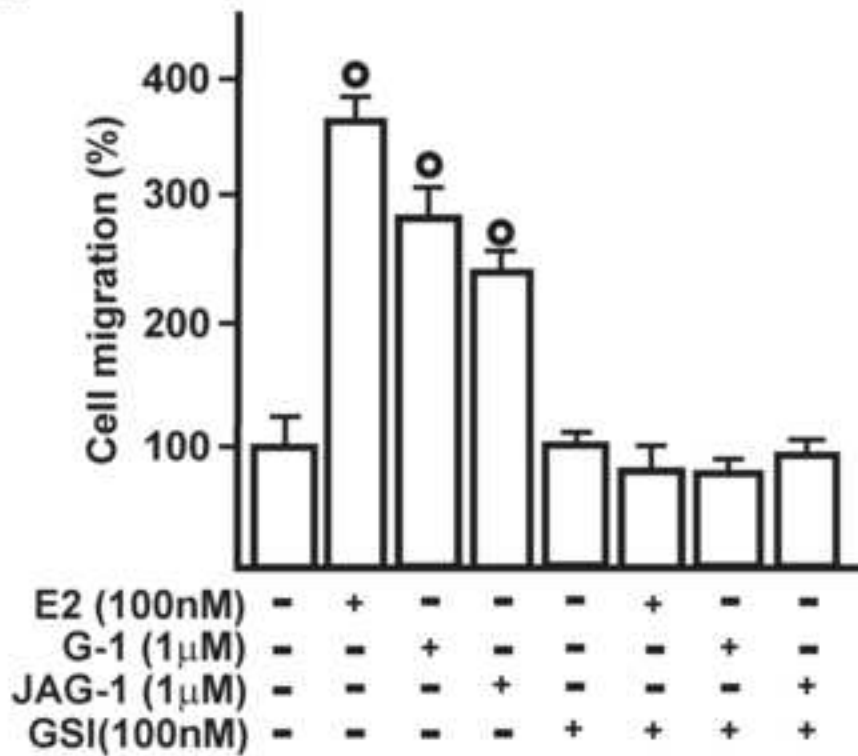


Fig. 7



## CAFs

A



B

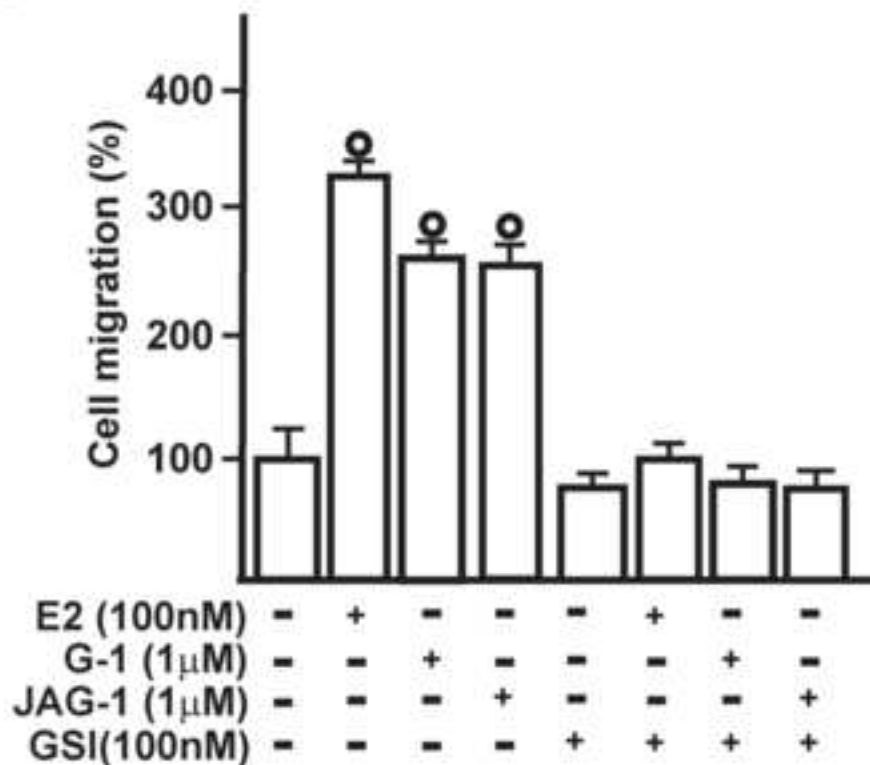


Fig. 8

# **(6-Bromo-1,4-dimethyl-9H-carbazol-3-yl-methylene)-hydrazine (“Carbhydraz”) as a novel GPER agonist**

Maria Stefania Sinicropi,<sup>1#</sup> Rosamaria Lappano,<sup>1#</sup> Anna Caruso,<sup>1</sup> Maria Francesca Santolla,<sup>1</sup> Assunta Pisano,<sup>1</sup> Camillo Rosano,<sup>2</sup> Anna Capasso,<sup>3</sup> Antonella Panno,<sup>1</sup> Jean Charles Lancelot,<sup>4</sup> Sylvain Rault,<sup>4</sup> Carmela Saturnino,<sup>3\*</sup> Marcello Maggiolini.<sup>1\*</sup>

<sup>1</sup>Department of Pharmacy, Health and Nutritional Sciences, University of Calabria, 87036 Arcavacata di Rende (CS), Italy;

<sup>2</sup>U.O.S. Biopolimeri e Proteomica, Azienda Ospedaliera Universitaria IRCCS San Martino IST - Istituto Nazionale per la Ricerca sul Cancro, Largo Benzi 10, 16132 Genova, Italy;

<sup>3</sup>Department of Pharmacy, University of Salerno via Giovanni Paolo II n° 132, 84084 Fisciano (SA), Italy;

<sup>4</sup> Université de Caen Basse-Normandie, Centre d'Etudes et de Recherche sur le Médicament de Normandie UPRES EA 4258 – FR CNRS 3038 INC3M, Bd Becquerel, 14032 Caen cedex, France.

<sup>#</sup>These Authors contributed equally to this work

\*Corresponding Authors: Carmela Saturnino, tel. +39 089 969769; e-mail address: saturnino@unisa.it; Marcello Maggiolini, tel. +39 0984 493076; e-mail address: marcellomaggiolini@yahoo.it.

## **Abstract**

Estrogens control a wide number of aspects of human physiology as well as play a key role in multiple diseases, including cancer, binding to and transactivating their cognate receptors (ERs). Numerous studies have recently revealed that the G protein-coupled receptor GPR30 contributes to diverse estrogen actions, including rapid signaling events and transcriptional activation. That is why it has been designated as G protein-coupled estrogen receptor (GPER). Because ERs and GPER share several features, including the ability to bind to same compounds, the availability of GPER-selective agonists and antagonists has advanced our understanding of the biological functions of GPER. In the present study, we designed and synthesized two novel carbazole derivatives. We investigated their ability to interact with and activate the GPER mediated transduction pathway in breast cancer cells. Both compounds did not show any ability to activate the classical ERs in ER-positive MCF7 cells, whereas one of the two compounds was able to trigger the rapid activation of the ERK transduction pathway in ER-negative SkBr3 cells, also demonstrating a good affinity for GPER in docking simulations. The characterization of this novel compound, identified as selective GPER agonist, could represent a potential useful tool to advance our understanding of the role of GPER in numerous biological systems as well as in cancer and to differentiate the functions elicited selectively by each estrogen receptor subtype.

**Keywords:** Breast cancer; Carbazole derivatives; Docking simulations; Estrogen/Estrogen Receptors; GPR30/GPER; Heterocycles.

## Introduction

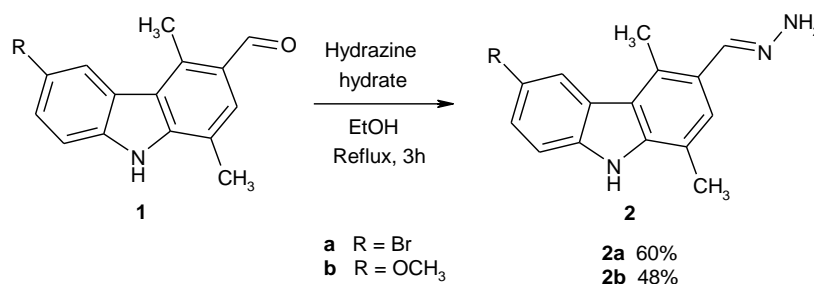
Nature is source of molecules with a deep impact on human health. Numerous natural metabolites have multiple and distinct biological properties, making them important health products or structural templates for drug discovery [1]. Today the literature provides a growing research on plant derived heterocycles, widely used in medicine, agriculture and technology [2]. Among nitrogen heterocycles, indole derivatives such as carbazole alkaloids display a wide variety of activities. Antibacterial, anti-inflammatory, psychotropic and anti-histamine properties have been attributed to many of them [3]. Moreover, carbazoles show significant antitumor activity in multiple cells derived from leukemia, melanoma, colon adenocarcinoma, kidney, brain and breast tumors [4-6]. For instance, a series of simple benzo[a]carbazoles has been shown to bind to estrogen receptor (ER) and inhibit the growth of mammary tumors of rats as well breast cancer cell proliferation [7]. ERs (ER $\alpha$  and ER $\beta$ ) are members of the superfamily of nuclear receptors, which regulate a large number of genes in many different target normal and cancer tissues, in response to estrogenic stimuli. Acting as ligand-dependent transcription factors, ERs exert distinct cellular functions. In particular, ER $\alpha$  plays a key role in the development and progression of breast cancer as well as is the principal biomarker for the response of breast tumors to endocrine therapy [8].

Although the biological responses to estrogens are mainly mediated by the classical ERs, the G protein-coupled receptor GPR30/GPER has been recently shown to mediate estrogen signaling in a variety of normal and cancer cell types [9]. In particular, GPER has been involved in rapid events induced by estrogens, including the transactivation of epidermal growth factor receptor (EGFR), the activation of the mitogen activated protein kinase (MAPK) and phosphoinositide3-kinase (PI3K) transduction pathways, the stimulation of adenylcyclase and the mobilization of intracellular calcium [10]. Furthermore, it exhibits many of the expected characteristics of an estrogen receptor, including the capability to bind to estrogens, antiestrogens, phyto- and xenoestrogens [11-14]. Accordingly, a recently synthesized compound, referred to as MIBE, displayed the property to bind to and inhibit both GPER- and ER $\alpha$ -mediated signaling in breast cancer cells, representing a promising pharmacological approach targeting breast carcinomas expressing one or both receptors [15]. However, the possibility to differentiate the pharmacology of GPER over that ERs by targeting each receptor subtype in a selective manner has represented a central point in dissecting estrogen signaling. The recent identification of novel compounds able to bind to and activate or inhibit GPER in a selective manner has greatly advanced our understanding of the role elicited by GPER in multiple biological systems as well as in cancer [16-18]. In this context, we have *in silico* designed, prepared and functionally characterized novel carbazole derivatives, one of which presented the ability to selectively activate the GPER-mediated signaling in ER-negative breast cancer cells.

## Results and discussion

### Chemistry

The starting 6-bromo-1,4-dimethyl-9H-carbazole-3-carbaldehyde (**1**) was prepared by a known procedure [19]. The synthesis of (6-bromo-1,4-dimethyl-9H-carbazol-3-yl-methylene)-hydrazine, referred to as Carbohydraz (**2a**), and its analogue **2b** was depicted in Scheme 1.



**Scheme 1.** Synthesis of Carbohydraz (**2a**) and of **2b**.

This is a convenient modification of the Wolff-Kishner [20] reduction and requires the heating of the aldehydic compound **1** with hydrazine hydrate in absolute ethanol by one-pot reaction. The desired hydrazines **2** were obtained in good yield (48-60%). From reaction of **1a** was also isolated, as a byproduct, bis-carbazole **3** (Fig.1) (yield of 15%) with potential interest in medicinal chemistry [3a].

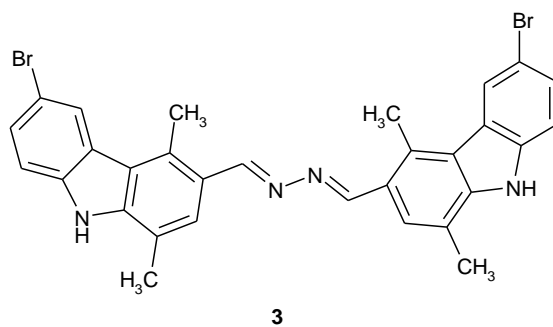


**Figure 1.** *N,N'*-bis-(6-bromo-1,4-dimethyl-9*H*-carbazol-3-yl-methylene)-hydrazine (**3**).

## Results

Our previous works [15, 18, 21-23] described the GPER binding pocket as a deep cleft in the protein core, surrounded by both hydrophobics and polar residues belonging to transmembrane helices TM III, TM V, TM VI and TM VII. Using a previously tested GPER molecular model as target [21], docking simulations confirmed a good affinity of the selective agonist G-1 for the protein, as previously demonstrated both *in silico* and *in vitro* [16]. Subsequently, we performed a docking simulation of the novel compounds Carbohydraz (**2a**) and **2b** for GPER using the same settings and parameters as used for G-1. Both molecules were positioned within the GPER binding site (Fig.2 A-B), similarly to G-1 (Fig.2 C-D). Particularly, the bromine atom of Carbohydraz (**2a**) is positioned about 2.9Å from the nitrogen atom of H307, which is a residue belonging to helix TM VII. The primary amine of Carbohydraz (**2a**) forms a hydrogen bond with N118 (TM II), while the carbazole moiety forms hydrophobic interactions with V116, L119, M133, F206 and F208, which contribute to stabilize the complex.

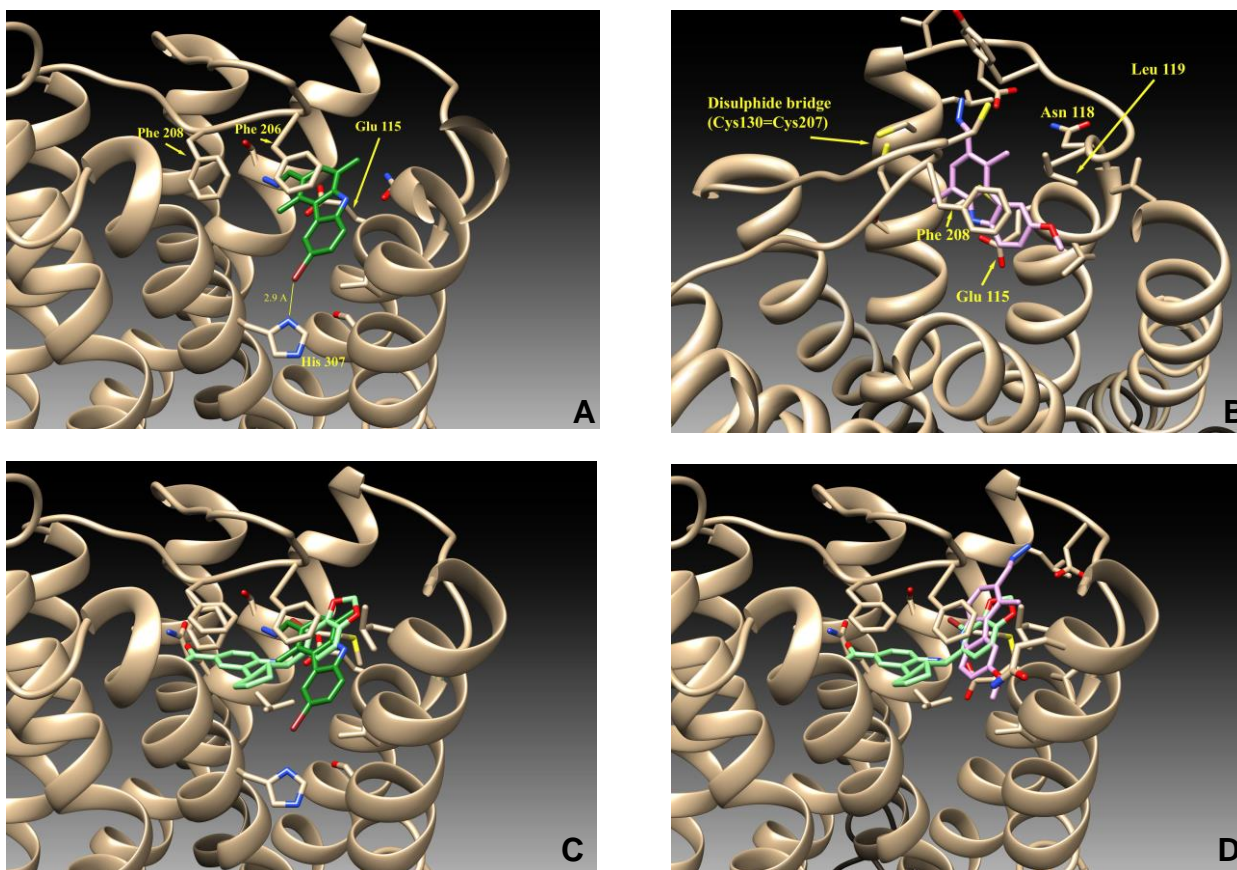


**Figure 2.** Ribbon representation of GPER (drawn in tan) bound to different compounds. Panel A reports the binding mode of Carbohydraz (**2a**), drawn as dark green sticks. A yellow line connects the bromine to the histidine indolic nitrogen atom. In Panel B the compound **2b** is drawn in purple. The G-1 moiety is drawn in light green and superposed to Carbohydraz (**2a**) in Panel C and to moiety **2b** in Panel D.

A synthetic plot illustrating the interactions of Carbohydraz (**2a**) and the GPER binding site is shown in figure 3. The hydrazinic group of Carbohydraz (**2a**) is in a favourable position to form hydrogen bonds with the carboxyl group of E115 and the hydroxyl group of C207. It should be noted that the functionalization of the carbazole nucleus in position 6 with a bromine present in Carbohydraz (**2a**) could be strategic for the affinity with GPER. In fact, the substitution of Br with OCH<sub>3</sub> in the same position (**2b**) could determine a 180° rotation of the carbazole ring and a subsequent reduction of interaction between this compound and GPER helices TM I and TM VII.

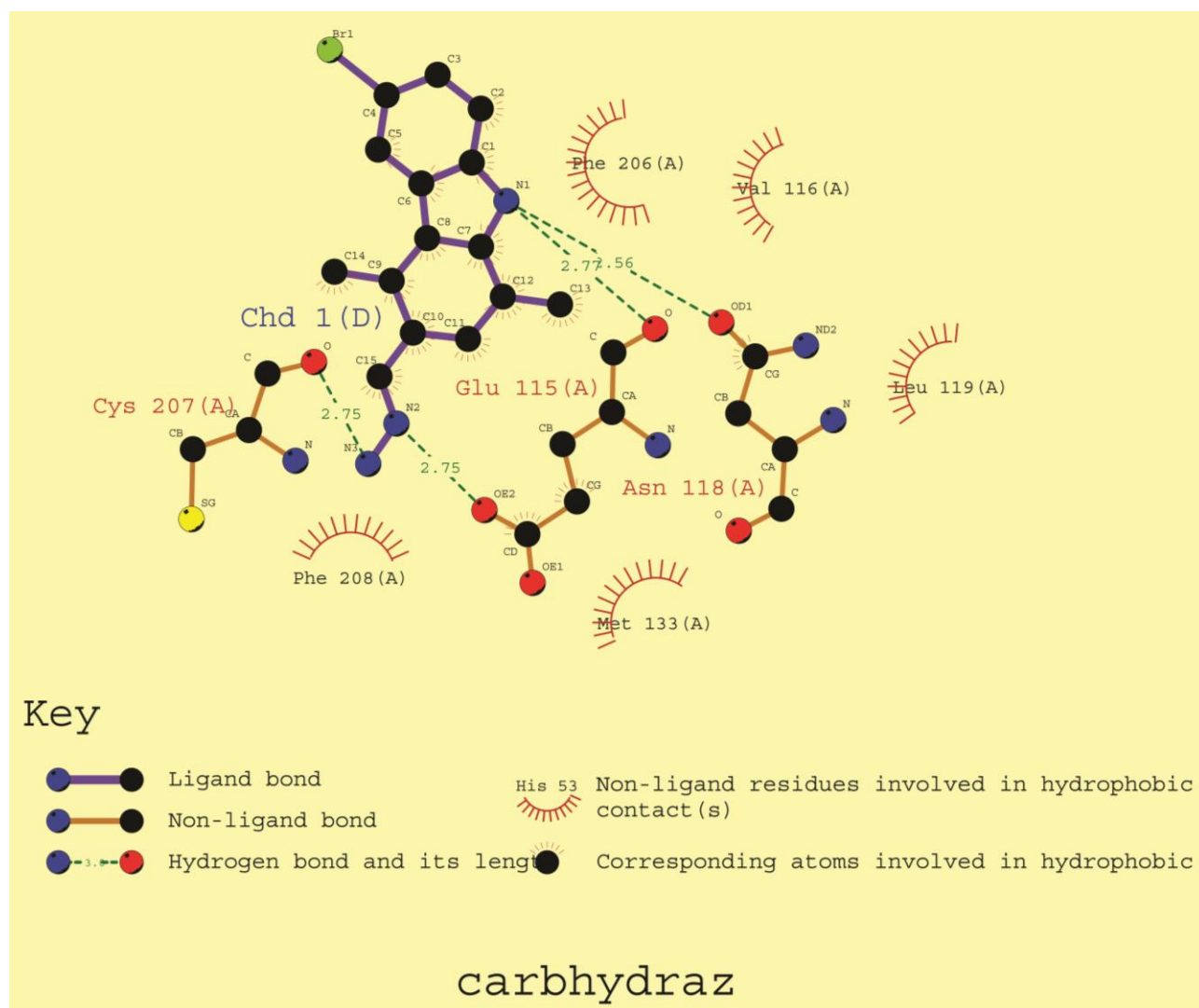


**Figure 3.** Plot illustrating the interactions of Carbohydraz (**2a**) and the GPER binding site.

*Carbohydraz induces ERK 1/2 phosphorylation through GPER in breast cancer cells.*

In order to verify the results obtained by docking simulation regarding the potential of the two novel synthesized compounds to potentially interact with GPER, we evaluated in ER-negative SkBr3 breast cancer cells the ERK1/2 phosphorylation, which is known to be a hallmark of ligand GPER activation [15, 18, 21, 22, 24-26]. As in dose-response studies only the compound referred to as Carbohydraz (**2a**) induced ERK1/2 phosphorylation (Fig. 4 A-B), we aimed to determine whether this effect occurs through GPER. To this end, we knocked-down GPER expression in SkBr3 cells by a shGPER, which abrogated the ability of Carbohydraz (**2a**) to induce ERK1/2 activation (Fig. 4 C-D). Taken together, these data suggest that Carbohydraz triggers ERK1/2 phosphorylation through GPER, confirming the findings obtained by docking simulation.

To further evaluate whether the synthesized compounds might be able to activate the classical ER $\alpha$ , we transiently transfected an ER reported gene in MCF7 breast cancer cells, which express ER $\alpha$  and not ER $\beta$  as judged by RT-PCR (data not shown). Only E2 transactivated the endogenous ER $\alpha$  in MCF7 cells demonstrating that Carbohydraz (**2a**) is selective for GPER, since did not exhibit activating properties for ER $\alpha$  (Fig. 5).

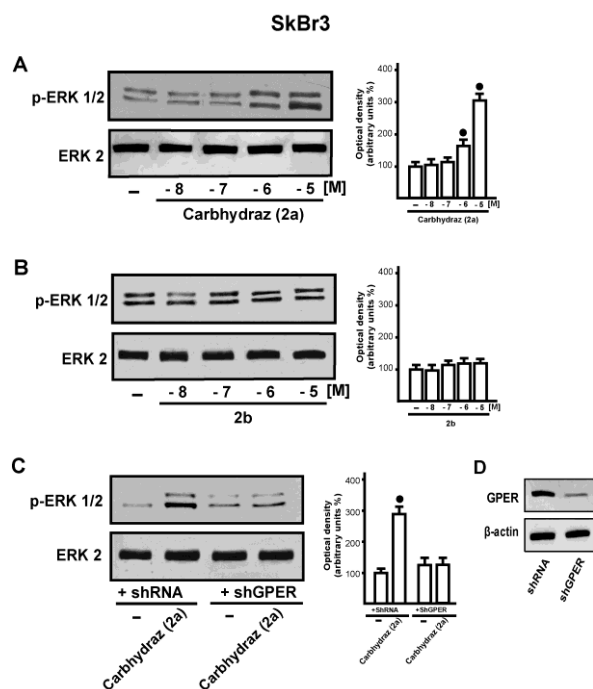


**Figure 4. Carbohydraz (2a) activates ERK1/2 in a GPER-dependent manner.** (A-B) ERK1/2 activation in SkBr3 cells treated for 15 min with increasing concentrations of Carbohydraz (2a) or 2b. (C) ERK1/2 activation in SkBr3 cells transfected with shRNA or shGPER and then treated for 15 min with vehicle (-) or 10  $\mu$ M Carbohydraz (2a). Side panels show densitometric analysis of the blots normalized to ERK2. (D) Efficacy of GPER silencing. Each data point represents the mean  $\pm$ SD of three independent experiments. (●) indicate  $p < 0.05$  for cells receiving vehicle (-) versus treatment.

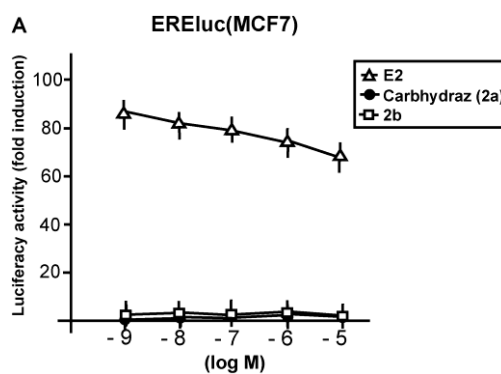


**Figure 5. Carbohydraz (2a) and 2b do not activate ER $\alpha$ .** MCF7 cells were transfected with an ER luciferase reporter gene along with the internal transfection control Renilla Luciferase and treated with increasing concentrations (logarithmic scale) of E2, Carbohydraz (2a) and 2b. The normalized luciferase activity values of cells treated with vehicle were set as 1-fold induction, upon which the activity induced by treatments was calculated. Each data point represents the mean  $\pm$  SD of three experiments performed in triplicate.

## Discussion and Conclusions

The seven-transmembrane G protein-coupled receptors (GPCRs), which belong to the largest superfamily of signal transduction proteins, play a crucial role in many physiological functions as well as in multiple diseases [27]. One member of this family, named GPR30/GPER, has largely proven to be a key mediator in the development and progression of several types of tumors, however it can also mediate relevant physiological responses in the reproductive, nervous, endocrine, immune and cardiovascular systems. As it concerns the potential role of GPER in cancer, its expression has been associated with aggressive features of breast, endometrial and ovarian tumors [28-30]. In

line with these findings, numerous investigations proved GPER expression and activation in different tumor cells, including breast, endometrial, ovarian, thyroid, prostate and testicular germ cells [11, 25, 26, 31-35]. While several GPCR family members, as GPER, control key biological functions in both physiological and pathological conditions, existing drugs that target this receptor superfamily are directed towards only a few members. Consequently, huge efforts are currently underway to develop new GPCR-based drugs, particularly for cancer treatment. Although their overexpression and solubility and consequently the crystallization process result particularly problematic, computer based methods have been increasing successful in identifying the atomic structure of a biological target like a GPCR on the basis of its primary structure [23]. In this context, the availability of a GPER 3D model allowed us to pursue a “protein-based” approach in order to characterize the potential interaction of different molecules with this receptor [23]. Moreover, following different approaches (“ligand-based” as well as mixed biomolecular and virtual screening), several GPER natural and synthetic ligands have been identified by our and other groups [16, 32-33, 36-41]. Ligand binding studies validated the results obtained by molecular modeling and docking simulations. Moreover, functional assays allowed the characterization of the biological effects elicited by numerous compounds through GPER in multiple contexts. In particular, the two well-known ER $\alpha$  ligands and activators 17 $\beta$ -estradiol and estradiol, as GPER ligands, showed the ability to activate or inhibit, respectively, GPER signaling. The ER antagonists tamoxifen and ICI182,780 displayed a high binding affinity for GPER and surprisingly acted as agonists of this receptor [12, 25, 31]. In addition a series of natural and synthetic compounds has been identified and characterized as GPER ligands with either agonist or antagonist properties [15-17, 42].

In the present study, we have designed and synthesized novel carbazole derivatives and performed docking simulations as well as functional assays in order to assess their potential affinity and activity for GPER. In particular, a compound, which we termed Carbohydraz (**2a**), displayed a better affinity than **2b** for the receptor in docking simulations. Accordingly, Carbohydraz (**2a**) showed the capability to trigger in breast cancer cells intracellular molecular signaling, such as ERK phosphorylation, which is known to characterize the ligand-induced activation of GPER. Moreover, Carbohydraz (**2a**) did not exhibit any activating properties for ER $\alpha$ , suggesting its specificity for GPER. Indeed, the ability of diverse molecules to bind to and activate both the classical estrogen receptors and GPER made difficult to differentiate the pharmacology of GPER over that of the classical ERs. In this context, Carbohydraz (**2a**) together with the other previously identified GPER selective ligands, either agonists or antagonists, would contribute to better dissect the distinct functions selectively mediated by each estrogen receptor.

## Materials and methods

### *Molecular modeling and docking simulations*

We used the program GOLD v.5.0.1 (the Cambridge Crystallographic Data Center, UK) to perform docking simulations. GOLD is a program using a genetic algorithm that allows to investigate the full range of ligand conformational flexibility and a partial protein side chain flexibility. We used, as the protein target for our docking simulation the three dimensional atomic coordinates of the GPER molecular model built by homology as described elsewhere [14]. We identified Phe 208 O atom, as the protein active site centre on the basis of our previous docking simulations [14] and we considered as the active site atoms, those located within 20 Å from this point. The default GOLD settings were used running the simulations. Residues Tyr123, Gln138, Phe206, Phe208, Glu275, Phe278 and His282 of GPER were defined with flexible side chains, allowing their free rotation. Ligand molecular structure was built and energy minimized with the programs InsightII and Discover3 (Biosym/MSI, San Diego, CA, USA). Figures were drawn with the program Chimera [43] and interaction diagram was built using the program Ligplot [44].

### *Cell culture*

SkBr3 human breast cancer cells were maintained in RPMI 1640 without phenol red supplemented with 10% FBS. MCF7 human breast cancer cells were maintained in DMEM with phenol red supplemented with 10% FBS. Cells were grown in a 37° C incubator with 5% CO<sub>2</sub>. The day before experiments for immunoblots cells were switched to medium without serum, thereafter cells were treated as indicated.

### *Western blot analysis*

SkBr3 was grown in 10-cm dishes and exposed to drugs for the appropriate time, then washed twice with ice-cold PBS and solubilized with 50 mM Hepes buffered solution, pH= 7.5, containing 150 mM NaCl, 1.5 mM MgCl<sub>2</sub>, 1mM EGTA, 10% glycerol, 1% Triton X-100, a mixture of protease inhibitors (Aprotinin, PMSF and Na-orthovanadate). Protein concentration in the supernatant was determined according to the Bradford method. Equal amounts (10-30 µg) of the whole cell lysate was electrophoresed through a reducing SDS/10% (w/v) polyacrylamide gel and electroblotted onto a nitrocellulose membrane which was probed with primary antibodies phosphorylated ERK1/2 (E-4), ERK2 (C-14), GPER (N-15) and  $\beta$ -actin (C-2) (all purchased from Santa Cruz Biotechnology, Inc). The levels of proteins and



phosphoproteins were detected, after incubation with the horseradish peroxidase-linked secondary antibodies, by the ECL® (enhanced chemiluminescence) System (GE Healthcare, Milan, Italy).

#### *Transfections and luciferase assays*

Plasmids and Luciferase Assays were previously described (19496085; 21304949). Cells were transferred into 24-well plates with 500  $\mu$ L of regular growth medium/well the day before transfection. MCF7 cell medium was replaced with DMEM supplemented with 1% charcoal-stripped (CS) FBS lacking phenol red and serum on the day of transfection, which was performed using the Fugene6 Reagent as recommended by the manufacturer (Roche Diagnostics, Mannheim, Germany) with a mixture containing 0.2  $\mu$ g of reporter plasmid and 1 ng of pRL-CMV. After 5–6 h the medium was replaced again with serum-free DMEM lacking phenol red and supplemented with 1% CS-FBS, ligands were added at this point and cells were incubated for 16–18 h. Luciferase activity was then measured with the Dual Luciferase kit (Promega) according to the manufacturer's recommendations. Firefly luciferase activity was normalized to the internal transfection control provided by the Renilla luciferase activity.

#### *Gene silencing experiments*

Cells were plated onto 10-cm dishes, maintained in serum-free medium for 24h and then transfected for additional 24h before treatments with a control vector or an independent shRNA sequence for each target gene using X-treamene (Roche Molecular Biochemicals, Milan, Italy). Short hairpin constructs against human GPER (shGPER) were generated and used as previously described [45, 46]. In brief, they were generated in lentiviral expression vector pLKO.1 purchased by Euroclone, Milan, Italy. The targeting strand generated from the GPER shRNA construct is 5'-CGCTCCCTGCAAGCAGTCTTT-3'.

## **Experimental section**

### **General**

Commercial reagents were purchased from Aldrich, Acros Organics and Alfa Aesar and were used without additional purification. Melting points were determined on a Gallenkamp melting point apparatus. The IR spectra were recorded on a Fourier Transform Infrared Spectrometer FT/IR-4200 for KBr pellets. <sup>1</sup>H-NMR (300 MHz) and <sup>13</sup>C-NMR (100 MHz) spectra were recorded on a Bruker 300 spectrometer. Chemical shifts are expressed in parts per million downfield from tetramethylsilane as an internal standard. Thin layer chromatography (TLC) was performed on silica gel 60F-264 (Merck). The 6-bromo-1,4-dimethyl-9H-carbazole-3-carbaldehyde **1** was prepared as described in the literature [19].

### **Preparation of 1,4-dimethyl-9H-carbazol-3-yl-methylene)-hydrazines (2a-c) and N,N'-bis-(6-bromo-1,4-dimethyl-9H-carbazol-3-yl-methylene)-hydrazine (3).**

Hydrazine hydrate, 98% (d= 1.029 g/mL; 5.97x10<sup>-3</sup> mol; 0.29 mL) and 1,4-dimethyl-9H-carbazole-3-carbaldehyde **1a-b** (1.48x10<sup>-3</sup> mol) were dissolved in absolute ethanol (37.4 mL).

The resulting solution was heated under reflux for 3h. After cooling to room temperature, the reaction solution was evaporated under reduced pressure. The remaining residue was washed twice with Et<sub>2</sub>O (20 mL). The filtrate was dried under reduced pressure and the solid residue obtained was recrystallized from Et<sub>2</sub>O to give **2a-b** as powder. The compound **3** has been isolated as cream powder for filtration of the reaction of **1a**.

#### *(6-Bromo-1,4-dimethyl-9H-carbazol-3-yl-methylene)-hydrazine (2a).*

Orange powder; yield 60%; mp > 270 °C. IR spectrum,  $\nu$ , cm<sup>-1</sup>: 3398-3354 (NH<sub>2</sub>); 3169 (NH); 1613 (CH=N); 1589; 1442; 857. <sup>1</sup>H NMR spectrum (DMSO-d<sub>6</sub>),  $\delta$ , ppm: 2.49 (s, 3H, CH<sub>3</sub>); 2.78 (s, 3H, CH<sub>3</sub>); 6.51 (s, 2H, NH<sub>2</sub>); 7.45-7.49 (m, 2H, Ar); 7.61 (s, 1H, Ar); 8.22 (s, 1H, CH=N-NH<sub>2</sub>); 8.26 (s, 1H, Ar); 11.47 (s, 1H, NH). <sup>13</sup>C NMR spectrum (DMSO-d<sub>6</sub>),  $\delta$ , ppm: 15.12; 16.77; 110.73; 112.95; 117.92; 119.87; 124.32; 124.39; 125.30; 125.38; 127.04; 127.45; 138.48; 138.68; 139.11. Found, %: C 56.98; H 4.46; N 13.29. C<sub>15</sub>H<sub>14</sub>BrN<sub>3</sub>. Calculated, %: C 56.95; H 4.50; N 13.31.

#### *(6-Methoxy-1,4-dimethyl-9H-carbazol-3-yl-methylene)-hydrazine (2b).*

Green powder; yield 48%; mp > 270 °C. IR spectrum,  $\nu$ , cm<sup>-1</sup>: 3430-3379 (NH<sub>2</sub>); 2924 (NH); 1612 (CH=N); 1464; 1210; 1130; 863. <sup>1</sup>H NMR spectrum (DMSO-d<sub>6</sub>),  $\delta$ , ppm:  $\delta$  2.79 (s, 3H, CH<sub>3</sub>); 3.53 (s, 3H, CH<sub>3</sub>); 3.87 (s, 3H, OCH<sub>3</sub>); 6.51 (s, 2H, NH<sub>2</sub>); 6.92-7.27 (m, 1H, Ar); 7.50-7.91 (m, 3H, 2 Ar, CH=N-NH<sub>2</sub>); 8.30 (s, 1H, Ar); 11.29 (s, 1H, NH). <sup>13</sup>C NMR spectrum (DMSO-d<sub>6</sub>),  $\delta$ , ppm: 15.32; 19.77; 55.87; 102.13; 105.95; 109.62; 112.19; 117.62; 121.39; 124.20; 125.05; 127.24; 134.67; 139.65; 143.06; 154.10. Found, %: C 71.89; H 6.41; N 15.72. C<sub>16</sub>H<sub>17</sub>N<sub>3</sub>O. Calculated, %: C 71.92; H 6.39; N 15.69.

#### *N,N'-bis-(6-bromo-1,4-dimethyl-9H-carbazol-3-yl-methylene)-hydrazine (3).*

Yield 15%; mp > 270 °C. IR spectrum,  $\nu$ , cm<sup>-1</sup>: 3419 (NH); 1614 (CH=N); 1589; 1438; 1247; 798. <sup>1</sup>H NMR spectrum (DMSO-d<sub>6</sub>),  $\delta$ , ppm: 2.58 (s, 6H, CH<sub>3</sub>); 3.00 (s, 6H, CH<sub>3</sub>); 7.55 (s, 4H, Ar); 8.01 (s, 2H, Ar); 8.34 (s, 2H, Ar); 9.18 (s, 2H, CH=N-); 11.52 (s, 2H, NH). <sup>13</sup>C NMR spectrum (DMSO-d<sub>6</sub>),  $\delta$ , ppm: 15.09; 16.72; 110.68; 112.94; 117.88; 119.86; 124.34; 124.38; 125.28; 125.37; 127.00; 127.41; 138.49; 138.68; 139.10. Found, %: C 60.02; H 4.03; N 9.33. C<sub>30</sub>H<sub>24</sub>Br<sub>2</sub>N<sub>4</sub>. Calculated, %: C 60.05; H 4.00; N 9.29.



## Acknowledgments

This work was supported by the Associazione Italiana per la Ricerca sul Cancro (AIRC project 12849 and Calabria project 2011) and the Fondazione Cassa di Risparmio di Calabria e Lucania.

## References

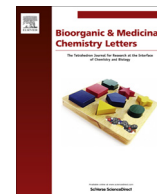
- [1] Kishore, N.; Mishra, B.B.; Tripathi, V.; Tiwari, V.K. Alkaloids as potential anti-tubercular agents. *Fitoterapia*, **2009**, *80*(3), 149-163.
- [2] Liu, Z.; Larock, R.C. Synthesis of Carbazoles and Dibenzofurans via Cross-Coupling of o-Iodoanilines and o-Iodophenols with Silylaryl Triflates and Subsequent Pd-Catalyzed Cyclization. *Tetrahedron*, **2007**, *63*(2), 347-355.
- [3] (a) Caruso, A.; Voisin-Chiret, A.S.; Lancelot, J.C.; Sinicropi, M.S.; Garofalo, A.; Rault, S. Efficient and Simple Synthesis of 6-Aryl-1,4-dimethyl-9H-carbazoles. *Molecules*, **2008**, *13*, 1312-1320; (b) Sinicropi, M.S.; Caruso, A.; Conforti, F.; Marrelli, M.; El Kashef, H.; Lancelot, J.C.; Rault, S.; Statti, G.A.; Menichini, F. Synthesis, inhibition of NO production and antiproliferative activities of some indole derivatives. *J. Enzym. Inhib. Med. Chem.* **2009**, *24*(5), 1148-1153; (c) Caruso, A.; Voisin-Chiret, A.S.; Lancelot, J.C.; Sinicropi, M.S.; Garofalo, A.; Rault, S. Novel and efficient synthesis of 5,8-dimethyl-9H-carbazol-3-ol via a hydroxydeboronation reaction. *Heterocycles*, **2007**, *71*(10), 2203-2210; (d) Caruso, A.; Lancelot, J.C.; El-Kashef, H.; Sinicropi, M.S.; Legay, R.; Lesnard, A.; Rault, S. A Rapid and Versatile Synthesis of Novel Pyrimido[5,4-b]carbazoles. *Tetrahedron*, **2009**, *65*, 10400-10405; (e) Caruso, A.; Chimento, A.; El-Kashef, H.; Lancelot, J.C.; Panno, A.; Pezzi, V.; Saturnino, C.; Sinicropi, M.S.; Sirianni, R.; Rault, S. Antiproliferative activity of some 1,4-dimethylcarbazoles on cells that express estrogen receptors: part I. *J. Enzym. Inhib. Med. Chem.*, **2012**, *27*, 609-613.
- [4] (a) Panno, A.; Sinicropi, M.S.; Caruso, A.; El-Kashef, H.; Lancelot, J.C.; Aubert, G.; Lesnard, A.; Cresteil, T.; Rault, S. New trimethoxybenzamides and trimethoxyphenylureas derived from dimethylcarbazole as cytotoxic agents. Part I. *J. Heterocyclic Chem.*, **2013**, *00*, 00. DOI 10.1002/jhet.1951. (b) Lancelot, J.C.; Letois, B.; Rault, S.; Dung, N.H.; Saturnino, C.; Robba M. Efficient synthesis of 6-substituted 3-nitro-1,4-dimethylcarbazoles and 3-amino-1,4-dimethylcarbazoles. *Gazz. Chim. Ital.*, **1991**, *121*, 301-307; (c) Andre, V.; Boissart, C.; Lechevrel, M.; Gauduchon, P.; Letalaer, J.Y.; Lancelot, J.C.; Letois, B.; Saturnino, C.; Rault, S.; Robba M. Mutagenicity of Nitrosubstituted and Amino-substituted Carbazoles In Salmonella-typhimurium .1. Monosubstituted Derivatives of 9H-carbazole. *Mut. Res.*, **1993**, *299*, 63-73; (d) Moinethedin, V.; Tabka, T. Poulain, L.; Goderd, T.; Lechevrel, M.; Saturnino, C.; Lancelot, J.C.; Le Tallaer, J.Y.; Gauduchon, P. Biological properties of 5,11-dimethyl-6H-pyrido-3,2-b carbazole: a new class of potent antitumor drugs. *Anti Canc. Drug Des.*, **2000**, *15*, 109-118; (e) Saturnino, C.; Buonerba, M.; Boatto, G.; Pascale, M.; Moltedo, O.; De Napoli, L.; Montesarchio, D.; Lancelot, J.C.; De Caprariis, P. Synthesis and preliminary biological evaluation of a new pyridocarbazole derivative covalently linked to a thymidine nucleoside as a potential targeted antitumoral agent. *Chem. Pharm. Bull.*, **2003**, *51*, 971-974; (f) Saturnino, C.; Palladino, C.; Napoli, M.; Sinicropi, M.S.; Botta, A.; Sala, M.; Carcereri de Prati, A.; Novellino, E.; Suzuki, H. Synthesis and biological evaluation of new N-alkylcarbazole derivatives as STAT3 inhibitors: preliminary study. *Eur. J. Med. Chem.*, **2013**, *60*, 112-119.
- [5] Moody, D.L.; Dyba, M.; Kosakowska-Cholody, T.; Tarasova, N.I.; Michejda, C.J. Synthesis and biological activity of 5-aza-ellipticine derivatives. *Bioorg. Med. Chem. Lett.*, **2007**, *17*(8), 2380-2384.
- [6] Stiborova, M.; Rupertova, M.; Schmeiser, H.H.; Frei, E. Molecular mechanism of antineoplastic action of an anticancer drug ellipticine. *Biomed. Pap. Med. Fac. Univ. Palacky Olomouc Czech. Repub.*, **2006**, *150*(1), 13-23.
- [7] von Angerer, E.; Prekajac, J. Benzo[a]carbazole derivatives. Synthesis, estrogen receptor binding affinities and mammary tumor inhibiting activity. *J. Med. Chem.*, **1986**, *26*, 113-116.
- [8] Ascenzi, P.; Bocedi, A.; Marino, M. Structurefunction relationship of estrogen receptor a and b: impact on human health. *Mol. Aspects Med.*, **2006**, *27*, 299-402.
- [9] Maggiolini, M.; Picard, D. The unfolding stories of GPR30, a new membrane bound estrogen receptor. *J. Endocrinol.*, **2010**, *204*, 105-114.
- [10] Prossnitz, E.R.; Maggiolini, M. Mechanisms of estrogen signaling and gene expression via GPR30. *Mol. Cell. Endocrinol.*, **2009**, *308*, 32-38.
- [11] Thomas, P.; Pang, Y.; Filardo, E.J.; Dong, J. Identity of an estrogen membrane receptor coupled to a G protein in human breast cancer cells. *Endocrinology*, **2005**, *146*, 624-632.
- [12] Revankar, C.M.; Cimino, D.F.; Sklar, L.A.; Arterburn, J.B.; Prossnitz, E.R. A transmembrane intracellular estrogen receptor mediates rapid cell signaling. *Science*, **2005**, *307*, 1625-1630
- [13] Thomas, P.; Dong, J. Binding and activation of the seven-transmembrane estrogen receptor GPR30 by environmental estrogens: a potential novel mechanism of endocrine disruption. *J. Steroid Biochem. Mol. Biol.*, **2006**, *102*, 175-179.
- [14] Lappano, R.; Rosano, C.; De Marco, P.; De Francesco, E.M.; Pezzi, V.; Maggiolini, M. Estriol acts as a GPR30 antagonist in estrogen receptor-negative breast cancer cells. *Mol. Cell. Endocrinol.*, **2010**, *320*, 162-170.

- [15] Lappano, R.; Santolla, M.F.; Pupo, M.; Sinicropi, M.S.; Caruso, A.; Rosano, C.; Maggiolini, M. MIBE acts as antagonist ligand of both estrogen receptor alpha and GPER in breast cancer cells. *Breast Cancer Res.*, **2012**, *14*(1), R12.
- [16] Bologna, C.G.; Revankar, C.M.; Young, S.M.; Edwards, B.S.; Arterburn, J.B.; Kiselyov, A.S.; Parker, M.A.; Tkachenko, S.E.; Savchuck, N.P.; Sklar, L.A.; Oprea, T.I.; Prossnitz, E.R. Virtual and biomolecular screening converge on a selective agonist for GPR30. *Nat. Chem. Biol.* **2006**, *2*, 207-212.
- [17] Dennis, M.K.; Field, A.S.; Burai, R.; Ramesh, C.; Petrie, W.K.; Bologna, C.G.; Oprea, T.I.; Yamaguchi, Y.; Hayashi, S.I.; Sklar, L.A.; Hathaway, H.J.; Arterburn, J.B.; Prossnitz, E.R. Identification of a GPER/GPR30 antagonist with improved estrogen receptor counterselectivity. *J. Steroid Biochem. Mol. Biol.*, **2011**, *127*, 358-366.
- [18] Lappano, R.; Rosano, C.; Santolla, M.F.; Pupo, M.; De Francesco, E.M.; De Marco, P.; Ponassi, M.; Spallarossa, A.; Ranise, A.; Maggiolini, M. Two novel GPER agonists induce gene expression changes and growth effects in cancer cells. *Curr. Cancer Drug Targets.*, **2012**, *12*(5), 531-542.
- [19] Vehar, B.; Hrast, M.; Kovac, A.; Konc, J.; Mariner, K.; Chopra, I.; O'Neill, A.; Janez, ic D.; Gobec, S. Ellipticines and 9-acridinylamines as inhibitors of D-alanine:D-alanine ligase. *Bioorg. Med. Chem.*, **2011**, 5137-5146.
- [20] Wolff, L. Chemischen Institut der Universität Jena: Methode zum Ersatz des Sauerstoffatoms der Ketone und Aldehyde durch Wasserstoff. *Justus Liebigs Annalen der Chemie*, **1912**, *394*(1), 86-108.
- [21] Lappano, R.; Rosano, C.; De Marco, P.; De Francesco, E.M.; Pezzi, V.; Maggiolini, M. Estriol acts as a GPR30 antagonist in estrogen receptor-negative breast cancer cells. *Mol. Cell. Endocrinol.*, **2010**, *320*, 162-170.
- [22] Pupo, M.; Pisano, A.; Lappano, R.; Santolla, M.F.; De Francesco, E.F.; Rosano, C.; Maggiolini, M. Bisphenol A induces gene expression changes and proliferative effects through GPER in breast cancer cells and cancer-associated fibroblasts. *Environ Health Perspect.*, **2012**, *120*(8), 1177-1182.
- [23] Rosano, C.; Lappano, R.; Santolla, M.F.; Ponassi, M.; Donadini, A.; Maggiolini, M. Recent advances in the rationale design of GPER ligands. *Curr. Med. Chem.*, **2012**, *19*(36), 6199-6206.
- [24] Albanito, L.; Lappano, R.; Madeo, A.; Chimento, A.; Prossnitz, E.R.; Cappello, A.R.; Dolce, V.; Abonante, S.; Pezzi, V.; Maggiolini, M. G-protein-coupled receptor 30 and estrogen receptor-alpha are involved in the proliferative effects induced by atrazine in ovarian cancer cells. *Environ Health Perspect.*, **2008**, *116*, 1648-1655.
- [25] Maggiolini, M.; Vivacqua, A.; Fasanella, G.; Recchia, A.G.; Sisci, D.; Pezzi, V.; Montanaro, D.; Musti, A.M.; Picard, D.; Andò, S. The G protein-coupled receptor GPR30 mediates c-fos up-regulation by 17beta-estradiol and phytoestrogens in breast cancer cells. *J. Biol. Chem.*, **2004**, *279*, 27008-27016.
- [26] Albanito, L.; Madeo, A.; Lappano, R.; Vivacqua, A.; Rago, V.; Carpino, A.; Oprea, T.I.; Prossnitz, E.R.; Musti, A.M.; Andò, S.; Maggiolini, M. G protein-coupled receptor 30 (GPR30) mediates gene expression changes and growth response to 17beta-estradiol and selective GPR30 ligand G-1 in ovarian cancer cells. *Cancer Res.*, **2007**, *67*, 1859-1866.
- [27] Lappano, R.; Maggiolini, M. G protein-coupled receptors: novel targets for drug discovery in cancer. *Nat. Rev. Drug Discov.*, **2011**, *10*(1), 47-60.
- [28] Filardo, E.J.; Graeber, C.T.; Quinn, J.A.; Resnick, M.B.; Giri, D.; DeLellis, R.A.; Steinhoff, M.M.; Sabo, E. Distribution of GPR30, a seven transmembrane spanning estrogen receptor in primary breast cancer and its association with clinicopathologic determinants of tumor progression. *Clin. Cancer Res.*, **2006**, *12*, 6359-6366.
- [29] Smith, H.O.; Leslie, K.K.; Singh, M.; Qualls, C.R.; Revankar, C.M.; Joste, N.E.; Prossnitz, E.R. GPR30: a novel indicator of poor survival for endometrial carcinoma. *Am. J. Obstet. Gynecol.*, **2007**, *196*, 386.e1-9, discussion 386.e9-e11.
- [30] Smith, H.O.; Arias-Pulido, H.; Kuo, D.Y.; Howard, T.; Qualls, C.R.; Lee, S.J.; Verschraegen, C.F.; Hathaway, H.J.; Joste, N.E.; Prossnitz, E.R. GPR30 predicts poor survival for ovarian cancer. *Gynecol. Oncol.*, **2009**, *114*, 465-471.
- [31] Filardo, E.J.; Quinn, J.A.; Bland, K.I.; Frackelton, A.R. Jr. Estrogen-induced activation of Erk-1 and Erk-2 requires the G protein-coupled receptor homolog, GPR30, and occurs via trans-activation of the epidermal growth factor receptor through release of HB-EGF. *Mol. Endocrinol.*, **2000**, *14*, 1649-1660.
- [32] Vivacqua, A.; Bonfiglio, D.; Recchia, A.G.; Musti, A.M.; Picard, D.; Ando, S.; Maggiolini, M. The G protein-coupled receptor GPR30 mediates the proliferative effects induced by 17 $\beta$ -estradiol and hydroxytamoxifen in endometrial cancer cells. *Mol. Endocrinol.*, **2006**, *20*, 631-646.
- [33] Vivacqua, A.; Bonfiglio, D.; Albanito, L.; Madeo, A.; Rago, V.; Carpino, A.; Musti, A.M.; Picard, D.; Ando, S.; Maggiolini, M. 17 $\beta$ -Estradiol, genistein, and 4-hydroxytamoxifen induce the proliferation of thyroid cancer cells through the G protein coupled-receptor GPR30. *Mol. Pharmacol.*, **2006**, *70*, 1414-1423.
- [34] Chan, Q.K.; Lam, H.M.; Ng, C.F.; Lee, A.Y.; Chan, E.S.; Ng, H.K.; Ho, S.M.; Lau, K.M. Activation of GPR30 inhibits the growth of prostate cancer cells through sustained activation of Erk1/2, c-jun/c-fos-dependent upregulation of p21, and induction of G(2) cell-cycle arrest. *Cell. Death Differ.*, **2010**, *17*, 1511-1523.
- [35] Chevalier, N.; Bouskine, A.; Fenichel, P. Role of GPER/GPR30 in tumoral testicular germ cells proliferation. *Cancer Biol. Ther.*, **2011**, *12*, 2-3.
- [36] Henry, D. Intercalation mechanisms: antitumor drug design based upon helical DNA as a receptor site. *Cancer Chemother Rep.*, **1972**, *3*, 50.

- [37] Balbi, A.; Anzaldi, M.; Macciò, C.; Aiello, C.; Mazzei, M.; Gangemi, R.; Castagnola, P.; Miele, M.; Rosano, C.; Viale, M. Synthesis and biological evaluation of novel pyrazole derivatives with anticancer activity. *Eur. J. Med. Chem.*, **2011**, *46*, 5293-5309.
- [38] Stec-Martyna, E.; Ponassi, M.; Miele, M.; Parodi, S.; Felli, L.; Rosano, C. Structural comparison of the interaction of tubulin with various ligands affecting microtubule dynamics. *Curr. Cancer Drug Targets.*, **2012**, *12*, 658-666.
- [39] Perdih, A.; Dolenc, M.S. Small molecule antagonists of integrin receptors. *Curr. Med. Chem.*, **2010**, *17*, 2371-2392.
- [40] Claffey, M.M.; Helal, C.J.; Verhoest, P.R.; Kang, Z.; Bundesmann, M.W.; Hou, X.; Liu, S.; Kleiman, R.J.; Vanasse-Frawley, M.; Schmidt, A.W.; Menniti, F.; Schmidt, C.J.; Hoffman, W.E.; Hajos, M.; McDowell, L.; O'Connor, R.E.; Macdougall-Murphy, M.; Fonseca, K.R.; Becker, S.L.; Nelson, F.R.; Liras, S. Application of Structure-Based Drug Design and Parallel Chemistry to Identify Selective, Brain Penetrant, *In Vivo* Active Phosphodiesterase 9A Inhibitors. *J. Med. Chem.*, **2012**, Oct 1. [Epub ahead of print].
- [41] Brvar, M.; Perdih, A.; Oblak, M.; Masic, L.P.; Solmajer, T. In silico discovery of 2-amino-4-(2,4-dihydroxyphenyl)thiazoles as novel inhibitors of DNA gyrase B. *Bioorg. Med. Chem. Lett.*, **2010**, *20*, 958-962.
- [42] Ramesh, C.; Nayak, T.K.; Burai, R.; Dennis, M.K.; Hathaway, H.J.; Sklar, L.A.; Prossnitz, E.R.; Arterburn, J.B. Synthesis and characterization of iodinated tetrahydroquinolines targeting the G protein-coupled estrogen receptor GPR30. *J. Med. Chem.*, **2010**, *53*, 1004-1014.
- [43] Pettersen, E.F.; Goddard, T.D.; Huang, C.C.; Couch, G.S.; et al. UCSF Chimera--a visualization system for exploratory research and analysis. *J. Computational Chem.*, **2004**, *25*, 1605-1612.
- [44] Wallace, A.C.; Laskowski, R.A.; Thornton, J.N. Ligplot. A program to generate schematic diagrams of protein-ligand interactions. *Protein Eng.*, **1996**, *8*, 127-134.
- [45] Pandey, D.P.; Lappano, R.; Albanito, L.; Madeo, A.; Maggiolini, M.; Picard, D. Estrogenic GPR30 signalling induces proliferation and migration of breast cancer cells through CTGF. *EMBO J.*, **2009**, *28*, 523-532.
- [46] Albanito, L.; Sisci, D.; Aquila, S.; Brunelli, E.; Vivacqua, A.; Madeo, A.; Lappano, R.; Pandey, D.P.; Picard, D.; Mauro, L.; Andò, S.; Maggiolini, M. Epidermal growth factor induces G protein-coupled receptor 30 expression in estrogen receptor-negative breast cancer cells. *Endocrinology.*, **2008**, *149*, 3799-3808.

Contents lists available at [SciVerse ScienceDirect](http://www.sciencedirect.com)

# Bioorganic & Medicinal Chemistry Letters

journal homepage: [www.elsevier.com/locate/bmcl](http://www.elsevier.com/locate/bmcl)

## Synthesis, characterization and cytotoxic activity on breast cancer cells of new half-titanocene derivatives

Esther Sirignano<sup>a,†</sup>, Carmela Saturnino<sup>a,†</sup>, Antonio Botta<sup>a</sup>, Maria Stefania Sinicropi<sup>b,\*</sup>, Anna Caruso<sup>b</sup>, Assunta Pisano<sup>c</sup>, Rosamaria Lappano<sup>c</sup>, Marcello Maggiolini<sup>c</sup>, Pasquale Longo<sup>d</sup>

<sup>a</sup> Department of Pharmaceutical and Biomedical Sciences, University of Salerno, Italy

<sup>b</sup> Department of Pharmaceutical Sciences, University of Calabria, 87036 Arcavacata of Rende Cosenza, Italy

<sup>c</sup> Department of Pharmaco-Biology, University of Calabria, 87036 Arcavacata of Rende Cosenza, Italy

<sup>d</sup> Department of Chemistry and Biology, University of Salerno, Italy

### ARTICLE INFO

#### Article history:

Received 18 December 2012

Revised 13 March 2013

Accepted 15 March 2013

Available online xxx

#### Keywords:

Metal-based anticancer drugs

Titanocene compounds

Breast cancer cells

### ABSTRACT

A series of novel titanocene-complexes has been prepared and evaluated for their growth regulatory effects in MCF7 and SkBr3 breast cancer cells. The capability of some of these compound to elicit relevant repressive effects on cancer cell growth could be taken into account towards novel pharmacological approaches in cancer therapy.

© 2013 Elsevier Ltd. All rights reserved.

Platinum based anticancer drugs like *cis*-platin, carboplatin and oxaliplatin are commonly used in the treatment of a wide number of tumors, including lung, colorectal, ovarian, head and neck, as well as genitourinary, and breast cancers. However, the efficacy of platinum-based drugs is often compromised because of the substantial risk for severe toxicities, including neurotoxicity.<sup>1</sup>

Over the last few years a lot of research has developed novel metal-based anticancer drugs, with the aim of improving clinical effectiveness, reducing general toxicity and broadening the spectrum of activity.<sup>2</sup>

The search for novel metal-based antitumor drugs, other than Pt agents, includes the investigation of the cytotoxic activity of copper(I/II)<sup>2</sup> and titanocene<sup>3</sup> compounds.

Particular attention has been recently devoted to new copper(I) complexes. Some of these were tested for their cytotoxic properties against several human tumor cell lines, such as HL60 (promyelocytic leukemia), MCF7 (breast cancer), HCT-15 (colon cancer), HeLa (cervix cancer), A549 (lung cancer), 2008 (ovarian cancer sensitive to *cis*-platin) and C13\* (ovarian cancer resistant to *cis*-platin).<sup>2</sup>

A great deal of research has been focused on a variety of transition metal complexes bearing labile *cis* chlorides or similar ligands. Among the candidate drugs, the pseudotetrahedral metallocene complexes of the type (C<sub>5</sub>H<sub>5</sub>)<sub>2</sub>MCl<sub>2</sub> represent a seemingly logical

extension of *cis*-platin derivatives and have received much attention.<sup>4</sup> These complexes are made up of a metal core consisting of transition metals as Ti, Nb, Mo, etc. The coordination sites of the metal are occupied by two cyclopentadienyl rings (C<sub>5</sub>H<sub>5</sub> or Cp) and two labile ligands (i.e., Cl). Köpf-Maier and Köpf<sup>5</sup> have investigated the antitumor activities of a whole series of metallocene dichloride complexes (varying the transition metal) *in vivo*. From this research, titanocene dichloride (TDC) (Fig. 1) exhibited the most promising chemotherapeutic activity among all other metallocenes tested.<sup>6</sup>

Consequently, numerous analogues of TDC were developed and well studied, such as titanocene Y (Fig. 1).

In particular, the anti-proliferative activity of titanocene Y and other titanocenes has been studied in 36 human tumor cell lines.<sup>7</sup> *In vitro* and *ex vivo* experiments showed that renal cancer is a major target for this novel class of titanocenes, although they showed a significant activity also against ovarian, prostate, cervix, lung, colon and breast tumors.<sup>8</sup>

Recently, we reported the synthesis and the cytotoxic activity of some titanocene derivatives obtained replacing the aryl-methoxylic group on cyclopentadienyl of titanocene Y with the ethenyl-methoxy group, in order to have a stronger electron donor effect on the cationic species responsible for the cytotoxic activity. We also verified the influence of leaving ligands on the activity by substituting chlorine atoms with dimethylamide, oxalate or aminoacid groups.<sup>3</sup> It is worth noting that in Ref. 3, the highest cytotoxic activity was reported for half-titanocene complex T<sub>1</sub>,

\* Corresponding author. Tel.: +39 0984 493200; fax: +39 0984 493298.

E-mail address: [s.sinicropi@unical.it](mailto:s.sinicropi@unical.it) (M.S. Sinicropi).

† These authors contributed equally to this work.

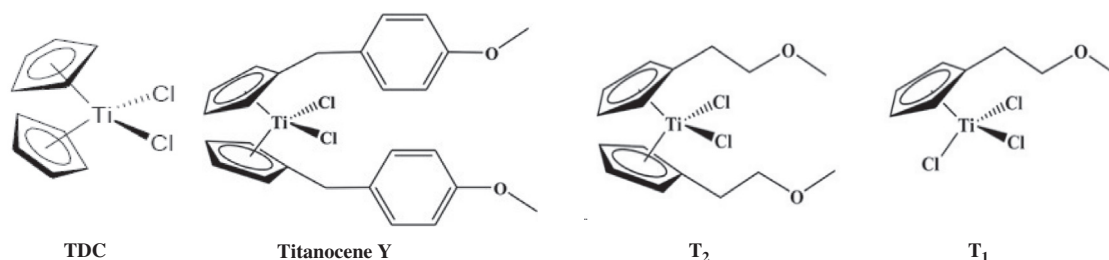


**Figure 1.** Titanocene dichloride (TDC); bis-[(*p*-methoxybenzyl)cyclopentadienyl]titanium dichloride (titanocene Y); bis-cyclopentadienyl-ethenylmethoxyl-titanium dichloride **T<sub>2</sub>** and cyclopentadienyl-ethenylmethoxyltitanium trichloride **T<sub>1</sub>**.

compared to that of titanocene **T<sub>2</sub>**, titanocene Y and *cis*-platin. Some of the synthesized compounds showed a good cytotoxicity, in particular complexes bis-cyclopentadienyl-ethenylmethoxyl-titanium dichloride **T<sub>2</sub>** and cyclopentadienyl-ethenylmethoxyl-titanium trichloride **T<sub>1</sub>** gave values very similar to *cis*-platin on MCF-7 cell lines, with the IC<sub>50</sub> comparable to the ones reported for titanocene Y. Moreover, the half-titanocene complex (**T<sub>1</sub>**) also showed a good cytotoxic activity, comparable to that of *cis*-platin, on HEK-293 cells. The results of hydrolysis of our titanocenes showed unequivocally that the leaving groups (Cl, N(CH<sub>3</sub>)<sub>2</sub>, C<sub>2</sub>O<sub>4</sub> or glycine) significantly affect even hydrolysis rate of cyclopentadienyl groups, being chloride and oxalate more stable.<sup>3</sup>

Thus, the presence of substituents, aryl methoxy group on cyclopentadienyl ring in titanocene Y or ethenyl-methoxy group in titanocene **T<sub>2</sub>** or in the half-titanocene **T<sub>1</sub>**, produce compounds with interesting cytotoxic activity. Although generalizations regarding structure-activity relationships are not yet clear, we could hypothesize that the neutral nucleophilic substituents of cyclopentadienyl (aryl methoxy or ethenyl-methoxy group) could intramolecularly coordinate the titanium cation, thus preventing decomposition reactions. On the other hand, this hypothesis was suggested for analogous complexes able to give polymerization of propene or styrene having microstructures strongly influenced by the possible coordination of neutral substituent of cyclopentadienyl to the metal center.<sup>9-11</sup>

As mentioned above, several examples of titanocene-complexes showing cytotoxic activity were reported, but to the best of our knowledge the cyclopentadienyl-ethenylmethoxyl-titanium trichloride represents the first example of half-titanocene complex with interesting cytotoxic activity.

Therefore, the aim of this study was the synthesis and the characterization of some half-titanocenes compounds (see Fig. 2) by nuclear magnetic resonance (NMR), mass spectroscopy and ele-

mental analysis. All these complexes contain different substituents on the Cp ligands, able to stabilize the titanium cation by intramolecular coordination. Preliminary cytotoxic studies of these titanocene based compounds have been carried out, as well.

Compound **5a** was synthesized in order to verify if the activity was higher for half-titanocene Y than titanocene Y, as it was for the bis-cyclopentadienyl-ethenylmethoxyl-titanium dichloride **T<sub>2</sub>** and cyclopentadienyl-ethenylmethoxyl-titanium trichloride **T<sub>1</sub>**. Compounds **5b**, **5e** and **5f** bear in different positions methoxyl groups, which may make ligands much more coordinating, except for the methoxyl in position 4. Compound **5d** has no substituents on the aryl, but the phenyl is of course able to coordinate to titanium. Finally, the dimethylamino group in position 4 of the aryl moiety of **5c** has a strong capabilities to bond metal-cation.

The synthesis of complexes was carried out according to Scheme 1. The syntheses of proligands fulvene **3a-d** and **3f** were carried out as outlined in references,<sup>12-15</sup> whereas **3e** (2,4-dimethoxyphenyl) fulvene was synthesized in good yield according to literature method<sup>14,16</sup> starting from 2,4-dimethoxy benzaldehyde.

The lithium salt of the ligand was obtained by reacting the suitable fulvene with Super Hydride (LiBEt<sub>3</sub>H) in dry diethyl ether. Then, it was isolated and subsequently reacted with 1 equiv of TiCl<sub>4</sub>·2THF in dry THF. The reaction product was purified following common procedures and isolated in high yield (see Scheme 1). Elemental analysis (C, H, N) was in accordance with the proposed formulation. <sup>1</sup>H COSY experiments allowed the assignment of all the proton resonances of the <sup>1</sup>H NMR spectrum, whereas DEPT experiments were useful for the attribution of <sup>13</sup>C NMR signals. The synthesized half-titanocenes were also characterized by mass spectrometry. The mass spectra show the molecular ion and the fragmentation of the complexes (i.e., ligand, [ligandTi]).<sup>17</sup> These data allowed us to have an unambiguous structural determination, as reported in Scheme 1.

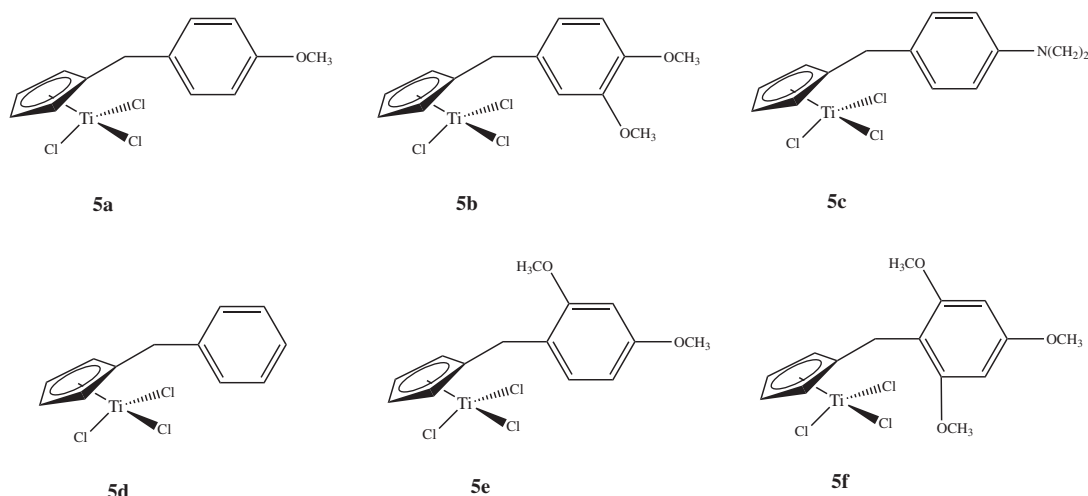
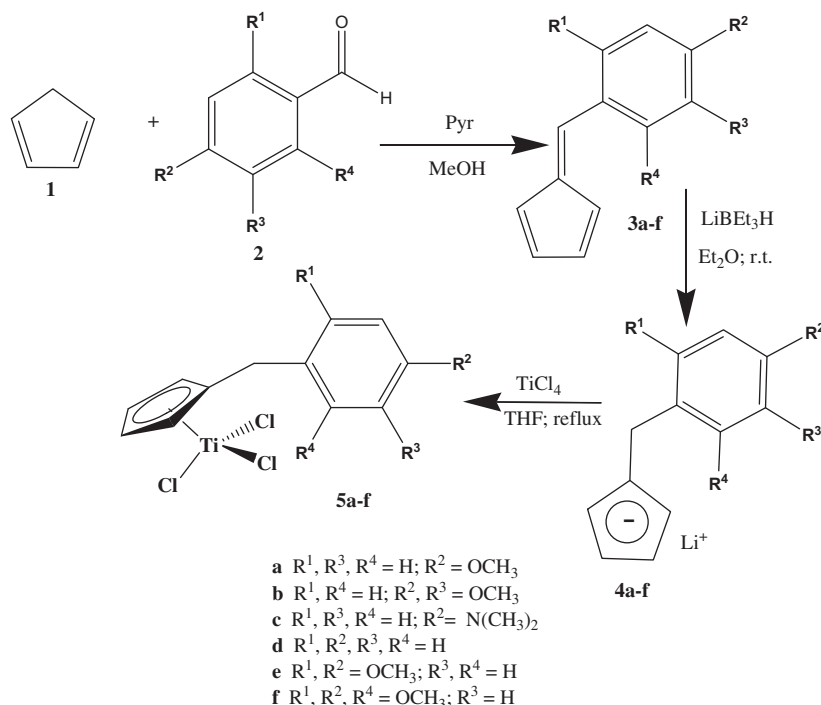


**Figure 2.** Structures of synthesized complexes.



**Scheme 1.** Synthetic route for the preparation of ligands and half-titanocene complexes **5a–f**.

**Table 1**  
Hydrolysis results of **5a–f** complexes in DMSO/D<sub>2</sub>O solution at rt followed by <sup>1</sup>H NMR

Complex	% Cp ring hydrolysis			
	5 min	4 h	8 h	24 h
<b>5a</b>	<1	<1	<1	<5
<b>5b</b>	<1	<1	<1	<5
<b>5c</b>	<1	<1	<5	17
<b>5d</b>	9	24	40	41
<b>5e</b>	<1	<1	<1	<5
<b>5f</b>	<1	<1	<1	<5

Hydrolysis stability of the six half-titanocene complexes (**5a–f**) has been determined in aqueous solution, 90% DMSO by <sup>1</sup>H NMR spectroscopy, in order to correlate the chemical stability and coordination chemistry of these complexes with their observed cytotoxic activity. Since we can expect that rapid hydrolysis of leaving group (–Cl) and cyclopentadienyl ligands could give way to biologically inactive species, active species could be generated if the Cp rings remain metal bound.

Hydrolysis of aromatic rings of **5a–f** was evaluated by integration of two signals of protons of cyclopentadienyl bonded to metal, as to newly formed multiplet of substituted cyclopentadiene. **Table 1** reports the results of our hydrolysis tests.

The complexes that show the highest hydrolytic stability are **5a**, **5b**, **5e** and **5f**. In particular, the cyclopentadienyl rings of complexes are hydrolyzed only for less than 5% after 24 h, whereas complexes **5c** and **5d** are hydrolyzed for 17% and 41%, respectively (**Table 1**).

These data provide sufficient evidence that the presence of coordinating groups on the aryl substituent of the cyclopentadienyl are effective for the stabilization of the complexes. Therefore, these coordinating groups might be fundamental to increase, if active, their biological effectiveness.

In order to investigate the effects on cancer cell proliferation of the novel synthesized compounds, we treated for 5 days MCF7 and SkBr3 breast cancer cells with each compound.<sup>18–20</sup> Cells were also exposed to *cis*-platin in order to compare the anticancer effects of the complexes to this well-known chemotherapeutic. It should be noted that by using the compounds mentioned above, SkBr3 cells

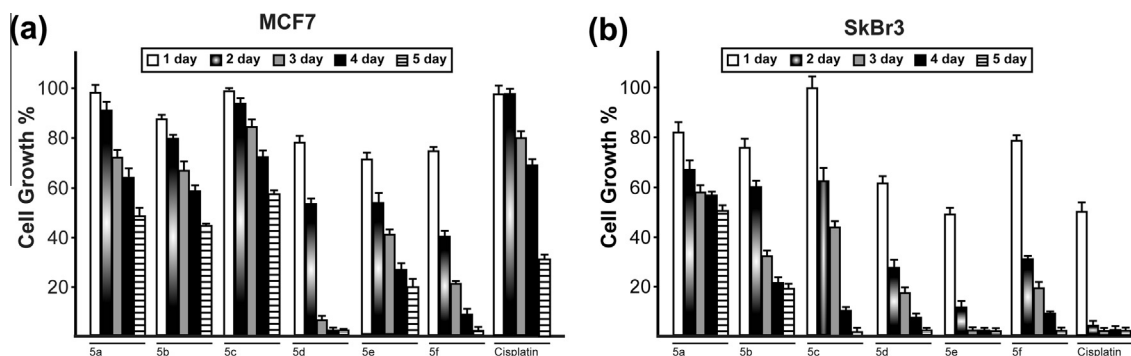


**Figure 3.** Evaluation of growth responses to 10  $\mu$ M of **5a–f** in MCF7 (a) and SkBr3 (b) breast cancer cells, as determined by using the MTT assay. Cell viability was expressed as the percentage of cells treated with the different compounds respect to cells treated with vehicle. Cells ( $5-8 \times 10^4 \text{ ml}^{-1}$ ) were treated for 1 day up to 5 days, as indicated.



resulted to be more responsive to the treatment compared to MCF7 cells. Among all tested compounds, **5d**, **5e** and **5f** elicited repressive effects on the proliferation of both cell lines (Fig. 3). In particular, **5d** strongly decreased the viability of MCF7 cells after 3 days of treatment, whereas **5e** showed the highest antitumor activity on SkBr3 cells after 2 days, being the most active compound on this cell line (Fig. 3). In particular, **5d**, **5e** and **5f** showed a strongest cytotoxic effect on MCF7 than *cis*-platin. Moreover **5e** showed a similar cytotoxic activity on SkBr3 compared to *cis*-platin.

In conclusion, a series of novel titanocene-complexes has been synthesized and evaluated for their growth regulatory effects in MCF7 and SkBr3 breast cancer cells. Among these compounds, that showed moderate to high antitumor activity, the strongest antiproliferative activity against MCF7 cells was displayed especially by **5d**, whereas **5e** elicited relevant repressive effects on SkBr3 cells. Hence, the capability of these compounds to elicit inhibitory effects on cancer cell growth could be taken into account towards novel pharmacological approaches in cancer therapy. Therefore further experiments would be helpful to investigate the molecular mechanism involved.

## Acknowledgments

We wish to thank Italian Minister of University and Research for financial support of this work. The authors are grateful to Dr. Rosanna Guarino for her contribute in the synthesis of the compounds.

## References and notes

- (a) McWhinney, S. R.; Goldberg, R. M.; McLeod, H. L. *Mol Cancer Ther.* **2009**, *8*, 10; (b) Bailly, C.; Viostat, B.; Labouze, X.; Morgant, G.; Saturnino, C.; Lancelot, J. C.; Robba, M.; Dung, N. H. *Met.-Based Drugs* **1998**, *5*, 279; (c) Saturnino, C.; Napoli, M.; Paolucci, G.; Bortoluzzi, M.; Popolo, A.; Pinto, A.; Longo, P. *Eur. J. Med. Chem.* **2010**, *45*, 4169.
- Zanella, A.; Gandin, V.; Porchia, M.; Refosco, F.; Tisato, F.; Sorrentino, F.; Scutari, G.; Rigobello, M. P. *Invest. New Drugs* **2011**, *29*, 1213.
- Napoli, M.; Saturnino, C.; Sirignano, E.; Popolo, A.; Pinto, A.; Longo, P. *Eur. J. Med. Chem.* **2011**, *46*, 122.
- Clarke, M. J.; Zhu, F.; Frasca, D. R. *Chem. Rev.* **1999**, *99*, 2511.
- Köpf-Maier, P.; Köpf, H. *Angew. Chem., Int. Ed. Engl.* **1979**, *18*, 477.
- Dombrowski, K. E.; Baldwin, W.; Sheats, J. E. *J. Organomet. Chem.* **1986**, *302*, 281.
- Kelter, G.; Sweeney, N. J.; Strohfeldt, K.; Fiebig, H.; Tacke, M. *Anti-Cancer Drug* **2005**, *16*, 1091.
- Claffey, J.; Gleeson, B.; Hogan, M.; Müller-Bunz, H.; Wallis, D.; Tacke, M. *Eur. J. Organomet. Chem.* **2008**, *26*, 4074.
- Longo, P.; Amendola, A. G.; Fortunato, E.; Boccia, A. C.; Zambelli, A. *Macromol. Rapid Commun.* **2001**, *22*, 339.
- De Rosa, C.; Auriemma, F.; Circelli, T.; Longo, P.; Boccia, A. C. *Macromolecules* **2003**, *36*, 3465.
- Napoli, M.; Grisi, F.; Longo, P. *Macromolecules* **2009**, *42*, 2516.
- Tacke, M.; Cuffe, L. P.; Gallagher, W. M.; Lou, Y.; Mendoza, O.; Müller-Bunz, H.; Rehmann, F.-J. K.; Sweeney, N. J. *Inorg. Biochem.* **1987**, *2004*, 98.
- Tacke, M.; Allen, L. T.; Cuffe, L. P.; Gallagher, W. M.; Lou, Y.; Mendoza, O.; Müller-Bunz, H.; Rehmann, F.-J. K.; Sweeney, N. J. *Organomet. Chem.* **2004**, *689*, 2242.
- Claffey, J.; Hogan, M.; Müller-Bunz, H.; Pampillon, C.; Tacke, M. *J. Organomet. Chem.* **2008**, *693*, 526.
- Stone, K. J.; Little, R. D. *J. Org. Chem.* **1984**, *49*, 11.
- Sweeney, N.; Mendoza, O.; Müller-Bunz, H.; Pampillon, C.; Rehmann, F.-J. K.; Strohfeldt, T.; Tacke, K. M. *J. Organomet. Chem.* **2005**, *690*, 4537.
- Experimental section*: The elemental analyses for C, H, N, were recorded on a ThermoFinnigan Flash EA 1112 series and performed according to standard microanalytical procedures. <sup>1</sup>H NMR, homodecoupled <sup>1</sup>H NMR, <sup>1</sup>H COSY and <sup>13</sup>C NMR spectra were recorded at 298 K on a Bruker Avance 300 Spectrometer operating at 300 MHz (<sup>1</sup>H) and 75 MHz (<sup>13</sup>C) and referred to internal tetramethylsilane. Molecular weights were determined by ESI mass spectrometry. ESI-MS analysis in positive and negative ion mode, were made using a Finnigan LCO ion trap instrument, manufactured by Thermo Finnigan (San Jose, CA, USA), equipped with the Excalibur software for processing the data acquired. The sample was dissolved in acetonitrile and injected directly into the electrospray source, using a syringe pump, which maintains constant flow at 5 µl/min. The temperature of the capillary was set at 220 °C. All manipulations were carried out under oxygen- and moisture-free atmosphere in an MBraun MB 200 glove-box. All the solvents were thoroughly deoxygenated and dehydrated under argon by refluxing over suitable drying agents, while NMR deuterated solvents (Euriso-Top products) were kept in the dark over molecular sieves. TiCl<sub>4</sub>, Titanium(IV) chloride tetrahydrofuran complex, Super Hydride (LiBEt<sub>3</sub>H, 1.0 M solution in THF), and all chemicals were obtained from Aldrich chemical Co. and used without further purification. Cyclopentadiene was obtained by freshly cracked dicyclopentadiene. The six fulvenes and their relative lithium salt were prepared by following the reported procedures.<sup>14,16</sup>
- Synthesis of half-titanocene complexes 5a,b*: Lithium cyclopentadienide intermediate (1.83 mmol) was dissolved in dry THF (20 ml) to give a colourless solution. TiCl<sub>4</sub> (18.30 mmol) was added at 0 °C to give a dark red solution. This was refluxed overnight and then cooled. The solvent was removed under reduced pressure. The remaining residue was extracted with dichloromethane (30 ml) and filtered through celite to remove the LiCl. The filtrate was washed twice with hexane (20 ml) and then dried under reduced pressure to give a solid.
- Spectral data of newly synthesized compounds*: [(4-Methoxybenzyl)cyclopentadienyl]-titanium-trichloride [C<sub>5</sub>H<sub>4</sub>-CH<sub>2</sub>-C<sub>6</sub>H<sub>4</sub>-OCH<sub>3</sub>]<sub>2</sub>TiCl<sub>3</sub> (**5a**). Black solid. <sup>1</sup>H NMR (δ ppm, CD<sub>2</sub>Cl<sub>2</sub>, 300 MHz): 3.78 [s, 3H, C<sub>5</sub>H<sub>4</sub>-CH<sub>2</sub>-C<sub>6</sub>H<sub>4</sub>-OCH<sub>3</sub>], 4.01 [s, 2H, C<sub>5</sub>H<sub>4</sub>-CH<sub>2</sub>-C<sub>6</sub>H<sub>4</sub>-OCH<sub>3</sub>], 6.80 [m, 4H, C<sub>5</sub>H<sub>4</sub>-CH<sub>2</sub>-C<sub>6</sub>H<sub>4</sub>-OCH<sub>3</sub>], 6.83–7.01 [d, 4H, C<sub>5</sub>H<sub>4</sub>-CH<sub>2</sub>-C<sub>6</sub>H<sub>4</sub>-OCH<sub>3</sub>]. <sup>13</sup>C NMR (δ ppm, CD<sub>2</sub>Cl<sub>2</sub>, 75 MHz): 55.90 [C<sub>5</sub>H<sub>4</sub>-CH<sub>2</sub>-C<sub>6</sub>H<sub>4</sub>-OCH<sub>3</sub>], 45.0 [C<sub>5</sub>H<sub>4</sub>-CH<sub>2</sub>-C<sub>6</sub>H<sub>4</sub>-OCH<sub>3</sub>], 114.0–128.70–130.0–132.0–135.90–147.80–158.60 [C<sub>5</sub>H<sub>4</sub>-CH<sub>2</sub>-C<sub>6</sub>H<sub>4</sub>-OCH<sub>3</sub>]. Mass (E.I., 70 eV, m/z): 273 [L-Ti-Cl]<sup>+</sup>, 186 [L]<sup>+</sup>. Calcd for C<sub>13</sub>H<sub>13</sub>Cl<sub>3</sub>O<sub>2</sub>Ti (%): C, 46.00; H, 3.86. Found (%): C, 46.21; H, 3.84.
- [(3,4-Di-methoxybenzyl)-cyclopentadienyl]-titanium-trichloride [C<sub>5</sub>H<sub>4</sub>-CH<sub>2</sub>-C<sub>6</sub>H<sub>3</sub>-(OCH<sub>3</sub>)<sub>2</sub>]<sub>2</sub>TiCl<sub>3</sub> (**5b**). Brown solid. <sup>1</sup>H NMR (δ ppm, THF-d<sub>8</sub>, 300 MHz): 3.73 [s, 6H, C<sub>5</sub>H<sub>4</sub>-CH<sub>2</sub>-C<sub>6</sub>H<sub>3</sub>-(OCH<sub>3</sub>)<sub>2</sub>], 3.98 [s, 2H, C<sub>5</sub>H<sub>4</sub>-CH<sub>2</sub>-C<sub>6</sub>H<sub>3</sub>-(OCH<sub>3</sub>)<sub>2</sub>], 6.29–6.42 [m, 4H, C<sub>5</sub>H<sub>4</sub>-CH<sub>2</sub>-C<sub>6</sub>H<sub>3</sub>-(OCH<sub>3</sub>)<sub>2</sub>], 6.71–6.76 [d, 2H, C<sub>6</sub>H<sub>3</sub>-(OCH<sub>3</sub>)<sub>2</sub>], 6.84 [s, 1H, C<sub>6</sub>H<sub>3</sub>-(OCH<sub>3</sub>)<sub>2</sub>]. <sup>13</sup>C NMR (δ ppm, CD<sub>2</sub>Cl<sub>2</sub>, 75 MHz): 55.50 [C<sub>5</sub>H<sub>4</sub>-CH<sub>2</sub>-C<sub>6</sub>H<sub>3</sub>-(OCH<sub>3</sub>)<sub>2</sub>], 36.80 [C<sub>5</sub>H<sub>4</sub>-CH<sub>2</sub>-C<sub>6</sub>H<sub>3</sub>-(OCH<sub>3</sub>)<sub>2</sub>], 112.20–113, 30–115.40–120.80–122.50–132.80–137.10–149.20–150.30 [C<sub>5</sub>H<sub>4</sub>-CH<sub>2</sub>-C<sub>6</sub>H<sub>3</sub>-(OCH<sub>3</sub>)<sub>2</sub>]. Mass (E.I., 70 eV, m/z): 286 [L-Ti-Na]<sup>+</sup>. Calcd for C<sub>14</sub>H<sub>15</sub>Cl<sub>3</sub>O<sub>2</sub>Ti (%): C, 45.51; H, 4.09. Found (%): C, 45.91; H, 4.04.
- (4-(*N,N*-Dimethylbenzylidene)-cyclopentadienyl)-titanium-trichloride [C<sub>5</sub>H<sub>4</sub>-CH<sub>2</sub>-C<sub>6</sub>H<sub>4</sub>-N(CH<sub>3</sub>)<sub>2</sub>]<sub>2</sub>TiCl<sub>3</sub> (**5c**). Red solid. <sup>1</sup>H NMR (δ ppm, THF, 300 MHz): 2.98 [s, 6H, C<sub>5</sub>H<sub>4</sub>-CH<sub>2</sub>-C<sub>6</sub>H<sub>4</sub>-N(CH<sub>3</sub>)<sub>2</sub>], 3.89 [s, 2H, C<sub>5</sub>H<sub>4</sub>-CH<sub>2</sub>-C<sub>6</sub>H<sub>4</sub>-N(CH<sub>3</sub>)<sub>2</sub>], 6.45–6.67 [m, 4H, C<sub>5</sub>H<sub>4</sub>-CH<sub>2</sub>-C<sub>6</sub>H<sub>4</sub>-N(CH<sub>3</sub>)<sub>2</sub>], 7.10–7.31 [d, 4H, C<sub>5</sub>H<sub>4</sub>-CH<sub>2</sub>-C<sub>6</sub>H<sub>4</sub>-N(CH<sub>3</sub>)<sub>2</sub>]. <sup>13</sup>C NMR (δ ppm, THF-d<sub>8</sub>, 75 MHz): 41.70 [C<sub>5</sub>H<sub>4</sub>-CH<sub>2</sub>-C<sub>6</sub>H<sub>4</sub>-N(CH<sub>3</sub>)<sub>2</sub>], 33.10 [C<sub>5</sub>H<sub>4</sub>-CH<sub>2</sub>-C<sub>6</sub>H<sub>4</sub>-N(CH<sub>3</sub>)<sub>2</sub>], 115.90–117.60–119.20–128.70–130.70–136.0–137.10 [C<sub>5</sub>H<sub>4</sub>-CH<sub>2</sub>-C<sub>6</sub>H<sub>4</sub>-N(CH<sub>3</sub>)<sub>2</sub>]. Mass (E.I., 70 eV, m/z): 371 [L-TiCl<sub>3</sub>-Na]<sup>+</sup>. Calcd for C<sub>14</sub>H<sub>16</sub>Cl<sub>3</sub>N<sub>2</sub>Ti (%): C, 47.70; H, 4.57. Found (%): C, 47.92; H, 4.17; N, 3.79.
- (Benzyl)-cyclopentadienyl-titanium-trichloride [C<sub>5</sub>H<sub>4</sub>-CH<sub>2</sub>-C<sub>6</sub>H<sub>5</sub>]<sub>2</sub>TiCl<sub>3</sub> (**5d**). Red solid. <sup>1</sup>H NMR (δ ppm, THF-d<sub>8</sub>, 300 MHz): 4.06 [s, 2H, C<sub>5</sub>H<sub>4</sub>-CH<sub>2</sub>-C<sub>6</sub>H<sub>5</sub>], 6.33–6.45 [m, 4H, C<sub>5</sub>H<sub>4</sub>-CH<sub>2</sub>-C<sub>6</sub>H<sub>5</sub>], 7.22–7.24 [m, 5H, C<sub>5</sub>H<sub>4</sub>-CH<sub>2</sub>-C<sub>6</sub>H<sub>5</sub>]. <sup>13</sup>C NMR (δ ppm, THF-d<sub>8</sub>, 75 MHz): 36.70 [C<sub>5</sub>H<sub>4</sub>-CH<sub>2</sub>-C<sub>6</sub>H<sub>5</sub>], 110.90–115.10–122.60–128.0–128.60–140.60 [C<sub>5</sub>H<sub>4</sub>-CH<sub>2</sub>-C<sub>6</sub>H<sub>5</sub>]. Mass (E.I., 70 eV, m/z): 242 [L-Ti-K]<sup>+</sup>, 163 [L-Li]<sup>+</sup>. Calcd for C<sub>12</sub>H<sub>11</sub>Cl<sub>3</sub>Ti (%): C, 46.58; H, 3.58. Found (%): C, 46.17; H, 3.32.
- (2,4-Di-methoxybenzyl)-cyclopentadienyl-titanium-trichloride [C<sub>5</sub>H<sub>4</sub>-CH<sub>2</sub>-C<sub>6</sub>H<sub>3</sub>-(OCH<sub>3</sub>)<sub>2</sub>]<sub>2</sub>TiCl<sub>3</sub> (**5e**). Brown solid. <sup>1</sup>H NMR (δ ppm, THF-d<sub>8</sub>, 300 MHz): 3.72–3.760 [s, 6H, C<sub>5</sub>H<sub>4</sub>-CH<sub>2</sub>-C<sub>6</sub>H<sub>3</sub>-(OCH<sub>3</sub>)<sub>2</sub>], 3.90 [s, 2H, C<sub>5</sub>H<sub>4</sub>-CH<sub>2</sub>-C<sub>6</sub>H<sub>3</sub>-(OCH<sub>3</sub>)<sub>2</sub>], 6.28–6.29 [m, 4H, C<sub>5</sub>H<sub>4</sub>-CH<sub>2</sub>-C<sub>6</sub>H<sub>3</sub>-(OCH<sub>3</sub>)<sub>2</sub>], 6.40–6.46 [d, 2H, C<sub>5</sub>H<sub>4</sub>-CH<sub>2</sub>-C<sub>6</sub>H<sub>3</sub>-(OCH<sub>3</sub>)<sub>2</sub>], 7.01 [s, 1H, C<sub>6</sub>H<sub>3</sub>-(OCH<sub>3</sub>)<sub>2</sub>]. <sup>13</sup>C NMR (δ ppm, CD<sub>2</sub>Cl<sub>2</sub>, 75 MHz): 55.40–55.50 [C<sub>5</sub>H<sub>4</sub>-CH<sub>2</sub>-C<sub>6</sub>H<sub>3</sub>-(OCH<sub>3</sub>)<sub>2</sub>], 31.80 [C<sub>5</sub>H<sub>4</sub>-CH<sub>2</sub>-C<sub>6</sub>H<sub>3</sub>-(OCH<sub>3</sub>)<sub>2</sub>], 99.10–104.80–116.60–121.90–123.30–131.40–137.60–159.20–161.0 [C<sub>5</sub>H<sub>4</sub>-CH<sub>2</sub>-C<sub>6</sub>H<sub>3</sub>-(OCH<sub>3</sub>)<sub>2</sub>]. Mass (E.I., 70 eV, m/z): 286 [L-Ti-Na]<sup>+</sup>. Calcd for C<sub>14</sub>H<sub>15</sub>Cl<sub>3</sub>O<sub>2</sub>Ti (%): C, 45.51; H, 4.09. Found (%): C, 45.91; H, 4.04.
- (2,4-Tri-methoxybenzyl)-cyclopentadienyl-titanium-trichloride [C<sub>5</sub>H<sub>4</sub>-CH<sub>2</sub>-C<sub>6</sub>H<sub>2</sub>-(OCH<sub>3</sub>)<sub>3</sub>]<sub>2</sub>TiCl<sub>3</sub> (**5f**). Black solid. <sup>1</sup>H NMR (δ ppm, THF, 300 MHz): 3.72–3.77 [s, 9H, C<sub>5</sub>H<sub>4</sub>-CH<sub>2</sub>-C<sub>6</sub>H<sub>2</sub>-(OCH<sub>3</sub>)<sub>3</sub>], 3.90 [s, 2H, C<sub>5</sub>H<sub>4</sub>-CH<sub>2</sub>-C<sub>6</sub>H<sub>2</sub>-(OCH<sub>3</sub>)<sub>3</sub>], 6.30–6.34 [m, 4H, C<sub>5</sub>H<sub>4</sub>-CH<sub>2</sub>-C<sub>6</sub>H<sub>2</sub>-(OCH<sub>3</sub>)<sub>3</sub>], 6.47 [s, 2H, C<sub>5</sub>H<sub>4</sub>-CH<sub>2</sub>-C<sub>6</sub>H<sub>2</sub>-(OCH<sub>3</sub>)<sub>3</sub>]. <sup>13</sup>C NMR (δ ppm, THF-d<sub>8</sub>, 75 MHz): 54.70 [C<sub>5</sub>H<sub>4</sub>-CH<sub>2</sub>-C<sub>6</sub>H<sub>2</sub>-(OCH<sub>3</sub>)<sub>3</sub>], 31.05 [C<sub>5</sub>H<sub>4</sub>-CH<sub>2</sub>-C<sub>6</sub>H<sub>2</sub>-(OCH<sub>3</sub>)<sub>3</sub>], 98.40–104.0–115.80–122.50–130.60–137.70–158.30–160.30 [C<sub>5</sub>H<sub>4</sub>-CH<sub>2</sub>-C<sub>6</sub>H<sub>2</sub>-(OCH<sub>3</sub>)<sub>3</sub>]. Mass (E.I., 70 eV, m/z): 317 [L-Ti-Na]<sup>+</sup>. Calcd for C<sub>15</sub>H<sub>17</sub>Cl<sub>3</sub>O<sub>3</sub>Ti (%): C, 45.09; H, 4.29. Found (%): C, 45.39; H, 4.24.
- (a) Caruso, A.; Chimento, A.; El-Kashef, H.; Lancelot, J. C.; Panno, A.; Pezzi, V.; Saturnino, C.; Sinicropoli, M. S.; Sirianni, R.; Rault, S. *J. Enzyme Inhib. Med. Chem.* **2012**, *27*, 60; (b) Gasparotto, V.; Castagliuolo, I.; Chiarello, G.; Pezzi, V.; Montanaro, D.; Brun, P.; Palù, G.; Viola, G.; Ferlin, M. *Eur. J. Med. Chem.* **1910**, *2006*, 49.
- Cell culture*: MCF7 breast cancer cells were maintained in DMEM/F-12 supplemented with 10% fetal bovine serum (FBS), 100 mg/ml penicillin/streptomycin and 2 mM L-glutamine (Invitrogen, Gibco, Milan, Italy). SkBr3 breast cancer cells were cultured in RPMI-1640 medium supplemented with 10% FBS, 100 mg/ml penicillin/streptomycin and 2 mM L-glutamine (Invitrogen, Gibco, Milan, Italy). Cells were switched to medium without serum the day before experiments and thereafter treated in medium supplemented with 1% FBS.
- Inhibition of cell proliferation*: The effects of each compound on cell viability were determined with the MTT [3-(4,5-dimethylthiazol-2-yl)-2,5-diphenyltetrazolium bromide] assay,<sup>20–23</sup> which is based on the conversion of MTT to formazan by mitochondrial enzyme. Cells were seeded in quadruplicate in 96-well plates in regular growth medium and grown until 70–80% confluence. Cells were washed once they had attached and then treated

- with 10  $\mu$ M each compound for indicated time (for 1 day up to 5 days). Relative cell viability was determined by MTT assay according to the manufacturer's protocol (Sigma–Aldrich, Milan, Italy). Mean absorbance for each drug dose was expressed as a percentage of the control untreated well absorbance and plotted versus drug concentration. IC<sub>50</sub> values represent the drug concentrations that reduced the mean absorbance at 570 nm to 50% of those in the untreated control wells.
20. Mosmann, T. J. *Immunol. Methods* **1983**, *65*, 55.
  21. Pascale, R.; Carocci, A.; Catalano, A.; Lentini, G.; Spagnoletta, A.; Cavalluzzi, M. M.; De Santis, F.; De Palma, A.; Scalera, V.; Franchini, C. *Bioorg. Med. Chem.* **2010**, *18*, 5903.
  22. Carocci, A.; Catalano, A.; Bruno, C.; Lovece, A.; Roselli, M. G.; Cavalluzzi, M. M.; De Santis, F.; De Palma, A.; Rusciano, M. R.; Illario, M.; Franchini, C.; Lentini, G. *Bioorg. Med. Chem.* **2013**, *21*, 847.
  23. Sinicropi, M. S.; Caruso, A.; Conforti, F.; Marrelli, M.; El Kashef, H.; Lancelot, J. C.; Rault, S.; Statti, G. A.; Menichini, F. *J. Enzyme Inhib. Med. Chem.* **2009**, *24*, 1148.





## The nuclear localization signal is required for nuclear GPER translocation and function in breast Cancer-Associated Fibroblasts (CAFs)



Marco Pupo<sup>a</sup>, Adele Vivacqua<sup>a</sup>, Ida Perrotta<sup>b</sup>, Assunta Pisano<sup>a</sup>, Saveria Aquila<sup>a</sup>, Sergio Abonante<sup>c</sup>, Anna Gasperi-Campani<sup>d</sup>, Vincenzo Pezzi<sup>a</sup>, Marcello Maggiolini<sup>a,\*</sup>

<sup>a</sup> Department of Pharmacy, Health and Nutritional Sciences, University of Calabria, Rende, Italy

<sup>b</sup> Department of Ecology, University of Calabria, Rende, Italy

<sup>c</sup> Regional Hospital, Cosenza, Italy

<sup>d</sup> Department of Experimental, Diagnostic and Specialty Medicine (DIMES) School of Medicine, Alma Mater Studiorum-University of Bologna, Italy and Interdepartmental Center for the Research on Cancer "Giorgio Prodi", University of Bologna, Italy

### ARTICLE INFO

#### Article history:

Received 9 January 2013  
Received in revised form 2 April 2013  
Accepted 30 May 2013  
Available online 5 June 2013

#### Keywords:

Breast cancer  
Cancer-associated fibroblasts  
Estrogen signaling  
GPER  
Nuclear localization signal

### ABSTRACT

Cancer associated fibroblasts (CAFs) actively contribute to the growth and invasion of cancer cells. In recent years, the G protein estrogen receptor (GPER) has been largely involved in the estrogenic signals in diverse types of normal and tumor cells. In CAFs, GPER was localized into the nucleus, however the molecular mechanisms which regulate its nuclear shuttle remain to be clarified. In the present study, we demonstrate that in breast CAFs GPER translocates into the nucleus through an importin-dependent mechanism. Moreover, we show that a nuclear localization signal is involved in the nuclear import of GPER, in the up-regulation of its target genes *c-fos* and *CTGF* and in the migration of CAFs induced by estrogens. Our data provide novel insights into the nuclear localization and function of GPER in CAFs toward a better understanding of the estrogen action elicited through these key players of the tumor microenvironment.

© 2013 Elsevier Ireland Ltd. All rights reserved.

### 1. Introduction

Cancer progression is not merely determined by malignant cell features as diverse elements present in the surrounding tumor stroma play a key role in the invasion, angiogenesis and metastasis (Kalluri, 2003). Among the components of the cancer microenvironment, vasculature which consist of endothelial and smooth muscle cells as well as pericytes provides the nutrients and oxygen (Lohela et al., 2009). In addition, the inflammatory and immune cells which are recruited by chemokines and cytokines, have both tumor-suppressing and promoting functions (Müller-Hübenthal et al., 2009). Notably, quiescent fibroblasts become activated in tumor stroma and act as important regulators of the paracrine signaling between stromal and cancer cells (Lorusso and Rugg, 2008). In particular, a specialized group of fibroblasts called Cancer-Associated Fibroblasts (CAFs) actively contribute to the growth and invasion of malignant cells by providing a unique tumor microenvironment (Xing et al., 2010). Considering that close relationships occur between cancer cells and CAFs, cancer development cannot be dissociated from its local microenvironment. For instance, CAFs

express a wide number of growth factors and matrix remodelling enzymes that modulate proliferation and invasion of cancer cells, angiogenesis and chemoresistance (Kenny and Bissell, 2003; Lafkas et al., 2008; Miyamoto et al., 2004; Orimo et al., 2005; Tlsty and Hein, 2001). In breast carcinomas, about 80% of stromal fibroblasts acquire the "activated" phenotype contributing to cancer progression through different mechanisms, including a functional cross-talk with the malignant cells and the local production of secreted factors and hormones like estrogens (Kalluri and Zeisberg, 2006; Pupo et al., 2012; Yamaguchi and Hayashi, 2009).

Estrogens are involved in a broad spectrum of physiological functions ranging from reproduction to modulation of bone density, brain function, and cholesterol mobilization (Koos, 2011). Moreover, estrogens may promote the development of certain types of tumors mainly through the estrogen receptor (ER) $\alpha$  and ER $\beta$  (Liang and Shang, 2012; Maggiolini et al., 2004a; Panno et al., 1996). An increasing number of studies has demonstrated that also the G protein-coupled estrogen receptor (GPER) mediates estrogenic signals in numerous normal and malignant cell types (Albanito et al., 2008a; Albanito et al., 2008b; Albanito et al., 2007; Bartella et al., 2012; Canonaco et al., 2008; Chimento et al., 2012; Chimento et al., 2011; Chimento et al., 2010; De Marco et al., 2012; Filice et al., 2009; Madeo et al., 2010; Maggiolini et al., 2004b; Maggiolini and Picard, 2009; Prossnitz and Maggiolini, 2009; Rago et al., 2011; Recchia et al., 2011; Revankar et al., 2005; Santolla et al., 2012; Sirianni et al.,

\* Corresponding author. Address: Department of Pharmacy, Health and Nutritional Sciences, University of Calabria, 87036 Rende, Italy. Tel.: +39 0984 493076; fax: +39 0984 493458.

E-mail address: [marcellomaggiolini@yahoo.it](mailto:marcellomaggiolini@yahoo.it) (M. Maggiolini).

2008; Vivacqua et al., 2009; Vivacqua et al., 2006a; Vivacqua et al., 2006b). In this regard, several studies have shown that not only 17 $\beta$ -estradiol (E2) binds to GPER (Filardo et al., 2000), but also estriol (Lappano et al., 2010) as well as the ER antagonists tamoxifen and ICI 182,780 (Filardo et al., 2002; Pandey et al., 2009; Thomas et al., 2005; Vivacqua et al., 2012; 2006a, 2006b). Furthermore, the identification of synthetic ligands of GPER acting as agonists or antagonists has extended our knowledge regarding the estrogenic GPER signaling (Bologa et al., 2006; Dennis et al., 2011; Lappano et al., 2012a, 2012b; Rosano et al., 2012). Interestingly, the ligand activation of GPER induced a specific gene signature consisting of a network of transcription factors involved in the proliferation and migration of ER-negative breast cancer cells (Pandey et al., 2009). In particular, the GPER signaling pathway recalled the well characterized transcriptional “immediate early response” of fibroblasts to serum, which includes among others c-fos and the connective tissue growth factor (CTGF) (Iyer et al., 1999; Pandey et al., 2009).

GPER was localized both at the cell membrane (Filardo et al., 2007; Pang et al., 2008; Thomas et al., 2005) and in subcellular compartments (Filardo and Thomas, 2012; Lin et al., 2009; Matsuda et al., 2008; Otto et al., 2008; Revankar et al., 2007; Revankar et al., 2005; Sakamoto et al., 2007; Wang et al., 2008). Moreover, GPER was detected within the nucleus in CAFs (Madeo and Maggiolini, 2010), mimicking the nuclear localization of other plasma membrane receptors, like certain tyrosine kinases receptors (RTKs) and GPCRs, in different cell types (Boivin et al., 2008; Gobeil et al., 2006; Wang et al., 2010). The presence of a peptide sequence referred to as nuclear localization signals (NLSs) was involved in the nuclear shuttle of these membrane receptors, for instance NLS motifs were identified in the eighth helix and/or in the third intracellular loops of diverse GPCRs (Gobeil et al., 2006).

In the present study, we demonstrate that a putative NLS located within the GPER protein sequence and an importin-dependent mechanism are involved in the receptor translocation within the nuclear compartment in CAFs. In addition, we show that nuclear GPER is required for the up-regulation of c-fos and CTGF as well as the migratory effects induced by E2. Our data provide novel insights into the molecular mechanisms by which GPER mediates the estrogen action in important players of the tumor microenvironment like CAFs.

## 2. Materials and methods

### 2.1. Reagents

17 $\beta$ -Estradiol (E2) and wheat germ agglutinin (WGA) were purchased from Sigma–Aldrich (Milan, Italy). E2 was dissolved in ethanol, WGA was solubilized in PBS.

### 2.2. Cell cultures

CAFs were extracted as previously described (Madeo and Maggiolini, 2010; Pupo et al., 2012) and maintained in a mixture of MEDIUM 199 and HAM'S F-12 (1:1) supplemented with 10% FBS. Primary breast fibroblasts were characterized by immunofluorescence. Briefly, cells were incubated with human anti-vimentin (V9) as well as human anti-cytokeratin 14 (LL001) and anti-fibroblast activated protein  $\alpha$  (FAP $\alpha$ ) (H-56) antibodies purchased from Santa Cruz Biotechnology (DBA, Milan, Italy) in order to select CAFs (data not shown). Signed informed consent from all the patients was obtained and all samples were collected, identified and used in accordance with approval by the respective local review boards.

### 2.3. Plasmids

Short hairpin construct against human GPER (shGPER) and the resistant version of GPER named GPER rescue (containing silent

mutations in the shRNA targeted sequence) were generated and used as previously described (Pandey et al., 2009; Vivacqua et al., 2009). The GPER rescue plasmid mutated in the NLS sequence referred to as GPER rescue (M) was generated from site directed mutagenesis experiments, as indicated below.

### 2.4. Site-directed mutagenesis

The PSORT II program was used to identify sequences in human GPER [Entrez Protein accession number Q99527] containing highly charged, basic amino acid residues that could potentially function as NLS. GPER rescue was mutated at the putative NLS by using the QuikChange™ site-directed mutagenesis kit from Stratagene (Agilent Technologies, Milan, Italy) to replace the arginine residues in the position 253 and 254 with alanine residues. The sequence for the sense primer was 5-caccgtgggctgcccGCGcgcagaaggcgtcccatg-3 (capital letters are mutated bases). Mutations were confirmed by DNA sequencing (PRIMM, Milan, Italy).

### 2.5. Gene silencing experiments

For the experiments performed using shRNA, cells were plated onto 10-cm dishes and transiently transfected with 5  $\mu$ g/plate of indicated plasmids in medium without serum for 24 h. All transfections were performed using X-treme Gene 9 reagent, as recommended by the manufacturer (Roche Diagnostics, Milan, Italy). For small interfering RNA (siRNA) transfection, siRNA oligonucleotides targeting importin  $\beta$  and nonspecific siRNA oligonucleotides were purchased from Ambion (Life Technologies, Milan Italy). The siRNA oligonucleotides were transfected using X-treme Gene 9 reagent, as recommended by the manufacturer (Roche Diagnostics, Milan, Italy); 48 h after transfection, cells were harvested and analyzed by immunogold assays.

### 2.6. Immunostaining assay

CAFs were seeded in Lab-Tek II chamber slides at a density of  $1 \times 10^5$  per well and incubated for 24 h in the corresponding maintenance media. For immunofluorescence staining, fibroblasts were transfected for 24 h, fixed in 4% paraformaldehyde, permeabilized with 0.1% TWEEN three times for 5 min and then were blocked for 30 min at room temperature with PBS containing 10% normal donkey serum (Santa Cruz Biotechnology, DBA, Milan, Italy), 0.1% Triton X-100, and 0.05% TWEEN. Thereafter, cells were incubated overnight at 4 °C with a primary antibody against GPER (K-19) (1:100 purchased from Santa Cruz Biotechnology, DBA, Milan, Italy) in PBS containing 0.05% TWEEN. After incubation, the slides were extensively washed with PBS and incubated with donkey anti-rabbit IgG-FITC (1:100, from Santa Cruz Biotechnology, DBA, Milan, Italy) and propidium iodide (1:1000, Sigma–Aldrich, Milan, Italy). Leica AF6000 Advanced Fluorescence Imaging System supported by quantification and image processing software Leica Application Suite Advanced Fluorescence (Leica Microsystems CMS, GbH Mannheim, Germany) were used for experiment evaluation.

### 2.7. Chromatin immune-precipitation (ChIP)

Cells grown in 10 cm plates were shifted for 24 h to medium lacking serum, permeabilized as previously described (Suh and Gumbiner, 2003) and then treated for 2 h with E2 1nM alone or in combination with WGA. ChIP assay was performed as previously described (Morelli et al., 2004). The immune-cleared chromatin was precipitated with anti-GPER (N-15, sc-48525-R) or nonspecific rabbit anti-IgG (sc-2027) antibodies both purchased from Santa Cruz Biotechnology (DBA, Milan, Italy). 5  $\mu$ l volume of each sample was used as template to amplify regions containing putative

AT-rich sequences (ATRS) located within the *c-fos* (from –46 to –41) (Lo et al., 2005) or *CTGF* (from –377 to –142) (Pupo and Maggiolini, unpublished data) promoters by real-time PCR (Applied Biosystems, Milan, Italy). The primers pairs used to amplify the fragments were: 5'-AGGGAGCTGCGAGCGCTGGG-3'(forward) and 5'-GTGGCGGTTAGGAGGCAAAGCCG-3'(reverse) for *c-fos* and 5'-GCTTTTTCAGACGGAGGAAT-3'(forward) and 5'-GAGCTGGAGG-TGGAGTCGC-3'(reverse) for *CTGF* promoter regions. Real-time PCR data were normalized with respect to input DNA whose quantification was performed by using 5  $\mu$ l of the template DNA. The relative antibody-bound fractions were normalized to a calibrator that was chosen to be the basal untreated sample.

## 2.8. Reverse transcription and semiquantitative RT-PCR

Total RNA was extracted using Trizol commercial kit (Invitrogen, Milan, Italy) according to the manufacturer's protocol. RNA was quantified spectrophotometrically and its quality was checked by electrophoresis through agarose gel stained with ethidium bromide. Total cDNA was synthesized from RNA by reverse transcription using the murine leukemia virus reverse transcriptase (Invitrogen, Milan, Italy) following the protocol provided by the manufacturer. The expression of selected genes, *c-fos*, *CTGF* and the internal control *RPLP0* (also known as *36B4*), was quantified by semiquantitative RT-PCR which was carried out as previously described (Maggiolini et al., 1999). cDNAs yielded bands of 420, 392 and 408 bp with 20, 20 and 10 PCR cycles, respectively. The primers used were: 5'-AGAAAAGGAGAATCCGAAGGGAAAG-3' (forward) and 5'-ATGATGCTGGGAACAGGAAGTC-3'(reverse) for *c-fos*; 5'-ATGGCATGAAGCCAGAGAGT-3'(forward) and 5'-GGTCAGTGACACGCTAAAA-3'(reverse) for *CTGF*; 5'-CTCAACATCTCCCCCTTCTC-3'(forward) and 5'-CAAATCCCATATCCTCGTCC-3'(reverse) for *RPLP0*.

## 2.9. Immunoblotting

Cells were grown in 10-cm dishes in regular growth medium and serum starved for 24 h before transfection or stimulation with ligands. For the experiments performed using WGA, cells were also permeabilized as previously described (Suh and Gumbiner, 2003). CAFs were then lysed in 500  $\mu$ l of 50 mmol/L NaCl, 1.5 mmol/L MgCl<sub>2</sub>, 1 mmol/L EGTA, 10% glycerol, 1% Triton X-100, 1% sodium dodecylsulfate (SDS), and a mixture of protease inhibitors containing 1 mmol/L aprotinin, 20 mmol/L phenylmethylsulfonyl fluoride, and 200 mmol/L sodium orthovanadate. Protein concentration was determined using Bradford reagent according to the manufacturer's recommendations (Sigma-Aldrich, Milan, Italy). Equal amounts of whole protein extract were resolved on a 10% SDS polyacrylamide gel and transferred to a nitrocellulose membrane (Amersham Biosciences, Milan, Italy). Membranes were probed overnight at 4 °C with the antibody against *c-fos* (H-125), *CTGF* (L-20), *GPER* (N-15), *Importin  $\beta$*  (H-300), *EGFR* (1005) and  $\beta$ -actin (C-2) which were purchased from Santa Cruz Biotechnology (DBA, Milan, Italy). The levels of proteins were detected, after incubation with the horseradish peroxidase-linked secondary antibodies, by the ECL<sup>®</sup> (enhanced chemiluminescence) System (GE Healthcare, Milan, Italy).

## 2.10. Immunogold assay

### 2.10.1. Preparation of CAFs

Cells were centrifuged at 1200g for 10 min, and the pellet was fixed with 4% paraformaldehyde and 0.25% glutaraldehyde in sodium phosphate buffer for 12 h at 4 °C. Samples were subsequently washed with phosphate buffer and dehydrated in ascending graded series of ethanol. Infiltration with LR white acrylic resin

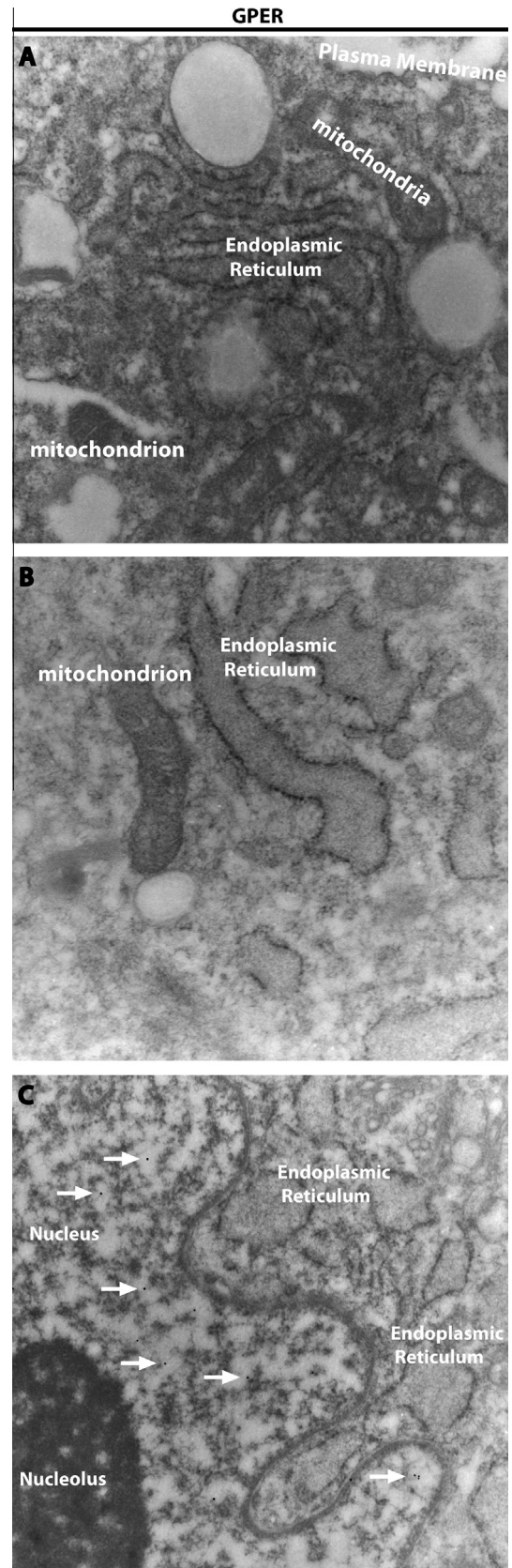


**Fig. 1.** Electron micrographs show the localization of GPER in the nucleus of CAFs. In CAFs serum-starved for 24 h, GPER is not distributed at the plasma membrane (A, 31,500 $\times$ ) or mitochondria (A, 31,500 $\times$  and B, 40,000 $\times$ ) and endoplasmic reticulum (A, 31,500 $\times$ , B, 40,000 $\times$  and C, 31,500 $\times$ ) but it localizes only in the nucleus (C, 31,500 $\times$ ). Arrows indicate immunoreactive gold particles.



(London Resin, Berkshire, UK) was performed with a mixture of ethanol and LR White (1:2) and pure LR White (twice) for 1 h each. All samples were then transferred to fresh LR White in gelatin capsules. The blocks were hardened and cured for 24 h at 50 °C.

#### 2.10.2. Postembedding immunogold

Ultrathin sections of 800–1200 Å were prepared using a diamond knife and collected on Formvar carbon-coated nickel grids. Non-specific binding sites were first blocked with 0.05 M glycine diluted in 0.1 M sodium phosphate buffer, pH 7.2, for 5 min then with 1% bovine serum albumin (BSA) in 0.1 M phosphate buffer, pH 7.2, for 30 min, and finally again with phosphate buffer-glycine for the next 10 min. After three washes with phosphate buffer-BSA for 5 min each, sections were incubated at 4 °C overnight with primary antibodies specific for GPER (N-15) (sc-48525-R) and pEGFR<sup>Tyr1173</sup> (sc-12351) (Santa Cruz Biotechnology (DBA, Milan, Italy)) diluted 1/10 in PBS + 1% BSA. Following three washes with phosphate buffer/BSA, grids with sections were incubated with 10-nm gold-conjugated goat anti-rabbit antibodies diluted 1/50 in phosphate buffer-BSA for 1 h at room temperature. After immunolabeling, sections were washed with PBS + 1% BSA and distilled water, dried, and then stained with uranyl acetate. Specificity of the reactions was confirmed by substituting the primary antibodies with nonimmune goat serum at 4 °C overnight. All sections were examined with a Zeiss EM 900 electron microscope.

#### 2.11. Migration assay

Migration assays were performed using Boyden chambers (Costar Transwell, 8 mm polycarbonate membrane). CAFs were transfected in medium without serum, after 24 h cells were seeded in the upper chambers. E2 was added to the medium without serum in the bottom wells. After 8 h cells on the bottom side of the membrane were fixed and counted.

#### 2.12. Statistical analysis

Statistical analysis was performed using analysis of variance followed by Newman-Keuls testing to determine differences in means. *p*-Values < 0.05 are considered statistically significant.

### 3. Results

#### 3.1. Nuclear localization of GPER

In order to provide novel insight into the functional activity elicited by GPER in our CAFs, which do not express the classical ERs (Madedo and Maggiolini 2010; Pupo et al., 2012), we initially evaluated its distribution pattern by electron microscopy. In CAFs, which were serum-deprived for 24 h, GPER localized in the nuclear compartment but not in the endoplasmic reticulum, mitochondria and plasma membrane (Fig. 1A–C and Supplementary Fig. 1A and B). To confirm the aforementioned observation, we transfected CAFs with a specific shGPER that silenced the expression (Supplementary Fig. 2) and the nuclear detection of GPER (Fig 2A and B). Considering that the GPER-mediated signaling involves the activation of EGFR, we assessed the localization of phosphorylated EGFR (pEGFR<sup>Tyr1173</sup>). As shown in Supplementary Fig. 3 (panels A and B), the activated EGFR was detected only at the plasma membrane in CAFs. Moreover, the silencing of EGFR did not alter the nuclear compartmentalization of GPER (Supplementary Fig. 4A–C). Collectively, these data suggest that in CAFs the peculiar localization of GPER within the nucleus does not depend on EGFR.

#### 3.2. Nuclear translocation of GPER occurs through an importin-dependent mechanism

On the basis of these data, we aimed to evaluate the mechanism involved in the translocation of GPER within the nucleus of CAFs. Considering that several GPCRs exhibit putative nuclear localization sequences which would allow their nuclear transport by importins (Gobeil et al., 2006), we performed electron microscopy experiments in CAFs exposed to WGA, which inhibits the importin-dependent nuclear translocation (Dittmann et al., 2005; Suh and Gumbiner, 2003). It is worth noting that WGA abolished the nuclear shuttle of GPER which localized within the cytoplasmic compartment (Fig. 3A and B). Similar results were obtained silencing importin  $\beta$  expression in CAFs (Supplementary Fig. 5A–C), suggesting that the nuclear localization of GPER involves an importin-dependent mechanism.

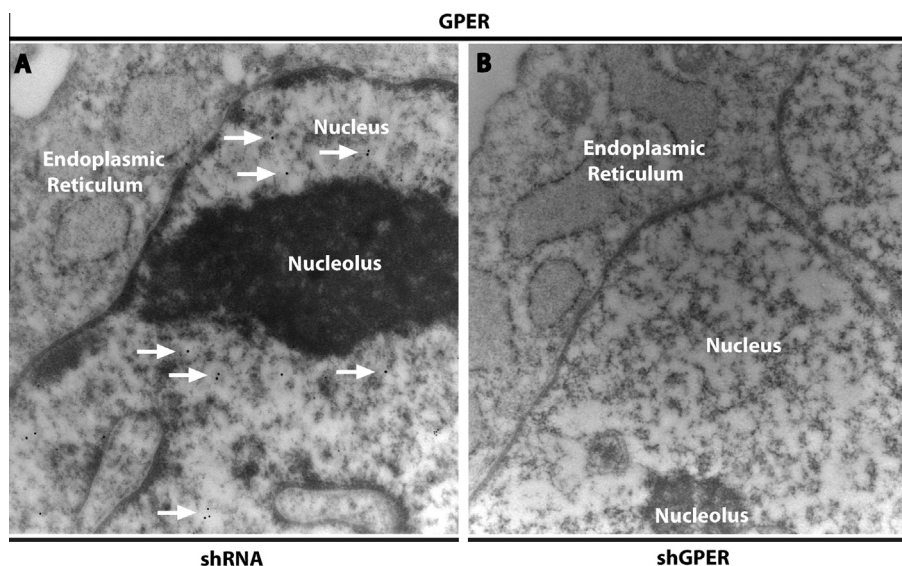


**Fig. 2.** (A,  $\times 31500$ ), electron micrographs showing the nuclear localization of GPER in CAFs transfected for 24 h with shRNA in medium without serum. (B,  $25,000\times$ ), CAFs transfected for 24 h with shGPER in medium without serum do not evidence nuclear GPER. Arrows indicate immunoreactive gold particles.

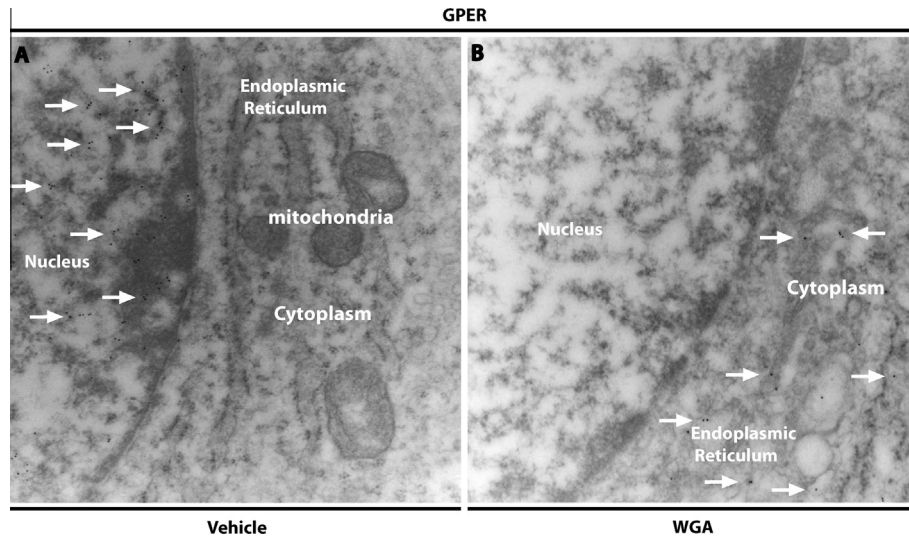


**Fig. 3.** Wheat germ agglutinin (WGA) prevents the nuclear translocation of GPER in CAFs. CAFs were serum-deprived for 24 h, then exposed to vehicle (A, 31,500 $\times$ ) or 5  $\mu$ g/ml nuclear transport inhibitor WGA for 2 h (B, 31,500 $\times$ ). Arrows indicate immunoreactive gold particles.

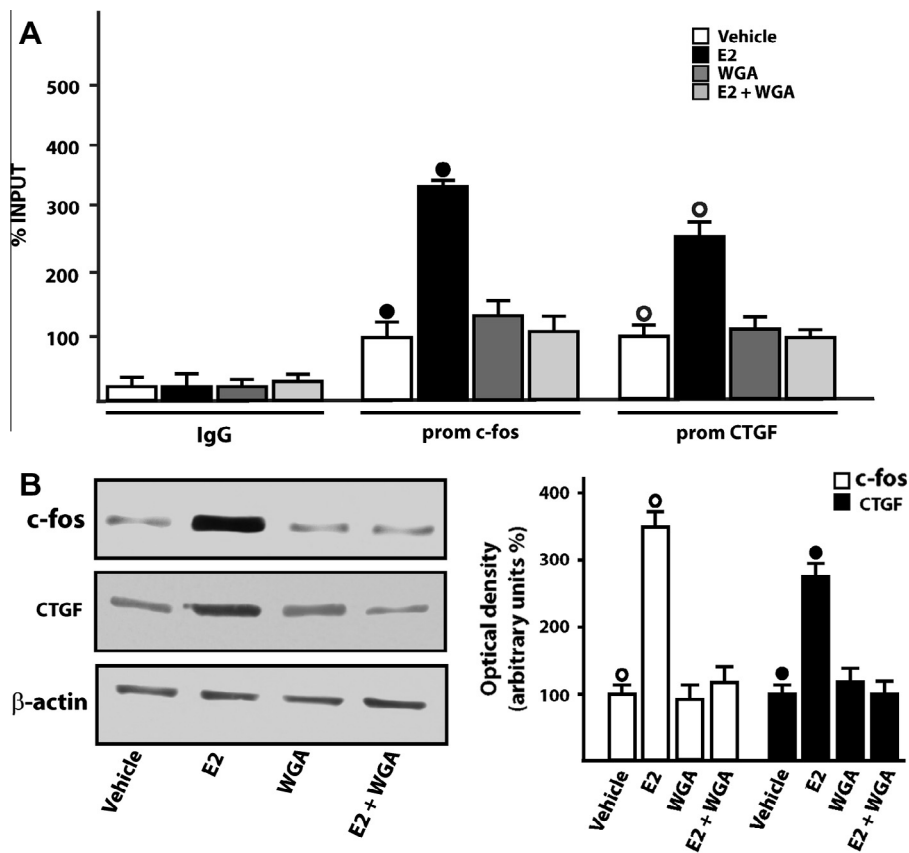


**Fig. 4.** Wheat germ agglutinin (WGA) abolishes the up-regulation of the GPER target genes *c-fos* and *CTGF* induced by E2. (A) WGA prevents the recruitment of GPER to the *c-fos* and *CTGF* promoter sequences induced by E2. CAFs were serum-deprived for 24 h, then treated with vehicle, 1 nM E2 for 2 h alone or in combination with 5  $\mu$ g/ml WGA. Cells were submitted to the ChIP analysis using anti-GPER or non-specific anti-IgG antibodies. The amplified sequences were evaluated by real-time PCR. Each column represents the mean  $\pm$  SD of three independent experiments performed in triplicate. (B) Immunoblots of *c-fos* and *CTGF* protein expression in CAFs serum-deprived for 24 h and then treated for 2 h with 1 nM E2 alone or in combination with 5  $\mu$ g/ml WGA. Side panel shows the densitometric analysis of the blots normalized to  $\beta$ -actin. Each data point represents the mean  $\pm$  SD of three independent experiments. (○), (●) indicate  $p < 0.05$  for cells receiving E2 treatment versus vehicle.

### 3.3. Inhibition of nuclear transport of GPER abrogates gene expression induced by E2

Next, we assessed the implication of the nuclear transport of GPER in the expression of *c-fos* and *CTGF* which mainly contribute

to the biological action of GPER (Madeo and Maggiolini, 2010; Pandey et al., 2009). In this vein, we first determined that the nuclear localization of GPER does not change upon treatment with E2 for 2 h (Supplementary Fig. 6A–B) or up to a 24 h treatment with E2 (data not shown). Then, we performed ChIP analysis immune-pre-

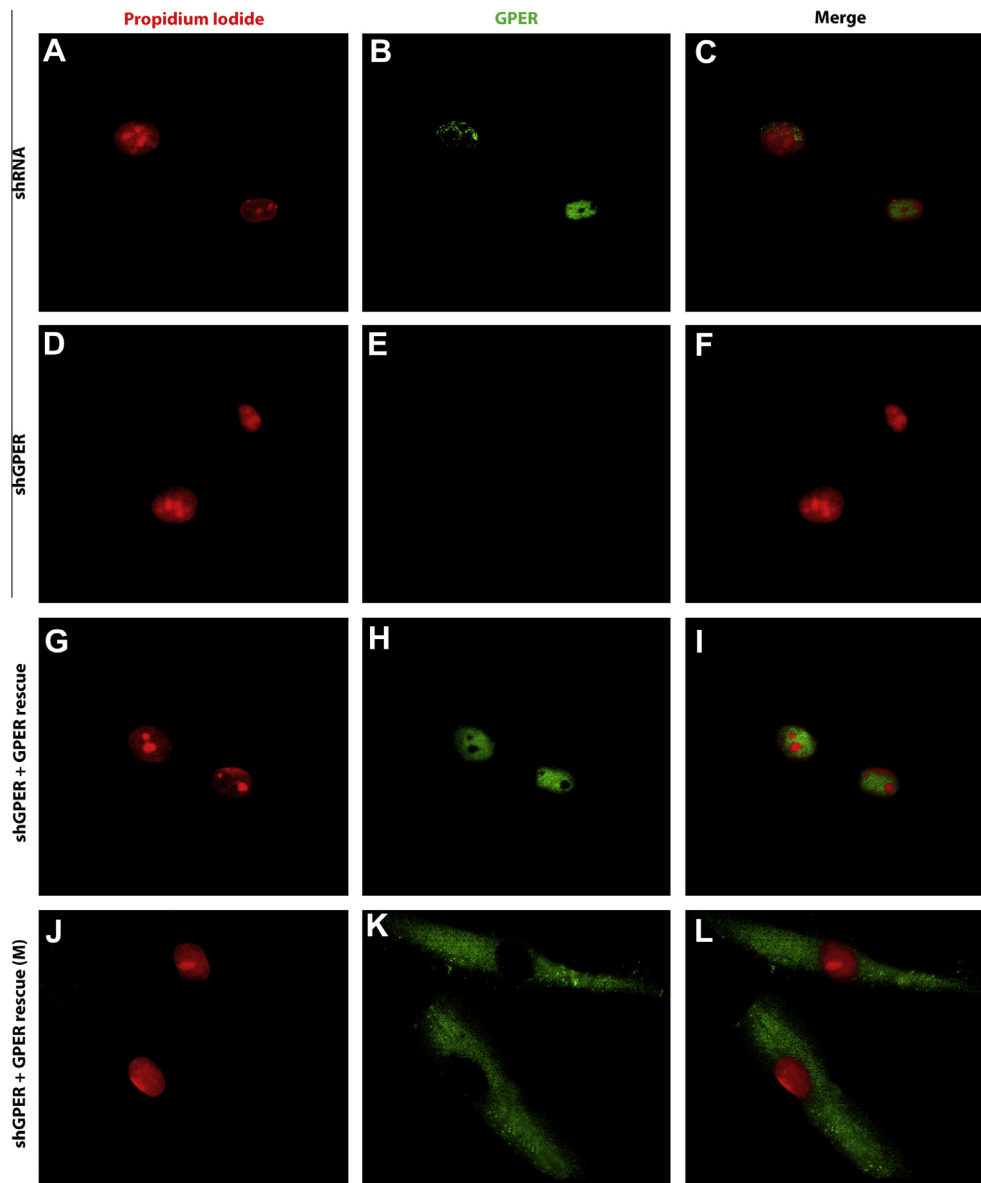


**Fig. 5.** Mutations of the NLS motif in the GPER sequence impair nuclear translocation of GPER in CAFs, as determined by fluorescence imaging. (A–L) Representative images of CAFs immunostained with anti-GPER antibody. (A, D, G, and J) nuclei stained with propidium iodide. (B, E, H and K) green signal localization of GPER. (A–C) GPER localizes in the nucleus of CAFs transfected for 24 h with shRNA in medium without serum. (D–F) The localization of GPER in the nucleus of CAFs is abrogated transfecting cells for 24 h with shGPER in medium without serum. (G–I) GPER localizes in the nucleus of CAFs transfected for 24 h with both shGPER and GPER rescue in medium without serum. (J–L) The localization of GPER in the nucleus of CAFs is abrogated transfecting cells for 24 h with shGPER and GPER rescue (M) in medium without serum. Each experiment shown is representative of 20 random fields observed each in three independent experiments. (For interpretation of the references to color in this figure legend, the reader is referred to the web version of this article.)

precipitating cell chromatin with an anti-GPER antibody and amplifying the regions containing putative ATRS motifs within the *c-fos* and *CTGF* promoter regions. In CAFs, the recruitment of GPER to *c-fos* and *CTGF* promoter sequences induced by E2 was abrogated in presence of WGA (Fig. 4A). In accordance with these data, the expression of *c-fos* and *CTGF* at both the mRNA (data not shown) and protein levels induced by E2 was abolished using WGA (Fig. 4B). Considering that WGA can lead to non-specific effects, we used the PSORTII program to verify whether the GPER protein sequence contains highly charged basic amino acid residues that could function as NLS. Having identified a putative NLS (Supplementary Fig. 7A and B), we modified this region in a resistant version of GPER named GPER rescue (see materials and methods), hence generating a further plasmid named GPER rescue (M) as shown in panel B of Supplementary Fig. 7. CAFs were therefore transfected with these mutated plasmids in order to evaluate the

role of NLS on the nuclear translocation of GPER. In fluorescence assays, cells transfected with shRNA evidenced a nuclear localization of GPER (Fig. 5A–C) while in cells transfected with shGPER the fluorescence signal was no longer present (Fig. 5D–F). Transfecting cells with both shGPER and GPER rescue, GPER was localized within the nucleus (Fig. 5G–I), whereas transfecting cells with both shGPER and GPER rescue (M) the fluorescence signal was clearly distributed within the cytoplasm compartment (Fig. 5J–L). Then, we analysed the protein expression of the GPER target genes *c-fos* and *CTGF* in CAFs transfected with a shRNA, shGPER alone and in combination with GPER rescue or GPER rescue (M). The up-regulation of *c-fos* and *CTGF* induced by E2 was abolished in presence of shGPER, but it was still present using shGPER along with GPER rescue (Fig. 6A). On the contrary, the treatment with E2 in cells transfected with both shGPER and GPER rescue (M) was not able to induce *c-fos* and *CTGF* expression (Fig. 6A). Col-

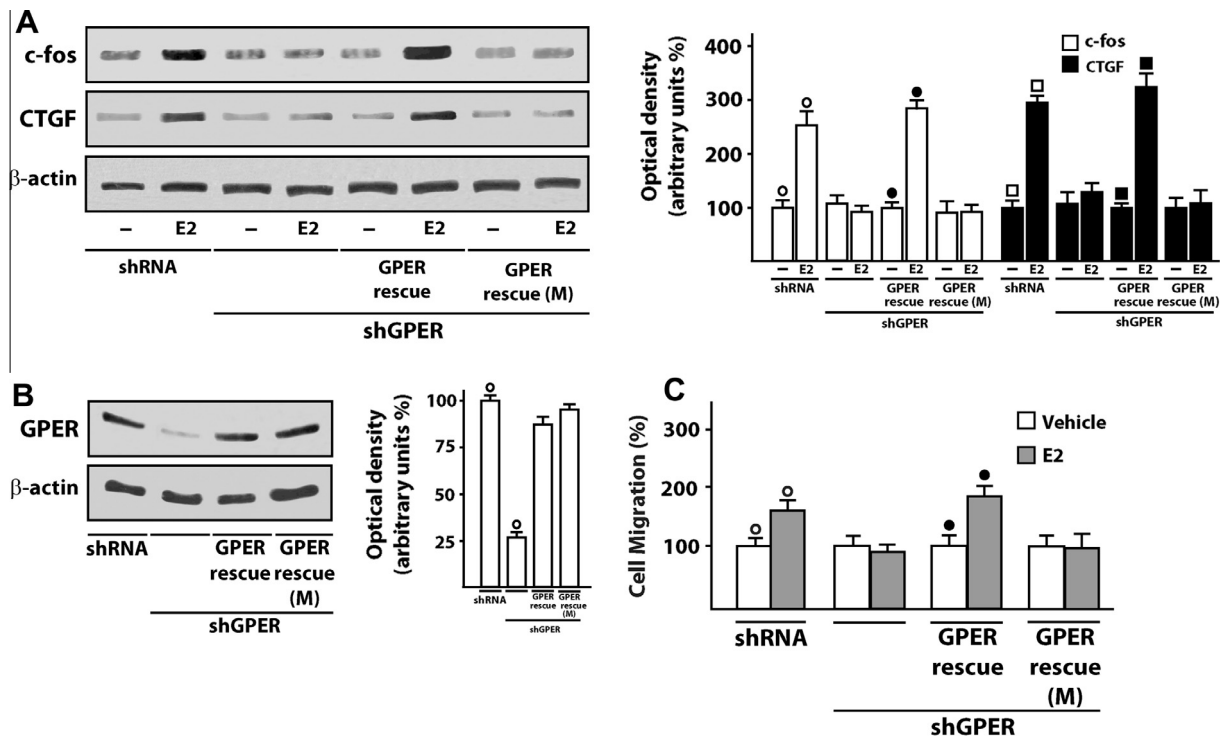


**Fig. 6.** Mutations of the NLS motif in the GPER sequence prevent the GPER-dependent up regulation of c-fos and CTGF as well as the migratory effects induced by E2 in CAFs. (A) Immunoblots of c-fos and CTGF protein expression in CAFs transfected for 24 h in medium without serum with shRNA, shGPER alone and in combination with GPER rescue or GPER rescue (M) before treatment with 1nM E2 for 2 h. (B) GPER protein expression in CAFs transfected for 24 h with shRNA, shGPER alone and in combination with GPER rescue or GPER rescue (M) in medium without serum. Side panels in A and B show the densitometric analysis of the blots normalized to  $\beta$ -actin. (C) Migration of CAFs treated with 1 nM E2 for 8 h in cells transfected for 24 h with shRNA, shGPER alone and in combination with GPER rescue or GPER rescue (M) in medium without serum. Values of cells receiving vehicle were set to 100% upon which the migration induced by E2 was calculated. Each data point represents the mean  $\pm$  SD of three independent experiments. (○), (●), (□), (■) indicate  $p < 0.05$  for cells receiving E2 versus vehicle.

lectively, these data suggest that a preserved NLS region on the GPER protein sequence is necessary in CAFs for the receptor translocation within the nucleus and the stimulation of GPER target genes by E2.

#### 3.4. The GPER nuclear transport is necessary for cell migration induced by E2

As a biological counterpart of the aforementioned results, we ascertained the role of the nuclear translocation of GPER on the migratory effects triggered by E2. The migration of CAFs upon exposure to E2 was abolished using shGPER alone but it was still evident transfecting cells with both shGPER and GPER rescue (Fig 6C). Interestingly, transfecting CAFs with both shGPER and GPER rescue (M) the migratory effects induced by E2 were no longer evident (Fig. 6C). Overall, these data suggest that the migration of CAFs observed upon E2 stimulation depends on the expression of GPER and its nuclear translocation.

#### 4. Discussion

The biological features of tumors do not exclusively rely on the properties of cancer cells as diverse elements of the tumor micro-environment synergistically cooperate towards cancer progression (Cirri and Chiarugi, 2011). For instance, factors secreted by the surrounding stromal cells together with cell interactions trigger a network of signaling pathways, which plays a pivotal role in driving tumorigenesis and metastasis (Xing et al., 2010). In particular, an increasing interest has been recently addressed to a specialized type of fibroblasts called CAFs, which actively contribute to the

growth and invasion of cancer cells (Mao et al., 2012). CAFs may originate from normal fibroblasts undergoing genetic alterations as well as from a transdifferentiation of epithelial and circulating cells recruited within the tumor mass (Ostman and Augsten, 2009). As it concerns breast cancer, over 80% of the fibroblasts exhibit the activated phenotype of CAFs, which therefore contribute to the growth, expansion and dissemination of neoplastic cells (Aboussekhra, 2011; Kalluri and Zeisberg, 2006). A better understanding regarding the signaling pathways which characterize the functional properties of CAFs, is therefore of paramount interest towards the identification of the molecular mechanisms involved in the pathological roles exerted by these cells in tumors and their potential consideration as a valuable prognostic marker and therapeutic target.

In recent years, the identification of GPER as a novel estrogen receptor has opened a new window among the molecular mechanisms involved by estrogens in triggering multifaceted biological actions (Prossnitz and Maggiolini, 2009). GPER has been found in a wide number of tumors including breast, endometrial, ovarian and thyroid carcinomas (Maggiolini and Picard, 2009). In cells derived from these types of cancer, estrogens can stimulate proliferative and migratory responses through GPER, which consequently contributes to tumor progression (Maggiolini and Picard, 2009). Further supporting the role elicited by GPER in well-characterized estrogen-sensitive tumors, its expression was associated with negative clinical features and poor survival rates in patients with breast, endometrial and ovarian carcinomas, suggesting that GPER may be considered as a predictor of aggressive diseases (Filardo et al., 2006; Smith et al., 2009; Smith et al., 2007).

In this study, we ascertained through electron microscopy that GPER localizes in the nuclear compartment in CAFs extracted from



breast cancer patients. In particular, we demonstrated for the first time the existence of a putative NLS in the GPER sequence, which regulates in CAFs the receptor nuclear translocation in an importin-dependent manner. Interestingly, the nuclear function of GPER is required for the expression of two main GPER target genes like *c-fos* and *CTGF* upon estrogen exposure (Pandey et al., 2009). In this regard, we found that GPER mediates the up-regulation of *c-fos* and *CTGF* by binding to putative ATRS motifs located within the promoter region of these genes. As a biological counterpart of these findings, we determined that the migration of CAFs stimulated by E2 relies on an importin-mediated process as shown by using a plasmid encoding the NLS-mutated GPER.

Although GPCRs are mainly considered as cell surface functional entities (Lappano and Maggiolini, 2012; Lappano and Maggiolini, 2011), our data are in accordance with previous studies showing that certain GPCRs including angiotensin II AT<sub>1</sub> (Chen et al., 2000), parathyroid hormone (Watson et al., 2000) and endothelin ETB (Boivin et al., 2003) receptors as well as some growth factor receptors like the epidermal growth factor receptor (EGFR) (Lin et al., 2001), can reside within the nucleus in diverse cell contexts. Different hypotheses have been proposed to elucidate the mechanisms through which GPCRs and growth factor receptors translocate into the nuclear compartment. In this regard, it has been shown that the nuclear shuttle of these receptors is generally mediated by the importin  $\alpha/\beta$  system which harbours a NLS sequence referred to as “pat4”, “pat7” or bipartite domains (Bedard et al., 2007; Lange et al., 2007). In particular, the armadillo-repeats within the importin  $\alpha$  protein allow the interaction with NLS-containing proteins (Christophe et al., 2000), while the arginine-rich N-terminal domain of the importin  $\alpha$  protein is responsible for the binding to the repeated HEAT motifs located within the importin  $\beta$  structure (Cingolani et al., 1999). Then, the importin  $\beta$  allows the translocation of the multiprotein complex across the nuclear membrane by interacting with nuclear pore proteins (Funasaka and Wong, 2011; Suh and Gumbiner, 2003). Several GPCRs have a clear NLS motif (Lee et al., 2004), therefore their nuclear import may occur through the association with carrier proteins recognizing NLS sequences (Gobeil et al., 2006). To date, the functions of GPCRs in cell nuclei remain to be fully characterized. Several studies have demonstrated that these receptors exhibit the ability to interact with membrane associated proteins which translocate into the nucleus (Gobeil et al., 2006; Marrache et al., 2005; Willard and Crouch, 2000), as well as to modulate gene transcription in a direct manner (Bhattacharya et al., 1999). Remarkably, the nuclear compartmentalization of GPER through a monopartite NLS, as we have demonstrated in the current study, opens new avenues to better understand the biology of this receptor towards its potential to regulate gene transcription.

Tumor microenvironment greatly contributes to the growth and invasion of cancer cells by diverse factors and mechanisms. As CAFs play a crucial action in cancer progression, understanding their role in tumorigenesis and metastasis would open further perspectives to identify therapeutic targets in the context of innovative anti-cancer strategies. In this regard, our data provide novel insights into the ability of GPER to act as a transcription regulator of genes involved in the biological responses to estrogens in CAFs.

## Acknowledgements

This work was supported by Associazione Italiana per la Ricerca sul Cancro (AIRC, Project n.12849/2012), AIRC project Calabria 2011 and Fondazione Cassa di Risparmio di Calabria e Lucania. AGC was supported by Roberto Pallotti's Legacy for Cancer Research, Cornelia Pallotti's Legacy for Cancer Research, RFO University of Bologna.

## Appendix A. Supplementary data

Supplementary data associated with this article can be found, in the online version, at <http://dx.doi.org/10.1016/j.mce.2013.05.023>.

## References

- Aboussekhra, A., 2011. Role of cancer-associated fibroblasts in breast cancer development and prognosis. *Int. J. Dev. Biol.* 55, 841–849.
- Albanito, L., Lappano, R., Madeo, A., Chimento, A., Prossnitz, E.R., Cappello, A.R., Dolce, V., Abonante, S., Pezzi, V., Maggiolini, M., 2008a. G-protein-coupled receptor 30 and estrogen receptor- $\alpha$  are involved in the proliferative effects induced by atrazine in ovarian cancer cells. *Environ. Health Perspect.* 116, 1648–1655.
- Albanito, L., Madeo, A., Lappano, R., Vivacqua, A., Rago, V., Carpino, A., Oprea, T.I., Prossnitz, E.R., Musti, A.M., Andò, S., Maggiolini, M., 2007. G protein-coupled receptor 30 (GPR30) mediates gene expression changes and growth response to 17 $\beta$ -estradiol and selective GPR30 ligand G-1 in ovarian cancer cells. *Cancer Res.* 67, 1859–1866.
- Albanito, L., Sisci, D., Aquila, S., Brunelli, E., Vivacqua, A., Madeo, A., Lappano, R., Pandey, D.P., Picard, D., Mauro, L., Andò, S., Maggiolini, M., 2008b. Epidermal growth factor induces G protein-coupled receptor 30 expression in estrogen receptor-negative breast cancer cells. *Endocrinology* 149, 3799–3808.
- Bartella, V., De Marco, P., Malaguarnera, R., Belfiore, A., Maggiolini, M., 2012. New advances on the functional cross-talk between insulin-like growth factor-I and estrogen signaling in cancer. *Cell. Signal.* 24, 1515–1521.
- Bedard, J.E., Purnell, J.D., Ware, S.M., 2007. Nuclear import and export signals are essential for proper cellular trafficking and function of ZIC3. *Hum. Mol. Genet.* 16, 187–198.
- Bhattacharya, M., Peri, K., Ribeiro-da-Silva, A., Almazan, G., Shichi, H., Hou, X., Varma, D.R., Chemtob, S., 1999. Localization of functional prostaglandin E2 receptors EP3 and EP4 in the nuclear envelope. *J. Biol. Chem.* 274, 15719–15724.
- Boivin, B., Chevalier, D., Villeneuve, L.R., Rousseau, E., Allen, B.G., 2003. Functional endothelin receptors are present on nuclei in cardiac ventricular myocytes. *J. Biol. Chem.* 278, 29153–29163.
- Boivin, B., Vaniotis, G., Allen, B.G., Hébert, T.E., 2008. G protein-coupled receptors in and on the cell nucleus: a new signaling paradigm? *J. Recept. Signal. Trans. Res.* 28, 5–28.
- Bologa, C.G., Revankar, C.M., Young, S.M., Edwards, B.S., Arterburn, J.B., Kiselyov, A.S., Parker, M.A., Tkachenko, S.E., Savchuck, N.P., Sklar, L.A., Oprea, T.I., Prossnitz, E.R., 2006. Virtual and biomolecular screening converge on a selective agonist for GPR30. *Nat. Chem. Biol.* 2, 207–212.
- Canonaco, M., Giusi, G., Madeo, A., Facciolo, R.M., Lappano, R., Canonaco, A., Maggiolini, M., 2008. A sexually dimorphic distribution pattern of the novel estrogen receptor G-protein-coupled receptor 30 in some brain areas of the hamster. *J. Endocrinol.* 196, 131–138.
- Chen, R., Mukhin, Y.V., Garnovskaya, M.N., Thielen, T.E., Iijima, Y., Huang, C., Raymond, J.R., Ullian, M.E., Paul, R.V., 2000. A functional angiotensin II receptor-GFP fusion protein: evidence for agonist-dependent nuclear translocation. *Am. J. Physiol. Renal Physiol.* 279, F440–F448.
- Chimento, A., Sirianni, R., Casaburi, I., Ruggiero, C., Maggiolini, M., Andò, S., Pezzi, V., 2012. 17 $\beta$ -Estradiol activates GPER- and ESR1-dependent pathways inducing apoptosis in GC-2 cells, a mouse spermatocyte-derived cell line. *Mol. Cell. Endocrinol.* 355, 49–59.
- Chimento, A., Sirianni, R., Delalande, C., Silandre, D., Bois, C., Andò, S., Maggiolini, M., Carreau, S., Pezzi, V., 2010. 17 Beta-estradiol activates rapid signaling pathways involved in rat pachytene spermatocytes apoptosis through GPR30 and ER  $\alpha$ . *Mol. Cell. Endocrinol.* 320, 136–144.
- Chimento, A., Sirianni, R., Zolea, F., Bois, C., Delalande, C., Andò, S., Maggiolini, M., Aquila, S., Carreau, S., Pezzi, V., 2011. Gper and ESRs are expressed in rat round spermatids and mediate oestrogen-dependent rapid pathways modulating expression of cyclin B1 and Bax. *Int. J. Androl.* 34, 420–429.
- Christophe, D., Christophe-Hobertus, C., Pichon, B., 2000. Nuclear targeting of proteins: how many different signals? *Cell. Signal.* 5, 337–341.
- Cingolani, G., Petosa, C., Weis, K., Müller, C.W., 1999. Structure of importin-beta bound to the IBB domain of importin-alpha. *Nature* 399, 221–229.
- Cirri, P., Chiarugi, P., 2011. Cancer-associated-fibroblasts and tumour cells: a diabolic liaison driving cancer progression. *Cancer Metast. Rev.* 31, 195–208.
- De Marco, P., Bartella, V., Vivacqua, A., Lappano, R., Santolla, M.F., Morcavallo, A., Pezzi, V., Belfiore, A., Maggiolini, M., 2012. Insulin-like growth factor-I regulates GPER expression and function in cancer cells. *Oncogene*. <http://dx.doi.org/10.1038/nc.2012.97>.
- Dennis, M.K., Field, A.S., Burai, R., Ramesh, C., Petrie, W.K., Bologa, C.G., Oprea, T.I., Yamaguchi, Y., Hayashi, S., Sklar, L.A., Hathaway, H.J., Arterburn, J.B., Prossnitz, E.R., 2011. Identification of a GPER/GPR30 antagonist with improved estrogen receptor counterselectivity. *J. Steroid Biochem. Mol. Biol.* 127, 358–366.
- Dittmann, K., Mayer, C., Fehrenbacher, B., Schaller, M., Raju, U., Milas, L., Chen, D.J., Kehlbach, R., Rodemann, H.P., 2005. Radiation-induced epidermal growth factor receptor nuclear import is linked to activation of DNA-dependent protein kinase. *J. Biol. Chem.* 280, 31182–31189.
- Filardo, E.J., Graeber, C.T., Quinn, J.A., Resnick, M.B., Giri, D., DeLellis, R.A., Steinhoff, M.M., Sabo, E., 2006. Distribution of GPR30, a seven membrane-spanning estrogen receptor, in primary breast cancer and its association with



- clinicopathologic determinants of tumor progression. *Clin. Cancer Res.* 12, 6359–6366.
- Filardo, E.J., Quinn, J.A., Bland, K.I., Frackelton Jr., A.R., 2000. Estrogen-induced activation of Erk-1 and Erk-2 requires the G protein-coupled receptor homolog, GPR30, and occurs via trans-activation of the epidermal growth factor receptor through release of HB-EGF. *Mol. Endocrinol.* 14, 1649–1660.
- Filardo, E.J., Quinn, J.A., Frackelton Jr., A.R., Bland, K.I., 2002. Estrogen action via the G protein-coupled receptor, GPR30: stimulation of adenylyl cyclase and cAMP-mediated attenuation of the epidermal growth factor receptor-to-MAPK signaling axis. *Mol. Endocrinol.* 16, 70–84.
- Filardo, E.J., Quinn, J.A., Pang, Y., Graeber, C., Shaw, S., Dong, J., Thomas, P., 2007. Activation of the novel estrogen receptor G protein-coupled receptor 30 (GPR30) at the plasma membrane. *Endocrinology* 148, 3236–3245.
- Filardo, E.J., Thomas, P., 2012. Minireview: G protein-coupled estrogen receptor-1, GPER-1: its mechanism of action and role in female reproductive cancer, renal and vascular physiology. *Endocrinology* 153, 2953–2962.
- Filice, E., Recchia, A.G., Pellegrino, D., Angelone, T., Maggiolini, M., Cerra, M.C., 2009. A new membrane G protein-coupled receptor (GPR30) is involved in the cardiac effects of 17beta-estradiol in the male rat. *J. Physiol. Pharmacol.* 60, 3–10.
- Funasaka, T., Wong, R.W., 2011. The role of nuclear pore complex in tumor microenvironment and metastasis. *Cancer Metast. Rev.* 30, 239–251.
- Gobeil Jr., F., Fortier, A., Zhu, T., Bossolasco, M., Leduc, M., Grandbois, M., Heveker, N., Bkaily, G., Chemtob, S., Barbaz, D., 2006. G-protein-coupled receptors signalling at the cell nucleus: an emerging paradigm. *Can. J. Physiol. Pharmacol.* 84, 287–297.
- Iyer, V.R., Eisen, M.B., Ross, D.T., Schuler, G., Moore, T., Lee, J.C., Trent, J.M., Staudt, L.M., Hudson Jr., J., Boguski, M.S., Lashkari, D., Shalon, D., Botstein, D., Brown, P.O., 1999. The transcriptional program in the response of human fibroblasts to serum. *Science* 283, 83–87.
- Kalluri, R., 2003. Basement membranes: structure, assembly and role in tumour angiogenesis. *Nat. Rev. Cancer* 3, 422–433.
- Kalluri, R., Zeisberg, M., 2006. Fibroblasts in cancer. *Nat. Rev. Cancer* 6, 392–401.
- Kenny, P.A., Bissell, M.J., 2003. Tumor reversion: correction of malignant behavior by microenvironmental cues. *Int. J. Cancer* 107, 688–695.
- Koos, R.D., 2011. Minireview: putting physiology back into estrogens' mechanism of action. *Endocrinology* 152, 4481–4488.
- Lafkas, D., Trimis, G., Papavassiliou, A.G., Kiaris, H., 2008. P53 mutations in stromal fibroblasts sensitize tumors against chemotherapy. *Int. J. Cancer* 123, 967–971.
- Lange, A., Mills, R.E., Lange, C.J., Stewart, M., Devine, S.E., Corbett, A.H., 2007. Classical nuclear localization signals: definition, function, and interaction with importin  $\alpha$ . *J. Biol. Chem.* 282, 5101–5105.
- Lappano, R., Maggiolini, M., 2012. GPCRs and cancer. *Acta Pharmacol. Sin.* 33, 351–362.
- Lappano, R., Maggiolini, M., 2011. G protein-coupled receptors: novel targets for drug discovery in cancer. *Nat. Rev. Drug Discov.* 10, 47–60.
- Lappano, R., Rosano, C., De Marco, P., De Francesco, E.M., Pezzi, V., Maggiolini, M., 2010. Estriol acts as a GPR30 antagonist in estrogen receptor-negative breast cancer cells. *Mol. Cell. Endocrinol.* 320, 162–170.
- Lappano, R., Rosano, C., Santolla, M.F., Pupo, M., De Francesco, E.M., De Marco, P., Ponassi, M., Spallarossa, A., Ranise, A., Maggiolini, M., 2012a. Two novel GPER agonists induce gene expression changes and growth effects in cancer cells. *Cancer Drug Targets* 12, 531–542.
- Lappano, R., Santolla, M.F., Pupo, M., Sinicropi, M.S., Caruso, A., Rosano, C., Maggiolini, M., 2012b. MIBE acts as antagonist ligand of both estrogen receptor  $\alpha$  and GPER in breast cancer cells. *Breast Cancer Res.* 14, R12.
- Lee, D.K., Lança, A.J., Cheng, R., Nguyen, T., Ji, X.D., Gobeil Jr., F., Chemtob, S., George, S.R., O'Dowd, B.F., 2004. Agonist-independent nuclear localization of the Apelin, angiotensin AT1, and bradykinin B2 receptors. *J. Biol. Chem.* 279, 7901–7908.
- Liang, J., Shang, Y., 2012. Estrogen and cancer. *Annu. Rev. Physiol.* <http://dx.doi.org/10.1146/annurev-physiol-030212-183708>.
- Lin, B.C., Suzawa, M., Blind, R.D., Tobias, S.C., Bulun, S.E., Scanlan, T.S., Ingraham, H.A., 2009. Stimulating the GPR30 estrogen receptor with a novel tamoxifen analogue activates SF-1 and promotes endometrial cell proliferation. *Cancer Res.* 69, 5415–5423.
- Lin, S.Y., Makino, K., Xia, W., Matin, A., Wen, Y., Kwong, K.Y., Bourguignon, L., Hung, M.C., 2001. Nuclear localization of EGF receptor and its potential new role as a transcription factor. *Nat. Cell Biol.* 9, 802–808.
- Lo, H.W., Hsu, S.C., Ali-Seyed, M., Gunduz, M., Xia, W., Wei, Y., Bartholomew, G., Shih, J.Y., Hung, M.C., 2005. Nuclear interaction of EGFR and STAT3 in the activation of the iNOS/NO pathway. *Cancer Cell* 7, 575–589.
- Lohela, M., Bry, M., Tammela, T., Alitalo, K., 2009. VEGFs and receptors involved in angiogenesis versus lymphangiogenesis. *Curr. Opin. Cell Biol.* 21, 154–165.
- Lorusso, G., Ruegg, C., 2008. The tumor microenvironment and its contribution to tumor evolution toward metastasis. *Histochem. Cell Biol.* 130, 1091–1103.
- Madeo, A., Maggiolini, M., 2010. Nuclear alternate estrogen receptor GPR30 mediates 17 $\beta$ -estradiol-induced gene expression and migration in breast cancer-associated fibroblasts. *Cancer Res.* 70, 6036–6046.
- Madeo, A., Vinciguerra, M., Lappano, R., Galgani, M., Gasperi-Campani, A., Maggiolini, M., Musti, A.M., 2010. C-Jun activation is required for 4-hydroxytamoxifen-induced cell death in breast cancer cells. *Oncogene* 29, 978–991.
- Maggiolini, M., Donzé, O., Picard, D., 1999. A non-radioactive method for inexpensive quantitative RT-PCR. *Biol. Chem.* 380, 695–697.
- Maggiolini, M., Picard, D., 2009. The unfolding stories of GPR30, a new membrane bound estrogen receptor. *J. Endocrinol.* 204, 105–114.
- Maggiolini, M., Recchia, A.G., Carpino, A., Vivacqua, A., Fasanella, G., Rago, V., Pezzi, V., Briand, P.A., Picard, D., Andò, S., 2004a. Oestrogen receptor beta is required for androgen-stimulated proliferation of LNCaP prostate cancer cells. *J. Mol. Endocrinol.* 32, 777–791.
- Maggiolini, M., Vivacqua, A., Fasanella, G., Recchia, A.G., Sisci, D., Pezzi, V., Montanaro, D., Musti, A.M., Picard, D., Andò, S., 2004b. The G protein-coupled receptor GPR30 mediates c-fos up-regulation by 17 $\beta$ -estradiol and phytoestrogens in breast cancer cells. *J. Biol. Chem.* 279, 27009–27016.
- Mao, Y., Keller, E.T., Garfield, D.H., Shen, K., Wang, J., 2012. Stromal cells in tumor microenvironment and breast cancer. *Cancer Metast. Rev.* <http://dx.doi.org/10.1007/s10555-012-9415-3>.
- Marrache, A.M., Gobeil, F., Zhu, T., Chemtob, S., 2005. Intracellular signaling of lipid mediators via cognate nuclear G protein-coupled receptors. *Endothelium* 12, 63–72.
- Matsuda, K., Sakamoto, H., Mori, H., Hosokawa, K., Kawamura, A., Itose, M., Nishi, M., Prossnitz, E.R., Kawata, M., 2008. Expression and intracellular distribution of the G protein-coupled receptor 30 in rat hippocampal formation. *Neurosci. Lett.* 441, 94–99.
- Miyamoto, H., Murakami, T., Tsuchida, K., Sugino, H., Miyake, H., Tashiro, S., 2004. Tumor-stroma interaction of human pancreatic cancer: acquired resistance to anticancer drugs and proliferation regulation is dependent on extracellular matrix proteins. *Pancreas* 28, 38–44.
- Morelli, C., Garofalo, C., Sisci, D., del Rincon, S., Cascio, S., Tu, X., Vecchione, A., Sauter, E.R., Miller Jr., W.H., Surmacz, E., 2004. Nuclear insulin receptor substrate 1 interacts with estrogen receptor alpha at ERE promoters. *Oncogene* 23, 7517–7526.
- Müller-Hübenthal, B., Azemar, M., Lorenzen, D., Huber, M., Freudenberg, M.A., Galanos, C., Unger, C., Hildenbrand, B., 2009. Tumour biology: tumour-associated inflammation versus antitumor immunity. *Anticancer Res.* 29, 4795–4805.
- Orimo, A., Gupta, P.B., Sgroi, D.C., Arenzana-Seisdedos, F., Delaunay, T., Naem, R., Carey, V.J., Richardson, A.L., Weinberg, R.A., 2005. Stromal fibroblasts present in invasive human breast carcinomas promote tumor growth and angiogenesis through elevated SDF-1/CXCL12 secretion. *Cell* 121, 335–348.
- Ostman, A., Augsten, M., 2009. Cancer-associated fibroblasts and tumor growth-bystanders turning into key players. *Curr. Opin. Genet. Dev.* 19, 67–73.
- Otto, C., Rohde-Schulz, B., Schwarz, G., Fuchs, I., Klewer, M., Brittain, D., Langer, G., Bader, B., Prelle, K., Nubbemeyer, R., Fritze, K.H., 2008. G protein-coupled receptor 30 localizes to the endoplasmic reticulum and is not activated by estradiol. *Endocrinology* 149, 4846–4856.
- Pandey, D.P., Lappano, R., Albanito, L., Madeo, A., Maggiolini, M., Picard, D., 2009. Estrogenic GPR30 signaling induces proliferation and migration of breast cancer cells through CTGF. *EMBO J.* 28, 523–532.
- Pang, Y., Dong, J., Thomas, P., 2008. Estrogen signaling characteristics of Atlantic croaker G protein-coupled receptor 30 (GPR30) and evidence it is involved in maintenance of oocyte meiotic arrest. *Endocrinology* 149, 3410–3426.
- Panno, M.L., Salerno, M., Pezzi, V., Sisci, D., Maggiolini, M., Mauro, L., Morrone, E.G., Andò, S., 1996. Effect of oestradiol and insulin on the proliferative pattern and on oestrogen and progesterone receptor contents in MCF-7 cells. *J. Cancer Res. Clin. Oncol.* 122, 745–749.
- Prossnitz, E.R., Maggiolini, M., 2009. Mechanisms of estrogen signaling and gene expression via GPR30. *Mol. Cell. Endocrinol.* 308, 32–38.
- Pupo, M., Pisano, A., Lappano, R., Santolla, M.F., De Francesco, E.M., Abonante, S., Rosano, C., Maggiolini, M., 2012. Bisphenol A induces gene expression changes and proliferative effects through GPER in breast cancer cells and cancer-associated fibroblasts. *Environ. Health Perspect.* 120, 1177–1182.
- Rago, V., Romeo, F., Giordano, F., Maggiolini, M., Carpino, A., 2011. Identification of the estrogen receptor GPER in neoplastic and non-neoplastic human testes. *Reprod. Biol. Endocrinol.* 9, 135.
- Recchia, A.G., De Francesco, E.M., Vivacqua, A., Sisci, D., Panno, M.L., Andò, S., Maggiolini, M., 2011. The G protein-coupled receptor 30 is up-regulated by hypoxia-inducible factor-1 $\alpha$  (HIF-1 $\alpha$ ) in breast cancer cells and cardiomyocytes. *J. Biol. Chem.* 286, 10773–10782.
- Revankar, C.M., Cimino, D.F., Sklar, L.A., Arterburn, J.B., Prossnitz, E.R., 2005. A transmembrane intracellular estrogen receptor mediates rapid cell signaling. *Science* 307, 1625–1630.
- Revankar, C.M., Mitchell, H.D., Field, A.S., Burai, R., Corona, C., Ramesh, C., Sklar, L.A., Arterburn, J.B., Prossnitz, E.R., 2007. Synthetic estrogen derivatives demonstrate the functionality of intracellular GPR30. *ACS Chem. Biol.* 2, 536–544.
- Rosano, C., Lappano, R., Santolla, M.F., Ponassi, M., Donadini, A., Maggiolini, M., 2012. Recent advances in the rationale design of GPER ligands. *Curr. Med. Chem.* 19, 6199–6206 (8).
- Sakamoto, H., Matsuda, K., Hosokawa, K., Nishi, M., Morris, J.F., Prossnitz, E.R., Kawata, M., 2007. Expression of G protein-coupled receptor-30, a G protein-coupled membrane estrogen receptor, in oxytocin neurons of the rat paraventricular and supraoptic nuclei. *Endocrinology* 148, 5842–5850.
- Santolla, M.F., Lappano, R., De Marco, P., Pupo, M., Vivacqua, A., Sisci, D., Abonante, S., Iacopetta, D., Cappello, A.R., Dolce, V., Maggiolini, M., 2012. GPER mediates the up-regulation of fatty acid synthase (FASN) induced by 17 $\beta$ -estradiol in cancer cells and cancer-associated fibroblasts (CAFs). *J. Biol. Chem.* 287, 43234–43245.
- Sirianni, R., Chimento, A., Ruggiero, C., De Luca, A., Lappano, R., Andò, S., Maggiolini, M., Pezzi, V., 2008. The novel estrogen receptor, G protein-coupled receptor 30, mediates the proliferative effects induced by 17beta-estradiol on mouse spermatogonial GC-1 cell line. *Endocrinology* 149, 5043–5051.

- Smith, H.O., Arias-Pulido, H., Kuo, D.Y., Howard, T., Qualls, C.R., Lee, S.J., Verschraegen, C.F., Hathaway, H.J., Joste, N.E., Prossnitz, E.R., 2009. GPR30 predicts poor survival for ovarian cancer. *Gynecol. Oncol.* 114, 465–471.
- Smith, H.O., Leslie, K.K., Singh, M., Qualls, C.R., Revankar, C.M., Joste, N.E., Prossnitz, E.R., 2007. GPR30: a novel indicator of poor survival for endometrial carcinoma. *Am. J. Obstet. Gynecol.* 196, 386.e1–386.e9.
- Suh, E.K., Gumbiner, B.M., 2003. Translocation of beta-catenin into the nucleus independent of interactions with FG-rich nucleoporins. *Exp. Cell Res.* 290, 447–456.
- Thomas, P., Pang, Y., Filardo, E.J., Dong, J., 2005. Identity of an estrogen membrane receptor coupled to a G protein in human breast cancer cells. *Endocrinology* 146, 624–632.
- Tlsty, T.D., Hein, P.W., 2001. Know thy neighbor: stromal cells can contribute oncogenic signals. *Curr. Opin. Genet. Dev.* 11, 54–59.
- Vivacqua, A., Bonofiglio, D., Albanito, L., Madeo, A., Rago, V., Carpino, A., Musti, A.M., Picard, D., Andò, S., Maggiolini, M., 2006a. 17 $\beta$ -Estradiol, genistein and 4-hydroxytamoxifen induce the proliferation of thyroid cancer cells through the G protein-coupled receptor GPR30. *Mol. Pharmacol.* 70, 1414–1423.
- Vivacqua, A., Bonofiglio, D., Recchia, A.G., Musti, A.M., Picard, D., Andò, S., Maggiolini, M., 2006b. The G protein-coupled receptor GPR30 mediates the proliferative effects induced by 17 $\beta$ -estradiol and hydroxytamoxifen in endometrial cancer cells. *Mol. Endocrinol.* 20, 631–646.
- Vivacqua, A., Lappano, R., De Marco, P., Sisci, D., Aquila, S., De Amicis, F., Fuqua, S.A., Andò, S., Maggiolini, M., 2009. G protein-coupled receptor 30 expression is up-regulated by EGF and TGF $\alpha$  in estrogen receptor  $\alpha$  positive cancer cells. *Mol. Endocrinol.* 23, 1815–1826.
- Vivacqua, A., Romeo, E., De Marco, P., De Francesco, E.M., Abonante, S., Maggiolini, M., 2012. GPER mediates the Egr-1 expression induced by 17 $\beta$ -estradiol and 4-hydroxytamoxifen in breast and endometrial cancer cells. *Breast Cancer Res. Treat.* 133, 1025–1035.
- Wang, C., Prossnitz, E.R., Roy, S.K., 2008. G protein-coupled receptor 30 expression is required for estrogen stimulation of primordial follicle formation in the hamster ovary. *Endocrinology* 149, 4452–4461.
- Wang, Y.N., Yamaguchi, H., Hsu, J.M., Hung, M.C., 2010. Nuclear trafficking of the epidermal growth factor receptor family membrane proteins. *Oncogene* 29, 3997–4006.
- Watson, P.H., Fraher, L.J., Natale, B.V., Kisiel, M., Hendy, G.N., Hodsmann, A.B., 2000. Nuclear localization of the type 1 parathyroid hormone/parathyroid hormone-related peptide receptor in MC3T3-E1 cells: association with serum-induced cell proliferation. *Bone* 26, 221–225.
- Willard, F.S., Crouch, M.F., 2000. Nuclear and cytoskeletal translocation and localization of heterotrimeric G-proteins. *Immunol. Cell Biol.* 78, 387–394.
- Xing, F., Saidou, J., Watabe, K., 2010. Cancer associated fibroblasts (CAFs) in tumor microenvironment. *Front Biosci.* 15, 166–179.
- Yamaguchi, Y., Hayashi, S., 2009. Estrogen-related cancer microenvironment of breast carcinoma. *Endocr. J.* 56, 1–7.

# Bisphenol A Induces Gene Expression Changes and Proliferative Effects through GPER in Breast Cancer Cells and Cancer-Associated Fibroblasts

Marco Pupo,<sup>1</sup> Assunta Pisano,<sup>1</sup> Rosamaria Lappano,<sup>1</sup> Maria Francesca Santolla,<sup>1</sup> Ernestina Marianna De Francesco,<sup>1</sup> Sergio Abonante,<sup>2</sup> Camillo Rosano,<sup>3</sup> and Marcello Maggiolini<sup>1</sup>

<sup>1</sup>Department of Pharmaco-Biology, University of Calabria, Rende, Italy; <sup>2</sup>Regional Hospital, Cosenza, Italy; <sup>3</sup>Department of Bioinformatics and Structural Proteomics, National Institute for Cancer Research, Genova, Italy

**BACKGROUND:** Bisphenol A (BPA) is the principal constituent of baby bottles, reusable water bottles, metal cans, and plastic food containers. BPA exerts estrogen-like activity by interacting with the classical estrogen receptors (ER $\alpha$  and ER $\beta$ ) and through the G protein-coupled receptor (GPR30/GPER). In this regard, recent studies have shown that GPER was involved in the proliferative effects induced by BPA in both normal and tumor cells.

**OBJECTIVES:** We studied the transduction signaling pathways through which BPA influences cell proliferation and migration in human breast cancer cells and cancer-associated fibroblasts (CAFs).

**METHODS AND RESULTS:** We used as a model system SKBR3 breast cancer cells and CAFs that lack the classical ERs. Specific pharmacological inhibitors and gene-silencing procedures were used to show that BPA induces the expression of the GPER target genes *c-FOS*, *EGR-1*, and *CTGF* through the GPER/EGFR/ERK transduction pathway in SKBR3 breast cancer cells and CAFs. Moreover, we observed that GPER is required for growth effects and migration stimulated by BPA in both cell types.

**CONCLUSIONS:** Results indicate that GPER is involved in the biological action elicited by BPA in breast cancer cells and CAFs. Hence, GPER-mediated signaling should be included among the transduction mechanisms through which BPA may stimulate cancer progression.

**KEY WORDS:** bisphenol A, breast cancer cells, cancer-associated fibroblasts, GPR30/GPER, tumor microenvironment. *Environ Health Perspect* 120:1177–1182 (2012). <http://dx.doi.org/10.1289/ehp.1104526> [Online 2 May 2012]

Bisphenol A (BPA), used largely in the manufacture of polycarbonate plastics, is the constituent of a wide array of consumer products, including plastic food containers, baby bottles, and the lining of metal food cans (Welshons et al. 2006). Humans are exposed to BPA mainly at the time of consumption of water and foods through the materials used for containers and packages (Vandenberg et al. 2009).

BPA is able to accelerate growth and puberty, alter the ovarian cycle in females (Mlynarciková et al. 2005; Rasier et al. 2006), interfere with embryonic development, and to induce aneuploidy (Takai et al. 2000). Moreover, a relationship between BPA blood levels, obesity, polycystic ovary syndrome, repeated miscarriage, and endometrial hyperplasia has been found in women, suggesting that it may act as an endocrine disruptor (Welshons et al. 2006). Exposure to BPA has also been correlated with the incidence of diverse types of tumors (Ho et al. 2006; Keri et al. 2007; Maffini et al. 2006).

BPA has estrogenic activity both *in vivo* and *in vitro* and is thought to be an environmental estrogen (Welshons et al. 2006). Previous investigations (reviewed by Vandenberg et al. 2009) have demonstrated that BPA binds to and activates the estrogen receptor (ER $\alpha$  and ER $\beta$ ), although the affinity of BPA for these receptors was approximately 10,000-fold weaker with respect to estradiol (Gould et al. 1998; Kuiper et al. 1998). In recent years, the identification

of G protein-coupled receptor (GPER) as a novel estrogen receptor has suggested new possibilities by which estrogenic compounds might cause biological effects in different cell types (Albanito et al. 2007; Maggiolini et al. 2004; Prossnitz and Maggiolini 2009; Vivacqua et al. 2006a, 2006b). In this regard, we reported a characteristic signature elicited by estrogenic GPER signaling in SKBR3 breast cancer cells and we identified a network of transcription factors, such as *c-FOS*, early growth response protein 1 (*EGR-1*), and connective tissue growth factor (*CTGF*), that may be involved in important biological functions (Pandey et al. 2009).

BPA is one of several environmental estrogens that have exhibited the ability to bind to GPER (Thomas and Dong 2006) and to activate transduction pathways (Dong et al. 2011) involved in the biological responses of both normal and neoplastic cells. For example, BPA stimulated the proliferation of mouse spermatogonial cells (Sheng and Zhu 2011) and human seminoma cells (Bouskine et al. 2009) and induced chemoresistance in breast cancer cells (Lapensee et al. 2009) through activation of GPER.

The contribution of the stromal microenvironment to the development of a wide variety of tumors has been highlighted by clinical evidence and the use of mouse models (Bhowmick et al. 2004a). A growing body of data has also suggested that tumor cells actively recruit cancer-associated fibroblasts (CAFs),

which remain activated and play a prominent role in cancer progression (Bhowmick et al. 2004b). In breast carcinoma approximately 80% of stromal fibroblasts may acquire the activated phenotype that promotes the proliferation of cancer cells at metastatic sites, stimulating tumor growth such as for the primary tumor (Kalluri and Zeisberg 2006).

In this study, we demonstrate that BPA exerts a stimulatory action through GPER in breast cancer cells and CAFs.

## Materials and Methods

**Reagents.** We purchased bisphenol A (BPA), *N*-[2-(*p*-bromocinnamylamino)ethyl]-5-soquinolinesulfonamide dihydrochloride (H89), PD98059 (PD), and arsenic trioxide (As<sub>2</sub>O<sub>3</sub>) from Sigma-Aldrich (Milan, Italy); AG1478 (AG) from Biomol Research Laboratories (DBA, Milan, Italy), and 1-(4-(6-bromobenzo[1,3]dioxol-5-yl)-3a,4,5,9b-tetrahydro-3H-cyclopenta[*c*]quinolin-8-yl)-ethanone (G-1) from Calbiochem (Merck KGaA, Frankfurt, Germany). As<sub>2</sub>O<sub>3</sub> was dissolved in phosphate-buffered saline, and BPA and PD were dissolved in ethanol; AG1478, H89, and G-1 were solubilized in dimethyl sulfoxide (DMSO).

**Cell culture.** SKBR3 cells. SKBR3 human breast cancer cells were maintained in phenol red-free RPMI 1640 medium supplemented with 10% fetal bovine serum (FBS). Cells were changed to medium without serum the day before experiments for immunoblotting and reverse-transcription polymerase chain reaction (RT-PCR).

**CAFs.** CAFs were extracted as previously described (Madeo and Maggiolini 2010). Briefly, breast cancer specimens were collected from primary tumors of patients who had undergone surgery. Signed informed consent

Address correspondence to M. Maggiolini, Department of Pharmaco-Biology, University of Calabria, 87036 Rende, Italy. Telephone: 39 0984 493076. Fax: 39 0984 493458. E-mail: marcellomaggiolini@yahoo.it

Supplemental Material is available online (<http://dx.doi.org/10.1289/ehp.1104526>).

This work was supported by the Associazione Italiana per la Ricerca sul Cancro (AIRC project 8925/2009 and Calabria project 2011), the Fondazione Cassa di Risparmio di Calabria e Lucania, and the Ministero dell'Università e Ricerca Scientifica e Tecnologica (Cofin project 2008PK2WCW/2008).

The authors declare they have no actual or potential competing financial interests.

Received 22 September 2011; accepted 2 May 2012.

was obtained from all the patients and from the institutional review board(s) of the Regional Hospital of Cosenza. Tissues from tumors were cut into smaller pieces (1–2 mm diameter), placed in digestion solution (400 IU collagenase, 100 IU hyaluronidase, and 10% serum, containing antibiotic and antimycotic solution), and incubated overnight at 37°C. The cells were then separated by differential centrifugation at  $90 \times g$  for 2 min. Supernatant containing fibroblasts was centrifuged at  $485 \times g$  for 8 min; the pellet obtained was suspended in fibroblasts growth medium (Medium 199 and Ham's F12 mixed 1:1 and supplemented with 10% FBS) and cultured at 37°C in 5% CO<sub>2</sub>. Primary cells cultures of breast fibroblasts were characterized by immunofluorescence. Briefly cells were incubated with human anti-vimentin (V9) and human anti-cytokeratin 14 (LL001), both from Santa Cruz Biotechnology DBA (Milan, Italy). To assess fibroblasts activation, we used anti-fibroblast activated protein  $\alpha$  (FAP $\alpha$ ) antibody (H-56; Santa Cruz Biotechnology DBA) (data not shown).

**Western blotting.** SKBR3 cells and CAFs were grown in 10-cm dishes, exposed to treatments or ethanol (or DMSO), which was used as the vehicle, and then lysed as described previously (Pandey et al. 2009). Protein concentrations were determined using Bradford reagent (Sigma-Aldrich) according to the manufacturer's recommendations. Equal amounts of whole protein extract were resolved on a 10% SDS-polyacrylamide gel

and transferred to a nitrocellulose membrane (Amersham Biosciences, Milan, Italy). Membranes were probed overnight at 4°C with antibodies against c-Fos (H-125),  $\beta$ -actin (C-2), phosphorylated extracellular signal-regulated kinase 1/2 (p-ERK1/2; E-4), Egr-1 (588), CTGF (L-20), ERK2 (C-14), ER $\alpha$  (F-10), or GPR30 (N-15), all from Santa Cruz Biotechnology, DBA (Milan, Italy), or ER $\beta$  from Serotec (Space Import Export, Milan, Italy). Results of densitometric analyses of Western blots, obtained using ImageJ software (Abramoff et al. 2004), are presented as optical density (OD; expressed in arbitrary units) relative to the control (ERK2 or  $\beta$ -actin).

**Plasmids and luciferase assays.** The *Ctcf* luciferase reporter plasmid p(-1999/+36)-luc, which is based on the backbone of vector pGL3-basic (Promega), was a gift from B. Chaour (Department of Anatomy and Cell Biology, State University of New York Downstate Medical Center, Brooklyn, NY, USA). The luciferase reporter plasmid for *c-FOS* encoding a -2.2-kb 5' upstream fragment of human *c-FOS* was a gift from K. Nose (Department of Microbiology, Showa University School of Pharmaceutical Sciences, Hatanodai, Shinagawa-ku, Tokyo, Japan). The *EGR-1* luciferase reporter plasmid pEgr-1A, which contains the -600 to +12 5'-flanking sequence from the human *EGR-1* gene was a gift from S. Safe (Department of Veterinary Physiology and Pharmacology, Texas A&M University, Houston, TX, USA). For the

luciferase assays, cells were transferred into 24-well plates containing 500  $\mu$ L of regular growth medium per well the day before transfection. On the day of transfection, SKBR3 cell medium was replaced with RPMI without phenol red and serum, and transfection was performed using Fugene6 Reagent (Roche Molecular Biochemicals, Milan, Italy) and a mixture containing 0.5  $\mu$ g of each reporter plasmid. Renilla luciferase (pRL-CMV; 1 ng) was used as a transfection control. After 5–6 hr, ligand was added and cells were incubated for 16–18 hr. We measured luciferase activity using the Dual Luciferase Kit (Promega, Milan, Italy) according to the manufacturer's recommendations. Firefly luciferase values generated by the reporter plasmid were normalized to Renilla luciferase values. Normalized values obtained from cells treated with ethanol vehicle were set as 1-fold induction, and the activity induced by treatments was calculated based on this value.

**RT-PCR and real-time PCR.** Total RNA was extracted using Trizol commercial kit (Invitrogen, Milan, Italy) according to the manufacturer's protocol. RNA was quantified spectrophotometrically, and cDNA was synthesized from the RNA by reverse transcription using murine leukemia virus reverse transcriptase (Invitrogen). We quantified the expression of selected genes by real-time PCR using SYBR Green as the detection method and the Step One sequence detection system (Applied Biosystems Inc., Milan, Italy).

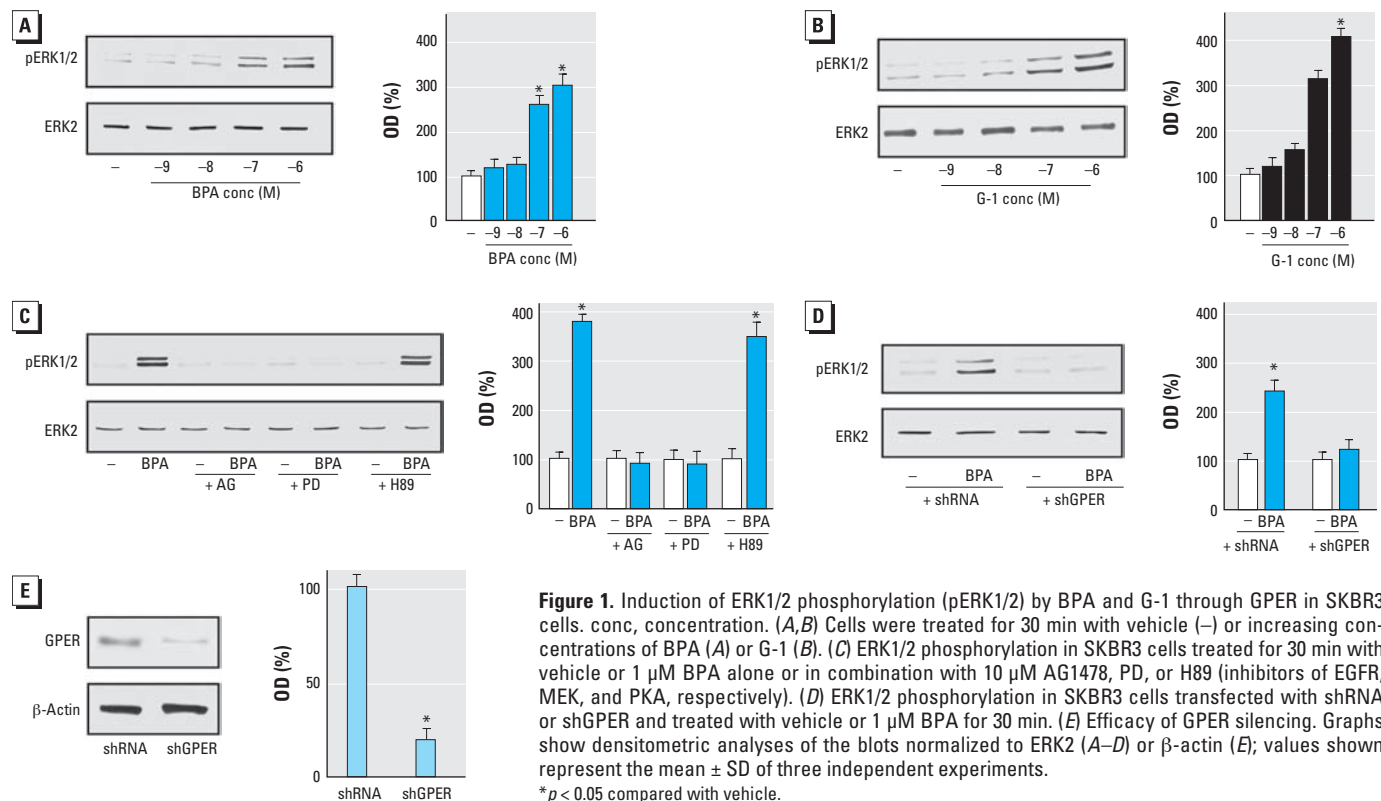


**Figure 1.** Induction of ERK1/2 phosphorylation (pERK1/2) by BPA and G-1 through GPER in SKBR3 cells. (A,B) Cells were treated for 30 min with vehicle (–) or increasing concentrations of BPA (A) or G-1 (B). (C) ERK1/2 phosphorylation in SKBR3 cells treated for 30 min with vehicle or 1  $\mu$ M BPA alone or in combination with 10  $\mu$ M AG1478, PD, or H89 (inhibitors of EGFR, MEK, and PKA, respectively). (D) ERK1/2 phosphorylation in SKBR3 cells transfected with shRNA or shGPER and treated with vehicle or 1  $\mu$ M BPA for 30 min. (E) Efficacy of GPER silencing. Graphs show densitometric analyses of the blots normalized to ERK2 (A–D) or  $\beta$ -actin (E); values shown represent the mean  $\pm$  SD of three independent experiments.

\* $p < 0.05$  compared with vehicle.



Gene-specific primers were designed using Primer Express software (version 2.0; Applied Biosystems Inc.). Assays were performed in triplicate. We used mean values to calculate expression levels by the relative standard curve method. For the sequences of primer used, see Supplemental Material, Table S1 (<http://dx.doi.org/10.1289/ehp.1104526>).

**Gene silencing experiments.** Cells were plated onto 10-cm dishes, maintained in serum-free medium for 24 hr, and then transfected for an additional 24 hr before treatments using Fugene6. The short hairpin (sh) RNA constructs to knock down the expression of *GPER* and *CTGF* and the unrelated shRNA control construct have been described previously (Pandey et al. 2009).

**Wound-healing assay.** CAFs were seeded into 12-well plates in regular growth medium. When at 70% to 80% confluency, the cells were transfected with shGPER using Fugene6 reagent for 24 hr. Transfected cells were washed once, medium was replaced with 2.5% charcoal-stripped FBS, and cells were treated. We then used a p200 pipette tip to scratch the cell monolayer. In experiments performed using conditioned medium, CAFs were plated into 12-well plates and transfected with 500 ng shRNA control plasmid or shGPER or shCTGF plasmids using Fugene6, as recommended by the manufacturer. After 24 hr, CAFs were treated with 1  $\mu$ M BPA, and the conditioned medium was collected and filtered through a sterile nonpyrogenic 0.2  $\mu$ m filter. The conditioned medium obtained was added to subconfluent SKBR3 cells, and a series of scratches were made using a p200 pipette tip. We evaluated cell migration in three independent experiments after 48 hr

of treatment; data are expressed as a percentage of cells in the wound area upon treatment compared with cells receiving vehicle.

**Proliferation assay.** SKBR3 cells and CAFs were seeded in 24-well plates in regular growth medium. After cells attached, they were washed, incubated in medium containing 2.5% charcoal-stripped FBS, and transfected with 500 ng shGPER or control shRNA plasmids using Fugene6 reagent. After 24 hr, cells were treated with 1  $\mu$ M BPA, and the transfection and treatment were renewed every 2 days. We counted the cells using the COUNTLESS automated cell counter (Invitrogen) following the manufacturer's recommendations.

**Statistical analysis.** For statistical analysis, we used analysis of variance followed by Newman-Keuls testing to determine differences in means. *p*-Values < 0.05 are considered statistically significant.

## Results

**BPA induces ERK1/2 activation through GPER.** Using SKBR3 cells and CAFs, which both express GPER and lack ERs [see Supplemental Material, Figure S1 (<http://dx.doi.org/10.1289/ehp.1104526>)], we evaluated ERK1/2 activation by increasing concentrations of BPA and the GPER ligand G-1, as GPER activation leads to ERK1/2 phosphorylation (Dong et al. 2011; Maggiolini and Picard 2010). BPA and G-1 induced ERK1/2 phosphorylation in both cell types in a dose-dependent manner (Figures 1A,B and 2A,B). When the epidermal growth factor receptor (EGFR) inhibitor AG1478 or the mitogen-activated protein kinase kinase MEK inhibitor PD was added, ERK1/2 activation

was not evident, but it was present when the protein kinase A (PKA) inhibitor H89 was added (Figure 1C). Interestingly, ERK1/2 phosphorylation by BPA was abolished by silencing GPER expression (Figures 1D, 2C), suggesting that GPER is required for ERK1/2 activation after exposure to BPA. We ascertained the efficacy of GPER silencing using immunoblots in SKBR3 cells and CAFs as shown in Figures 1E and 2D, respectively. Moreover, to demonstrate the specificity of BPA action, we used the environmental contaminant arsenic (Nordstrom 2002), which elicits the ability of breast cancer cells to activate ERK1/2 (Ye et al. 2005). We observed that ERK1/2 phosphorylation induced by 10  $\mu$ M As<sub>2</sub>O<sub>3</sub> was still present in SKBR3 cells transfected with shGPER (data not shown).

**BPA stimulates the expression of GPER target genes.** GPER-mediated signaling regulates the transcription of diverse target genes (Pandey et al. 2009). In the present study, BPA transactivated the promoter sequence of *c-FOS*, *EGR-1*, and *CTGF* (Figure 3A), and accordingly stimulated mRNA expression of these genes (Figures 3B, 4A). In accordance with these findings, BPA induced the protein levels of c-FOS, EGR-1, and CTGF (Figure 3C). As observed with ERK1/2 activation, the EGFR inhibitor AG1478 and the ERK inhibitor PD, but not the PKA inhibitor H89, repressed the up-regulation of these proteins by BPA (Figure 3C). Notably, the c-FOS, EGR-1, and CTGF protein increases after exposure to BPA were abrogated by silencing GPER in both SKBR3 cells and CAFs (Figures 3D, 4B). The efficacy of GPER silencing was ascertained by immunoblotting experiments in SKBR3 cells

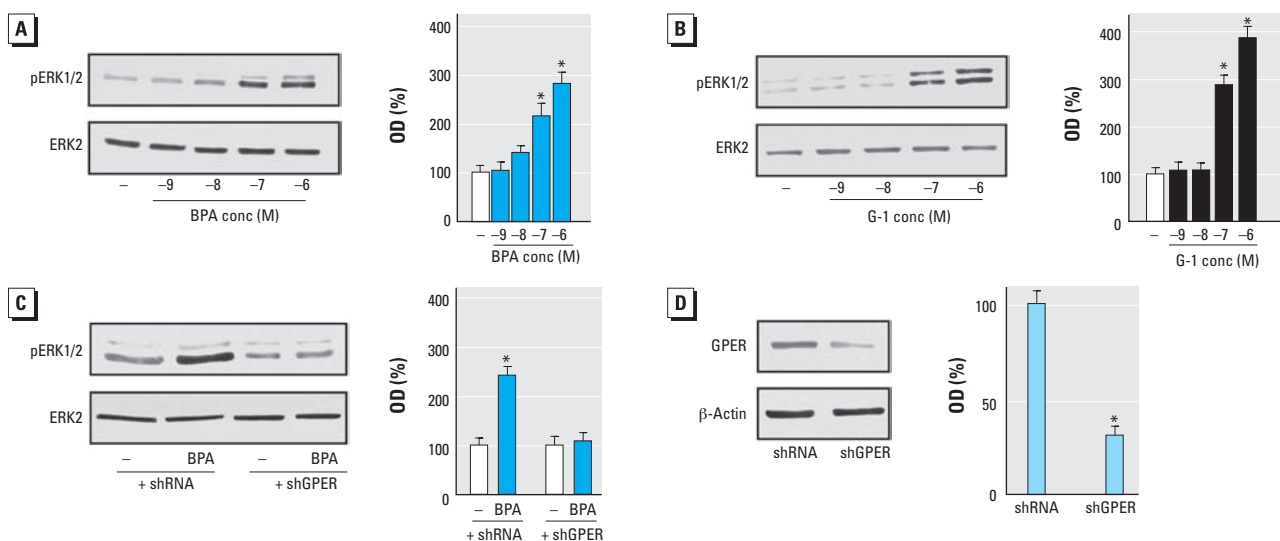


**Figure 2.** Induction of ERK1/2 phosphorylation (pERK1/2) by BPA and G-1 through GPER in CAFs. conc, concentration. (A,B) CAFs were treated for 30 min with vehicle (–) or increasing concentrations of BPA (A) or G-1 (B). (C) ERK1/2 phosphorylation in CAFs transfected with shRNA or shGPER and treated with vehicle or 1  $\mu$ M BPA for 30 min. (D) Efficacy of GPER silencing in CAFs. Graphs show densitometric analyses of the blots normalized to ERK2 (A–C) or  $\beta$ -actin (D); values shown represent the mean  $\pm$  SD of three independent experiments.

\**p* < 0.05 compared with vehicle.

and CAFs as shown in Figures 3E and 4C, respectively. Taken together, these results demonstrate that BPA regulates the expression of *c-FOS*, *EGR-1*, and *CTGF* through the GPER/EGFR/ERK transduction pathway.

**BPA induces cell proliferation and migration through GPER.** The aforementioned results were recapitulated in the complex physiologic responses such as cell proliferation and migration. The proliferative effects observed in both SKBR3 cells and CAFs after 5-day treatment with BPA were cancelled when GPER expression was silenced by shGPER (Figure 5A,B). Moreover, in wound-healing assays in CAFs, migration induced by BPA was abolished by knocking down GPER expression (Figure 5C). To evaluate whether the treatment of CAFs with BPA could induce the migration of tumor cells through secreted factor(s), we performed wound-healing assays

in SKBR3 cells cultured with conditioned medium from CAFs. Interestingly, the migration of SKBR3 cells was not evident after silencing GPER or CTGF expression in CAFs (Figure 5D). Overall, these findings demonstrate that BPA induces stimulatory effects as a GPER agonist in both ER-negative SKBR3 breast cancer cells and CAFs.

## Discussion

There has been increased interest in understanding the molecular mechanisms involved in the endocrine-disrupting effects of BPA (Vandenberg et al. 2009). In this regard, fetal and perinatal exposures to BPA in rodents have been shown to affect the brain, mammary gland, and reproductive tract, as well as to stimulate the development of hormone-dependent tumors (Durando et al. 2007; Munoz-de-Toro et al. 2005). Moreover, the

estrogenic actions of BPA, including increased uterine wet weight, luminal epithelial height, and increased expression of the estrogen-inducible protein lactoferrin, were reported in prepubescent CD-1 mice (Markey et al. 2001). Analogously, BPA induced the proliferation of uterine and vaginal epithelial cells in ovariectomized rats (Steinmetz et al. 1998). In regard to the mechanisms by which BPA can exert estrogen-like effects, it has been reported that BPA's two benzene rings and two (4,4')-OH substituents fitting in the ER binding pocket allow the binding to and activation of both ER $\alpha$  and ER $\beta$ , which in turn mediate the transcriptional responses to BPA (Gould et al. 1998; Kuiper et al. 1998; Vivacqua et al. 2003). In addition, rapid nongenomic effects involving diverse transduction pathways were observed upon exposure to BPA in pancreatic islet, endothelial, and hypophysial cells and in

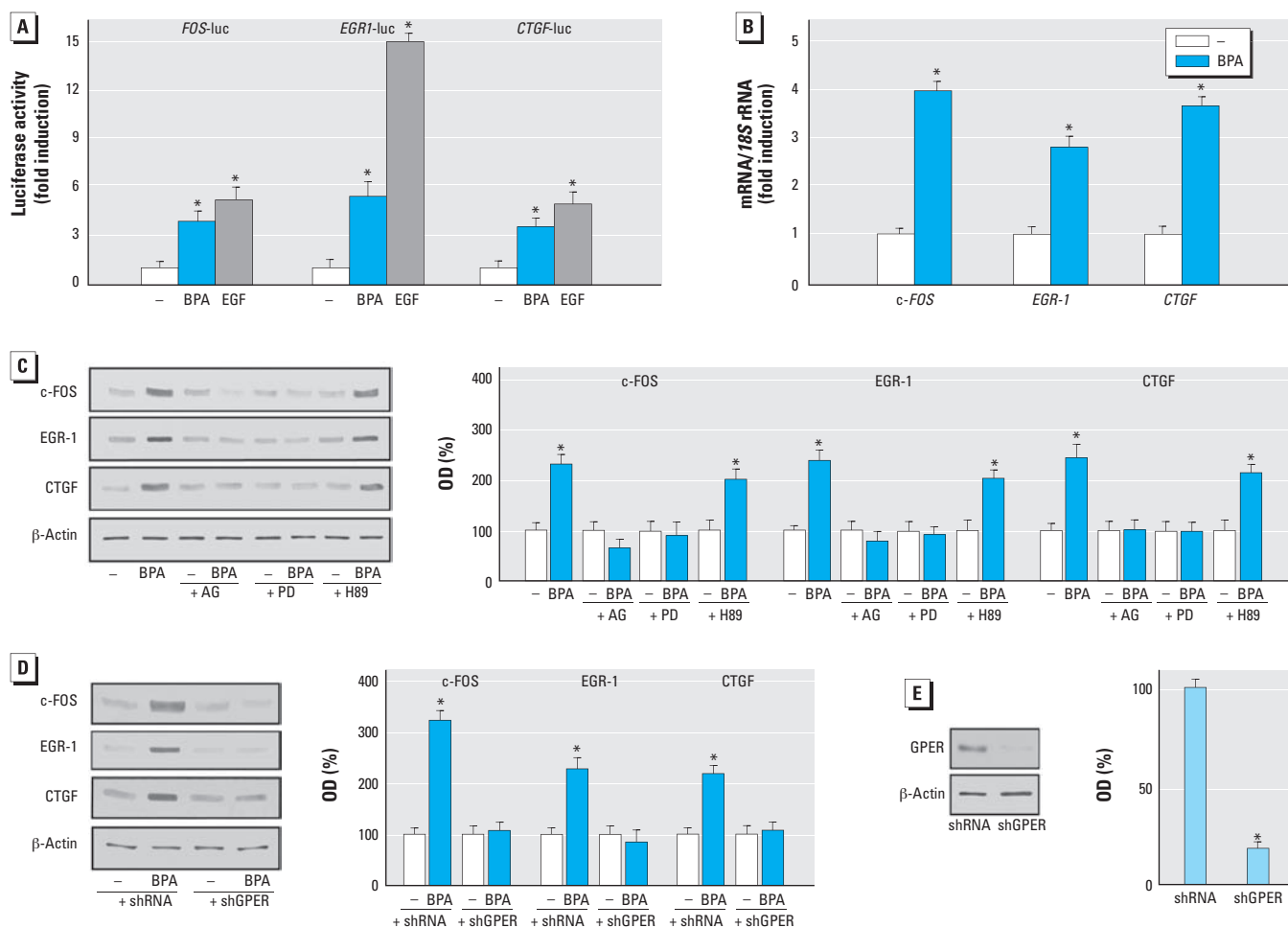


**Figure 3.** Expression of GPER target genes (*c-FOS*, *EGR-1*, and *CTGF*) in SKBR3 cells in response to BPA treatment. (A) Evaluation of *c-FOS*, *EGR-1*, and *CTGF* luciferase reporter genes in transfected SKBR3 cells treated with vehicle (–), 1  $\mu$ M BPA, or EGF (50 ng/mL; positive control). Luciferase activity was normalized to the internal transfection control; values are presented as fold change (mean  $\pm$  SD) of vehicle control and represent three independent experiments, each performed in triplicate. (B) Evaluation of *c-FOS*, *EGR-1*, and *CTGF* mRNA expression by real-time PCR in cells treated with 1  $\mu$ M BPA for 4 hr. Gene expression was normalized to *18S* expression, and values are presented as fold change (mean  $\pm$  SD) of vehicle control. (C) Immunoblots showing *c-FOS*, *EGR-1*, and *CTGF* protein expression in SKBR3 cells treated with vehicle or 1  $\mu$ M BPA alone or in combination with 10  $\mu$ M AG1478, PD, or H89 (inhibitors of EGFR, MEK, and PKA respectively). (D) Protein levels of *c-FOS*, *EGR-1*, and *CTGF* in SKBR3 cells transfected with shRNA or shGPER and treated with vehicle or 1  $\mu$ M BPA for 6 hr. (E) Efficacy of GPER silencing. Graphs show densitometric analyses of the blots normalized to  $\beta$ -actin; values represent the mean  $\pm$  SD of three independent experiments.

\* $p < 0.05$  compared with vehicle.

breast cancer cells (Alonso-Magdalena et al. 2005; Noguchi et al. 2002; Watson et al. 2007). In this context, the novel estrogen receptor GPER was recently shown to mediate the BPA-dependent rapid activation of intracellular signaling (Dong et al. 2011) and the proliferation of both human seminoma cells (Bouskine et al. 2009) and mouse spermatogonial cells (Sheng and Zhu 2011).

To investigate the potential of GPER to mediate estrogenic signals such as those elicited by BPA, we used SKBR3 breast cancer cells and CAFs, both of which express GPER and lack ERs. Interestingly, we found that in both cell types BPA triggers rapid ERK activation through the GPER/EGFR transduction pathway and induces the expression of genes that characterize estrogenic GPER-mediated signaling (Pandey et al. 2009). In addition, we determined that BPA stimulates the proliferation and migration of SKBR3 cells and CAFs through GPER. Of note, conditioned medium from BPA-treated CAFs induced the migration of SKBR3 cells, suggesting that BPA may also promote a functional crosstalk between cancer cells and CAFs. These data regarding CAFs are particularly intriguing given that these cells actively contribute to cancer growth and progression even at metastatic sites (Bhowmick and Moses 2005).

The present findings are relevant to the results obtained in a previous study (Albanito et al. 2008) in which we found that atrazine, another environmental contaminant, triggered estrogen-like activity through the GPER/EGFR/ERK transduction pathway in hormone-sensitive ovarian cancer cells. Moreover, in that study (Albanito et al. 2008) we observed that atrazine induced functional crosstalk between GPER and ER $\alpha$  in accordance with the results of Sheng and Zhu (2011) who demonstrated a similar interaction

in mouse spermatogonial cells after exposure to BPA. Overall, these findings, together with results of the present study, contribute to a better understanding on the multifaceted mechanisms by which environmental estrogens may act as endocrine stimulators in hormone-dependent malignancies.

BPA is consistently detected in almost all individuals in developed nations (Welshons

et al. 2006), suggesting that humans are exposed to BPA continuously. In addition, the rapid metabolic clearance of BPA and its detectable levels in human blood and urine suggest that the intake of BPA may be higher than indicated by diverse studies and that long-term daily intake may lead to its bioaccumulation. In this regard, previous studies (Vandenberg et al. 2009) have estimated

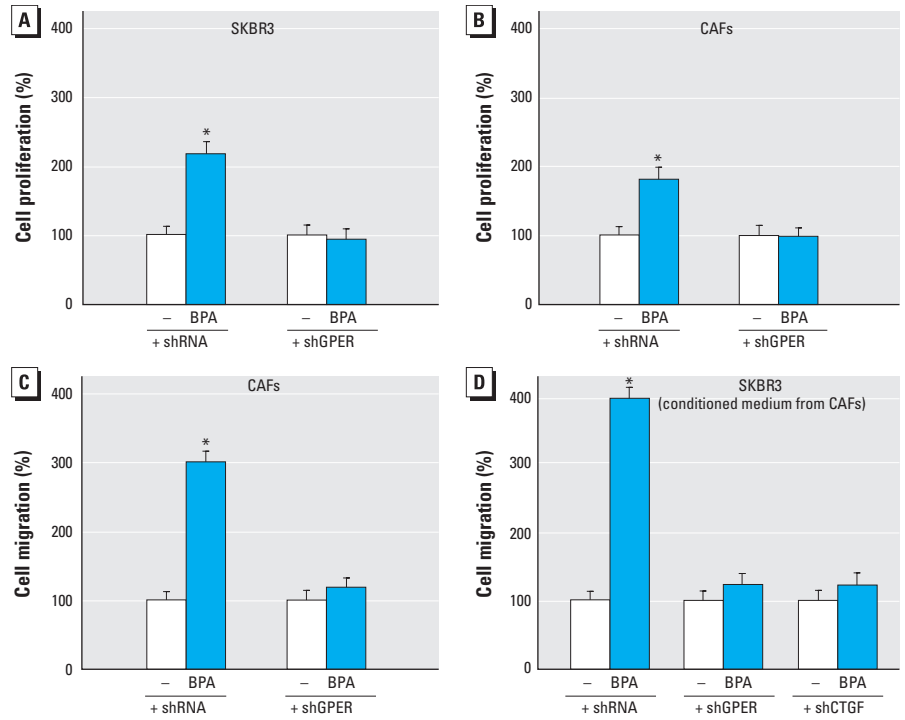


**Figure 5.** Induction of proliferation and migration in SKBR3 cells and CAFs. (A,B) Proliferation in SKBR3 cells (A) and CAFs (B) treated with vehicle (-) or 1  $\mu$ M BPA for 5 days after silencing GPER expression. (C) Migration in CAFs treated with vehicle or 1  $\mu$ M BPA for 48 hr after silencing GPER expression. (D) Migration in SKBR3 cells cultured in conditioned medium from CAFs with silenced expression of GPER and CTGF. Values shown represent the mean  $\pm$  SD percent of vehicle control of three independent experiments, each performed in triplicate. \* $p$  < 0.05 compared with vehicle.

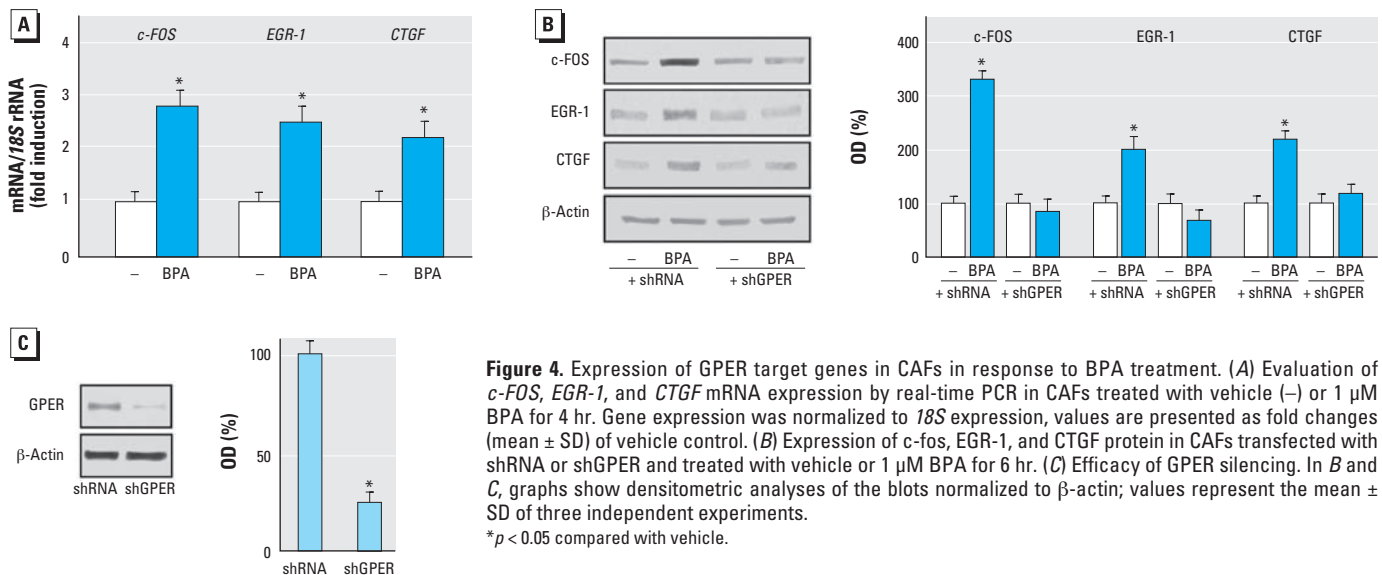


**Figure 4.** Expression of GPER target genes in CAFs in response to BPA treatment. (A) Evaluation of *c-FOS*, *EGR-1*, and *CTGF* mRNA expression by real-time PCR in CAFs treated with vehicle (-) or 1  $\mu$ M BPA for 4 hr. Gene expression was normalized to 18S expression, values are presented as fold changes (mean  $\pm$  SD) of vehicle control. (B) Expression of *c-fos*, *EGR-1*, and *CTGF* protein in CAFs transfected with shRNA or shGPER and treated with vehicle or 1  $\mu$ M BPA for 6 hr. (C) Efficacy of GPER silencing. In B and C, graphs show densitometric analyses of the blots normalized to  $\beta$ -actin; values represent the mean  $\pm$  SD of three independent experiments. \* $p$  < 0.05 compared with vehicle.

that human exposure ranges from  $< 1 \mu\text{g}/\text{kg}/\text{day}$  to almost  $5 \mu\text{g}/\text{kg}/\text{day}$  ( $0.325 \text{ mg}/\text{day}/\text{adult}$ ). However, pharmacokinetic modeling data have shown that oral intakes up to  $100 \text{ mg}/\text{day}/\text{adult}$  would be required to explain the reported human circulating levels (Vandenberg et al. 2009). Hence, future studies should include mathematical models of potential exposures, particularly because many sources of BPA exposure have been identified (Vandenberg et al. 2009). These observations suggest that the BPA concentration used in the present study is achievable in humans. In the present study, we found that BPA is able to trigger GPER-mediated signaling in breast cancer cells and CAFs, which contributes to tumor progression. Thus, GPER may be a potential mediator of the estrogen-like activity of BPA, as well as a further biological target in estrogen-sensitive tumors.

## REFERENCES

- Abramoff MD, Magalhaes PJ, Ram SJ. 2004. Image processing with ImageJ. *Biophotonics Int* 11(7):36–42.
- Albanito L, Lappano R, Madeo A, Chimento A, Prossnitz ER, Cappello AR, et al. 2008. G-protein-coupled receptor 30 and estrogen receptor- $\alpha$  are involved in the proliferative effects induced by atrazine in ovarian cancer cells. *Environ Health Perspect* 116:1648–1655.
- Albanito L, Madeo A, Lappano R, Vivacqua A, Rago V, Carpino A, et al. 2007. G protein-coupled receptor 30 (GPR30) mediates gene expression changes and growth response to  $17\beta$ -estradiol and selective GPR30 ligand G-1 in ovarian cancer cells. *Cancer Res* 67:1859–1866.
- Alonso-Magdalena P, Laribi O, Ropero AB, Fuentes E, Ripoll C, Soria B, et al. 2005. Low doses of bisphenol A and diethylstilbestrol impair  $\text{Ca}^{2+}$  signals in pancreatic  $\alpha$ -cells through a nonclassical membrane estrogen receptor within intact islets of Langerhans. *Environ Health Perspect* 113:969–977.
- Bhowmick NA, Chytil A, Plieth D, Gorska AE, Dumont N, Shappell S, et al. 2004a. TGF- $\beta$  signaling in fibroblasts modulates the oncogenic potential of adjacent epithelia. *Science* 303:848–851.
- Bhowmick NA, Moses HL. 2005. Tumor-stroma interactions. *Curr Opin Genet Dev* 15:97–101.
- Bhowmick NA, Neilson EG, Moses HL. 2004b. Stromal fibroblasts in cancer initiation and progression. *Nature* 432:332–337.
- Bouskine A, Nebout M, Brucker-Davis F, Benahmed M, Feniche P. 2009. Low doses of bisphenol A promote human seminoma cell proliferation by activating PKA and PKG via a membrane G-protein-coupled estrogen receptor. *Environ Health Perspect* 117:1053–1058.
- Dong S, Terasaka S, Kiyama R. 2011. Bisphenol A induces a rapid activation of Erk1/2 through GPR30 in human breast cancer cells. *Environ Pollut* 159:212–218.
- Durando M, Kass L, Piva J, Sonnenschein C, Soto AM, Luque EH, et al. 2007. Prenatal bisphenol A exposure induces preneoplastic lesions in the mammary gland in Wistar rats. *Environ Health Perspect* 115:80–86.
- Gould JC, Leonard LS, Maness SC, Wagner BL, Conner K, Zacharewski T, et al. 1998. Bisphenol A interacts with the estrogen receptor  $\alpha$  in a distinct manner from estradiol. *Mol Cell Endocrinol* 142:203–214.
- Ho SM, Tang WY, Belmonte de Frausto J, Prins GS. 2006. Developmental exposure to estradiol and bisphenol A increases susceptibility to prostate carcinogenesis and epigenetically regulates phosphodiesterase type 4 variant 4. *Cancer Res* 66(11):5624–5632.
- Kalluri R, Zeisberg M. 2006. Fibroblasts in cancer. *Nat Rev Cancer* 6:582–601.
- Keri RA, Hob SM, Hunt PA, Knudsen KE, Soto AM, Prins GS. 2007. An evaluation of evidence for the carcinogenic activity of bisphenol A. *Reprod Toxicol* 24:240–252.
- Kuiper GG, Lemmen JG, Carlsson B, Corton JC, Safe SH, Van Der Saag PT, et al. 1998. Interaction of estrogenic chemicals and phytoestrogens with estrogen receptor  $\beta$ . *Endocrinology* 139:4252–4263.
- Lapensee EW, Tuttle TR, Fox SR, Ben-Jonathan N. 2009. Bisphenol A at low nanomolar doses confers chemoresistance in estrogen receptor- $\alpha$ -positive and -negative breast cancer cells. *Environ Health Perspect* 117:175–180.
- Madeo A, Maggolini M. 2010. Nuclear alternate estrogen receptor GPR30 mediates  $17\beta$ -estradiol-induced gene expression and migration in breast cancer-associated fibroblasts. *Cancer Res* 70:6036–6046.
- Maffini MV, Rubin BS, Sonnenschein C, Soto AM. 2006. Endocrine disruptors and reproductive health: the case of bisphenol-A. *Mol Cell Endocrinol* 255:179–186.
- Maggolini M, Picard D. 2010. The unfolding stories of GPR30, a new membrane-bound estrogen receptor. *J Endocrinol* 204:105–114.
- Maggolini M, Vivacqua A, Fasanella G, Recchia AG, Sisci D, Pezzi V, et al. 2004. The G protein-coupled receptor GPR30 mediates *c-fos* up-regulation by  $17\beta$ -estradiol and phytoestrogens in breast cancer cells. *J Biol Chem* 279:27009–27016.
- Markey CM, Luque EH, Munoz De Toro M, Sonnenschein C, Soto AM. 2001. In utero exposure to bisphenol A alters the development and tissue organization of the mouse mammary gland. *Biol Reprod* 65(4):1215–1223.
- Mlynarciková A, Kolena J, Ficková M, Scsuková S. 2005. Alterations in steroid hormone production by porcine ovarian granulosa cells caused by bisphenol A and bisphenol A dimethacrylate. *Mol Cell Endocrinol* 244:57–62.
- Munoz-de-Toro M, Markey CM, Wadia PR, Luque EH, Rubin BS, Sonnenschein C, et al. 2005. Perinatal exposure to bisphenol-A alters peripubertal mammary gland development in mice. *Endocrinology* 146(9):4138–4147.
- Noguchi S, Nakatsuka M, Asagiri K, Habara T, Takata M, Konish H, et al. 2002. Bisphenol A stimulates NO synthesis through a non-genomic estrogen receptor-mediated mechanism in mouse endothelial cells. *Toxicol Lett* 135:95–101.
- Nordstrom DK. 2002. Public health. Worldwide occurrences of arsenic in ground water. *Science* 296:2143–2145.
- Pandey DP, Lappano R, Albanito L, Madeo A, Maggolini M, Picard D. 2009. Estrogenic GPR30 signalling induces proliferation and migration of breast cancer cells through CTGF. *EMBO J* 28:523–532.
- Prossnitz ER, Maggolini M. 2009. Mechanisms of estrogen signaling and gene expression via GPR30. *Mol Cell Endocrinol* 308:32–38.
- Rasier G, Toppari J, Parent AS, Bourguignon JP. 2006. Female sexual maturation and reproduction after prepubertal exposure to estrogens and endocrine disrupting chemicals: a review of rodent and human data. *Mol Cell Endocrinol* 254–255:187–201.
- Sheng ZG, Zhu BZ. 2011. Low concentrations of bisphenol A induce mouse spermatogonial cell proliferation by G-protein-coupled receptor 30 and estrogen receptor- $\alpha$ . *Environ Health Perspect* 119:1775–1780.
- Steinmetz R, Mitchner NA, Grant A, Allen DL, Bigsby RM, Ben-Jonathan N. 1998. The xenoestrogen bisphenol A induces growth, differentiation, and *c-fos* gene expression in the female reproductive tract. *Endocrinology* 139:2741–2747.
- Takai Y, Tsutsumi O, Ikezuki Y, Hiroi H, Osuga Y, Momoeda M, et al. 2000. Estrogen receptor-mediated effects of a xenoestrogen, bisphenol A, on preimplantation mouse embryos. *Biochem Biophys Res Commun* 270:918–921.
- Thomas P, Dong J. 2006. Binding and activation of the seven-transmembrane estrogen receptor GPR30 by environmental estrogens: a potential novel mechanism of endocrine disruption. *J Steroid Biochem Mol Biol* 102:175–179.
- Vandenberg LN, Maffini MV, Sonnenschein C, Rubin BS, Soto AM. 2009. Bisphenol-A and the great divide: a review of controversies in the field of endocrine disruption. *Endocr Rev* 30(1):75–95.
- Vivacqua A, Bonofiglio D, Albanito L, Madeo A, Rago V, Carpino A, et al. 2006a.  $17\beta$ -Estradiol, genistein and 4-hydroxytamoxifen induce the proliferation of thyroid cancer cells through the G protein-coupled receptor GPR30. *Mol Pharmacol* 70:1414–1423.
- Vivacqua A, Bonofiglio D, Recchia AG, Musti AM, Picard D, Andò S, et al. 2006b. The G protein-coupled receptor GPR30 mediates the proliferative effects induced by  $17\beta$ -estradiol and hydroxytamoxifen in endometrial cancer cells. *Mol Endocrinol* 20:631–646.
- Vivacqua A, Recchia AG, Fasanella G, Gabriele S, Carpino A, Rago V, et al. 2003. The food contaminants bisphenol A and 4-nonylphenol act as agonists for estrogen receptor  $\alpha$  in MCF7 breast cancer cells. *Endocrine* 22(3):275–284.
- Watson CS, Bulayeva NN, Wozniak AL, Alyea RA. 2007. Xenoestrogens are potent activators of nongenomic estrogenic responses. *Steroids* 72:124–134.
- Welshons WV, Nagel SC, vom Saal FS. 2006. Large effects from small exposures. III. Endocrine mechanisms mediating effects of bisphenol A at levels of human exposure. *Endocrinology* 147:S56–S69.
- Ye J, Li A, Liu Q, Wang X, Zhou J. 2005. Inhibition of mitogen-activated protein kinase enhances apoptosis induced by arsenic trioxide in human breast cancer MCF-7 cells. *Clin Exp Pharmacol Physiol* 32(12):1042–1048.



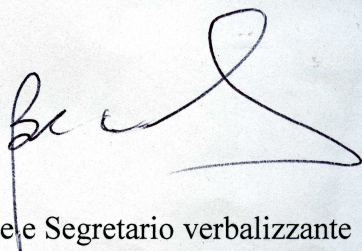
## ALLEGATO E - GIUDIZIO DELLA CANDIDATA ASSUNTA PISANO

Il Collegio dei Docenti ha valutato l'attività di ricerca della candidata Assunta Pisano che si è sviluppata nel campo della Biologia Molecolare, Chimica Organica e Proteomica in relazione alla caratterizzazione strutturale e funzionale del recettore estrogenico GPER in cellule tumorali ormono-sensibili e alla sintesi e caratterizzazione dell'attività biologica esercitata da nuovi composti derivati dal titanio sulla proliferazione cellulare tumorale, e ha preso in esame i risultati conseguiti, riportati in n° 5 lavori a stampa o in corso di stampa su riviste internazionali con referee con buon IF medio, n° 2 comunicazioni in congressi internazionali e n° 1 comunicazioni in congressi nazionali.

Il Collegio ha inoltre valutato:

- l'attività svolta dalla candidata presso il laboratorio di Patologia Generale ed Oncologia Molecolare dell'Università della Calabria, sotto la guida del Prof. Marcello Maggiolini;
- l'attività formativa della candidata che si è realizzata attraverso la partecipazione a n° 2 Convegni internazionali e n° 1 Convegno nazionale;
- l'attività formativa della candidata che si è realizzata a seguito della assidua frequenza all'attività didattica proposta dalla Scuola di Dottorato.

Con riferimento a quanto sopra richiamato, il Collegio dei Docenti del corso di Dottorato di Ricerca in Scienza e Tecnica – Curriculum OMPI (Organic Materials of Pharmaceutical Interest), giudica l'attività della candidata Assunta Pisano ampiamente positiva e la presenta con piena soddisfazione al giudizio della Commissione.



Il Presidente e Segretario verbalizzante  
(Prof. Bartolo GABRIELE)